Analysis of metallothionein gene expression in oxidative stress related disorders

BY

BOITUMELO SEMETE, M.Sc.

Thesis submitted for the degree Philosophiae Doctor (Ph.D.)
in Biochemistry at the North-West University

SUPERVISOR: Professor Antonel Olckers
Centre for Genome Research, North-West University (Potchefstroom Campus)

CO-SUPERVISOR: Doctor Francois van der Westhuizen
Biochemistry, North-West University (Potchefstroom Campus)

CO-SUPERVISOR: Doctor Izelle Smuts
Department of Paediatrics, University of Pretoria

December 2004

Analise van metallotionien geenekspressie in oksidatiewe stres verwante afwykings

DEUR

BOITUMELO SEMETE, M.Sc.

Proefskrif voorgelê vir die graad Philosophiae Doctor (Ph.D.)
in Biochemie aan die Noordwes-Universiteit

PROMOTOR: Professor Antonel Olckers
Sentrum vir Genomiese Navorsing, Noordwes-Universiteit (Potchefstroom Kampus)

MEDEPROMOTOR: Doktor Francois van der Westhuizen
Biochemie, Noordwes-Universiteit (Potchefstroom Kampus)

MEDEPROMOTOR: Dokter Izelle Smuts
Departement Pediatrie, Universiteit van Pretoria

Desember 2004

This thesis is dedicated to my parents

ABSTRACT

Increased reactive oxygen species (ROS) have been reported to be at the centre of various diseases. Although several reports have implicated elevated levels of ROS in the pathogenesis of diabetes mellitus, the early detection of ROS is still not attainable. This limitation causes difficulty in the early diagnosis of ROS related disorders. The presence of high levels of ROS was reported to result in differential expression of antioxidant genes involved in protecting cells from their deleterious effects.

Among the antioxidant genes that are expressed, it was postulated that expression of metallothioneins (MTs) are also induced. MTs are low molecular weight, cysteine-rich proteins involved in metal homeostasis and reported to harbour antioxidant function. The aim of this investigation was to explore MTs as biomarkers for elevated levels of ROS in whole blood of type 2 diabetic (T2D) individuals. The level of ROS in diabetic, non-diabetic as well as individuals at risk of developing T2D was determined via the use of biochemical assays. Real-Time PCR was utilised to analyse the expression of MTs and the presence of MT proteins was analysed via the ELISA.

In this study it was observed that diabetic individuals had elevated levels of ROS. However, no significant difference in the expression of MTs and the presence of MT proteins between the diabetic and non-diabetic individuals was observed. *In vitro* experimental conditions indicated that MT expression is induced by elevated levels of ROS. In pathological conditions the ROS-dependent induction of MT expression needs to be elucidated further. It therefore can be suggested that MTs can not yet be utilised as biomarkers for the detection of elevated levels of ROS in pathological conditions with ROS aetiology. This investigation also highlights the fact that blood is not an optimal medium in which this objective can be attained.

Key Terms: enzyme-linked immonusorbent assay (ELISA); Metallothioneins (MTs); mitochondria; Reactive Oxygen species (ROS); Real-Time PCR; Type 2 diabetes mellitus (T2D).

OPSOMMING

Dit word berig dat die toename in reaktiewe suurstofspesies (ROS) sentraal is tot verskeie siektes. Alhoewel etlike berigte verhoogde vlakke van ROS in die patogenese van diabetes mellitus impliseer, is die vroeë opsporing van ROS nog nie moontlik nie. Hierdie beperking is 'n struikelblok in die vroegtydige diagnose van ROS-verwante afwykings. Dit word berig dat die voorkoms van hoë ROS vlakke lei tot verskille in die uitdrukking van anti-oksidant gene betrokke in die beskerming van selle teen hul skadelike uitwerking.

Dit word veronderstel dat, onder die anti-oksidant gene wat uitgedruk word, die uitdrukking van metallotioniene (MTs) ook teweeggebring word. MTs het lae molekulêre gewig, en is sisteïenryke proteïne betrokke in metaalhomeostase en dit word berig dat hulle anti-oksidant aktiwiteit besit. Die doel van hierdie studie was om MTs te ondersoek as biomerkers vir verhoogde vlakke van ROS in heelbloed van tipe 2 diabetiese (T2D) individue. Die vlak van ROS in diabetiese, nie-diabetiese, sowel as individue met die risiko om T2D te ontwikkel, is biochemies bepaal. Kwantitatiewe PKR is gebruik om die uitdrukking van MTs te ondersoek en die aanwesigheid van MT proteïene is geanaliseer via ELISA.

In hierdie studie is dit waargeneem dat individue met diabetes verhoogde vlakke van ROS besit. Geen betekenisvolle verskil in die uitdrukking van MTs en die aanwesigheid van MTs is egter waargeneem tussen diabetiese en nie-diabetiese individue nie. *In vitro* eksperimentele toestande het aangedui dat MT uitdrukking teweeggebring word deur verhoogde vlakke van ROS. Die uitdrukking van MTs in ROS geassosieerde toetstande moet nog verder verklaar word. Dus kan MTs tans nog nie aangewend word vir die opsoor van verhoogde ROS aktiwiteit in geassosieerde toetstande nie. Hierdie studie bring die feit na vore dat bloed nie die geskikste medium is vir hierdie tipe bepalings nie.

Sleutelterme: ensiem-gekoppelde immonusorbent assay (ELISA); Metallothioniene (MTs); mitochondria; Reaktiewe Suurstofspesies (ROS); Kwantitatiewe PKR; Tipe 2 diabetes mellitus (T2D).

TABLE OF CONTENTS

CHAPTER FOUR
METALLOTHIONEINS 40

CHAPTER FIVE
MATERIALS AND METHODS 58

CHAPTER SIX
RESULTS AND DISCUSSION 81

LIST OF ABBREVIATIONS AND SYMBOLS

LIST OF SYMBOLS

I	respiratory chain complex I
II	respiratory chain complex II
III	respiratory chain complex III
IV	respiratory chain complex IV
V	oxidative phosphorylation system complex V
≤	equal to or less than
ca.	circa: approximately
α	alpha
β	beta
γ	gamma
μ	micro: 10^{-6}
δ	delta
ε	epsilon (indicating the extinction coefficient of NADH)

LIST OF ABBREVIATIONS

Abbreviations are listed in alphabetical order.

3' UTR	3' untranslated region
5' UTR	5' untranslated region
12S rRNA	12 Svedberg units ribosomal RNA
16S rRNA	16 Svedberg units ribosomal RNA
18S rRNA	18 Svedberg units ribosomal RNA
ΔAbs	mean difference in absorbance
A	adenine (in DNA sequence)
A	alanine (in amino acid sequence)
A_1	first absorbance reading taken
A_2	second absorbance reading taken
AAPH	2,2' azobis (2-amidinopropane) dihydrochloride
ADH	alcohol dehydrogenase
ADP	adenosine diphosphate
Ala	alanine
A-NH_2	N,N,-diethylparaphenylen-diamine
$[A\text{-}NH_2]^+$	coloured radical cation of N,N,-diethylparaphenylen-diamine
ANOVA	analysis of variance
ANT	adenine nucleotide translocator
AP-1	activator protein-1
AP-2	activator protein-2
apo-MT	demetallated metallothionein
AR	aldolase reductase

ARE	antioxidant response element
Asn	asparagine
AST	aspartate aminotransferase
Asp	aspartic acid
ATP	adenosine triphosphate
ATPase 6	adenosine triphosphatase 6
ATPase 8	adenosine triphosphatase 8
BLAST	basic local alignment search tool
BCA	bicinchoninic acid
BLE	basal level enhancers
BMI	body mass index
bp	base pairs
BSA	bovine serum albumin
C	cytosine (in DNA sequence)
C	cysteine (in amino acid sequence)
°C	degrees Celsius
CARR U	carrateli units; 1 CARRU = 0.08 mg. 100 ml^{-1} H_2O_2
CCl_4	carbon tetrachloride
Cd	cadmium
cDNA	complementary DNA, obtained by reverse transcription of the mRNA
cm^3	cubic centimetre
cm	centimetre
CNS	central nervous system
Co	cobalt
CO I	cytochrome *c* oxidase I
CO II	cytochrome *c* oxidase II
CO III	cytochrome *c* oxidase III
CoA	coenzyme A
CoQ	coenzyme Q
$CoQH^-$	semiquinone anion form of CoQ
$CoQH_2$	reduced coenzyme Q
CO_2	carbon dioxide
CPCP	Cys-Pro-Cys-Pro
CRS	Cambridge reference sequence
CSBs	conserved sequence blocks
Ct	cycle threshold
CTP	cytidine triphosphate
Cu	copper
Cu^+	copper ion
Cu^{2+}	copper II ion
Cu_2SO_4	copper II sulphate
Cys	cysteine
Cyt	cytochrome
cyt *a*	cytochrome *a*
cyt *b*	cytochrome *b*
cyt *c*	cytochrome *c*
d	path of cuvette
D	aspartic acid

Da	Dalton
dATP	2'-deoxyadenosine-5'-triphosphate
DCF	2',7'-dichlorofluorescein
dCTP	2'-deoxycytidine-5'-triphosphate
ddH_2O	double distilled water
dGTP	2'-deoxyguanosine-5'-triphosphate
D-loop	displacement loop
DMEM	Dulbecco's Modified Eagle's Medium
DMSO	dimethyl sulfoxide
DNA	deoxyribonucleic acid
dNTP	2'-deoxynucleotide-5'-triphosphate
DTNB	5,5'dithiobis-(2-nitrobenzoic acid) solution
dTTP	2'-deoxythymidine-5'-triphosphate
d-ROMs	reactive oxygen metabolites
e^-	electron
E	glutamic acid (in amino acid sequence)
E	PCR efficiency
Eco RI	restriction endonuclease isolated from an *E. coli* strain that carries the cloned ecoRI gene from *Escherichia coli* RY 13, with recognition site 5'-G↓AATTC-3'
EDTA	ethylenediamine tetra-acetic acid: $C_{10}H_{16}N_2O_8$
ELISA	enzyme-linked immonusorbent assay
et al.	*et alii*
EtBr	ethidium bromide: $C_{21}H_{20}BrN_3$
F	phenylalanine (in amino acid sequence)
F	correction factor utilised for the determination of the CARR U with an assigned value of 9000
F0	initial fluorescence
F_1	portion of complex V which projects into the mitochondrial matrix
FAD	flavin adenine dinucleotide
$FADH_2$	flavin adenine dinucleotide (reduced form)
FCS	foetal calf serum
Fe	iron
Fe^{2+}	ferrous iron
Fe^{3+}	ferric iron
Fe-S	iron-sulphur
Fi	fluorescence measured at time i
FMN	flavin mononucleotide (oxidised)
$FMNH_2$	flavin mononucleotide (reduced)
F_0	portion of complex V embedded into the mitochondrial inner membrane
FSHD	fascioscapulohumeral muscular dystrophy
fwd	forward primer
G	glycine (in amino acid sequence)
G	guanine (in DNA sequence)
$g.l^{-1}$	grams per litre
$g.mol^{-1}$	grams per mole
GAPDH	glyceraldehyde-3-phosphate dehydrogenase
GIF	growth inhibitory factor
Gly	glycine

GLUT	glucose transporter
GR	glutathione reductase
GRE	glucocorticoid responsive element
GSH	reduced glutathione
GSH_t	reduced glutathione + oxidised glutathione
GSSG	oxidised glutathione
GSHPx	glutathione peroxidase
GPT	glutamate-pyruvate transaminase
H	histidine (in amino acid sequence)
H	hydrogen
H^+	hydrogen ion
H_2DCFDA	2',7'-dichlorodihydrofluorescein diacetate
H_2O	water
H_2O_2	hydrogen peroxide
HCl	hydrochloric acid
HeLa	cells which were originally obtained from the cervical cancer cell line of Henrietta Lacks
Hg	mercury
HKG	housekeeping gene
HPLC	high performance liquid chromatography
hrs	hours
HRP	horse radish peroxidase
H-strand	heavy strand
I	isoleucine
IAA	iodoacetic acid
IDDM	insulin dependent diabetes mellitus
IgG	immunoglobulin G
IκB	inhibitor of nuclear factor κB
IL1	interleukin 1
IL6	interleukin 6
IL6-REs	interleukin 6 responsive elements
Ile	isoleucine
IRS	insulin receptor substrate
IT_{H1}	heavy strand initiation of transcription site 1
IT_{H2}	heavy strand initiation of transcription site 2
IT_L	initiation of transcription site located on the light strand
JAK	Janus kinase
K	lysine in amino acid sequence
k	sample dilution factor
K_2HPO_4	di-potassium hydrogen phosphate
kb	kilo basepairs
KCl	potassium chloride
kDa	kilo Dalton
kg	kilogram
L	Leucine (in amino acid sequence)
L	litre
L^{CUN}	leucine with anticodon CUN
L^{UUR}	leucine with anticodon UUR

LDH	lactate dehydrogenase
LDL	low density lipoproteins
Leu	leucine
LHON	Leber's hereditary optic neuropathy
L/P	lactate:pyruvate ratio
Lys	lysine
L-strand	light strand
µl	microlitres
µM	micromolar
µm	micrometres
μmol^{-1}	micromole
µg	microgram
$\mu g.ml^{-1}$	microgram per millilitre
m	meter
M	methionine (in amino acid sequence)
M	molar: moles per litre
M2VP	1-methyl-2-vinyl-pyridinium trifluoromethane sulfonate: 30 mM in 0.1 N HCl
MELAS	mitochondrial encephalomyopathy lactic acidosis and stroke-like episodes
MERRF	myoclonic epilepsy and ragged red muscle fibres
Met	methionine
mg	milligrams
Mg^{2+}	magnesium ion
$MgCl_2$	magnesium chloride
min	minutes
min	minimum
ml	millilitre
mm	millimetre
MLTF	major late transcription factor
mM	millimolar
M-MLV-RT	moloney murine leukemia virus reverse transcriptase
Mn	manganese
Mn-SOD	manganese superoxide dismutase
mol	moles
MODY	maturity onset diabetes of the young
MPA	metaphosphoric acid
MPT	mitochondrial permeability transition pore
MRE	metal responsive element
mRNA	messenger RNA
MSUD	maple syrup urine disease
MT	metallothionein
mtDNA	mitochondrial DNA
MTF-1	metal responsive element binding transcription factor
MTT	3-[4,5-dimethylthiazol-2-yl]-2,5-diphenyltetrazoliumbromide
mtTFA	mitochondrial transcription factor
mtTERM	mitochondrial transcription terminator
mtRNA	mitochondrial ribonucleic acid
mtRNase P	mitochondrial RNase P

MW	molecular weight
N	normality
N	asparagine (in amino acid sequence)
n	total number of house keeping genes
NAD^+	nicotinamide adenine dinucleotide (oxidised form)
NADH	nicotinamide adenine dinucleotide (reduced form)
$NADP^+$	nicotinamide adenine dinucleotide phosphate (oxidised form)
NADPH	nicotinamide adenine dinucleotide phosphate (reduced form)
Na_2CO_3	di-sodium carbonate
Na_2EDTA	disodium EDTA: $C_{10}H_{14}N_2Na_2O_8.2H_2O$
$NaHCO_3$	sodium carbonate
NaH_2PO_4	di-sodium hydrogen phosphate
$NaPO_4$	sodium phosphate
NARP	neurogenic ataxia and retinitis pigmentosa
ND 1-6	NADH dehydrogenase subunit 1-6
nDNA	nuclear DNA
NE	normalised expression
NEM	*N*-ethylmaleimide
NF	normalisation factor
NF κB	nuclear factor κB
ng	nanogram
NIDDM	non-insulin dependant diabetes mellitus
nm	nanometres
nM	nanomolar
NMR	nuclear magnetic resonance
NRBM	national repository for biological materials
N-terminal	amino terminal of a polypeptide
O	oxygen
O_2^-	superoxide anion
8-OHdG	8-hydroxy-2-guanosine
OH	hydroxy
OH^-	hydroxyl radical
O_H	heavy-strand origin of replication
O_L	light-strand origin of replication
OMIM	Online Mendelian Inheritance in Man
ORAC	oxygen radical absorbance capacity
OXPHOS	oxidative phosphorylation
%	percentage
P	proline
PBS	phosphate buffered saline
PCA	perchloric acid
PCR	polymerase chain reaction
PEP	phosphoenol pyruvate
PES	N-ethyldibenzopyrazine ethyl sulphate
pH	a measure of acidity: numerically equal to the negative logarithm of H^+ concentration expressed in molarity
P_H	heavy strand promoter
Phe	phenylalanine

P_i	inorganic phosphate
P_L	light strand promoter
pO_2	high pressure oxygen
P/O	phosphate/oxygen ratio
POWIRS2	Profiles of Obese Women with Insulin Resistance Syndrome
Pro	proline
Q	glutamine (in amino acid sequence)
Q	relative quantity of gene expression
Q_i	compartment facing the mitochondrial matrix where the Q-cycle occurs
Q_o	compartment where the Q-cycle occurs oriented towards the inner membrane space
r	correlation coefficient
R	arginine
REST	relative expression software tool
Rev	reverse primer
RFU	relative fluorescence units
RNA	ribonucleic acid
ROS	reactive oxygen species
$R\text{-}O^{\cdot}$	alkoxyl radical of hydroperoxide
$R\text{-}OO^{\cdot}$	hydroperoxyl radical of hydroperoxide
R-OOH	hydroperoxide
rRNA	ribosomal RNA
RT-PCR	reverse transcription polymerase chain reaction
s	slope of graph
S	serine (in amino acid sequence)
S	area under the fluorescence curve for the ORAC assay
S^{AGY}	serine with anticodon AGY
SD	standard deviation
$SDNF_n$	standard deviation of the normalisation factor
SDQ	standard deviation of the relative quantity of gene expression
Ser	serine
SOD	superoxide dismutase
STAT	signal transducer and activator of transcription kinase
S^{UCN}	serine with anticodon UCN in mitochondrial DNA
t	time
T	threonine (in amino acid sequence)
T	thymine (in DNA sequence)
T1D	type one diabetes
T2D	type two diabetes
T_a	annealing temperature
TBARS	thiobarbituric acid-reactive substances
TBE	tris borate-EDTA buffer: 89.15 mM Tris® (pH 8.0), 88.95 mM boric acid, 2.498 mM Na_2EDTA
t-BHP	*tert*-butyl hydroperoxide
TE buffer	tris EDTA buffer: 10 mM Tris·HCl (pH 8.0), 1 mM Na_2EDTA
TCA cycle	tricarboxylic acid cycle or citric acid cycle
TFIID	transcription factor IID
tGSH	total GSH

Thr	threonine
TMB	3,5,3', 5'-tetramethylbenzidine
TNF-α	tumour necrosis factor-α
Tris-HCl	tris-hydrochloric acid (2-amino-2-hydroxymethyl)-1,3-propanediol hydrochloride: $C_4H_{11}NO_3.H_3O$
Triton X-100®	Triton X-100®[1]: Octylphenolpoly(ethylene-glycoether)$_n$: $C_{34}H_{62}O_{11}$; for n=10
Trolox	6-hydroxy-2,5,7,8-tetramethylchroman-2-carboxylic acid
tRNA	transfer RNA
$tRNA^{leu}$	transfer RNA for leucine
$tRNA^{Leu(UUR)}$	transfer RNA for leucine with anticodon UUR
Tyr	tyrosine
U	units of enzyme activity, which is the amount of enzyme required to digest 1 µg of λDNA in 1 hour at 37 °C
$U.ml^{-1}$	units per millilitre
UV	ultra violet
V	valine (in amino acid sequence)
v	sample volume utilised for analysis
V	total reaction volume
Val	valine
$V.cm^{-1}$	volts per centimetre
v/v	volume per total volume
W	tryptophan (in amino acid sequence)
WHR	waist hip ratio
w/v	weight per volume
X	stop codon
x g	gravitational acceleration
Y	tyrosine
Zn	zinc

[1]Triton X-100® is a registered trademark of Rohm & Haas Company, Philadelphia, PA, U.S.A.

LIST OF EQUATIONS

LIST OF FIGURES

LIST OF GRAPHS

LIST OF TABLES

ACKNOWLEDGEMENTS

The accomplishment of this thesis is as a result of the contribution of many individuals who directly or indirectly added value by sharing their wisdom and time. I would like to express my sincere gratitude to the following people and institutions. Without their contribution, effort and encouragement this study would not have been possible.

The patients who participated in this study, and their respective families.

Prof. A Olckers, for being an extraordinary supervisor, always willing to go the extra mile. Her contribution to my scientific career has been phenomenal. **Dr. I Smuts**, her commitment and clinical knowledge that she imparted to this study is greatly appreciated. **Dr. F H van der Westhuizen**, for always willing to share his in depth scientific and biochemical knowledge. I would also like to thank him for the opportunity to work in his laboratory. His involvement in this study is greatly appreciated. **Dr. Annelize van der Merwe**, her commitment and her willingness to help a team member is greatly admired. To the Centre for Genome Research team (**Wayne Towers and Marco Alessandrini, Jake Darby, Dan Isabirye, Michelle Freeman, Desire-lee Dalton** and **Desire Hart**), your support, encouragement, and reliability has been exceptional. **Martha Sebogoli** for making sure that we work in a clean environment as well as her friendliness.

To the team at Biochemistry, **Fanie Rautenbach** for helping me with the biochemical analyses, **Dr. Oksana Levanets,** for helping me with the Real-Time-PCR, **Yolanda Oliver**, for her assistance with the optimisation of the ELISA, **Fimmie Reinecke** and **Leigh Cooper** for helping me with the cell culture work as well as the rest of the department, thank you for your hospitality during my time there as well as your support. I would also like to express my gratitude to **Dr. Suria Ellis** for the help with the statistical analysis of data. My immeasurable gratitude also goes to **Dr. Anna-Marie Kruger, Sister Chrissy Lessing** and **Chrizet Venter** for helping me with the recruitment of patients into the investigation. Your assistance is highly appreciated.

The **North West University (Potchefstroom campus)** administrative and library staff, for the infrastructure and making my experience as a student at the University a great delight. The **Centre for Genome Research**, for funding for this study as well as providing the

infrastructure to perform my studies. Thank you for awarding me a bursary for the years of my study. To **Pharmacology** (Potchefstroom campus), thank you for making available to me the use of the Bio-Rad Real-Time-PCR machine. **DNAbiotec**, for providing the infrastructure and funding to complete this study. The **NRF** for the scholarship awarded to me for the two years of my study.

I would like to express my eternal gratitude to my parents, my brother and sister, for their unconditional love and support throughout my studies. To my friends, for their constant encouragement, prayers, support and most of all their love. Most of all, the **Lord**, my source of strength, comfort and wisdom, to whom I will be eternally grateful.

CHAPTER ONE

INTRODUCTION

Reactive oxygen species (ROS) are an array of free radicals which, upon interacting with cellular components, results in the degradation thereof. Various types of cellular damage occur as a result of exposure to high levels of ROS, eventually leading to apoptosis or necrosis. ROS are produced by various cellular organelles such as peroxisomes, the plasma membrane, mitochondria and in the cytosol. This investigation focuses on ROS produced via the activity of mitochondria. Most of the energy required for various cellular functions is produced via oxidative phosphorylation (OXPHOS) which occurs within the mitochondrion. During energy production in the form of ATP, superoxide radicals are formed as by products, resulting in the accumulation of ROS within the cell.

The role of mitochondria in the pathogenesis of various disorders is associated mainly with the aforementioned ROS production via OXPHOS. In addition to ROS damaging the cellular organelles, these species also cause damage to deoxyribonucleic acid (DNA), resulting in the occurrence of mutations within both the nuclear DNA as well as the mitochondrial DNA. These mutations together with the altered cellular state manifest as disorders with a primary or secondary mitochondrial involvement such as mitochondrial cytopathies, type 2 diabetes mellitus (T2D) and neurodegenerative diseases. An elaborate discussion of the features of the mitochondria as well as the mitochondrial DNA is presented in Chapter Two. Due to the mitochondria being at the centre of various energy production pathways, which are integral for cellular metabolism, these pathways are discussed in Chapter Three.

In addition to an altered energy state, which is a result of ROS production, differential expression of genes involved in bioenergetics as well as protecting the cell has been reported (Van der Westhuizen *et al.*, 2003). Among the class of genes whose protein products have a protective role against ROS, are a group of proteins known as Metallothioneins (MT). These are low molecular weight metal binding proteins that are postulated to be involved in the detoxification and homeostasis of heavy metals, as well as scavenging ROS (Bühler and Kagi, 1974). The physical and chemical properties of this class of proteins are reviewed in Chapter Four. Based on these suggested roles of MTs as

well as the reported tissue specific expression (Fornace *et al.*, 1988), it was the aim of this research programme to investigate the expression pattern of these proteins, in whole blood of individuals affected with T2D. This programme was divided into three phases, where the first and the second phases were *in vitro* approaches performed along with Olivier (2004) and Reinecke (2004) with the aim of elucidating the expression of MTs in complex I deficient and ROS producing HeLa cell lines. To determine the functional role of MTs, Reinecke (2004) over expressed these proteins in the aforementioned cell lines and investigated their effect.

The third approach was aimed at investigating the expression pattern of these proteins *in vivo*. This was preformed via the analysis of MT expression in whole blood of T2D individuals, non-diabetic and individuals at risk for developing T2D. Biochemical parameters listed in Chapter Five were measured and the expression of MTs was investigated utilising the techniques described in Chapter Five. The objective of this *in vivo* investigation was to analyse the expression of MTs in pathological cases and exploring these proteins as possible biomarkers for increased oxidative stress. To verify that ROS induces expression of MTs, as reported (Fornace *et al.*, 1988), an *in vitro* approach utilising ROS producing HeLa cells was followed.

It was hypothesised during this molecular investigation that increased ROS production in patients with T2D, will result in an increased expression of MTs. The study reported in this thesis is the first to investigate the effect of ROS in T2D on the expression of MT genes. The results of this analysis are discussed in Chapter Six. A summary of the clinical data for the individuals included in this investigation is presented in Appendix A. The data from the biochemical parameters analysed are presented in Appendix B, whereas those from the Real-Time PCR and enzyme-linked immonusorbent assay (ELISA) are presented in Appendix C and Appendix D respectively. Conclusions drawn from the results obtained in this study are discussed in Chapter Seven.

CHAPTER TWO

THE MITOCHONDRION

Since the recognition of the pathophysiological significance of oxygen radicals in a variety of clinical diseases, the role of mitochondria has increasingly become a subject of investigation in this context. This stems from the ability of mitochondria to produce reactive oxygen species (ROS), which are detrimental to cellular bioenergetics.

2.1 THE MITOCHONDRIAL GENOME

Mitochondria are endosymbiotic organelles located in all mammalian cells and metabolic pathways involved in energy production occur within this organelle (Campbell, 1995). The mitochondrion was identified in 1898 by Benda, upon observation of insect spermatogenesis. The mitochondrion is involved in aerobic respiration which is coupled to oxidative phosphorylation i.e. production of adenosine triphosphate (ATP) from adenosine diphosphate (ADP) and inorganic phosphate (P_i). These functions are interrelated as ATP synthesis is obligatory coupled to aerobic respiration (Campbell, 1995). The mitochondrion is not solely involved in these two processes but also in lipid metabolism, the citric acid cycle and beta (β)-oxidation of fatty acids.

The mitochondrion contains its own DNA, and is the only cellular organelle other than the nucleus to contain DNA in animal cells (Bogenhagen and Clayton, 1974). It has an outer membrane that is permeable to most metabolites and an inner membrane, which is selectively permeable. The inner membrane contains folds which enclose the matrix. The presence of DNA within the mitochondrion was discovered in 1963 by Nass and Nass, when the 'fibres' within the mitochondria exhibited characteristics similar to that of DNA when fixated, after electron staining reactions (Nass and Nass, 1963a), and enzymatic treatment (Nass and Nass, 1963b). The mitochondrial genome, as depicted in Figure 2.1 is a circular double-stranded molecule consisting of 16,569 base pairs (bp) of known sequence (Anderson *et al.*, 1981). Its physical length reported by Bogenhagen and Clayton (1974) and Borst (1977), has been estimated to be approximately five micrometres (μm) with a molecular mass of 10^7 Daltons (Da).

Figure 2.1: Diagrammatic representation of the mitochondrial genome

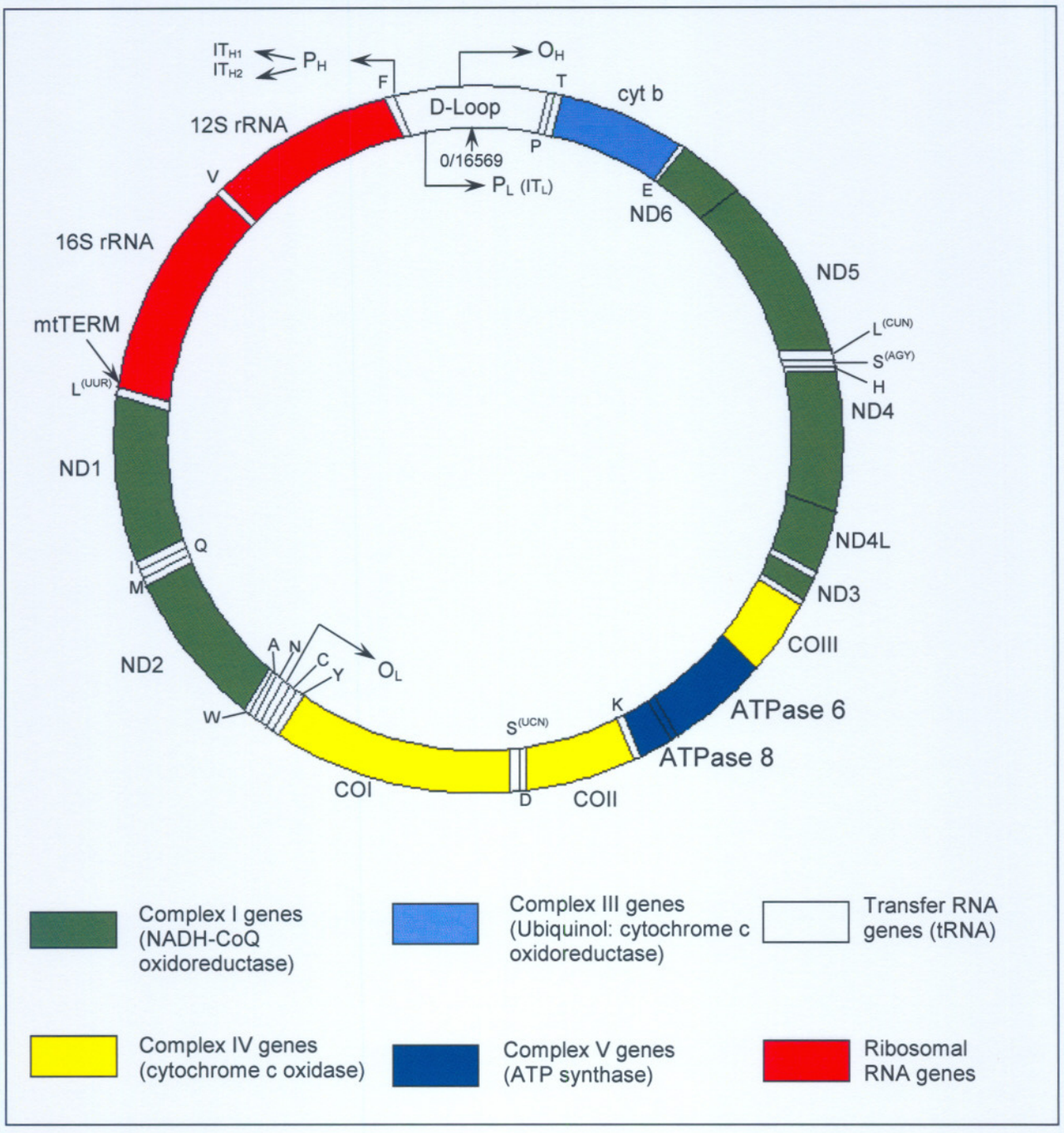

The outer circle illustrates the heavy strand and the inner circle represents the light strand. All tRNA's are indicated in white and the single letters correspond to the amino acid abbreviations. A = alanine; C = cysteine; D = aspartic acid; E = glutamic acid; F = phenylalanine; G = glycine; H = histidine; I = isoleucine; K = lysine; L = leucine; M = methionine; N = asparagine; P = proline; Q = glutamine; R = arginine; S = serine; T = threonine; V = valine; W = tryptophan; Y = tyrosine; Cyt b = cytochrome b; D-loop = displacement loop; ND1-6 = NADH dehydrogenase subunits 1-6; CO I – III = cytochrome *c* oxidase I – III; ATPase 6 = ATP synthase subunit 6; ATPase 8 = ATP synthase subunit 8; O_H = heavy strand origin of replication; O_L = light strand origin of replication; P_H = heavy strand promoter; P_L = light strand promoter. NADH = nicotinamide adenine dinucleotide; ATP = adenosine triphosphate; IT_{H1} and IT_{H2} = heavy strand initiation of transcription sites 1 and 2; IT_L = light strand initiation of transcription site; S^{UCN} = serine with anticodon UCN; S^{UCN} = serine with anticodon UCN; L^{UUR} = leucine with anticodon UUR; L^{CUN} = leucine with anticodon CUN. mtTERM = binding site for the mitochondrial transcription terminator. 12S rRNA = 12 Svedberg unit ribosomal RNA; 16S rRNA = 16 Svedberg unit ribosomal RNA. Adapted from MITOMAP (2003).

The published mitochondrial DNA (mtDNA) sequence is referred to as the Cambridge reference sequence (CRS) and is used to compare mtDNA sequence data generated (Anderson *et al.*, 1981). Andrews *et al.* (1999) reanalysed the mtDNA sequence and identified variations such as substitutions and rare polymorphisms. The mtDNA utilised

(Clayton, 1991). The mtDNA contains 37 genes of which 22 are transfer ribonucleic acid (tRNA) genes, two are ribosomal ribonucleic acid (rRNA) genes and 13 are polypeptide genes. The heavy strand codes for the two rRNAs, 14 tRNAs and 12 polypeptide genes. The light strand encodes eight tRNAs and a single polypeptide (Anderson *et al.*, 1981). The 13 polypeptide coding genes encode for polypeptides embedded within the mitochondrial inner membrane and are involved in the respiratory chain and oxidative phosphorylation. These include genes encoding for seven subunits of complex I, i.e. reduced nicotinamide adenine dinucleotide (NADH) dehydrogenase-ubiquinone oxidoreductase, one for complex III (ubiquinone-cytochrome *c* oxidoreductase), three subunits of complex IV (cytochrome *c* oxidase) and two subunits of complex V also termed the ATP synthase (Borst, 1977).

Each of the aforementioned respiratory chain complexes is not solely encoded by the mtDNA but also contain subunits encoded by the nDNA (Anderson *et al.*, 1981). The nDNA encoded subunits are discussed in Section 3.1. The nDNA encoded proteins are translated into precursor polypeptides, which are subsequently transported to the mitochondria where they are further processed into their functional moieties together with the mtDNA encoded polypeptides. These nuclear encoded polypeptides are synthesised with cleavable amino terminal (N-terminal) pre-sequences for targeting towards the mitochondria (Braun and Schmitz, 1997). Thus mutations within the nuclear genes encoding for mitochondrial polypeptides may result in a defective protein, hence affecting the assemblage of the various subunits. This dual genetic control allows nDNA mutations to result in aberrant metabolism of the mitochondria and thus affect the energy production of the respective cell (Von Kleist-Retzow *et al.*, 1998).

2.1.1 mtDNA transcription

Mitochondrial DNA, unlike nDNA, has only one promoter for all genes on the heavy strand and another for those on the light strand, whereas in the nDNA a single gene has its own promoter and generally does not share it with any other genes (Bogenhagen *et al.*, 1984). The heavy-strand (P_H) and the light strand (P_L) promoters are both located within the displacement loop (D-loop) and initiate transcription of each of the respective strands resulting in polycistronic transcripts. These promoter elements have a consensus 15-bp sequence motif, i.e. 5'-CANACC(G)CC(A)AAAGAYA-3', which surrounds the transcription initiation sites. Additional upstream elements, which are composed of binding sites for the mitochondrial transcription factor (mtTFA) are required for optimal transcription (Borst, 1977; Bogenhagen *et al.*, 1984). Another difference between the mitochondrial genome and the nuclear genome is the variation in the genetic code illustrated in Table 2.1 (Barrell *et al.*, 1979; Anderson *et al.*, 1981).

Table 2.1: Differences between the mitochondrial and the nuclear genetic code

Codon	nDNA	mtDNA
AGA	Arginine	STOP
AGG	Arginine	STOP
AUA	Isoleucine	Methionine
UGA	STOP	Tryptophan

Adapted from Barrell *et al.* (1979) and Anderson *et al.* (1981).

In addition to these differences, the mitochondrial genetic system uses a simplified decoding mechanism that allows translation of all codons with less than the 32 tRNAs. These differences ensure the incompatibility of mtDNA genes within the nuclear environment, i.e. if any DNA is transferred from the mtDNA to the nucleus it would result in non-functional genes.

The transcripts produced via transcription of the heavy strand are present in different relative amounts. The 12 Svedberg units (S) and the 16S rRNAs, which are proximal to the promoter are 50-100 times more abundant than the more distal transcripts (Clayton, 1984). This observation can be explained due to the existence of two initiation sites (IT_{H1} and IT_{H2}) within the P_H. It is proposed that the H-strand follows a dual transcription model, whereby transcription starts relatively frequent at the IT_{H1} and then terminates at the downstream end of the 16S rRNA gene (Montoya *et al.*, 1982; Montoya *et al.*, 1983). The factor mediating attenuation of transcription has been termed the mitochondrial transcription terminator (mtTERM) and it binds at the border of the 16S rRNA and the $tRNA^{Leu(UUR)}$ genes preventing the mitochondrial ribonucleic acid (mtRNA) polymerase from transcribing any further (Hess *et al.*, 1991). This process is responsible for the

synthesis of the high levels of rRNA species. In contrast, transcription starting at the IT_{H2} is less frequent but results in polycistronic molecules corresponding to almost the entire H-strand transcripts. This process results in the production of all the messenger ribonucleic acid (mRNA) and tRNAs encoded on this strand (Montoya *et al.*, 1982; Montoya *et al.*, 1983). The P_L, unlike the P_H is comprised of only a single initiation site for the light strand (IT_{L1}) recognised by the mtTFA and transcribes the L-strand as a single polycistronic precursor RNA encompassing all the genes encoded by this strand. Transcription of both these strands is facilitated by a mtRNA polymerase, and its efficiency is enhanced by the unwinding of the mtDNA by DNA gyrase (Clayton, 1984; Larsson and Clayton, 1995).

Processing of the long polycistronic H- and L- strands is a relatively simple process due to the lack of intergenic DNA sequences within the mtDNA. However, there is a need for post-transcriptional modifications of the genes expressed. Maturation of the tRNAs involves cleavage at the 5'-end by mitochondrial RNase P (mtRNase P) and cleavage at the 3'-end by an endonuclease (DiMauro and Schon, 2001). Maturation of the tRNA is completed by addition of the sequence CCA to the 3'-end, a process catalysed by ATP cytidine triphosphate (CTP): tRNA nucleotidyltransferase (Rossmanith *et al.*, 1995). The mitochondrial mRNAs are polyadenylated by a mitochondrial poly(A) polymerase immediately after cleavage, and the 3'-ends of the two rRNAs are modified by the addition of short polyadenylate tails (DiMauro and Schon, 2001).

2.1.2 mtDNA replication

The replication of the mt genome is similar to that of a prokaryote, whereby a single origin of replication is present on each strand (Clayton, 1982). This supports the endosymbiotic theory postulated for the existence of mitochondria within the cell. It is hypothesised that these organelles evolved from the symbiotic relationship between the aerobic prokaryotic bacteria and the anaerobic host cell. During this symbiotic relationship, the mitochondria transferred many of its genes to the nuclear chromosomes (DiMauro and Wallace, 1993).

The heavy strand origin of replication (O_H) is located within the control D-loop and that of the light strand (O_L) within a cluster of five tRNA genes located two-thirds of the genomic distance away from the O_H. The D-loop is so termed due to the presence of a short nucleic acid strand complementary to the light strand displacing the H-strand and residing there until replication commences (Clayton, 1982).

mtDNA replication starts at the O_H with the unidirectional synthesis of the daughter H-strand via the aid of the mitochondrial DNA polymerase gamma (γ). Prior to mtDNA replication, a helicase catalyses the unwinding of duplex DNA by disrupting the hydrogen bonds that hold the two strands together, therefore providing single stranded templates for DNA polymerase. It has been postulated that short mitochondrial transcripts originating at the initiation transcription site located on the light strand (IT_L) serve as primers for the initiation of the H-strand synthesis. This process therefore suggests a link between mitochondrial replication and transcription (Chang and Clayton, 1985). There is no known difference between transcripts that prime replication and those for L-strand transcription. Transition from RNA to DNA synthesis takes place at sites that constitute the O_H. These sites consist of three short evolutionary conserved sequence blocks (CSBs). The transition from RNA to DNA is not fully understood, but it is postulated that it occurs within the region of the CSBs (Taanman, 1999).

The L-strand origin of replication is flanked by five tRNA genes and is only activated when the parental H-strand is displaced by the growing daughter strand. After strand displacement, O_L changes conformation to form a stem loop structure that serves as a recognition site for the DNA primase which provides a short RNA primer. RNA priming starts at the thymine rich portion of the predicted O_L-loop. The transition from RNA to DNA synthesis takes place at a specific site near a crucial GC-rich site at the base of the hairpin (Hixson *et al.*, 1986). Synthesis is then completed by the mitochondrial DNA polymerase γ and results in a concatenated pair of circles, whose links are broken and ligated by DNA ligase to form closed circular structures. A DNA gyrase subsequently introduces supercoils into the mtDNA helix (Clayton, 1982).

The mitochondrial genome lacks protective histones, which are present within the nuclear genome (Wallace, 1992a). The inefficiency of the post-transcriptional mitochondrial base excision repair mechanism and the high levels of ROS produced within the mitochondria, as discussed in Section 3.3, contribute to the high mutation rate observed (Crouteau *et al.*, 1999) in mitochondria.

2.1.3 Mitochondrial inheritance

The mode of inheritance of the mtDNA is fundamentally different from the Mendelian mode of nDNA inheritance. mtDNA is maternally inherited (Giles *et al.*, 1980) and has a high copy number, with a single cell containing 1,000 – 10,000 mtDNA molecules (Bogenhagen

and Clayton, 1974). Paternal mtDNA transmission does not normally occur due to the fact that the midpiece portion of the spermatozoa, which contains the mtDNA, does not penetrate the ovum, therefore making negligible contribution to the mtDNA content of the ovum (Hecht *et al.*, 1984). Other studies have, however, indicated that sperm derived mitochondria are transmitted, but are lost early in embryogenesis (Kaneda *et al.*, 1995). Each mitochondrion contains 2-10 copies of the mt genome, and the number of mtDNA copies within a cell depends on the energy demand of the respective cell.

2.1.4 Mitochondrial segregation

Mitochondrial replication and division are processes that are independent of the cell cycle or the timing of nuclear replication. Thus, during mitotic division, as depicted in Figure 2.2, a cell may donate different proportions of mutant mtDNA to its daughter cells. This varied transmission of mtDNA suggests that in a heteroplasmic cell any of the various populations of mtDNA will be randomly transmitted to the daughter cells, affecting the level of heteroplasmy in the respective cells (Wallace, 1992a).

2.1.5 Heteroplasmy

Homoplasmy refers to the exclusive presence of identical copies of mtDNA within a single cell. These could be either all normal or all mutant. On the other hand, heteroplasmy denotes the existence of two populations of mtDNA species. In a heteroplasmic state, the fraction of mutated mtDNA varies between different tissues of an individual and also between different cells of the same tissue. As illustrated in Figure 2.2, a mother with heteroplasmic mtDNA may transmit varying levels of mutated mtDNA to her offspring since mitochondria segregate independently. It is also possible that a heteroplasmic mother does not transmit any of the mutated mtDNA copies to her offspring. Thus, the percentage of heteroplasmy within a cell may result in offspring with different mtDNA content and consequently varying severity and nature of clinical symptoms (Wallace, 1992b). The level of heteroplasmy inherited from the mother is therefore not predictable, thus complicating prenatal diagnosis and counselling in mitochondrial disorders.

Figure 2.2: Schematic representation of heteroplasmy and mitotic segregation

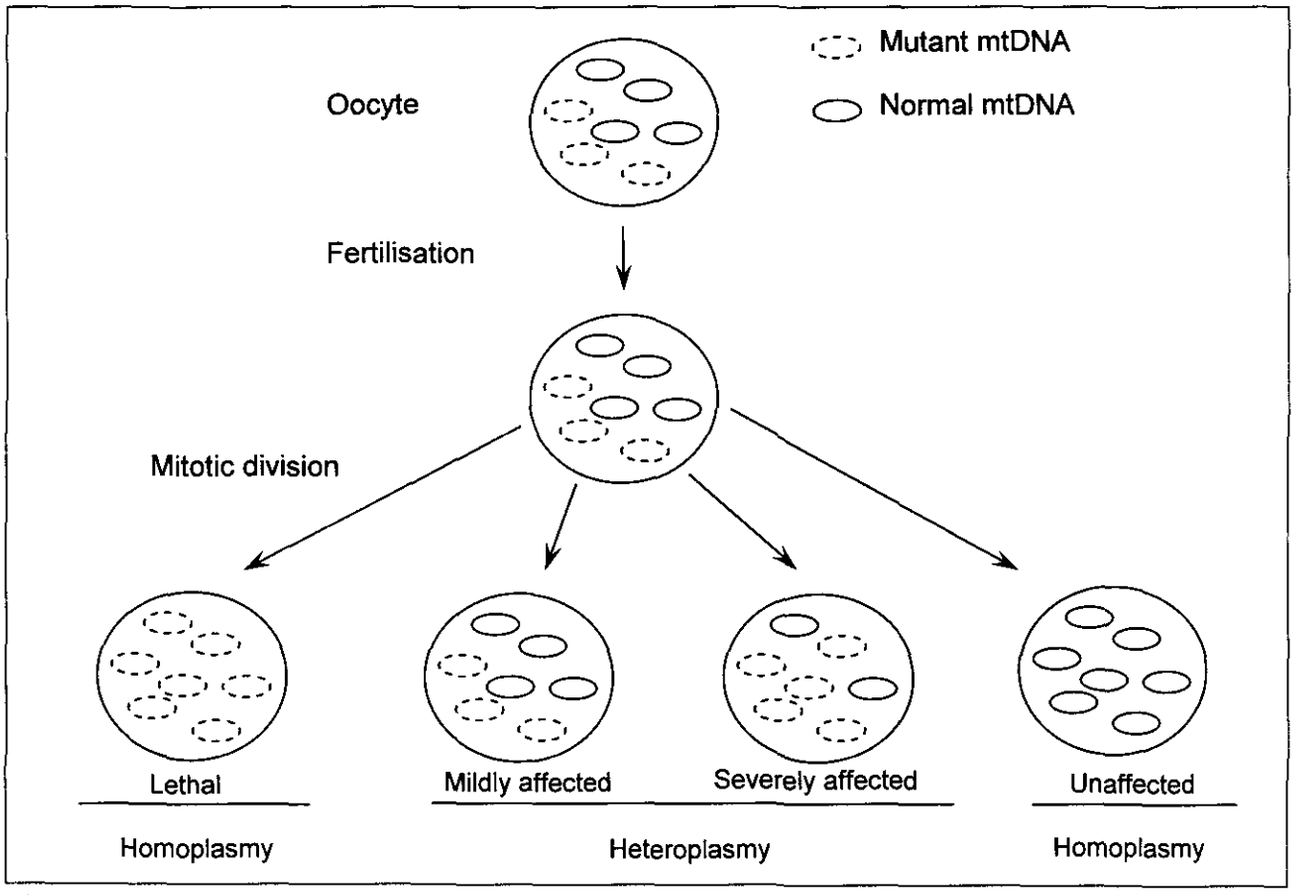

Adapted from DiMauro and Wallace (1993).

The risk of transmission of mutated mtDNA depends mainly on the degree of heteroplasmy and the fact that above a certain threshold level, as discussed in Section 2.1.6, mutated mtDNA are likely to be transmitted to all children (Wallace, 1992b). The occurrence of a severe homoplasmic pathogenic mutation, as illustrated in Figure 2.2, will result in a profound reduction of energy recognised to be incompatible with life. The level of heteroplasmy may in some cases be correlated to the severity of the disorder and also the age of onset (DiMauro and Wallace, 1993).

2.1.6 Threshold effect

The threshold effect refers to the proportion of the mutant to normal genomes that must be exceeded in order to induce presentation of the clinical phenotype. The threshold effect, or level of the mutant mtDNA, has been correlated to the severity and the age of onset of a mitochondrial disorder or the severity of defective OXPHOS. The threshold effect varies between cell types, tissue, and organs and also depends on the energy demand of the respective tissues (Wallace, 1992a). The progressive accumulation of mutations results in an age-related decline of OXPHOS capacity and this effect is illustrated in Figure 2.3 for different tissues with different energy requirements in normal individuals and patients.

Figure 2.3 Graphical representation of threshold effect consequences with regards to phenotypic expression and the age of onset

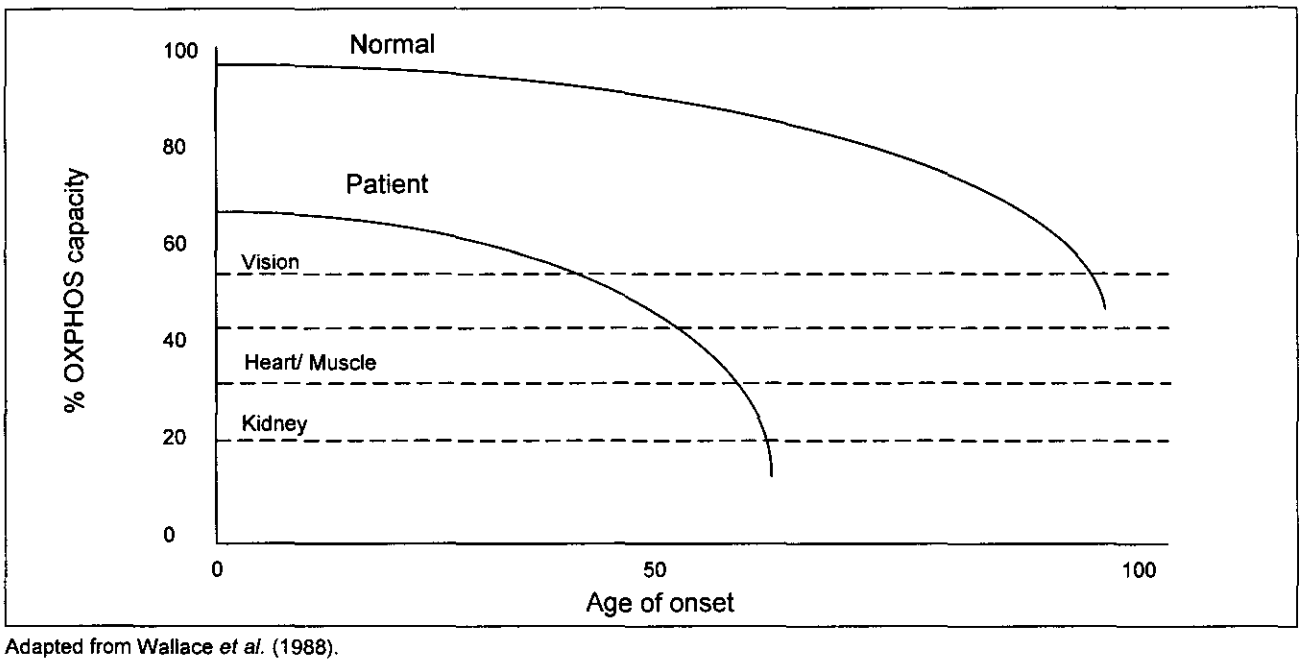

Adapted from Wallace *et al.* (1988).

2.1.7 Haplogroups

Throughout the years, analysis of human mtDNA variation has identified specific combinations of polymorphisms that have been utilised to systematically classify mtDNA into haplogroups. This technique of haplogrouping is extensively employed in studying human origins, dispersal and evolution as well as disease progression (Cann *et al.*, 1987). In a study by Wallace *et al.* (1992a) it was suggested that certain mtDNA polymorphisms in combination with environmental factors and pathogenic mtDNA mutations result in varied functionality of the mitochondria within a specific haplogroup. This study was supported by Brown *et al.* (2002), where it was observed that the 10,663 mutation which is involved in the pathogenesis of Leber's hereditary optic neuropathy (LHON) is pathogenic when co-occurring with haplogroup J. It is therefore important to consider mitochondrial diseases in the context of specific haplogroups. The role of the mitochondrion and its aforementioned characteristics in the progression of diseases is further discussed in Chapter Three.

CHAPTER THREE

BIOCHEMICAL PATHWAYS INTERGRAL TO THE MITOCHONDRIA

Almost all cells in humans depend on OXPHOS to generate energy in the form of ATP to drive cellular metabolism. The catabolism of glucose is another pathway that yields ATP. However, the ATP yield in the latter pathway is less than that produced via the OXPHOS pathway, as discussed in subsequent Sections. Much of the ROS are that produced by the OXPHOS pathway as toxic by-products ultimately leading to programmed cell death, DNA damage and various other forms of damage to the cell. The relatively high levels of ROS within the mitochondria also contribute to the high mutation rate noted within the mtDNA (Wallace, 1992a).

3.1 MITOCHONDRIAL RESPIRATORY COMPLEXES

Complexes involved in the OXPHOS pathway are embedded within the inner mitochondrial membrane (with the exception of complex II) and are arranged in order of increasing redox potential (Harris, 1995). A summary of these complexes and their functions are provided in Table 3.1.

Table 3.1: Summary of mitochondrial complexes involved in OXPHOS

Complex	Name	Reaction	Proton flow	nDNA subunits	mtDNA subunits
I	NADH-CoQ oxidoreductase	$NADH + H^+ + CoQ \rightarrow NAD^+ + CoQH_2$	into inter-membrane space	39	7
II	Succinate-CoQ oxidoreductase	$Succinate + CoQ \rightarrow fumarate + CoQH_2$	none	4-5	0
III	ubiquinone-cytochrome *c* oxidoreductase	$CoQH_2 + 2cyt\ c\ [Fe^{3+}] \rightarrow CoQ + 2cyt\ c\ [Fe^{2+}] + 2H^+$	into inter-membrane space	9-10	1
IV	cytochrome *c* oxidase	$2cyt\ a\ [Fe^{2+}] + \frac{1}{2} O_2 + H^+ \rightarrow 2cyt\ a\ [Fe^{3+}] + H_2O$	outward	10	3
V	ATP synthase	$ADP + P_i \rightarrow ATP$	into matrix	14	2

NADH = reduced nicotinamide adenine dinucleotide; NAD^+ = oxidised nicotinamide adenine dinucleotide; CoQ = coenzyme Q (ubiquinone); $CoQH_2$ = reduced coenzyme Q (ubiquinol); cyt *c* = cytochrome *c*; Fe^{2+} = ferrous iron; Fe^{3+} = ferric iron; O_2 = oxygen; H_2O = water; H^+ = hydrogen ion; ATP = adenosine triphosphate; ADP = adenosine diphosphate; P_i = inorganic phosphate. Adapted from Scholte (1987).

These complexes are involved in the electron transport from the more electronegative components to the more electropositive oxygen, as well as proton transfer across the inner membrane, leading to the production of energy in the form of ATP.

3.1.1 Complex I

The first complex, NADH-coenzyme Q (CoQ) oxidoreductase (EC 1.6.99.3), is an integral part of the inner mitochondrial membrane. Complex I is composed of proteins which contain iron-sulphur clusters, a flavoprotein which oxidises NADH, and other protein subunits. It is the largest of the four complexes with a molecular weight of 10^6 Da (Walker, 1995). Complex I catalyses the first step of electron transport from NADH to CoQ, and couples the redox reaction with an active proton transport across the inner membrane into the inter-membrane space. The 46 subunits are assembled into two domains. The peripheral domain is encoded by the nuclear genes and bears the catalytic NADH binding site.

Table 3.2: Electron transfer reactions within complex I

Reaction number	Reaction
1	$NADH + H^+ + E\text{-}FMN \rightarrow NAD^+ + E\text{-}FMNH_2$
2	$E\text{-}FMNH_2 + Fe\text{-}S_{oxidised} \rightarrow E\text{-}FMN + Fe\text{-}S_{reduced} + 2H^+$
3	$Fe\text{-}S_{reduced} + CoQ + 2H^+ \rightarrow Fe\text{-}S_{oxidised} + CoQH_2$

E-FMN = Enzyme - flavin mononucleotide (oxidised); $E\text{-}FMNH_2$ = Enzyme - flavin mononucleotide (reduced); CoQ = coenzyme Q (ubiquinone); $CoQH_2$ = reduced coenzyme Q (ubiquinol); Fe-S = iron – sulphur; H^+ = hydrogen ion; NAD^+ = oxidised nicotinamide adenine dinucleotide.

The membrane embedded domain is composed mainly of the seven NADH dehydrogenase subunits (ND) encoded by the mitochondrial genome. The reaction occurs in several steps as presented in Table 3.2, with the oxidation of the flavoprotein and reduction of the iron-sulphur moieties. The initial process is the transfer of electrons, as indicated in Reaction 1, from NADH to the flavin portion of the flavoprotein. The second, as illustrated in Reaction 2, involves the re-oxidation of the reduced flavoprotein followed by the transfer of electrons to the iron-sulphur clusters and subsequent reduction of CoQ (also termed ubiquinone) to reduced CoQ ($CoQH_2$) as depicted in Reaction 3. CoQ is free to move within the membrane and to pass electrons to the third complex for further transport to oxygen (Adams and Turnbull, 1996). This reaction catalysed by complex I is one of the reactions that are responsible for the proton pumping that creates a pH gradient across the inner mitochondrial membrane (Murray *et al.*, 1993; Campbell, 1995).

To date, over sixty families of natural and commercial compounds are known to inhibit complex I activity. Inhibition at the site of NADH oxidation, located on the matrix side, results in increased ROS production by causing electron leakage. Therefore, ROS production, due to inhibition of complex I activity at this site, is directed into the mitochondrial matrix where these reactive species could lead to mitochondrial DNA damage or could alternatively be inactivated by the matrix-antioxidant enzyme systems (Cadenas *et al.*, 1977). One of the compounds that results in electron leakage is rotenone, the most potent natural inhibitor of complex I belonging to the family of isoflavanoids (Grigorieff, 1999; Chen *et al.*, 2003). The effect of this compound on the altered expression of metallothionein (MT) was explored by other members of our research team.

Human complex I deficiency is one of the most frequently encountered defects of mitochondrial energy metabolism with an incidence of approximately 1:10,000 live births (Smeitink, 1999). Other disorders such as diabetes mellitus also have a defective mitochondrial OXPHOS aetiology, lending credence to this investigation including diabetic patients, as discussed is Section 3.3.2. The biochemical and the physiological effect of OXPHOS deficiency are further discussed in Section 3.2.

3.1.2 Complex II

The second of the four membrane-bound complexes is succinate-CoQ oxidoreductase (EC 1.6.99.1). It is the only complex not embedded into the mitochondrial inner membrane. It has a molecular mass of 140 kilo Dalton (kDa) and is encoded exclusively by the nDNA. Similar to complex I, this complex also transfers electrons to the ubiquinone pool. However, as illustrated in Table 3.3, the source of electrons in this case is not NADH, but succinate from the citric acid cycle. As summarised in Reaction 4, succinate is oxidised to fumarate by the flavin moiety of complex II, followed by the oxidation of the flavin group (Reaction 5) and simultaneous reduction of CoQ to $CoQH_2$ (Adams and Turnbull, 1996). The oxidation of succinate to fumarate also forms part of the citric acid cycle catalysed by the enzyme succinate dehydrogenase, which forms part of this enzyme complex.

Table 3.3: Electron transfer reactions in complex II

Reaction number	Reaction
4	Succinate + E-FAD → Fumarate + E-$FADH_2$
5	E-$FADH_2$ +CoQ → E-FAD + $CoQH_2$

E = enzyme; FAD = Flavin adenine dinucleotide (oxidised); $FADH_2$ = flavin adenine dinucleotide (reduced); CoQ = coenzyme Q (ubiquinone); $CoQH_2$ = reduced coenzyme Q (ubiquinol).

Succinate dehydrogenase is composed of a flavoprotein subunit containing a succinate binding site, a covalently bound flavin adenine dinucleotide (FAD) moiety of the enzyme and an iron-sulphur subunit (Campbell, 1995). The other components of complex II are cytochrome *b* (cyt *b*) which forms part of the two polypeptides that are required for anchoring succinate dehydrogenase to the mitochondrial membrane and for binding CoQ (Adams and Turnbull, 1996; Campbell, 1995).

3.1.3 Complex III

Complex III, ubiquinone-cytochrome *c* oxidoreductase (EC 1.10.2.2), is an integral part of the inner mitochondrial membrane and is composed of cytochrome *b*, cytochrome c_1 and several iron-sulphur proteins. Cytochrome *b* is the only subunit in this complex encoded and synthesised by the mitochondrial genome (Anderson *et al.*, 1981). Complex III catalyses the oxidation of $CoQH_2$ in a multistep process, passing the electrons to cytochrome *c*. Cytochrome *c* is, however, not part of the complex but is loosely bound to the outer surface of the inner membrane facing the intermembrane space. The oxidation of CoQ involves two electrons and since cytochrome *c* can only accept one electron, two molecules of cytochrome *c* are required for every molecule of CoQ that is involved in this reaction (Adams and Turnbull, 1996). Complex III translocates 4 hydrogen ions (H^+) from the matrix across the inner mitochondrial membrane for each pair of electrons that are transferred from CoQ to cytochrome *c*. Because of the crucial involvement of CoQ, this process is termed the Q cycle, and is schematically represented in Figure 3.1

Figure 3.1: Schematic representation of the Q-cycle

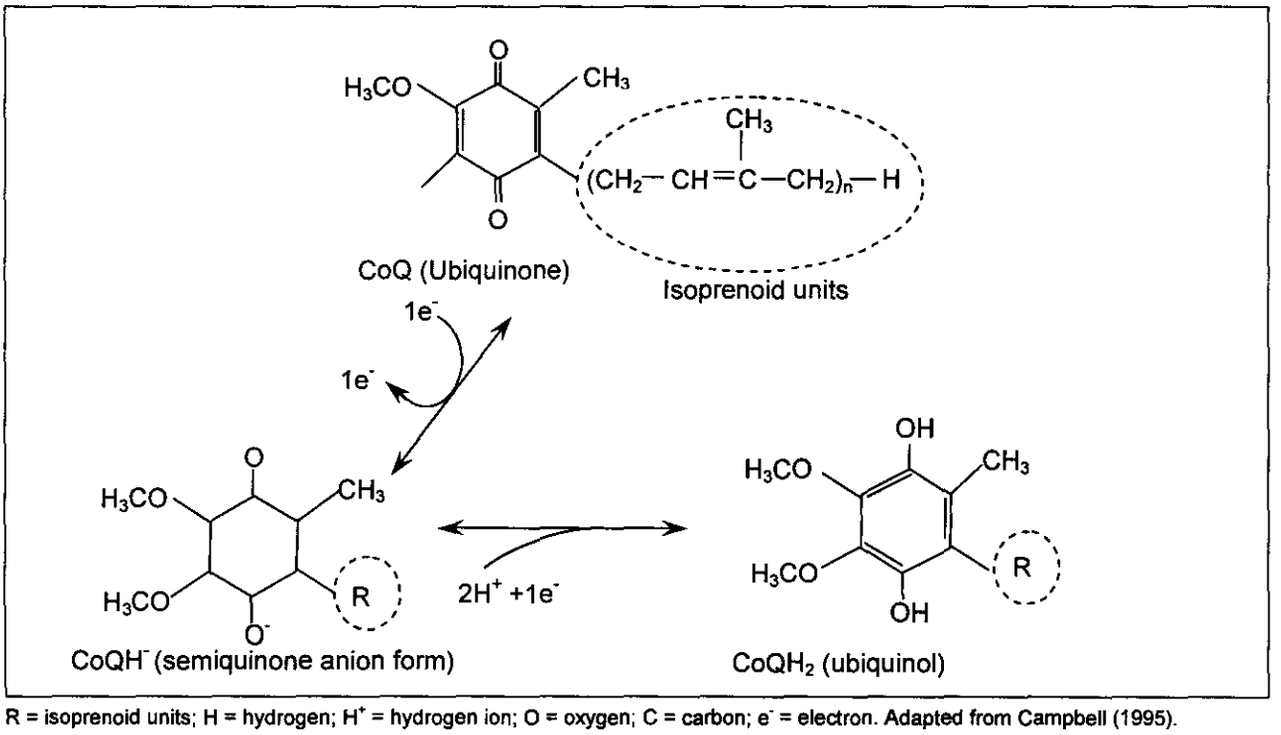

R = isoprenoid units; H = hydrogen; H^+ = hydrogen ion; O = oxygen; C = carbon; e^- = electron. Adapted from Campbell (1995).

One electron is passed from the reduced CoQ to the iron-sulphur cluster to cytochrome c_1, leaving CoQ in the semiquinone form as illustrated in Figure 3.1. The semiquinone, along with the oxidised and the reduced forms of CoQ, participate in the cyclic process where the two cytochrome *b* molecules are oxidised. The second molecule of CoQ is involved in transferring a second electron to cytochrome c_1 and finally to the mobile carrier cytochrome *c*. Cytochrome *c* acts as an intermediate carrier for the transfer of electrons from complex III to complex IV (Campbell, 1995). The compartment facing the mitochondrial matrix where the Q-cycle occurs is referred to as the Q_i centre, with the Q_o centre oriented towards the inner membrane space.

It was suggested from various investigations, including that of Gille and Nohl (2001), that conditions affecting the transfer of electrons within the Q-cycle lead to the production of superoxide anion (O_2^-). It was concluded from these studies that any effect compromising the bifurcated transfer of electrons from $CoQH_2/CoQH^-$ to cytochrome *b* may induce the transfer of these electrons to O_2 (Gille and Nohl, 2001). Turrens *et al.* (1985) clearly illustrated that semiquinone is the direct electron donor responsible for most of the O_2^- generated by complex III. Antimycin A, one of the classical inhibitors of the respiratory chain acts by intercepting the aforementioned electron transfer within the Q-cycle, thus leading to increased production of O_2^-. ROS produced at the Q_i centre due to this inhibition is therefore directed towards the matrix.

3.1.4 Complex IV

Cytochrome *c* oxidase (EC 1.9.3.1) catalyses the final steps of the electron transport from cytochrome *c* to oxygen resulting in the formation of water (H_2O). This complex consists of 13 protein subunits, namely subunits I-III which are encoded by the mitochondrial genome and form part of the catalytic core of the complex as well as subunits IV-VIII which are encoded by the nuclear genome. The functions of the nuclear encoded subunits are unknown, but are probably involved in the tissue specific developmental regulation of cytochrome *c* oxidase. During the reaction carried out by this complex, two hydrogen ions and one electron are translocated from the matrix to the intermembrane space. Electron transfer into complex IV is initiated by the binding of cyt *c* to subunit II on the external side of the membrane. The electrons are transferred as indicated in Table 3.4 into subunit I. Subunit III has no redox centres and thus no role in proton pumping but may be important in the assembly of complex IV (Campbell, 1995).

Table 3.4: Electron transfer within complex IV

Reaction number	Reaction
6	cyt $c \rightarrow Cu_a \rightarrow$ haem of $cyt_a \rightarrow$ haem of cyt_{a3} - Cu_b

Cyt $c_{,a,a3}$ = cytochrome $c_{,a,a3}$; $Cu_{a,b}$ = copper $_{a,b}$.

As previously mentioned, these energy releasing electron transfer reactions are catalysed by complexes I to IV, which are schematically depicted in Figure 3.2. These reactions give rise to proton pumping which culminates in a pH gradient across the inner membrane. Any impairment in the maintenance of the pH gradient will result in an altered membrane potential whose effects are further discussed in Section 3.3.3. The energy released by the oxidation reaction in the electron transport chain is used to drive the phosphorylation of three molecules of ADP by the coupling process (Adams and Turnbull, 1996).

Figure 3.2: The composition and localisation of the respiratory chain complexes

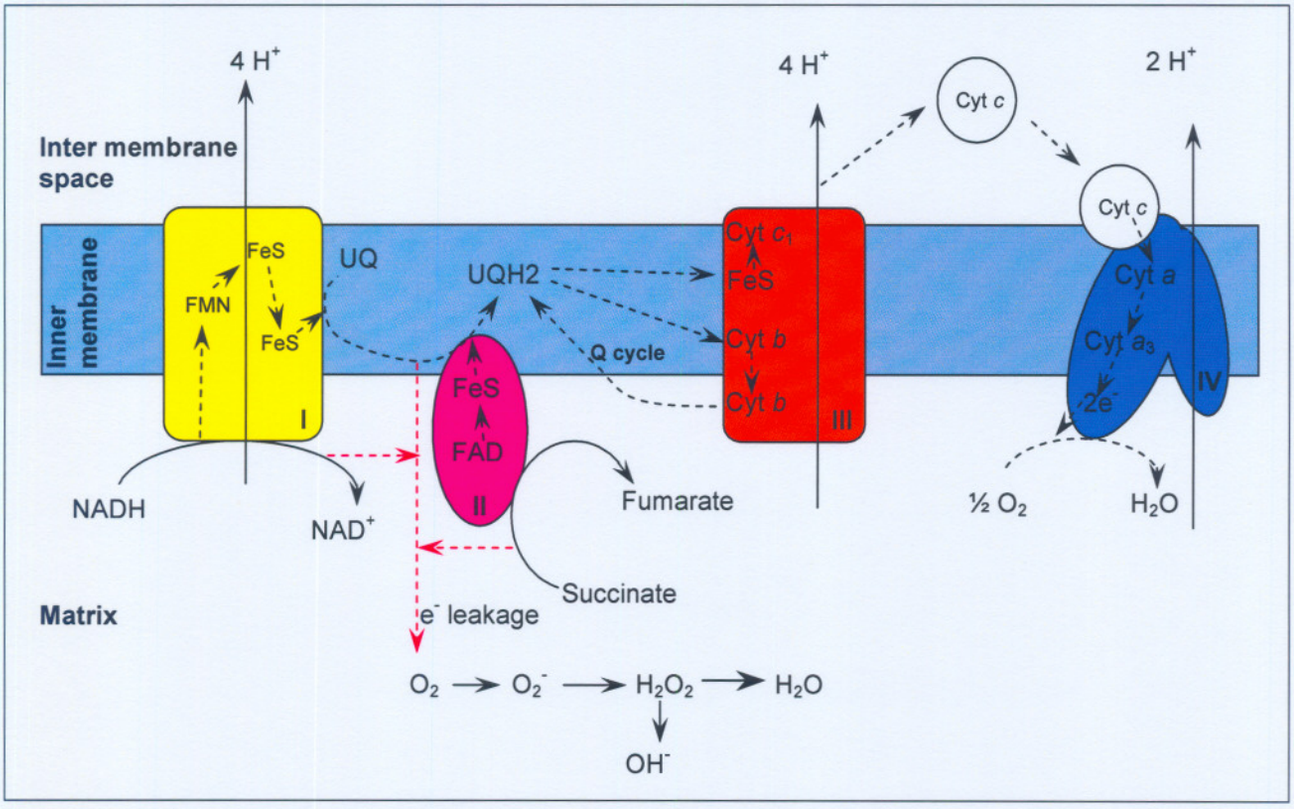

FMN = flavin mononucleotide; FeS = iron-sulphur clusters; FAD = Flavin adenine dinucleotide; UQ = ubiquinone; NADH = reduced nicotinamide adenine dinucleotide; NAD^+ = oxidised nicotinamide adenine dinucleotide; UQH_2 = ubiquinol; Cyt *a, b, c,* = cytochrome *a, b, c*; H^+ = hydrogen; O_2 = oxygen; H_2O = water; H_2O_2 = hydrogen peroxide; OH^- = hydroxyl radical; e^- = electron. I = complex I; II = complex II; III = complex III; IV = complex IV. Dashed arrows indicate electron flow; red dashed arrows indicate electron leakage. Adapted from MITOMAP (2003).

3.1.5 The coupling of oxidation to phosphorylation by complex V

The coupling of ATP production to electron transport is termed the phosphate/oxygen (P/O) ratio. This ratio gives the number of moles of P_i required in the reaction with ADP to yield ATP for each mole of oxygen atoms consumed in the reaction illustrated in Table 3.5. A coupling factor is thus required to link oxidation and phosphorylation. This is facilitated by a complex protein oligomer, separate from the electron transport complexes, namely ATP synthase or complex V (Koolman and Röhm, 1996).

Table 3.5: Electron transfer reactions in complex V

Reaction number	Reaction
7	$1/2\ O_2 + 2H^+ + 2e^- \rightarrow H_2O$

O_2 = oxygen; H^+ = hydrogen ion; H_2O = water; e^- = electrons.

This protein complex is assembled from 16 different polypeptides. Two of these polypeptides, adenosine triphosphatase (ATPase) 6 and ATPase 8, are encoded by the mitochondrial genome (Anderson *et al.*, 1981). The entire complex has a molecular weight of circa (ca.) 400 kDa (Koolman and Röhm, 1996). The complete protein spans the inner mitochondrial membrane and projects into the matrix. The portion embedded into the membrane is called the F_0 subunit, whereas the portion which projects into the matrix is called F_1. The F_0 portion contains four subunits and facilitates the flow of protons down the electrochemical gradient, back to the matrix side of the inner mitochondrial membrane. F_1 is a soluble protein consisting of five different subunits in a stoichiometric ratio of $\alpha_3\beta_3\gamma\delta\varepsilon$ involved in the production of ATP from ADP and P_i. Some of the ATP generated is utilised by the mitochondrion, and the rest transported outside to the cytosol by the adenine nucleotide translocator (ANT).

Due to the coupled nature of oxidation and phosphorylation, the rate of mitochondrial respiration can be controlled by the concentration of ADP. There are five states summarised in Table 3.6 that control the rate of respiration within the mitochondria. The overall process of OXPHOS is blocked by inhibitors such as cyanide and Antimycin A which inhibit electron flow and oligomycin which inhibit the action of the ATP synthase. Uncouplers, such as 2,4-dinitrophenol and other acidic aromatic compounds, inhibit phosphorylation of ADP without affecting the electron transport chain (Murray *et al.*, 1993; Harris, 1995). These substances carry protons across the inner mitochondrial membrane. In their presence, electron transport from NADH to O_2 proceeds normally, but ATP is not

formed due to the dissipation of the proton-motive force across the inner mitochondrial membrane (Campbell, 1995).

Table 3.6: States of respiration control

State number	Conditions limiting the rate of respiration
1	Respiration is controlled by the availability of ADP and substrates
2	Respiration is controlled by the availability of substrate only
3	When all substrates and components are present in saturating amounts and the capacity of the respiratory chain becomes saturated (e.g. during exercise)
4	Respiration is controlled by the availability of ADP only (e.g. when cell is in a resting state)
5	The rate of respiration is controlled by the availability of oxygen only

ADP = adenosine diphosphate. Adapted from Murray *et al.* (1993).

The OXPHOS pathway is the more important of the two mechanisms responsible for cellular production of ATP. The second pathway is cytosolic glycolysis, where ATP production involves the oxidation of glucose to pyruvate, a process coupled to the reduction of oxidised nicotinamide adenine dinucleotide (NAD^+) to NADH. Thus for this pathway to be maintained there must be a continuous supply of NAD^+ via OXPHOS. In mammals with OXPHOS pathway defects the reduction of pyruvate to lactate by lactate dehydrogenase is favoured. This pathway replenishes NAD^+, resulting in an aberrant NADH:NAD^+ ratio (Minniti *et al.*, 2001; Nadlinger *et al.*, 2002). The accumulation of lactic acid via this pathway leads to lactic acidosis, one of the characteristic symptoms of patients with mitochondrial cytopathies and various other metabolic diseases. The electron transport system is a complex process and a defect within this pathway would have a profound effect on cellular metabolism. Many complications within this pathway have been identified, all presenting with complex clinical features (Naviaux, 1997).

3.1.6 Metabolic pathways integral to those within the mitochondrion

If mitochondria are the 'power house' of the cell, then the citric acid cycle, which occurs within the mitochondrial matrix is its engine. This is where the metabolic fuels, i.e glucose derived from carbohydrates, amino acids from proteins and fatty acids from lipids, are all fed into the citric acid cycle in the form of acetyl-coenzyme A (acetyl-CoA). The entry of these substrates into the citric acid cycle is illustrated in Figure 3.3. These substrates are ultimately oxidised to carbon dioxide (CO_2) and H_2O. The energy derived from this pathway is transferred to electron carriers which subsequently enter the OXPHOS pathway.

The citric acid cycle is involved in both anabolic and catabolic reactions. In the citric acid cycle two molecules of CO_2 are produced for each molecule of acetyl-CoA and electrons are also lost. The electron acceptors are NAD^+ and FAD. Subsequent to the reduction of these electron acceptors, to form NADH and reduced flavin adenine dinucleotide ($FADH_2$) respectively, these carriers transport the electrons as previously illustrated in Figure 3.2 to the electron transport chain of the OXPHOS pathway (Harris, 1995). It is therefore evident that a defect in these pathways would affect the citric acid cycle and ultimately the OXPHOS pathway.

Figure 3.3: Metabolic pathways within the mitochondria

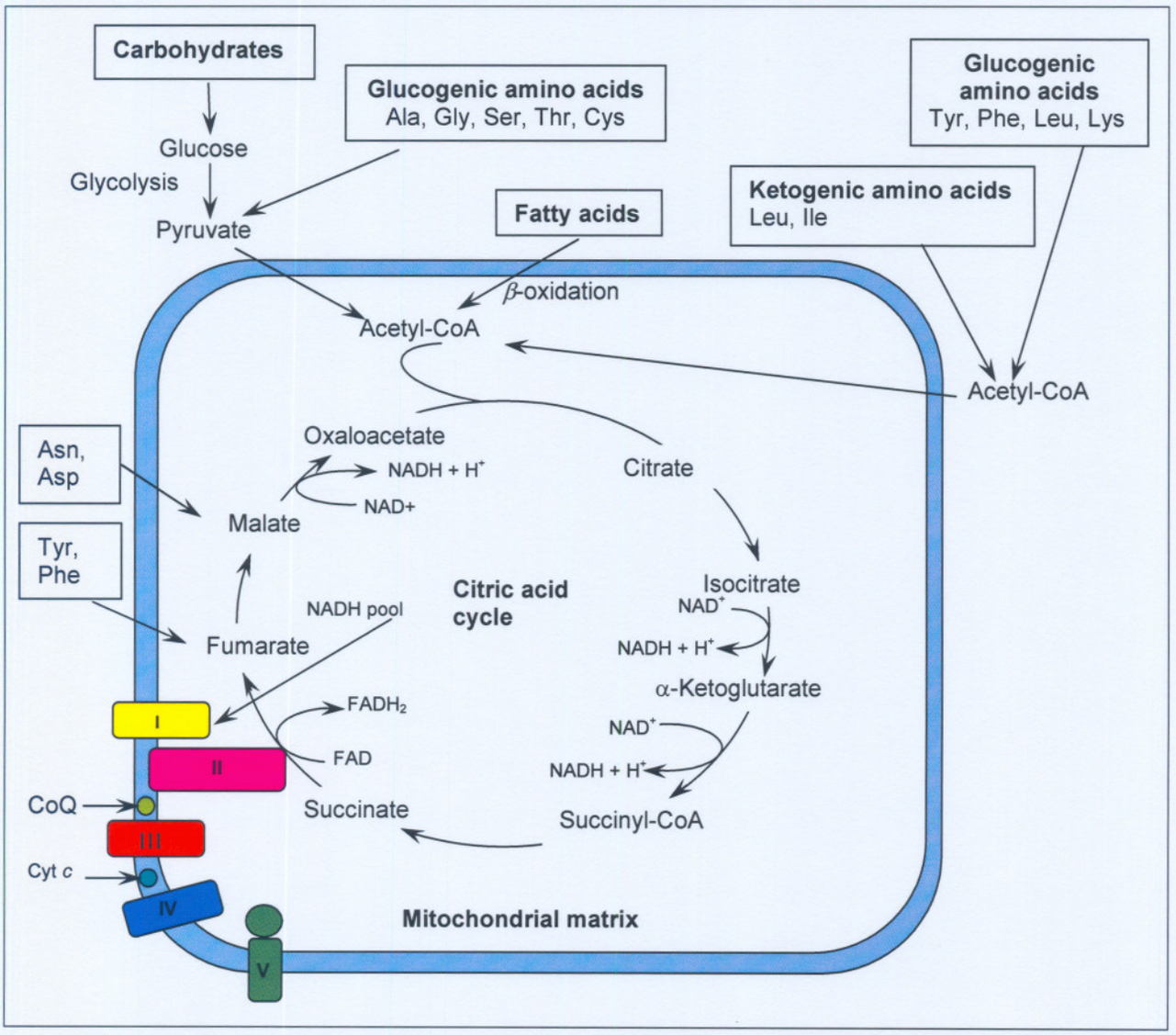

I = complex I; II = complex II; III = complex III; IV = complex IV; V = complex V; FAD = Flavin adenine dinucleotide; FADH = reduced flavin adenine dinucleotide; NADH = reduced nicotinamide adenine dinucleotide; NAD^+ = oxidised nicotinamide adenine dinucleotide; Cyt *c* = cytochrome *c*; CoQ = coenzyme Q; Ala = alanine; Gly = glycine; Ser = serine; Thr = threonine; Cys = cysteine; Ile = isoleucine; Leu = leucine; Tyr = tyrosine; Phe = phenylalanine; Lys = lysine; Asn = asparagine; Asp = aspartic acid; H^+ = hydrogen ion. Adapted from Campbell (1995).

3.2 DISORDERS OF MITOCHONDRIAL DYSFUNCTION

Mitochondrial cytopathies are a group of metabolic disorders that result from mutations within multiple genes involved in mitochondrial biogenesis and function, resulting in defects within the mitochondrial OXPHOS (Smeitink *et al.*, 2001). These mutations usually manifest in tissues with higher energy demands. The first association linking this group of disorders with the mitochondrial genome was described by Wallace *et al.* (1988), demonstrating that LHON resulted from a mutation in the mitochondrial genome. Subsequent to this report, the role of mitochondria in a variety of metabolic syndromes has been reported by others (Adams and Turnbull, 1996; Brown *et al.* 2002).

Nuclear mutations may also interfere with the biogenesis and functioning of the mitochondria, for example, the loss or impaired function of one of the nuclear encoded respiratory chain subunits. This results in a deficiency of the corresponding enzyme complex in the respiratory chain and consequently an altered OXPHOS. Nuclear genes do not only encode for the respiratory chain subunits, but also for other proteins required in mitochondrial biogenesis and maintenance. These include proteins, discussed in Section 2.1.1 and 2.1.2, required for mtDNA replication, transcription, translation, processing and additional proteins involved in mitochondrial protein importation (Larson and Clayton, 1995).

Another class of mutations are those which result in defective intergenomic communication. These may result in the altered control of mtDNA replication, translation or transcription, ultimately leading to multiple mtDNA deletion or mtDNA depletion within specific tissues. Communication between the mitochondria and the nucleus is also facilitated by metabolic signals and signal transduction pathways. These are vital and intricate processes, which together with the complexity of the OXPHOS, explain the wide range of clinical variability observed in patients with metabolic disorders (Larson and Clayton, 1995).

The biochemical consequences of a defective OXPHOS pathway, observed in most patients with mitochondrial cytopathies and OXPHOS related deficiencies are complex. However, the conditions summarised in Table 3.7 are frequently observed in these patients, and form the basis of the biochemical diagnosis of disorders with a defective OXPHOS.

Table 3.7: The biochemical consequences of defective OXPHOS

a	Altered ATP/ADP ratio
b	Disruption of the membrane potential
c	Changes in ion homeostasis
d	Increased ROS production
e	Impaired carbohydrate and amino acid metabolism
f	Inhibition of fatty-acid oxidation

ATP = adenosine triphosphate; ADP = adenosine diphosphate; ROS = reactive oxygen species. Compiled from Piccolo *et al.* (1991) and Adams and Turnbull (1996).

The characteristics of the mitochondria discussed in the previous chapter result in mitochondrial disorders and these vary on the clinical level. The variability within this class of disorders is discussed in Section 3.2.1.

3.2.1 Clinical features of defective OXPHOS

Defects in the electron transport chain may present in several ways, ranging from catastrophic neonatal illness with lactic acidosis to neurological abnormalities. The common clinical presentations that are observed in these individuals are as follows:

a. The symptoms may be atypical to a particular disorder, incomplete or overlap with symptoms observed in other disorders with a mitochondrial involvement.

b. A maternal pattern of inheritance of a particular disorder may indicate mitochondrial involvement. However, disorders linked to primary defects in the OXPHOS or mitochondrial biogenesis can also be inherited in an autosomal dominant, recessive or sex-linked manner.

c. Almost all tissues in the body depend on oxidative metabolism to some extent and can therefore be affected by a defect in the electron transport chain, which leads to systemic manifestation.

d. Due to neuronal tissue being post-mitotic and highly dependent on oxidative metabolism, they are susceptible to any defect in OXPHOS. The affected individuals present with neurological abnormalities. The high energy requirements of this tissue also allude to their susceptibility.

e. Skeletal muscle weakening may be present (myopathy) as well as drooping eyelids (ptosis), heart muscle weakness (cardiomyopathy), brain malfunctioning (encephalopathy) and seizures. These symptoms and the respective disorders are summarised in Table 3.8 (Larson and Clayton, 1995). Recently, Wolf and Smeitink (2002) proposed the use of the Mitochondrial Disease Criteria for the diagnosis of mitochondrial disorders. These criteria takes into consideration clinical, metabolic,

imaging as well as histopathological features versus biochemical investigations of skeletal muscle, to make a more accurate diagnosis. It was suggested in the report that these form of diagnosis be employed in various metabolic disorders in order to increase the sensitivity of the current diagnostic procedures.

Table 3.8: Disorders associated with mitochondrial impairment

Disorders	Main clinical features
Disorders associated with mtDNA mutations	
LHON	Central optic nerve degeneration
Leigh Syndrome	Impaired mental functioning, lactic acidosis
MELAS	Progressive mental impairment, stroke like episodes
MERRF	Cardiomyopathy, dementia, neurosensory hearing loss
NARP	Seizures, dementia, developmental delay
nDNA disorders involving mitochondrial function	
Leigh Syndrome	Mental retardation, lactic acidosis
Pyruvate dehydrogenase deficiency	Neurological complications, lactic acidosis
Glucose-6-phosphate dehydrogenase deficiency	Neonatal jaundice, chronic haemolytic anaemia
MODY	Early onset hyperglycaemia
Diabetes mellitus	Hyperglycaemia, irregular metabolism
Malignant hyperthermia	Skeletal muscle calcium dysregulation, hypermetabolism and elevated body temperatures
Primary disorders of intramitochondrial enzymes	
Methylmalonic acidaemia	Hypotonia, developmental delay
Variegate porphyria	Photosensitivity and CNS effects
Propionic acidaemia	Acidosis, hypoglycaemia, developmental delay
MSUD	Mental retardation

LHON = Leber's hereditary optic neuropathy; MELAS = mitochondrial encephalomyopathy, lactic acidosis and stroke-like episodes; MERRF = myoclonic epilepsy and ragged red muscle fibres; NARP = neurogenic ataxia and retinitis pigmentosa; MODY = Maturity onset diabetes of the young; CNS = central nervous system; MSUD = Maple syrup urine disease. Adapted from Mueller *et al.* (1995); Naviaux (1997).

3.3 REACTIVE OXYGEN SPECIES

Within a cellular environment, ROS are produced during physiological activities either spontaneously or as a result of reactions catalysed by enzymes or transition metals. The five primary metabolic sources of free radicals are plasma membrane, mitochondria, peroxisomes, endoplasmic reticulum and the cytosol. The mechanisms that these organelles utilise to produce ROS as well as their relation to clinical conditions is presented in Table 3.9. The plasma membrane is largely involved in the production of ROS, particularly during inflammation and infection. The membrane uses ROS production to destroy the infected cells and prevent the spreading of the infection. Of the various sites mentioned above, the mitochondria are the principal metabolic source of ROS.

Table 3.9: Primary mechanisms of oxidative stress production and their relation to pathological conditions and lifestyle factors

Site of ROS production	Type oxidative stress	Primary mechanism	Type of ROS produced	Aetiology and clinical correlation
Plasma membrane	Oxidative stress by reactive changes of cell surfaces	NADPH oxidase activation and arachidonic acid production	Hydroperoxides and superoxide anion	Inflammation, immunological reactions and infectious diseases
Mitochondria	Respiration induced Oxidative stress	Metabolic activation and mitochondrial dysfunction	Hydrogen peroxide and superoxide anion	Obesity, mitochondrial genetic diseases (primary) and mitochondrial diseases (secondary)
Microsomes	Pharmaco-metabolic induced oxidative stress	Cytochrome P_{450}/b_5 activation	Various	Alcohol and xenobiotic exposure
Cytosol	Intracellular oxygen pressure induced oxidative stress	Xanthine oxidase activation	Hydrogen peroxide and superoxide anion	Ischemia-reperfusion diseases (infarctions)
Other mechanisms	Oxidative stress by multiple mechanisms	Multiple forms	Hydrogen peroxide and superoxide anion and various others	Cigarette smoking, pollutants and radiation

Adapted from Iorio (2002).

It has been estimated that 1-2 percent (%) of the respiratory oxygen, the final electron acceptor of the respiratory chain, is converted to O_2^- by the transfer of electrons to molecular oxygen (Fahn and Cohen, 1992; Kondoh *et al.*, 2001). The unpaired electron of a free radical is usually exchangeable, thus providing the chemical basis for the reactivity and instability of superoxide and most other radical species (Harris, 1995).

As depicted in Figure 3.2, the free electrons within the mitochondria originate from the leakage of electrons from the OXPHOS pathway and from the transfer of electrons via the electron carriers (Staneik and Nohl, 2000). The O_2^- production also occurs when the respiratory chain is blocked or impaired, which is often the case in patients with mitochondrial cytopathies. Most of the O_2^- is dismutated to hydrogen peroxide (H_2O_2) by manganese superoxide dismutase (Mn-SOD) under physiological conditions, and in turn converted to H_2O and O_2 by glutathione peroxidase (GSHPx). However H_2O_2 may also be converted to the highly toxic hydroxyl radicals (OH^-). All these ROS share the same property, which is to oxidise other chemical species by an electron transfer mechanism. This reaction is terminated when the free radical reacts with another free radical producing an entity without unpaired electrons. The latter radical therefore acts as an antioxidant thus blocking the auto-oxidation process (Harris, 1995).

Antioxidants are classified by their mode of action, i.e. preventative antioxidants, radical scavengers, repair agents, and adaptation agents. Preventative antioxidants include chelators, ROS quenchers and peroxide breakers, whereas repair agents comprise several enzymes such as lipases, DNA repair enzymes and transferases. Radical scavengers are composed mainly of hydrophilic or hydrophobic compounds which lower the free radical concentration in a biological environment by removing one or more reactive species. In the group of radical scavengers, thiol compounds such as those discussed in Section 4.1 play a crucial role against ROS attack.

ROS are continually produced in tissues by the action of the mitochondrial electron transport system (Cadenas *et al.*, 1977; Kondoh *et al.*, 2001) and systems such as the action of reduced nicotinamide adenine dinucleotide phosphate (NADPH) oxidase (Griendling and Harrison, 2001). Exposing cells to high levels of ROS results in tissue injury and inflammation, which subsequently elicit an acute-phase response characteristic of hepatic synthesis of acute-phase proteins such as α-2-macroglobulin, fibrinogen and ceruloplasmin. An increased production of ROS as a result of exposure to ionizing radiation, environmental pollutants and heavy metals (Prithivirajsingh *et al.*, 2004). Cigarette smoking, alcohol intake and other incorrect lifestyles also increase ROS production (Dhindsa *et al.*, 2004).

The chemical reactivity of ROS also results in damage to organic compounds, amino acids, membranes, DNA, and lipids, particularly those composed of unsaturated fatty acids (Piccolo *et al.*, 1991). In addition to their deleterious effects, ROS modulate gene transcription, affect tyrosine phosphorylation and influence the activity of metalloproteins. The presence of ROS also propagates the initiation of apoptosis, a common pathology of mitochondrial cytopathies and other diseases such as diabetes mellitus and Alzheimer's disease. Irregular cell development due to the presence of ROS has previously been reported including various other features in the pathogenesis of neurodegenerative disorders. In addition to these, oxidative stress is implicated in the pathogenesis of several diseases such as atherosclerosis and hypertension. The induction of a cellular mechanism in response to the effects of high levels of ROS is thus imperative and indicates that a cell is under oxidative stress. The various systems and their mechanism of action are summarised in Table 3.10.

Table 3.10: Cellular mechanism developed to overcome the effects of ROS

Enzyme antioxidants	**Mode of action**
a. Superoxide dismutase	$2O_2^- + 2H^+ \rightarrow H_2O_2 + O_2$ (dismutation of O_2^- to H_2O_2)
b. Catalase	$2H_2O_2 \rightarrow O_2 + 2H_2O$ (scavenging of H_2O_2)
c. Glutathione peroxidase or reductase	$2GSH + H_2O_2 \rightarrow GSSG + 2H_2O$ (conversion of H_2O_2 to H_2O and degradation of lipid peroxides)
Chemical antioxidants	**Mode of action**
i. Ascorbic acid	Hydrophilic radical scavenger
ii. Glutathione	Degrades peroxides
iii. Vitamin E	Hydrophobic radical scavenger

H_2O_2 = hydrogen peroxide; O_2 = oxygen; H_2O = water; H^+ = hydrogen ion (proton); O_2^- = superoxide; GSH = oxidised glutathione; GSSG = reduced glutathione. Adapted from Campbell (1995).

To date, no effective antioxidant system has been observed for the most potent of all reactive oxygen species, namely the OH^- radicals. OH^- induces DNA damage by producing a wide range of oxidative damage including strand breaks and base modifications such as the conversion of guanosine in DNA to 8-hydroxy-2-guanosine (8-OHG), characteristic of oxidative damage to the cell, which inhibits replication and transcription (Dandona *et al.*, 1996).

3.3.1 ROS and complex I deficiency

The presence of ROS within the mitochondria is one of the mechanisms that make mtDNA susceptible to acquiring mutations (Cadenas , 1977). These mutations have been reported to be the basis of a number of pathologies with mitochondrial involvement, due to the eventual defective OXPHOS that is as a result of increased ROS (Choksi *et al.*, 2004). Diseases such as those that are due to point mutations within either the tRNA or structural genes, or deletions of mtDNA segments have been characterised (Adams and Turnbull, 1996). The complexity and the observed variability within this group of disorders may be attributed to the intricate nature of mitochondria, as discussed in the previous chapter.

Of the mitochondrial cytopathies, deficiencies of complex I are the most variable, presenting with features that are non-specific, thus making an early and precise diagnosis difficult (Scholte, 1987). Since this investigation focused more on the molecular role of ROS in disorders with a mitochondrial involvement and not the clinical aspects, a summary of these symptoms of mitochondrial dysfunction is provided in Table 3.11, to highlight the widespread clinical symptoms of mitochondrial dysfunction.

Table 3.11: A summary of symptoms of mitochondrial dysfunction

Organ involved	Symptom
Central nervous system	seizures, hypotonia, hypertonia, dystonia, developmental delay and regression, stroke like episodes, acute encephalopathy and dementia
Endocrine system	diabetes mellitus and irregular hormone production
Metabolic system	lactic acidosis and hypoglycaemia
Muscle	muscle weakness and exercise intolerance
Liver	liver dysfunction and failure
Heart	cardiomyopathy and conduction defects
Gastrointestinal	chronic diarrhoea and exocrine/pancreatic dysfunction
Lung	respiration insufficiency
Eye/Ear	sensorineural hearing loss, ptosis and progressive external ophthalmoplegia cataract/corneal opacities, retinal pigmentary degeneration

Adapted from Bhattacharya *et al.* (2003).

3.3.2 The involvement of ROS in type 2 diabetes mellitus (T2D)

Diabetes mellitus is a clinically and genetically heterogeneous disorder characterised by impaired insulin secretion that is often combined with insulin resistance. This impairment may be due to both environmental and genetic factors. Diabetes mellitus is recognised as one of the leading causes of mortality and morbidity in the world, affecting ca. 5-6% of the world population (King *et al.*, 1998). The observed prevalence is also due to its association with hypertension, cardiovascular disorders, renal dysfunction and dyslipidaemias (Orie *et al.*, 1999; Dandona *et al.*, 2004). Diabetes mellitus is divided into two major groups, i.e. non-insulin dependent diabetes mellitus (NIDDM) also termed T2D and insulin dependent diabetes mellitus (IDDM) or type one diabetes (T1D) according to the report by Himsworth, 1936. However, both types are characterised by a systemic defect in the insulin dependent energy metabolism.

T1D results from insulin deficiency that is due to cell mediated autoimmune destruction of the β-cells of the pancreas. This form of diabetes generally develops in the young and is responsible for ca. 10-15% of the diabetic population (Hovi, 1998). T2D, however results from a combination of insulin resistance and insulin deficiency, and unlike T1D it is observed in adults (Sonksen and Sonksen, 2000). It can also develop at a younger age, and this form is known as maturity-onset diabetes of the young (MODY). T2D accounts for 85% of the diabetic population (Owen and Hattersley, 2001).

Under normal conditions, subsequent to the ingestion of nutrients, the levels of glucose increases resulting in an increase in insulin secretion, a hormone produced by the β-cells of the islet of Langerhans of the pancreas. Within a tissue, glucose is metabolised to

glycogen by glycogen synthase (non-oxidative metabolism), or is alternatively oxidised to carbon dioxide and water via pyruvate dehydrogenase (oxidative metabolism). Insulin signalling results in the uptake of glucose by respective tissues, followed by its breakdown via glycolysis, as indicated in Figure 3.4 and the utilisation thereof for energy requirements. This prevents the utilisation of other sources of energy such as lipolysis, proteolysis, ketogenesis, gluconeogenesis and glycogenolysis.

Figure 3.4: Schematic representation of the glycolytic pathway

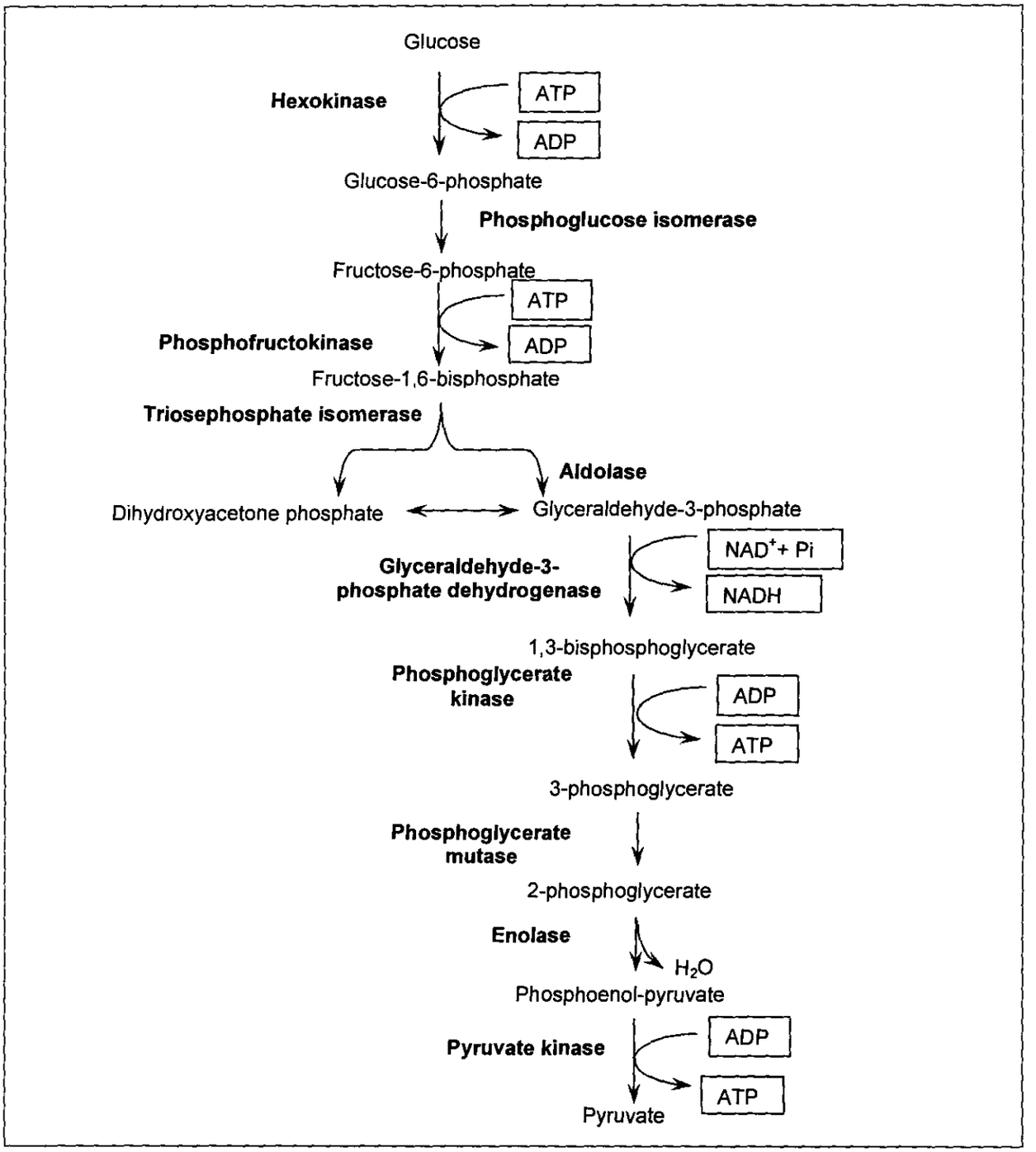

H_2O = water; ATP = adenosine triphosphate; ADP = adenosine diphosphate; P_i = inorganic phosphate NADH = reduced nicotinamide adenine dinucleotide; NAD^+ = oxidised nicotinamide adenine dinucleotide. Adapted from Campbell (1995).

In addition to the role of insulin in glucose uptake, it is also postulated to exert an anti-inflammatory response at both the cellular and molecular levels (Dandona and Aljada, 2002). The maintenance of normal glucose homeostasis is dependent upon hepatic glucose production, glucose uptake by the muscle and adipocytes as well as stimulated insulin secretion.

3.3.2.1 Metabolic impairment in T2D

In a type 2 diabetic state, there is a decreased glucose uptake in response to insulin by the respective cells, resulting in a hyperglycaemic condition, with the consequence being the preferential use of other pathways for energy production. Increased lipolysis in adipose tissues will result in high concentrations of free fatty acids and glycerol which eventually lead to ketoacidosis. In T2D individuals, even though low levels of glucose are ingested, the rate of gluconeogenesis and glycogenolysis is increased and these pathways serve as sources of energy, with the nett effect being the secretion of glucose produced by the hepatocytes into the circulation leading to glycosuria. To overcome the impaired glucose uptake, insulin secretion is initially increased to overcome the insulin resistance and maintenance of normal glucose level, leading to hyperinsulinaemia, impaired glucose tolerance and subsequently hyperglycaemia (Sonksen and Sonksen, 2000).

In a fasting state, hepatic glucose production occurs via glycogen breakdown and gluconeogenesis. In T2D patients with high levels of fasting glucose, hepatic glucose production is increased. In mild cases of T2D, hepatic glucose production is normal, however glucose uptake is impaired. Therefore hyperglycaemia and ketone overproduction are the hallmarks of insulin deficiency (Sonksen and Sonksen, 2000). Patients also present with various other symptoms such as susceptibility to lipid peroxidation which eventually leads to atherosclerosis, a major complication of diabetes mellitus (Dandona and Aljada, 2002).

Recent studies have implicated the production of excessive levels of ROS in the pathogenesis of diabetes mellitus, including vascular diabetic complications which are the main cause of morbidity and mortality within this group of patients (Sakai *et al.* 2003). It is postulated that these reactive species within the pancreas result in β-cell dysfunction and apoptosis of these cells. Sakai *et al.* (2003) provided evidence that high levels of glucose increase intracellular ROS production from the mitochondria in the β-cells, which in turn results in reduced glucose induced insulin secretion. Hyperglycaemia not only increases

ROS production in the β-cells, but also attenuates antioxidative mechanisms. The presence of ROS has not only been identified in the pancreatic cells, but in blood cells (Dandona *et al.*, 1996; Dincer *et al.*, 2002), the vascular endothelial system (Sydow and Münzel, 2003) and other tissues. Friedman *et al.* (2003) illustrated in their investigation that increased production of ROS alters the oxidisability of the low density lipoproteins (LDL), thus resulting in endothelial dysfunction observed in individuals diagnosed with diabetes mellitus.

The lipid peroxidation observed in diabetic individuals has been associated with the increased level of oxidative stress reported for both T1D and T2D. Other events resulting in increased oxidative stress are glucose auto-oxidation (catalysed by trace amount of transition metals) and non-enzymatic protein glycation, including an increase in levels of inflammatory mediators. Metabolic stress resulting from changes in energy metabolism as well as antioxidant defence mechanisms also contribute to the formation of ROS in diabetic individuals. These factors present strong evidence that diabetes mellitus is associated with oxidative stress, which eventually leads to cell and DNA damage (Dandona *et al.*, 1996), therefore lending credence to the investigation of the effects of ROS in T2D individuals on the expression of MT genes.

As previously mentioned, a significant proportion of the ROS is produced via the action of the mitochondria, predominantly the OXPHOS, as discussed in Section 3.1. Lipid peroxidation within the mitochondria due to either ROS production or insulin insensitivity also increase the formation of 8-OHdG, which is found at a higher frequency in mtDNA than in nuclear DNA (Dandona *et al.*, 1996). Several reports, including that of Dandona *et al.* (1996) and Suzuki *et al.* (1999) have demonstrated that a diabetic state increases oxidative damage to DNA. Few other DNA alterations have been reported to be linked to diabetes and ROS production. Şardaş *et al.* (2001) reported that the supplementation of diabetic patients (both T1D and T2D) with Vitamin E yielded a decrease in the extent of DNA damage upon analysis of the DNA via the comet assay. It was postulated in their report that the decrease in DNA damage may have been as a result of the enhanced antioxidant capacity in these individuals.

In the context of the current study, where the effect of ROS production in diabetes mellitus was investigated, it was important to note that some of the alterations reported in diabetic amyotrophy and myotrophy are located with the genes that encode the subunits of complex I (Williams *et al.*, 1976). Thus, as discussed in Section 3.1.1, a defect in the

functioning of complex I eventually leads to the overproduction of ROS, which results in complications in the cellular metabolism ultimately manifesting as pathological conditions i.e. diabetes mellitus. Diabetes has also been reported to be associated with malfunctioning of the mitochondrial permeability transition pore (MPT), which is involved in the maintenance of the membrane potential (Kristal *et al.*, 1996). Impaired functioning of the transition pore, as discussed in Section 3.3.3, is characteristic of an early event of apoptosis. These reports support analysis of ROS in the pathogenesis of various disorders on a more holistic level. Obesity found in most of the T2D patients also constitutes a great risk for the development of this disease, even though the precise mechanism is not yet elucidated (Hotamisligil and Spiegelman, 1994; Greenfield and Campbell, 2004).

3.3.2.2 Anti-inflammatory effects of insulin

Under hyperglycaemic conditions, the pentose phosphate pathway is utilised as an alternative to glycolysis. The ensuing flux of glucose into this pathway may alternatively result in the production of sorbitol by the enzyme aldolase reductase (AR) and thus the depletion of NADPH. The regeneration of reduced glutathione (GSH), an H_2O_2 scavenger, by the GSH-reductase, requires NADPH. Thus the consumption of NADPH leads to an increased concentration the aforementioned radical species. GSH induces its antioxidant properties by increasing the bioavailability of reducing equivalents GSHPx, which then catalyzes the reduction of free radicals such as H_2O_2 and lipid hydroperoxides with the subsequent formation of oxidised glutathione (GSSG) and H_2O. The presence of GSH is vital for the maintenance of the integrity of the cell by reacting with peroxides that would degrade the fatty acid side chains of the cell membrane. Hyperglycaemia is an indirect cause of GSH depletion (Lee and Chung, 1999). In an investigation by Seghrouchni *et al.* (2002) it was observed that T1D patients which were on insulin treatment had low levels of oxidative stress when compared to T2D individuals. However, T2D patients that were also under going treatment presented with less oxidative stress (Seghrouchni *et al.*, 2002). The aforementioned report supports the hypothesis that insulin reduces oxidative stress due to its anti-inflammatory effects (Dandona *et al.*, 2004).

It is postulated by Dandona *et al.* (2004), that insulin exerts an anti-inflammatory response by reducing ROS production via the inhibition or suppression of the NADPH oxidase in mononuclear cells as well as suppression of the intracellular cytokine nuclear factor κB (NF-κB). The suppression of NF-κB thus results in an increase in the inhibitor of NF-κB (IκB) with the loss of the proinflammatory effects of tumour necrosis factor-α (TNF-α).

NADPH oxidase is integral to the pentose phosphate pathway and is involved in the oxidation of NADPH produced via this pathway, resulting in oxidised nicotinamide adenine dinucleotide phosphate ($NADP^+$) and superoxide (Cross and Jones, 1991; Dandona *et al.*, 2004).

TNF-α has been illustrated to interfere with the action of insulin by various mechanisms such as inhibiting autophosphorylation of the insulin receptor in the adipocytes including the human aortic endothelial cells, conversion of insulin receptor substrate-1 into an inhibitor of insulin receptor tyrosine kinase activity or decreasing the glucose transporters (GLUT) -4 in muscle cells (Hotamisligil *et al.*, 1994). Neutralisation of TNF-α in animal models of obesity as well as diabetes led to a decrease in insulin resistance via binding of TNF-α to the receptor. The decrease in the concentration of TNF-α resulted in an increase in insulin stimulated uptake of glucose (Hotamisligil *et al.*, 1993). Even though this approach has been effective in animal models, the neutralisation of TNF-α with antibodies is to date not effective in diabetic individuals (Schmidt *et al.*, 1999). Based on the report by Schmidt *et al.* (1999) the presence of high levels of proinflammatory cytokines in obese individuals could be utilised to predict the development of T2D.

Hotamisligil *et al.* (1995) reported that expression of TNF-α is also induced in obese humans and that its expression was decreased subsequent to weight loss. From this report it was suggested that there is a significant correlation (with a p-value less than 0.01) between the body mass index (BMI) and plasma concentrations of TNF-α. A G308A polymorphism in the promoter region of TNF-α has been associated with increased plasma levels of TNF-α with a subsequent 1.8 times higher risk of developing T2D when compared to non-carriers (Vendrell *et al.*, 2003) as well as an increase in abdominal fat distribution in T2D individuals (Furuta *et al.*, 2002). In addition, the C174G mutation of the interleukin 6 (IL6) promoter was reported to cause an increase in the risk to insulin resistance (Stephens *et al.*, 2004).

Leptin, an adipocyte specific protein that is elevated in obese individuals (Unger *et al.*, 1999), also regulates immune function via the stimulation of responses to inflammation (Kondoh *et al.*, 2002). In addition, this protein regulates body weight by inducing hypophagia as well as the preferential use of lipids as opposed to glucose as an energy source (Unger *et al.*, 1999). Low leptin concentrations observed under fasting stress, or in obese individuals, is postulated to play an important role in the observed suppression of immune regulation. The resultant impairment of the immune response leads to the

production of proinflammatory cytokines such as TNF-α (Kondoh *et al.*, 2002). This process could explain the observed susceptibility to infections during periods of starvation or in obese individuals.

Insulin resistance due to the loss of the signalling effect of insulin promotes inflammation, via the counter production of proinflammatory cytokines such as TNF-α (Hotamisligil *et al.*, 1994). An important implication of the inflammatory effect of T2D and obesity is atherosclerosis, a major cause of death in both obese and diabetic individuals (Schmidt *et al.*, 1999). Atherosclerosis is an inflammatory process, which is induced by the increased levels of ROS in the circulating mononuclear cells and increase lipid peroxidation eventually leading to thrombosis (Dandona and Aljada, 2002). As discussed in Section 3.3, during oxidative stress endogenous mechanisms are employed to destroy these reactive species. In normal individuals, these mechanisms are sufficient to counteract the free radical production, but in a diabetic individual they are overwhelmed because of the increased oxidative stress (Seghrouchni *et al.*, 2002). Gene expression data reported by van der Westhuizen *et al.* (2003) suggested that patients with high levels of ROS due to complex I deficiencies have common gene expression profiles. These include high levels of MT transcripts as well as a decrease in mtDNA transcripts. It thus appears that oxidative stress via the production of ROS plays a significant role in the induction of genes that may protect a cell against the deleterious effects of ROS. The determination of various molecular markers for oxidative stress will prove to be beneficial for the early detection of this inflammatory disorder.

Liang *et al.* (2002) investigated the effect of MTs in cardiomyocytes of diabetic mice. From this investigation it was concluded that oxidative stress in the heart of these mice resulted in an upregulation of antioxidant enzymes. Over expression of MTs in these cells prevented the depletion of GSH, therefore protecting the heart from oxidative damage. A schematic summary of the effect of ROS generation, inflammation, obesity as well as genetic factors on insulin signalling is presented in Figure 3.5.

Figure 3.5: A model suggesting the role of inflammation in insulin resistance, obesity and a possible role in the induction of metallothionein

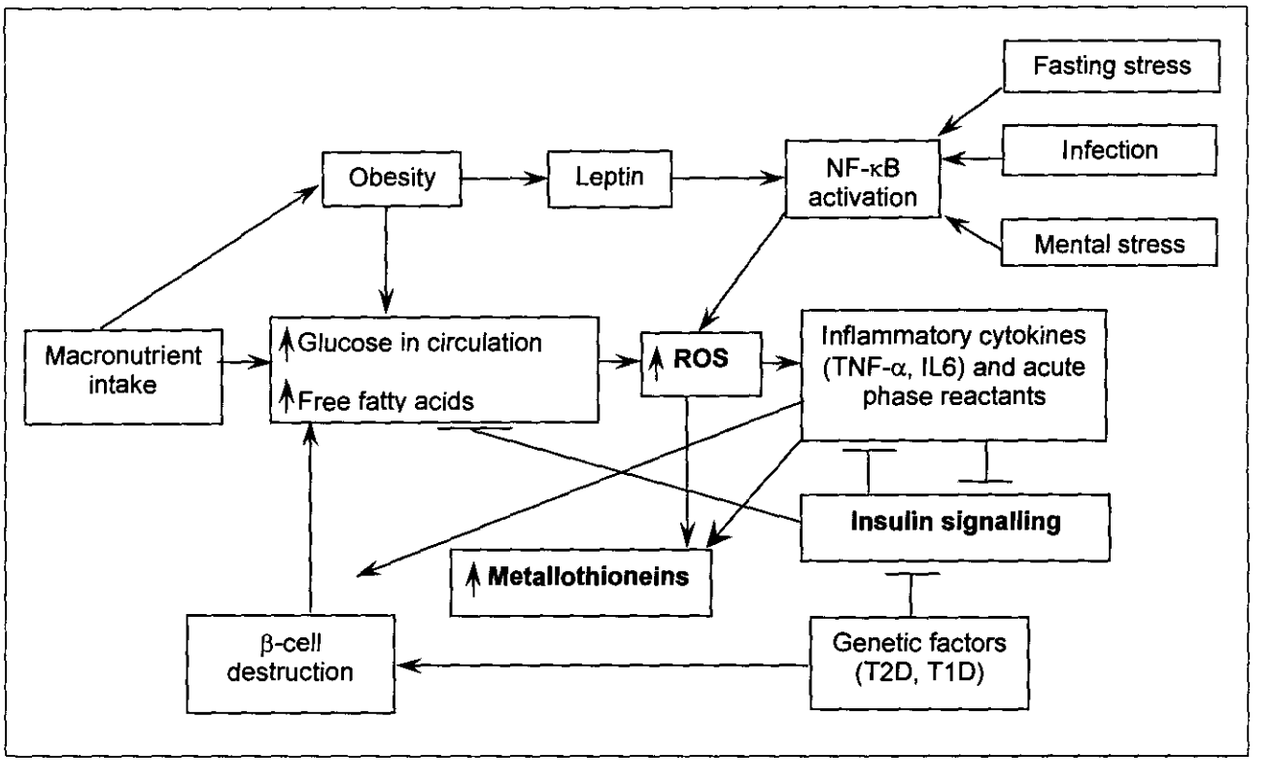

T2D = type 2 diabetes mellitus; T1D = type 1 diabetes mellitus; ROS = reactive oxygen species; NF-κB = nuclear factor κB; TNF-α = tumour necrosis factor-α; IL6 = interleukin 6. Adapted from Dandona *et al.* (2004).

It can be deduced from Figure 3.5 that the factors indicated play a role in the pathogenesis of diabetes mellitus and eventually the increased expression of MTs. The anti-inflammatory aspect of insulin function will be the focus of this molecular investigation which is to elucidate the combined effect of oxidative stress and insulin resistance in T2D patients. As depicted in Figure 3.5, it is not only oxidative stress that results the induction of MT but mediators such as cytokines, nutrient intake and various other forms of stress. These conditions and their effect on MT synthesis are further discussed in Chapter Four. Thornalley and Vašák (1985) and Miura *et al.* (1997) indicated in their investigations that there is a constant high rate reaction of MT with hydroxyl radicals when compared to GSH. The detection of genes expressed when a cell is under oxidative stress, may be a major step in identifying common transcriptional markers characteristic of a disease, particularly those resulting from the production of ROS.

3.3.2.3 Genetic basis of T2D

T2D is currently thought to be caused by environmental factors, as well as being highly influenced by an array of genes involved in insulin secretion, the utilisation of insulin, obesity genes as well as genes involved in β-cell function (Jun *et al.*, 1999). This

conclusion was made due to the high familial segregation, high prevalence in certain ethnic groups as well as the high concordance rate of the disease in identical twins (Barnett *et al.*, 1981).

In most genetically predisposed individuals, there is a slow progression from a normal state to insulin resistance, hyperinsulinaemia, glucose desensitisation, defects in insulin secretion, impaired glucose tolerance and eventually hyperglycaemia, which are characteristic of T2D (Green, 1996). This slow progression supports the analysis of individuals at risk for developing diabetes in the current investigation. The progression is affected by the environment as well as genetic predisposition of the individual in a specific population group. The cumulative effect of these two factors is summarised in Figure 3.6.

3.3.2.3.1 Candidate genes

As discussed in Section 3.3 high levels of ROS lead to DNA damage. Thus, due to the postulated role of ROS in the pathogenesis of diabetes, it is also possible that mutations within genes whose protein products are involved in the processes mentioned in Section 3.3.2.3 and those listed in Figure 3.6 are caused by the ROS damage to the DNA. The search for candidate genes has been cumbersome due to the complexity of this disorder. These genes can be classified into those that are involved in insulin secretion and those involved in insulin resistance.

The insulin gene was the first defective insulin secretory candidate gene identified for the deficiency observed in T2D. Mutations in the insulin gene have been identified resulting in the alteration of the amino acid sequence of the A and B chains involved in the binding of insulin to the receptor, thus resulting in free circulating insulin molecules with abnormal bioactivity (Campbell, 1995). Other mutations that occur in proteins involved in the processing of proinsulin, result in high concentrations of circulating proinsulin (Jun *et al.*, 1999).

Figure 3.6: Schematic illustration of the effect of the environment as well as genetic predisposition to the development of T2D

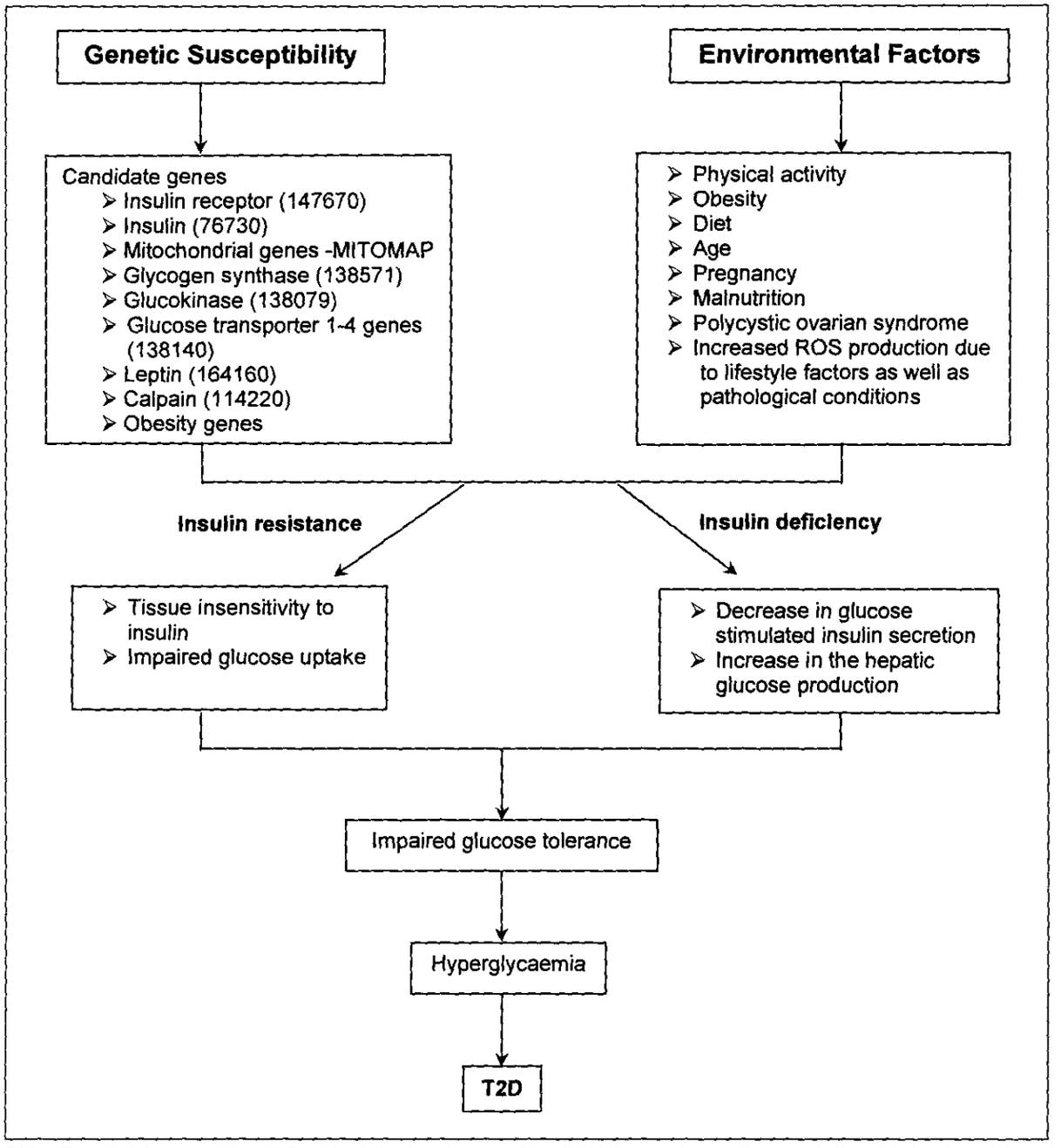

T2D = Type 2 diabetes mellitus. Online Mendelian Inheritance in Man (OMIM) accession numbers are indicated in brackets. Adapted from Jun *et al.* (1999).

As a result of the mitochondria being involved in energy production as well as glucose stimulated insulin secretion in pancreatic β-cells, the role of mitochondrial genes in the pathogenesis of T2D is broadly investigated, therefore supporting their inclusion in Figure 3.6. Another factor that supports the analysis of the mitochondria is the maternal mode of transmission of some forms of T2D. A mutation at position 3243 in the $tRNA^{Leu}$ gene of the mitochondria has been identified in ca. 2% of the diabetic population (Suzuki *et al.*, 2003). The presence of this mutation results in decrease ATP concentration, increased activities

of antioxidant enzymes as well as impaired insulin secretion, to name a few consequences of the presence of this mutation (Rusanen *et al.*, 2000). Deletions as well as duplications in the mtDNA have also been identified in T2D patients (Suzuki *et al.*, 2003). The prevalence as well as the role of these mutations remains to be elucidated.

The insulin receptor gene has been considered as the primary candidate gene contributing to insulin resistance. Mutations in this gene have been linked to severe insulin resistance (Moller *et al.,* 1991). Polymorphisms within this gene have also been identified, however, the association of these changes to T2D requires more investigation (Okazawa *et al.*, 2004). The insulin receptor substrate (IRS) -1, a substrate for the insulin receptor tyrosine kinase, involved in the insulin signalling pathway has also been under investigation (Clausen *et al.*, 1995). Various other genes as summarised in Figure 3.6 are currently under investigation. No single gene has been detected to have a strong association with T2D, thus supporting the multigenic hypothesis of the role that genes play in the predisposition to T2D (Jun *et al.*, 1999; Suzuki *et al.*, 1999).

3.3.3 Oxidative stress, apoptosis and its effects on ageing

The role of ROS produced by the mitochondria in the pathogenesis of diseases, together with its role in cell death is discussed in Section 3.3 and supports the theory that ROS are involved in the ageing process. The concept that mitochondria is involved in the ageing process stems from the theory put forward by Harman in 1988, that associates cell senescence to the deleterious effects of free radicals produced during metabolism as discussed in his report, Harman (1998). In accordance with this theory, Lass *et al.* (1998) described an inverse relationship between auto-oxidation and the metabolism of animal species. The life expectancy of *C. elegans* was also found to be negatively affected by a high metabolic rate in terms of O_2 consumption. In rodents, it was determined that a restriction in caloric intake resulted in an increase in longevity, accompanied by a decreased state 4 respiration (listed in Table 3.6) as well as decreased superoxide production (Esposito *et al.*, 2000).

The possible involvement of the mitochondria in the degenerative diseases of old age has been extensively evaluated (Fahn and Cohen, 1992; Agarwal and Sohal, 1995; Staniek and Nohl, 2000; Eckert *et al.*, 2003). In disorders such as Alzheimer's, Huntington's and Parkinson's diseases, the impairment of energy metabolism due to the progressive failure of the mitochondria has been suggested (Eckert *et al.*, 2003; Zhu *et al.*, 2004). A common

denominator of all these diseases is the increased levels of free radicals in the respective tissues as well as decreased ATP synthesis (Staniek and Nohl, 2000). These disturbances lead to membrane depolarisation which results in activation of cell death. Oxidative stress due to a defect in the mitochondria is at the epitome of programmed cell death i.e. apoptosis (Lundberg and Sweda, 2004). This process as depicted in Figure 3.7 has been implicated in the course of ageing (Lenaz, 1998).

Figure 3.7: Schematic illustration of the central role of ROS

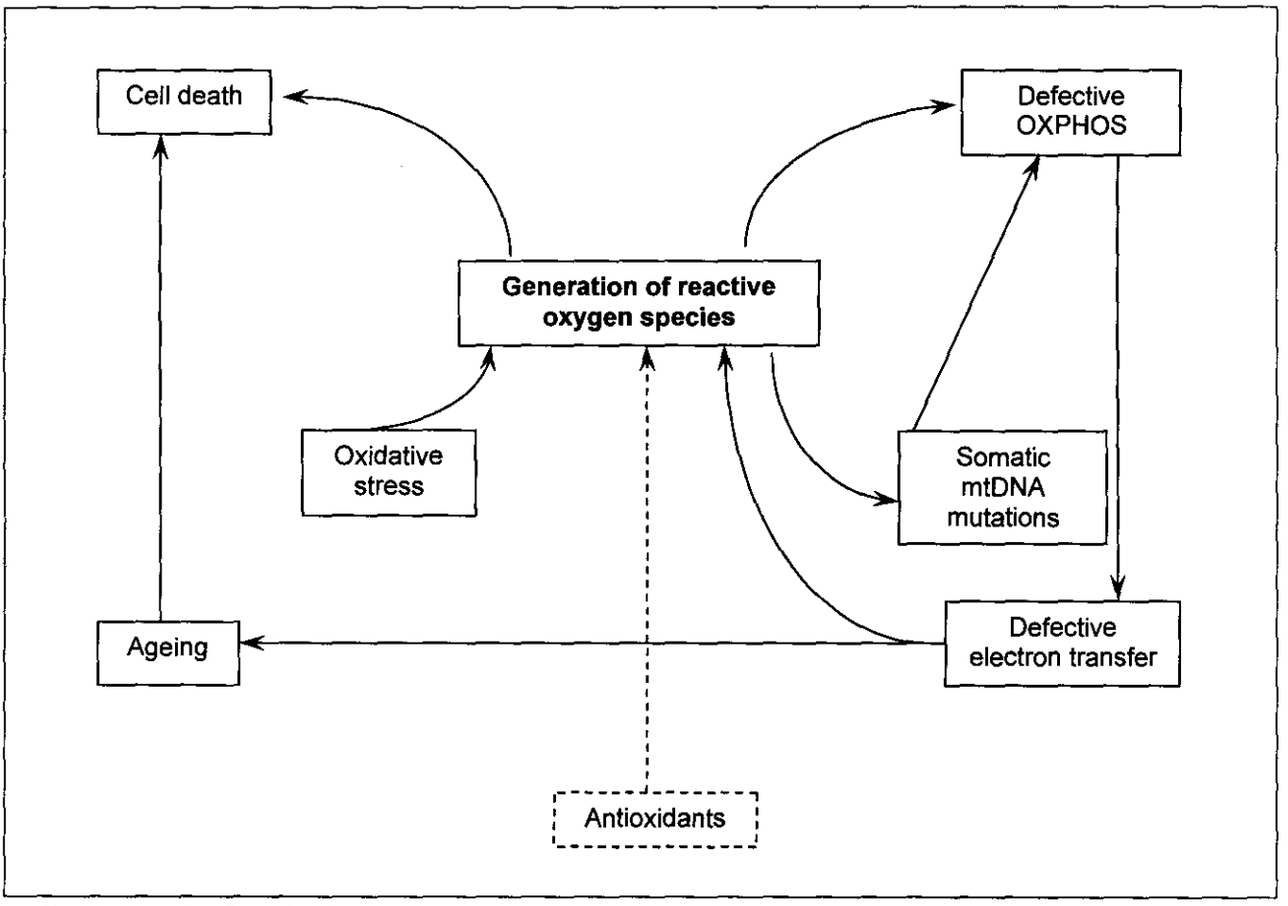

mtDNA = mitochondrial DNA; OXPHOS = oxidative phosphorylation. Adapted from Lenaz (1998).

The release of cytochrome c from the intermembrane space is an early event within mitochondria that triggers apoptosis. As illustrated in Figure 3.8, this event together with the recruitment of Apaf-1 activates caspase 3, a cysteine-aspartate protease. Caspase 3 is inhibited by the action of Bcl-2, a member of the family of anti-apoptotic proteins. These proteins are located in the outer mitochondrial membrane where the pro-apoptotic proteins such as Bax and Bad are also localised (Alberts *et al.*, 1998). The aforementioned release of cytochrome *c* as well as the opening of the MPT lead to decreased membrane potential. These features are characteristic of the mitochondrially produced ROS induced apoptosis (Alberts *et al.*, 1998; Kristal *et al.*, 1996). Oxidative stress is an early intrinsic component of the apoptotic cascade committing a cell to apoptosis (Talbot *et al.*, 2004). p53 expression

and dexamethasone (an anti-cancer drug) have been reported to induce apoptosis, however, at the core of the mechanism of induction is the production of reactive oxygen species (Samuni *et al.*, 2004).

Figure 3.8: Schematic representation of the oxidative stress induced apoptosis

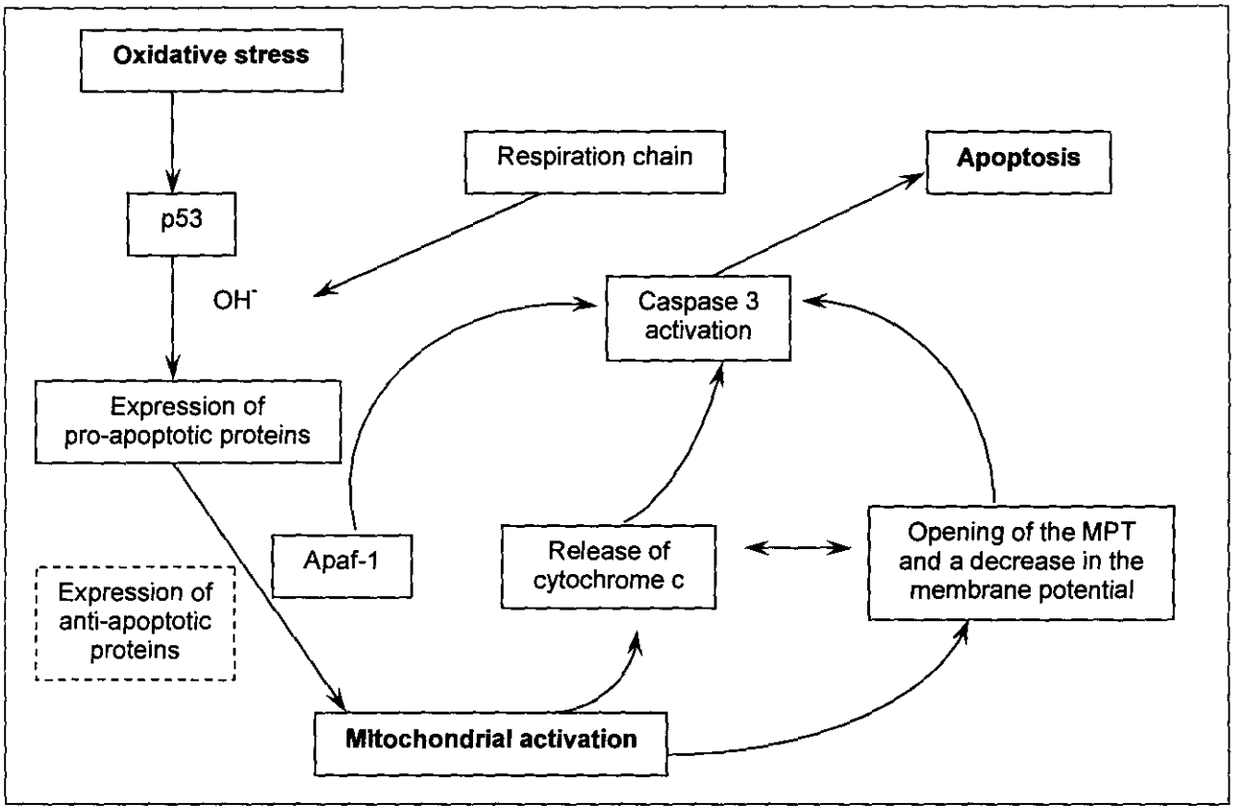

OH^- = hydroxide radical; MPT = mitochondrial permeability transition pore; p53 = pro-apoptotic protein; Apaf-1 = activator of caspase 3. Adapted from Lenaz (1998).

Eckert *et al.* (2003) and Zhu *et al.* (2004) have illustrated that in Alzheimer's disease, the affected brain areas exhibit an increased induction of 8-OHdG from mtDNA, indicative of increased oxidative stress. Lowered levels of reduced glutathione in the substantia nigra of old asymptomatic individuals with Parkinson's disease also alludes to early involvement of oxidative stress in the pathogenesis of this disease (Fahn and Cohen, 1992). From the reports by Fahn and Cohen (1992); Eckert *et al.* (2003) and Zhu *et al.* (2004), it is evident that oxidative stress is the underlying phenomenon in the pathogenesis of most disorders. It is therefore suggested that, an early detection of free radicals is imperative for the diagnosis as well as the therapeutic intervention of ROS related disorders such as diabetes mellitus. The detection of ROS is challenging due to the instability of these species (Harris, 1995). The use of molecular markers that are indicative of oxidative stress will thus aid in the detection of these free radicals.

CHAPTER FOUR

METALLOTHIONEINS

Metallothionein is a collective name for a superfamily of ubiquitously expressed low molecular weight proteins with high sulphur content and a high metal binding capacity. They were originally discovered in equine models as cadmium (Cd) and Zinc (Zn) associated proteins (Margoshes and Vallee, 1957), and have since been reported to have an antioxidant function (Kling and Olsson, 2000).

4.1 METALLOTHIONEINS

Metallothioneins occur throughout the animal kingdom and are also found in higher plants, eukaryotic micro organisms as well as in some prokaryotes (Margoshes and Vallee, 1957; Kägi and Vallee *et al.*, 1960; Zhou *et al.*, 1995). These genetically polymorphous proteins are most abundant in the liver and kidney, since these are the primary sites for heavy metal accumulation as well as in the pancreas and intestines of animal species (Kagi *et al.*, 1974). This distribution of MT proteins is similar to that of GSHPx, which is also highly expressed in the liver and kidney. There is a high level of variation in the concentration of these proteins in different species and tissues, reflecting effects of age, stage of development, and cell function (Miura *et al.*, 1997; Esposito *et al.*, 2000).

In view of their metal binding capacity, MTs are implicated in the detoxification, transport and maintenance of homeostasis of essential and toxic heavy metals (Bühler and Kägi, 1974). Zn and Copper (Cu), participate in a variety of enzymatic reactions and are essential trace metals for all life forms. However, high levels of these metal ions may be toxic, thus they have to be maintained in homeostasis. This family of proteins has also been postulated to have a putative role in scavenging ROS, based on the presence of thiol groups, as discussed in Section 3.3. Their synthesis has been observed to be induced under various forms of cellular stress including fasting stress (Kondoh *et al.*, 2003). Much is known about the physical and the chemical properties of MTs including their genetic regulation. However, the physiological role of MTs, is still unclear. The conditions under which these proteins are expressed as well as their function is a subject of controversy (Thomas *et al.*, 1986; Sato and Bremner, 1993; Romero-Isart and Vašák, 2002).

Although MTs are cytoplasmic proteins they also accumulate in lysosomes and have been observed in the nucleus during development. The nuclear localisation of MTs may be related to interactions with micronutrients such as Zn and Cd metal ions and with various constituents during cell cycle regulation and differentiation (Andrews *et al.*, 1991; Lazo *et al.*, 1995; Riggio *et al.*, 2003). Thus, the nuclear localisation of MTs may be a vital factor for determining the protective role of MTs against the genotoxic effects of certain compounds within the nucleus (Rossman *et al.*, 1997). MTs could also modulate gene expression by exchanging the bound Zn as well as free Zn between histones, transcription factors and other enzymes. The Sp1 transcription factor is a classical example of a transcription factor common to all vertebrates with a Zn finger DNA binding domain at its carboxyl terminus to which MT transfers Zn ions (Zeng *et al.*, 1991).

4.1.1 Classification of metallothioneins

Metallothioneins were initially divided into three classes. Class I included all proteinaceous MTs with locations of Cysteine (Cys) similar to those in the mammalian forms, whereas the positions of the Cys residues in class II were different to those in class I. Class III comprised of metalloisopolypeptides containing gammaglutamyl-Cysteinyl units similar to proteinaceous MTs (Margoshes and Vallee, 1957). Due to the continuous identification of variation within the classes of metallothioneins, this classification system has become non-specific. A new nomenclature defining the MTs based on the length of sequence, amino acid composition and the number and recurrence of the Cys residues is currently utilised. This system differentiates MTs based on their sequence similarity, phylogenetic relationships and also subdivides the MTs into families, subfamilies and isoforms or allelic forms. Four mammalian isoforms have been described and are classified as MT-1, MT-2, MT-3 and MT-4 (Karin and Richards, 1982a).

4.1.2 The genetic organisation of metallothioneins

The four human MT genes are all located on chromosome 16q13 resulting in a multigene family of MTs within an 82.1 kilo basepair (kb) region (Karin *et al.*, 1984). In vertebrates, genes for all isoforms consist of a 5'-untranslated region (5'-UTR), three coding exons separated by two introns with AG/CT conserved exon/intron boundaries and a polyadenylation signal at the 3'-untranslated region (3'-UTR) end. The 5'-UTR contains one or more copies of the regulatory metal responsive elements (MRE) which are involved in the basal transcription of MT genes. These elements harbour a consensus sequence CTNTGC(G/A)CNCGGCCC which acts as a binding target for the metal responsive

element binding transcription factor (MTF-1) that regulates MT gene expression. The MTF-1 gene is located on chromosome 1p33, and encodes a 72.5 kDa protein composed of six Cys_2His_2 zinc finger motifs in the N-terminus that mediate the binding of the protein to the DNA sequence and multiple domains which are involved in transcription activation (Heuchel *et al.*, 1994). Even though the composition of the regulatory elements within the MTs is similar, the induction ratios and transcription efficiencies of the various isoforms differ (Quaife *et al.*, 1994).

MT-1 is composed of 13 sub-isoforms encoded by genes within the MT gene cluster. MT-1A, MT-1B, MT-1E (Karin and Richards, 1982b) and MT-1F, MT-1G, MT-1H, MT-1X (Schmidt *et al.*, 1984; Stennard *et al.*, 1994) have been demonstrated to be functional. West *et al.* (1990) identified four additional MT-1 genes which are also located within the MT gene cluster. These include MT-1I, MT-1J, MT-1K and MT-1L, however, these are classified as nonfunctional on the basis of the non-conserved positions of the Cysteine residues, the presence of in frame stop codons and the occurrence of aromatic amino acids such as tyrosine and tryptophan as well as phenylalanine including histidine due to the susceptibility of these amino acids to oxidation (Hamer, 1986). Partial sequencing of the MT-1I sub-isoform, revealed a major deletion at the start of the second exon, which was postulated to result in the inhibition of expression of this particular isoform (Stennard *et al.*, 1994). Since the publication of these results, no further investigations have been performed to test the aforementioned postulation. MT-1C and MT-1D were also categorised as being nonfunctional sub-isoforms due to the presence of in-frame termination codons and deletions that would affect the reading frame (Hamer, 1986). A summary of the various isoforms is presented in Table 4.1.

Table 4.1: Summary of mammalian MT isoforms

Isoform	**Functionality**	**Reference**
MT-1	Functional and non-functional sub-isoforms	Karin *et al.*, 1980
MT-2	Functional and non-functional sub-isoforms	Kissling and Kägi, 1977
MT-3	Functional	Blaauwgeers *et al.*, 1996
MT-4	Functional	Hildago *et al.*, 2001
Sub-isoform	**Functionality**	**Reference**
MT-1A	Functional	Karin and Richards, 1982b;
MT-1B	Functional	Karin and Richards, 1982b;
MT-1C	Non-functional	Hamer, 1986
MT-1D	Non-functional	Hamer, 1986
MT-1E	Functional	Karin and Richards, 1982b;

Table 4.1: continued...

Isoform	Functionality	Reference
MT-1F	Functional	Schmidt *et al.*, 1985; Stennard *et al.*, 1994
MT-1G	Functional	Schmidt *et al.*, 1984; Stennard *et al.*, 1994
MT-1H	Functional	Schmidt *et al.*, 1984; Stennard *et al.*, 1994
MT-1I	Non-functional	Hamer, 1986; West *et al.*, 1990; Stennard *et al.*,1994
MT-1J	Non-functional	Hamer, 1986; West *et al.*, 1990; Stennard *et al.*,1994
MT-1K	Non-functional	Hamer, 1986; West *et al.*, 1990; Stennard *et al.*,1994
MT-1L	Non-functional	Hamer, 1986; West *et al.*, 1990; Stennard *et al.*,1994
MT-1X	Functional	Schmidt *et al.*, 1984; Stennard *et al.*, 1994
MT-2A	Functional	Huang *et al.*, 1998
MT-2B	Non-functional	Huang *et al.*, 1998

MT-2A as well as MT-3, also known as the growth inhibition factor (GIF), are classified as functional. The structural organisation of the various MT genes is illustrated in Figure 4.1, where MT-4 is depicted at the 5'-end of the gene cluster and MT-1X at the 3'-end. The orientation of the genes indicated in Figure 4.1 is also the 5' to 3' direction of transcription for all genes except MT-1G (West *et al.*, 1990). The physiological requirement for such a large number of genes is unclear. A common element of the functional isoforms is the cis-acting elements in the 5'-UTR which induce differential MT expression in response to metal ions and various agents released during cellular stress (Sadhu and Godamu, 1988).

Figure 4.1: Physical map of the human metallothionein locus on chromosome 16q13

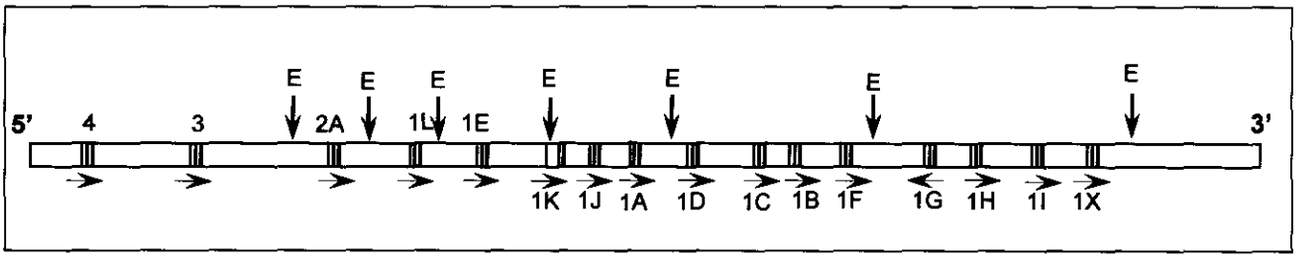

E = *Eco* RI sites; the arrows indicate the transcriptional orientation of the MT genes; vertical bars represent the exons within each gene. Numbers 4 to 1 indicate the respective MT isoforms. A-X = sub-isoforms of MT-1. Adapted from West *et al.* (1990).

An MT-like gene located on chromosome 11q13 has been identified. This gene has been illustrated to be actively regulated in the male germ line cells. The synthesis of the 32 kDa

protein, the testis-specific metallothionein-like protein (tesmin) is a clear marker of early male germ cell differentiation (Sugihara *et al.*, 1999). This observation coincides with the noted increase of MT-1A and MT-1B during development as discussed in Section 4.1.7.2, as well as the high level of expression of MTs in testis unexposed to metal ions. Even though tesmin has several characteristics similar to MT, its amino acid content is different to that of other MTs. The differences include the low Cys content of the protein and the presence of leucine residues, which are not present in MT isoforms (Waalkes and Peratoni, 1986, West *et al.*, 1990). In addition to these characteristics, this protein is composed of aromatic amino acids. Based on the aforementioned properties, it can be suggested that even though tesmin is MT-like with reference to molecular weight and its metal binding nature it can not be classified as a metallothionein isoform (Waalkes and Peratoni, 1986).

It was also illustrated by Schmidt *et al.* (1985) via the analysis of human-rodent cell hybrids that, in addition to the MT genes located on chromosome 16 and tesmin, there are other pseudogenes that are located on other autosomes. A processed MT-2 pseudogene (MT-2B), in which no introns interrupt the coding sequence, is located on chromosome 4 and displays allelic variation distinguished by *Eco* RI digestion (Karin and Richards, 1982b). The other MT-like genes are located on chromosome 1, with one being on the long arm of the chromosome and the other on the short arm. An additional two MT-like genes were detected, one on chromosome 18 and the other on chromosome 20 (Schmidt *et al.*, 1985). The location of the aforementioned pseudogenes is dispersed throughout the genome and the chromosomal linkage of the functional isoforms and non-functional ones is characteristic of a multigene family of higher eukaryotes, thus supporting the classification of MTs as a gene family.

4.1.3 Biochemical properties of metallothioneins

The mammalian forms of MT proteins are characterised by a molecular weight of 6-7 kDa, containing 60-68 amino acid residues. The primary structure contains 20 Cys residues, 6-8 lysine (Lys) residues and 7-10 serine (Ser) residues, all involved in the binding of a total of seven equivalents of bivalent metal ions per mole of protein as illustrated in Figure 4.2. The distribution of the Cys residues within the amino acid sequence is characteristic for each isoform (Hamer, 1986; Banci, 2003). All Cys residues occur in the reduced form, thus do not form any disulphide bonds, and are bound to the metal ions via mercaptide bonds. MTs are also heat stable and do not contain aromatic amino acids.

MTs contain two separate metal-thiolate clusters with differential capacity to associate with metal ions. One cluster binds four metal ions and the other cluster binds three metal ions, as depicted in Figure 4.2 by the three-dimensional structure of a metal bound MT. The three-metal binding cluster (β-domain) consisting of nine Cys residues is located in the N-terminal containing amino acid residues 1-30. The four-metal binding cluster (alpha (α)-domain) is located in the C-terminal composed of amino acids 31-61, including eleven Cys residues. The two metal thiolate clusters are connected by a flexible hinge region composed of a conserved Lys-Lys segment (Winge and Miklossy, 1982). The protein folding patterns in the α and β domains are topologically similar but achiral and characterised by a high proportion of reverse turns. In both the clusters, the polypeptide chain makes three turns to spiral around the metal atoms. The hydrophobic residues are clustered in the two exposed loops of the clusters (Vašák and Hasler, 2000; Romero-Isart and Vašák, 2002).

Figure 4.2: Crystal structure of Cd_5,Zn_2-MT-2 from rat liver

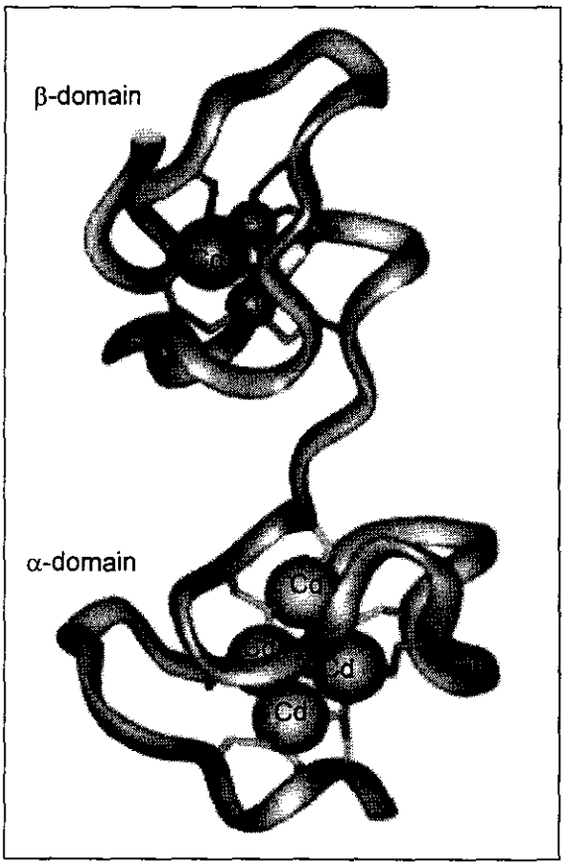

The large circles represent Cd ions and the smaller circles indicate the position of the Zn ions. Adapted from Romero-Isart and Vašák (2002).

The synthesis of the predominantly disordered apoprotein (thionine or apometallothionein) is induced by heavy metals, such as Cd, Zn, Cu and mercury (Hg), which bind to it and result in a folded metallothionein protein (Galdes *et al.*, 1978; Vašák *et al.*, 1984). Other metals such as cobalt (Co) and manganese (Mn) induce MT synthesis but do not bind to the newly synthesised protein, which usually contains Zn as the bound metal. The affinity of metal ions for the binding sites on MTs differs in the following order: Zn<Cd<Cu<Hg (Bühler and Kägi, 1974). At an acidic pH, the metal ions are released resulting in an apoprotein (Karin *et al.*, 1980).

Metallothioneins contain an alanine at the carboxyl terminus (C-terminus) and N-acetylmethionine at the N-terminus of the polypeptide (Karin and Richards, 1982a). However, this composition differs between isoforms. Two major isoforms of MT, MT-1 and

MT-2, are found in most vertebrate tissues. These two isoforms are ubiquitously expressed and have similar amino acid composition. Their synthesis is induced by a variety of stress conditions, which are discussed in the subsequent sections. MTs isolated from human livers contain mainly Zn, whereas those from human kidney consist primarily of Cd. These differences reflect the variable natural heavy metal exposure of the different organs. MT-2 has a higher affinity for Zn and is the more predominant of the two even though the relative proportion of these isoforms depends upon the stimulus resulting in their synthesis (Kägi *et al.*, 1961; Sato and Bremner, 1993; Sato *et al.*, 1995). In higher organisms, MTs are the sole proteins in which Cd accumulates naturally.

The expression of MT-3 and MT-4 is, however, highly restricted to the brain, predominantly in the glutaminergic neurons (Palmiter *et al.*, 1992; Giacconi *et al.*, 2003) and squamous epithelial cells of the skin, tongue and intestinal lining (Quaife *et al.*, 1994) respectively. Even though these two isoforms are not inducible, they both bind Zn and Cu. A report by Blaauwgeers *et al.* (1996) indicated that MT-3 is not primarily brain specific but is rather a central nervous system-specific isoform. Over expression of MT-3 in cultured human fibroblasts has been reported to have a protective role against oxidative stress (You *et al.*, 2002).

Whether or not the various isoforms have different functions remains to be elucidated. The variation in the expression profiles of MT isoforms can be correlated to that of the GSHPx isoforms, with GSHPx-4 highly expressed in the testis and brain but not in the liver and kidney whereby the predominant isoform is GSHPx-1 (Esposito *et al.*, 2000).

The primary structure of the four isoforms is illustrated in Table 4.2, where a distinct MT-3 conserved Cys-proline (Pro)-Cys-Pro (CPCP) sequence motif is illustrated. When compared to MT-1 and 2, MT-3 has a threonine (Thr) at position 5 and an acidic hexapeptide at position 53 which are depicted in Table 4.2. The presence of the aforementioned amino acid sequence has been illustrated to be decisive for the activity of MT-3. MT-3 exhibits a 70% sequence identity to MT-1 and MT-2. However, MT-4 is less homologous to MT-1 and MT-2 due to the difference in the majority of the Cys residues (Quaife *et al.*, 1994).

Table 4.2: Representation of amino acid sequences of mammalian MT isoforms

MT isoforms	amino acid sequence
MT1	MDPNCSCATG GSCTCTGSCK CKECKCNSCK KSCCSCCPMS CAKCAQGCIC KGASEKCSCC A
MT2	MDPNCSCAAG DSCTCAGSCK CKECKCTSCK KSCCSCCPVG CAKCAQGCIC KGASDKCSCC A
MT3	MDPE[redacted]CPCPS GGSCTCADSC KCEGCKCTSC KKSCCSCCPA ECEKCAKDCV CKGG[redacted] [redacted]KCSCCQ
MT4	MDPR[redacted]CVCMS GGICMCGDNC KCTTCNCKTC RKSCCPCCPP GCAKCARGCI CKGGSDKCSC CP

M = methionine; D = aspartic acid; F = phenylalanine; N = asparagine; C = Cysteine; S = Serine; A = alanine; T = threonine; G = Glycine; K = lysine; E = glutamic acid; P = proline; Q = glutamine; I = isoleucine; R = arginine. The amino acids highlighted in purple represent the distinct difference at position five of the respective isoforms. The tetranucleotide indicated in yellow denotes the conserved amino acid sequence of the MT-3 isoform. The distinguishing hexapeptide of MT-3 is illustrated in green.

As discussed in Section 4.1.2, MT-1 is further subdivided into the various sub-isoforms, whose amino acid sequence is depicted in Table 4.3. Though these sub-isoforms have numerous amino acid differences, there are characteristic differences at various positions within the amino acid sequence, that result in some of these sub-isoforms being classified as non-functional, such as those indicated with open boxes.

Table 4.3: A comparison of amino acid sequences of mammalian MT-1 sub-isoforms

MT-1 sub-isoform	amino acid sequence
MT1A	MDPNCSCATG GSCTCTGSCK CKECKCNSCK KSCCSCCPMS CAKCAQGCIC KGASEKCSCC A
MT1B	MDPNCSCTTG GSCACAGSCK CKECKCTSCK KCCCSCCPVG CAKCAQGCVC KGSSEKCRCC A
MT1E	MDPNCSCAAA GVSCTCASSC KCKECKCTSC KKSCCSCCPV GCAKCAQGCI CKGASEKCSC CA
MT1F	MDPNCSCAAG VSCTCAGSCK CKECKCTSCK KSCCSCCPVG CSKCAQGCVC KGASEKCSCC D
MT1G	MDPNCSCAAA GVSCTCASSC KCKECKCTSC KKSCCSCCPV GCAKCAQGCI CKGASEKCSC CA
MT1H	MDPNCSCEAG GSCACAGSCK CKKCKCTSCK KSCCSCCPLG CAKCAQGCIC KGASEKCSCC A
MT1K	MDPNCSCTTG VSCACTGSCK CKECKCTSCK KSCCSCCPVG CAKCA□GCVC KGTLENCSCC A
MT1J	MDPN□SCTTG GSCTCAGSCK CKECKCTSCK KSCC□CCPMG XAKCA□GCIC KGTSEKCSCC A
MT1X	MDPNCSCSPV GSCACAGSCK CNECKCTSCK KSCCSCCPVG CAKCAQGCIC KGTSDKCSCC A

M = methionine; D = aspartic acid; N = asparagines; C = Cysteine; S = Serine; A = alanine; T = threonine; G = Glycine; K = lysine; E = glutamic acid; P = proline; Q = glutamine; I = isoleucine; H = Histidine; F = phenylalanine; R = arginine. X = in-frame stop codon. □ = characteristic differences in amino acids.

4.1.4 Evolutionary conservation of metallothioneins

The organisation of the rodent and primate MT gene family has been extensively studied via hybridisation, cloning and chromosomal localisation experiments. Mice appear to contain only two functional and tightly linked MT-1 and MT-2 genes. Rats on the other hand seem to harbour at least four MT-related sequences within the genome. Even though there are differences between the different isoforms, the coding regions of these mammalian isoforms are strongly conserved, as illustrated by the following list.

- Monkey MT-2 and human MT-2 differ by 1.2% non-synonymous and 4.8% synonymous changes.
- Rat MT-1 and human MT-1F differ by 9.9% non synonymous and 28% synonymous changes (Karin and Richards, 1982a; Karin and Richards, 1982b).

Within the mammalian MT genes, there is no clear relationship between the MT-1 and MT-2 classes in the divergent species. In primates, the MT-1 genes of humans and monkeys are more closely related to one another than the MT-2 genes in other species. Similarly, within rodents, the mouse, rat and hamster MT-1 genes are more closely related to one another than to their MT-2 counterparts. A comparison of primate to rodent MT genes indicates that the primate MT-1s are less divergent from primate MT-2 than from rodent MT-1s. A possible explanation for this is that both rodents and primates independently acquired the two gene isoforms (Karin and Richards, 1982b).

The MTs of *Drosophila*, *Neurospora* and crab are homologous to the mammalian MTs and are designated as class 1 MTs. The positions of the Cys residues in the polypeptides are highly conserved with the major difference being in their length in comparison to the mammalian isoform. The two crab MTs are 57 and 58 amino acids in length and correspond to the α and β domain of the mammalian MT isoforms. *Drosophila* MTs consist of 40 amino acids and correspond primarily to the β domain, whereas the *Neurospora* MT contains only 25 amino acids homologous to the β domain. A comparison of these proteins to mammalian MT gives an evolutionary rate of 7×10^{-10} substitutions/codon/year. As predicted from the conservation of mammalian MT proteins structure, the coding regions are highly homologous and the non-coding regions are more divergent (Hamer, 1986).

4.1.5 The reactivity of metallothioneins

The abundance of the conserved polarisable Cys thiolate ligands within the MT results in a high metal ion binding affinity in these proteins. The metal-thiolate complexes of MTs have a high thermodynamic stability and as a consequence of their structural flexibility they are kinetically very labile. Therefore, the thiolate ligands undergo both metallation and demetallation rapidly, producing apo-MT and metal bound MT. This property allows the intramolecular transfer of metals, for example, Zn between other enzymes and MTs (Romero-Isart and Vašák, 2002).

Although the thiol groups of MTs are masked through their interaction with metal ions, they retain a substantial degree of the nucleophilicity. This together with the protein's thermostability and kinetic lability could explain the reactivity of the coordinated Cysteine side chains with oxidising agents. The interaction of the Cys residues of the metal thiolate clusters with cellular oxidants result in the release of the bound metal via the free radical attack at the metal-bound thiolates, leading to protein oxidation or modification and subsequent metal release (Thornalley and Vašák, 1985).

4.1.6 Basal MT gene expression

The core promoters of MT-1 and MT-2 genes are composed of the classical TATA box and initiator regions. These regions are recognised by transcription factor IID (TFIID) resulting in the assembly of the pre-initiating complex that mediates basal transcription. As discussed in Section 4.1.2, the 5'-UTR also contains one or more MREs which function in conjunction with the MTF-1. However, the MTF-1 is primarily involved in metal-induced MT expression. Therefore the MREs, together with the essential metal ions, such as Zn that associate with MTF-1 at levels required to support life, contribute to the basal as well as inducible MT expression. MTF-1 is not only essential for induction by Zn but also mediates responses to Cd, Cu and other heavy metals (Heuchel *et al.*, 1994). Kimura *et al.* (2002) illustrated that activation of MTF-1 can also be mediated by MT via the increase of intracellular levels of Zn.

It has previously been demonstrated that in mice and chicken MT-1 genes, expression during H_2O_2 –induced oxidative stress is mediated through an E box motif which is a binding site of the adeno major late transcription factor (MLTF). This binding site overlaps with an antioxidant response element (ARE) to form a MLTF/ARE sequence that is necessary for both basal and inducible MT expression. Subsequent to the binding of the MLTF (a member of the basic helix-loop-helix-Zip protein family) to the E box, its interaction with other transcription factors regulates MT gene expression (Dalton *et al.*, 1994; 1997). It is of interest for the purpose of elucidating the role of MT to note that the AREs are also found in regulatory sequences involved in the expression of genes responsive to free radicals (Dalton *et al.*, 1994). These include genes encoding the phase II detoxification enzymes and the Ya-subunit of the glutathione-*S*-transferase. This feature lends credence to the proposed function of MTs being radical scavengers.

All MT gene promoters also consist of at least a single GC box (consensus sequence, GGGGCGGGG) which contributes to the basal level expression of MT via interaction with members of the Zn finger transcription factors. Enhancer elements, known as basal level enhancers (BLE) are also present within the 5'-UTR of MT. These elements function similar to the classical enhancer elements (Lee *et al.*, 1987) and interact with the proinflammatory activator protein -1 (AP-1) and activator protein 2 (AP-2) to enhance the expression of MT under conditions inducing the expression of these genes.

4.1.7 Induction of MT gene expression

In addition to basal expression of the MT genes, the biosynthesis of these proteins is induced by a variety of agents and conditions such as metal ions, hormones, cytokines, growth factors, tumour enhancers, chelators and many other forms of stress (Karin *et al.*, 1980; Sato and Bremner, 1993; Fraga and Oteiza, 2002). MTs are also induced under non-physiological conditions such as infection, irradiation, hot or cold exposure and starvation (Sato and Bremner, 1993). Physiological MT synthesis and concentration have been observed to be increased during cell proliferation and particularly during development. Variations in the expression and extracellular localisation of MT isoforms have also been noted during differentiation and monocyte activation (Riggio *et al.*, 2003). These proteins have been postulated to protect tissues against various forms of oxidative damage, including radiation, lipid peroxidation, detoxification of potentially toxic heavy metal ions and in the homeostasis of essential trace elements during development. MTs also regulate the synthesis, assembly and activity of Zn metalloproteins (Bremner and Davies, 1975).

4.1.7.1 Induction by metal ions

The initial observation indicating that MTs are induced by high levels of metal ions were provided by an investigation which illustrated that an increase in the level of Zn resulted in a proportional increase in the concentration of Zn-MT in rat liver and other organs (Bremner and Davies, 1975). A similar result was observed in HeLa cells with a high Zn content, where high MT expression was detected (Chimienti *et al.*, 2001). The concentration of the metal ions required for peak transcription levels varies according to the metal ions and the time required to reach these levels. Zn and Cd are two of the most potent inducers of MT expression.

As discussed in Section 4.1.2, MTF-1 is vital for the metal ion induced MT gene expression. Following cellular exposure to metal ions, MTF-1 translocates from the cytoplasm to the nucleus, where it binds to the MRE of the MT gene promoter sequences and regulates transcription. This regulation is attained via the interaction of MTF-1 with components of the RNA polymerase II transcriptional unit (Smirnova *et al.*, 2000). Although the activity of MTF-1 is induced by a variety of metal ions, its binding ability to the MREs DNA sequence is mediated by allosteric interactions with Zn. It is therefore only responsive to Zn (Heuchel *et al.*, 1994). The ratio of thiol groups to Zn atoms in the MT-Zn complexes was observed to be approximately 3:1. This is consistent with the view that each metal atom is bound to three Cysteine residues in the protein (Kägi and Vallee, 1961).

4.1.7.2 Induction by chemical stress

Although the concentration of heavy metals is a major determinant of tissue MT levels, induction of MT synthesis may also be due to a variety of chemical stimuli. Cisplatin, an anticancer drug which is known to exert its action through free radical generation leading to lipid peroxidation, has also been noted to induce an increased expression of MTs (Satoh *et al.*, 1988). Other agents such as *tert*-butyl hydroperoxide (*t*-BHP) which produces ROS (Wang *et al.*, 2000; Baumann *et al.*, 1991) and paraquat, a superoxide radical generator, causes *in vitro* MT induction (Sato, 1991; Choi 2003). *In vivo* rat studies indicated that the liver is the most responsive to these oxidising agents, with the pancreas and the kidney being the second most responsive organs (Fornace *et al.*, 1988; Baumann *et al.*, 1991).

Ultra violet (UV) irradiation has also been postulated to lead to an induction of MT synthesis resulting from the production of ROS by the radiolysis of water, which in turn damages DNA. MT synthesis in this instance is postulated to induce resistance to DNA damage via scavenging ROS. In a study reported by Fornace *et al.* (1988), induction of MT1 and MT2 mRNA peaked at four hours (hrs) after exposure to UV irradiation in Chinese hamster lung fibroblasts. The non-induction of the other MT isoforms support the postulated inducer specificity observed within MT isoforms. An increase in MT expression has also been observed in rainbow trout when they hatch, due to the exposure to UV light. However, the expression profile seems to be tissue specific or at least mediated by tissue specific factors (Fornace *et al.*, 1988).

The role of MT in free radical regulation and scavenging in aquatic species has been extensively investigated (Anderson *et al.*, 1999; Kling and Olsson, 2000; Filipović and Rapor, 2003). Since high oxygen pressure (pO_2) leads to an excessive load of ROS (Iorio, 2002), and fish often encounter high pO_2 levels and more frequently than terrestrial animals, it is important for fish to respond well to raised ROS levels. One such protective mechanism for free radicals damage may be the upregulation of MT. A previous study by Kling and Olsson (2000) indicated that exposure of rainbow trout gonadal cells to H_2O_2 led to the upregulation of MT protein synthesis. These products were detected by Northern blot analysis and immunohistochemistry respectively. The authors also compared the cell survival rate subsequent to treatment with metals prior to the exposure to H_2O_2. This illustrated that metal treatment of the cells induced MT expression and led to a significant raise in H_2O_2 tolerance. There was, however, a difference in the cell survival of the gonadal cells compared to the embryonic cells, which showed a less significant MT induction. This observation emphasises the tissue specific expression of MT (Huang *et al.*, 1998).

4.1.7.3 Physiological inducers of MT synthesis

Cytokines such as TNFα, interleukin 1(IL1) and IL6 are secreted from a variety of cells during an inflammatory, immune or stimulus response and are the major mediators of hepatic acute phase protein synthesis, including MTs (Hernández *et al.*, 2000). These cytokines have a two fold function, that is, they induce inflammation through the production of ROS and also down regulate the inflammation by inducing synthesis of acute phase responses (Min *et al.*, 1992). They have been observed to induce synthesis of Mn-SOD, a mitochondrial localised enzyme essential for the conversion of O_2^- to H_2O_2 and O_2. Mn-SOD is also thought to be an acute-phase protein vital for the protection of cells against oxygen toxicity, via scavenging of free radicals. Among the inflammatory cytokines, IL6 is a key regulator for the induction of a wide variety of the acute-phase proteins. It has also been observed to be the major mediator of MT gene expression (Sato *et al.*, 1995).

The mechanism by which the cytokines induce Mn-SOD and MT expression is not clear, but it has been postulated that the secreted IL6 associates with the membrane bound IL6 receptor. This results in the formation of a complex that activates *Janus kinases* (JAK), which in turn phosphorylates the signal transducer and activator of transcription kinases (STAT). The resulting complex translocates to the nucleus and induces transcription of MT

by binding to STAT response elements in the regulatory sequences (Hirano *et al.*, 1997; Haq *et al.*, 2003). Deletion experiments in an attempt to characterise the MT promoter region, demonstrated the presence of overlapping IL6 response elements (IL6-REs) in the mouse MT1 promoter sequences (Kasutani *et al.*, 1998). Sequences to which the STAT transcription factors bind to were demonstrated to be located 259 bp upstream of the MT gene transcription initiation site, in close proximity to the IL6-REs. The presence of various responsive elements within the MT gene promoter is consistent with the observed difference in induction and transcriptional efficiency in the various isoforms.

In the investigation by Sato *et al.* (1995) on the role of Mn-SOD and MT, it was demonstrated that the pre-treatment of rats with TNFα and IL6 prevented lipid peroxidation and subsequent liver damage induced by carbon tetrachloride (CCl_4). These cytokines increased the activity of the mitochondrial Mn-SOD and synthesis of cytoplasmic MT. The difference in the subcellular localisation of MT and Mn-SOD suggests that they may play a cooperative antioxidative role in various compartments of the cell.

Glucocorticoid hormones also induce MT expression, however, the induction is independent of other regulatory sequences present within the MT promoter (Godowski *et al.*, 1987; Hernández *et al.*, 2000). The MT regulatory sequences include glucocorticoid responsive elements (GREs) which upon binding of the glucocorticoid hormones as well as the RNA polymerase II transcription unit induce transcription. Human MT2 consists of only a single copy of the GRE and this element is absent in MT1 genes, whereas there are two copies in mouse MT2 and MT1. In mice, MT1 and MT2 are induced at equal levels by glucocorticoid hormones (Karin *et al.*, 1984; Kadonaga *et al.*, 1987).

As described in the previous sections, cytokines induce MT synthesis, however, pre-treatment with dexamethasone, a steroid hormone that inhibits cytokine production, prevented the increase on MT concentration *in vitro* (Min *et al.*, 1992; Sato *et al.*, 1995). These results suggest that even though glucorcorticoids are direct inducers of MT synthesis, they inhibit MT synthesis during inflammation by suppressing cytokine production (Karin *et al.*, 1980; Min *et al.*, 1992).

4.1.7.4 Induction due to lipid peroxidation

Since ROS increases membrane permeability by oxidation of membrane lipids, it results in the induction of lipid peroxidation which subsequently leads to tissue damage. It is expected that some mediators released during this process may induce MT synthesis. The

hepatic concentration of MT indirectly induced by these ROS was well correlated with lipid peroxide levels by the measurement of thiobarbituric acid-reactive substances (TBARS). To evaluate the relationship between lipid peroxidation and MT synthesis, the effect of vitamin E (a lipid soluble antioxidant which prevents lipid oxidation) on the production of MT was investigated by Sato and Bremner, (1993). The administration of CCl_4 to rats increased hepatic concentration of TBARS and induced leakage of aspartate aminotransferase (AST) from liver to plasma indicating the occurrence of lipid peroxidation and liver damage. However, the MT concentration was similar in untreated rats versus those pre-treated with vitamin E, illustrating that lipid peroxidation in the liver is not necessary for induction of MT synthesis by CCl_4 (Cagen and Klaassen, 1979; Sato and Bremner, 1993; Sato *et al.*, 1995). This could reflect sequestration of the reactive metabolite of CCl_4 by MT, or alternatively support the hypothesis that MTs are not directly induced by free radicals but rather by the release of cytokines or other mediators released during oxidative stress (Sato *et al.*, 1995). Lipid peroxidation also occurs when a cell is exposed to alkylating agents such as bromobenzene, which in turn results in a reduced GSHPx concentration (Chvapil *et al.*, 1972).

4.1.8 Radical scavenging mechanism of metallothioneins

The exact mechanism by which MTs scavenge free radicals is not clear, but a variety of mechanisms have been proposed. Four of the proposed mechanisms are listed below.

a. The Cys residues of MTs, particularly their thiolate groups, seem to be the primary target for the reaction with OH^- forming diamagnetic metal-thiolate clusters. The thiolate ions of MT are bound to the transition metals, however, these metals are constantly undergoing intramolecular exchange thereby making the thiolate ions of MT accessible to electron acceptors such as ROS (Simpkins *et al.*, 1996). The primary structure of MT, in particular the presence of Cys residues, has been postulated to be a crucial feature in their reactivity with OH^-. The chemical composition, mainly the sulphur content, is a more important factor than the size of the MT. Thornalley and Vašák (1985) utilised bovine serum albumin (BSA) as a control to investigate the effects of MT on free radical scavenging. It was observed that the effective concentration of Cys sulphur in MT is 20-times the molar concentration of Cys residues in GSH and 4-times that of BSA. It was suggested from this investigation that MTs have multiple sites for OH^- attack, rendering them with a more effective OH^- scavenging ability than GSH (Thornalley and Vašák,

1985). In contrast, the quenching of superoxide radicals by MT appeared to be inefficient when compared to that of superoxide dismutase (SOD) and GSH.

b. It has also been hypothesised that the primary determinant of MT protection is the release of the Zn followed by its uptake into the membrane. Subsequent to the uptake of Zn, the membrane will be stabilised since Zn protects against lipid peroxidation by a variety of mechanisms such as a decrease in iron (Fe) uptake, induction of MT or an increase in GSHPx activity (Chvapil *et al.*, 1972; Thomas *et al.*, 1986).

c. Thirdly, MT can chelate Fe or mediate its conversion to an unstable form. Fe leads to the production of hydroxyl radicals that can subsequently initiate lipid oxidation (Fraga and Oteiza, 2002).

d. MT may also play a physiological role as a cofactor of GSHPx for the degradation of harmful oxidants. It is also hypothesised that MT may increase the cellular levels of Zn and Cu which may activate antioxidant enzymes.

Whether any of these functions are dominant in the defence system against oxidative stress remains to be elucidated. Even though there is evidence of the protective role of MT against ROS generated by various mechanisms, several studies as described in the subsequent text, have indicated that MTs do not function as antioxidants *in vivo*.

Conrad *et al.* (2000) demonstrated that MT null mice and parental controls were equally sensitive to oxidative damage induced by γ-radiation and 2-nitropropane. In contrast to this investigation, initial studies by Lazo *et al.* (1995) and Zheng *et al.* (1996) with cells from MT null and wild-type mice, indicated that MTs function as antioxidants. Lazo *et al.* (1995) utilised embryonic cells which were treated with paraquat to induce production of ROS. It was reported that the wild-type cells were less sensitive to the growth inhibitory effects of ROS. Zheng *et al.* (1996) reported that the MT null hepatocyte cultures that were utilised were more sensitive to the cytotoxic action of *t*-BHP and produced more lipid peroxidation compared to the wild-type derived hepatocytes. A similar study was performed in astrocytes (Suzuki *et al.*, 2000) and results supporting those by Zheng *et al.* (1996) were obtained.

A possible explanation for the contrasting results is that Lazo *et al.* (1995) and Zheng *et al.* (1996) exposed the cells in culture directly to ROS generated by *t*-BHP and paraquat, whereas those in Conrad *et al.* (2000) were exposed to physiological doses of oxidative

stress caused by γ-radiation. Therefore it is possible that MT only exerts a protective effect under extreme conditions of oxidative stress observed when cells are directly exposed to overwhelming oxidative damage. However, the *in vivo* level of oxidative stress may never reach a level where MTs function as antioxidants. These observations also emphasise the tissue specific nature of MTs. Similar findings to those of Conrad *et al.* (2000), were reported by Liu *et al.* (1999), illustrating that transgenic mouse models that over express MT were not protected from any oxidative damage caused by γ-radiation, similar to the control mice.

Oxygen free radicals formed in tissues can be spontaneously degraded by any of the other aforementioned biological systems, such as GSH or SOD. The particularly short half-life of the hydroxyl radical is another constituent that may lead to the non-functioning of MTs *in vivo*. Thus MTs and other scavengers can only be effective if they are within close proximity of the site of radical production in order to interact with the radicals before reacting with other cellular compartments. It is evident from the literature presented in the previous sections that the precise role of metallothioneins is still to be elucidated. However, many studies have demonstrated that the presence of ROS within a cell has detrimental effects that lead to the pathogenesis of a variety of disorders.

Based on these previous reports, the role of ROS in mitochondrial cytopathies and other disorders such as diabetes, particularly T2D in the context of this investigation has become apparent. It is evident that future research should be focused on elucidating the role of these reactive oxygen species in the pathogenesis of ROS-related disorders and the effects thereof on the expression of genes. At the start of the current study, it was hypothesised that an increase in the level of MT expression is expected in the group of individuals affected with T2D that were included in this investigation, and that a lower expression level will be detected in individuals not affected. The analysis of the gene expression profiles of metallothioneins in individuals with ROS related disorders will prove to be imperative for the elucidation of their role in these respective disorders.

4.2. RESEARCH OBJECTIVES

The objective of this research project was to explore the use of metallothioneins as biomarkers for ROS related disorders, specifically T2D in this investigation. This will aid in the pre-symptomatic detection of increased levels of ROS.

4.2.1 Specific objectives of this investigation

In order to address the research objective outlined in Section 4.2, the following specific objectives were investigated in this study.

a. The first objective of this investigation was to determine the levels of ROS *in vivo* i.e. in whole blood of the following three groups of individuals.
   i. Individuals affected with T2D, which were designated as Group-1,
   ii. Individuals not affected with T2D, which were referred to as Group-2 and
   iii. Individuals at risk for developing T2D who were classified as Group-3.

b. The second objective was to investigate whether there is a ROS-dependant induction on MT gene expression in whole blood of individuals with elevated levels of ROS as compared to those with lower ROS levels. This second goal also entailed that the presence of MT protein had to be determined.

c. The final objective was to elucidate the expression of MT genes in HeLa cell lines with high levels of ROS, and to compare the results obtained from the *in vitro* study to those of the *in vivo* study as listed in the first objective for the three groups of individuals.

CHAPTER FIVE

MATERIALS AND METHODS

This project forms part of the broader mitochondrial project which has been approved by the Ethics Committee of the North-West University (Potchefstroom campus), under the title "*Mitochondrial DNA (mtDNA) mutations in patients with suspected mitochondrial disorders in the South African context*", approval number 02M02. This study was also approved by the Ethics committee of the Faculty of Medicine of the University of Pretoria, and the Pretoria Academic Hospital. The approval number 91/98 was assigned to the study entitled "*Mitochondrial DNA (mtDNA) mutations in patients with suspected mitochondrial disorders in the South African context*". Due to the inclusion of diabetic individuals in this study, ethical approval for the diabetes project was also obtained under the title *"Molecular analysis of non-insulin dependant diabetes mellitus (NIDDM) in the South African population"* and has been assigned the approval number 02M08.

5.1 PATIENT POPULATION

All individuals included in this investigation were recruited from Potchefstroom, in the North-West province of South Africa. Patients who were clinically diagnosed with diabetes mellitus, in particular T2D, were recruited into the investigation subsequent to the acquisition of written informed consent. The inclusion criterion for these individuals was based on a previous clinical diagnosis of T2D, by their respective clinicians. This group, which was composed of one Indian, one Black and 17 Caucasian South African individuals, is referred to as Group-1 throughout this report. Clinically unaffected aged matched individuals were also recruited into the investigation following attainment of written informed consent and were referred to as Group-2. This group was composed of one Black and 11 Caucasian South African individuals. The selection of non-diabetic, aged matched individuals to include in this investigation, was based on a negative diagnosis for T2D. Individuals comprising these two groups were randomly selected from the Centre for Diabetes at the North-West University (Potchefstroom campus). Medical data for the diabetic and non-diabetic individuals was also obtained where possible. During the recruitment of these individuals, questions pertaining to the lifestyle factors, which may have had an influence in the parameters measured in this investigation, were asked for

both groups. The information, which was obtained from all the individuals during the recruitment phase, is presented in Table 5.1.

Table 5.1: Summary of the information required from the individuals recruited into the investigation

Number	Information
1	Age and gender
2	Mass in kilograms (kg), height in metres (m), waist size in cm and hip size in cm
3	Alcohol intake, cigarette smoking, laser treatment and cataract removal
4	Family history of diabetes
5	Medication for T2D, hypertension or other types of medication

T2D = type two diabetes mellitus.

A group of individuals classified as being at risk of developing diabetes were also included in this investigation. These individuals formed part of the Profiles of Obese Women with Insulin Resistance Syndrome (POWIRS2) study, and were referred to as Group-3. This group was composed of female Caucasian South African individuals The selection criteria for these individuals were that they had to have BMI values above the normal value of 25, due to the association of high BMI and obesity with diabetes (Hotamisligil *et al.*, 1995) as well as family history of diabetes mellitus. Screening of the genes associated with the pathogenesis of T2D as listed in Figure 3.6, was not the aim of this study. A family history of diabetes was regarded as indicative of possible genetic predisposition to developing diabetes.

Medical history as well as the information outlined in Table 5.1 were also obtained for these individuals when recruiting them onto the research programme. After 10 hrs of fasting, whole blood from these individuals was obtained with informed consent. The blood obtained from individuals comprising these three groups was pre-treated as required for each of the biochemical parameters described in Section 5.2.

5.2 BIOCHEMICAL ANALYSES

Various biochemical parameters were analysed to determine the level of ROS and the energy status in whole blood of the individuals in the three groups. ROS levels were also measured in *t*-BHP-treated and control cell lines. The analyses listed as numbers 1-6 in Table 5.2, were performed in whole blood. Due to the large quantity of cells required, which could not even be attained via culturing for the assays listed as 1-6, these analyses were not performed on cell cultures. To determine the production of ROS and to analyse the effects of ROS on cell viability in cell cultures, the analyses numbered as 7 and 8 were

performed. Therefore, different biochemical assays were performed for whole blood and cell cultures and these assays would indicate the oxidative stress within the respective material analysed. All the reagents utilised in the biochemical analyses were purchased from Sigma Aldrich, unless stated otherwise.

Table 5.2: Biochemical parameters analysed

Assay number	Tissue	Biochemical assay	Method utilised
1	Whole blood	Reactive oxygen metabolites (d-ROMs) assay	Spectrophotometry
2		Oxygen radical absorbance capacity (ORAC) assay	Fluorometry
3		Glutathione redox status analysis	Spectrophotometry
4		NADH:NAD^+ ratio analysis	Spectrophotometry
5		Lactate and Pyruvate analysis	Spectrophotometry
6		ATP and ADP analysis	Spectrophotometry
7	Cell culture	ROS production assay	Fluorometry
8		Cell viability assay	Spectrophotometry

ATP = adenosine triphosphate; ADP = adenosine diphosphate; NADH = reduced nicotinamide adenine dinucleotide; NAD^+ = oxidised nicotinamide adenine dinucleotide; ROS = reactive oxygen species.

5.2.1 Reactive oxygen metabolites (d-ROMs) analysis

The d-ROMs test is a colorimetric test that allows analysis of the concentration of hydroperoxides (R-OOH, Reactions 1, 3, and 4 in Table 5.3) or any other reactive oxygen metabolites (Reaction 2 in Table 5.3) generated by ROS attack on a number of organic substrates in a biological sample. A summary of these metabolites is presented in Table 5.3. For the analysis, 10 microlitres (μl) of the choromogenic reagent, N,N,-diethylparaphenylen-diamine (A-NH_2) and 1 millilitre (ml) of acetate buffer at a measure of acidity (pH) of 4.8, provided with the kit (Diacron International) were aliquoted to 10 μl of the serum sample. The low pH facilitates the availability of the iron ions, which were initially bound to the serum proteins to catalyse the *in vitro* breakdown of blood hydroperoxides to the alkoxyl and peroxyl radicals presented in Table 5.3.

Table 5.3: Reaction of the reactive metabolites involved in the d-ROMs test kit

Reaction number	Reaction
1	$R\text{-}OOH + Fe^{2+} \rightarrow R\text{-}O^{\cdot} + Fe^{3+} + OH^-$
2	$R\text{-}O^{\cdot} + A\text{-}NH_2 \rightarrow R\text{-}O^- + [A\text{-}NH_2]^+$
3	$R\text{-}OOH + Fe^{3+} \rightarrow R\text{-}OO^{\cdot} + Fe^{2+} + H^+$
4	$R\text{-}OOH + A\text{-}NH_2 \rightarrow R\text{-}OO^{\cdot} + [A\text{-}NH_2]^+$

R-OOH = hydroperoxide; $R\text{-}O^{\cdot}$ = alkoxyl radical of hydroperoxide; $R\text{-}OO^{\cdot}$ = hydroperoxyl radical of hydroperoxide; Fe^{2+} = ferrous ion; Fe^{3+} = ferric ion; A-NH_2 = N,N,-diethylparaphenylen-diamine; $[A\text{-}NH_2]^+$ = coloured radical cation of N,N,-diethylparaphenylen-diamine; H^+ = hydrogen ion; $OH^{\cdot}$ = hydroxyl radical.

In the d-ROMs test, the hydroperoxides react with a chromogenic substrate, which results in a coloured solution. The coloured complex is detected and quantified via spectrometric analysis as Carratelli Units (CARR U). A blank was also prepared in a similar manner to the samples as well as the control serum sample provided with the kit, with the exception that the biological material was replaced with water. The absorbance was recorded kinetically at 505 nanometres (nm), in 1 min time intervals for 5 min. The absorbance of the blank was subtracted from those of the standards and the samples. The hydroperoxide concentration was calculated from the formula in Equation 5.1.

Equation 5.1: Determination of the concentration of hydroperoxides

$$\text{CARR U} = \frac{\Delta\text{Abs}}{\text{min}} \times F$$

CARR U = Carratelli units, where 1 CARR U corresponds to 0.08 mg.100 ml^{-1} H_2O_2; ΔAbs = mean difference in absorbance; min = minutes; *F* = correction factor with an assigned value of 9000. Adapted from Iorio (2002).

Reference intervals determined by Lubrano *et al.* (2002) as listed in Table 5.4 were utilised as a reference in this investigation to characterise oxidative stress levels in the serum samples.

Table 5.4: Reference intervals for oxidative stress levels

CARR U	mg.100 ml^{-1} H_2O_2	Oxidative stress level
250-300	16-20	Normal range
300-320	20-24	Range of border line threshold
320-340	24-27	Range of mild oxidative stress
340-400	27-32	Range of oxidative stress
400-500	32-40	Range of high oxidative stress
>500	>40	Range of very high oxidative stress

CARR U = Carratelli units, where 1 CARR U corresponds to 0.08 mg.100 ml^{-1} H_2O_2; H_2O_2 = hydrogen peroxide. Adapted from Lubrano *et al.* (2002).

5.2.2 Oxygen Radical Absorbance Capacity (ORAC) assay

The Oxygen Radical Absorbance Capacity (ORAC) assay was utilised to measure the total antioxidant capacity of biological samples. It is based on the induced free radical damage of fluorescein, that is observed by a decrease in fluorescence emission. In the presence of an antioxidant, such as Trolox (6-hydroxy-2,5,7,8-tetramethylchroman-2-carboxylic acid, a water-soluble analogue of α–tocopherol) which was used as a standard in this assay, the inhibition of free radical damage was measured. This measurement reflects the protection against a decrease in fluorescence of fluorescein (Cao and Prior, 1998).

The ORAC assay was performed in blood samples collected in serum tubes. The serum was obtained subsequent to it being separated from the blood cells via centrifugation. Due to the sensitivity of the ORAC assay, the samples were diluted 100 - 200 fold with phosphate buffer. The serum was also pre-treated with 0.5 molar (M) perchloric acid (PCA) and centrifuged at 10,000 x gravitational acceleration (x g) to precipitate the proteins and to prevent oxidation of the antioxidants. The resulting supernant was utilised for the ORAC assay.

A Trolox standard series were prepared on microtitre plates from a 500 micromolar (μM) stock solution in a 75 mM phosphate buffer (di-potassium hydrogen phosphate (K_2HPO_4), di-sodium hydrogen phosphate (NaH_2PO_4) at pH 7.4) as illustrated in Table 5.5, giving the final concentration indicated. The serum samples were diluted in the phosphate buffer and aliquoted to the wells in duplicate to a total reaction volume of 20 μl as in the standards.

Table 5.5: Illustration of the layout of the microtitre plate for the ORAC assay

Reagent	1	2	3	4	5	6
Phosphate Buffer (μl)	20	19	18	16	14	12
Trolox (μl)	0	1	2	4	6	8
[final] μM	0	25	50	100	150	200

To each well, 160 μl of a fluorescein solution (56 nM in phosphate buffer) was added. Temperature plays a critical role in the ORAC because the reaction can be affected by the thermal decomposition of 2, 2' Azobis (2-amidinopropane) dihydrochloride (AAPH), a peroxyl radical generator utilised in the assay. To eliminate the problem of temperature non-homogeneity across the plate, the plate was pre-incubated at 37 degrees Celsius (°C) for 15 min (Huang *et al.* 2002). The reaction was initialised by adding 20 μl AAPH (240 nanomolar (nM) in the phosphate buffer) and the plate immediately placed in the FL600 Bio-Tek microplate reader pre-heated to 37 °C. Fluorescence measurements were taken every two minutes (excitation at 485 nm and emission at 520 nm from the top of the plate) until the final reading was circa (ca.) 5% of the initial reading. The area under the curve was calculated according to Equation 5.2 to quantify the antioxidant capacity of the respective tissues. The area under curve technique that was utilised to determine the ORAC is further discussed in Section 6.2.1.2.

Equation 5.2: Determination of the area under the curve

$$S = (0.5 + F5/F0 + F10/F0 + F15/F0 + \ldots + Fi/F0 + Fi/F0) \times 5$$

F0 = initial fluorescence at 0 min; Fi = fluorescence measurement at time i; S = area under the curve. Adapted from Cao and Prior (1998).

The final readings (ORAC value) were expressed as Trolox equivalents, as illustrated in Equation 5.3. The data was analysed utilising Microsoft Excel®[1] to calculate the total cellular antioxidant capacity applying both Equation 5.2 for the area under the curve and 5.3 for the final ORAC value. The ORAC activity against peroxyl radicals measured in serum of healthy individual has been estimated to ca. 1,800 – 1,900 μM Trolox Units (Cao and Prior, 1998).

Equation 5.3: Determination of the ORAC value

$$\text{ORAC value } (\mu M) = 20k\,(S_{sample}-S_{blank})/(S_{trolox}-S_{blank})$$

k = sample dilution factor; *S* = area under the fluorescence curve. Adapted from Cao and Prior (1998).

5.2.3 Glutathione redox analysis

This method of analysis is based on the recycling process of glutathione by the enzyme glutathione reductase. This reaction is vital within the cell, since it is one of the enzymatic mechanisms that a cell utilises to scavenge ROS. The exact mode of action is discussed in Section 3.3. As GSSG is only present in minimal amounts in comparison to GSH, auto-oxidation of the latter will result in a false GSSG representation. The accurate determination of the GSH:GSSG ratio was accomplished by the exploitation of a GSH scavenger, 1-methyl-2-vinyl-pyridinium trifluoromethane sulfonate (M2VP), a sulfhydryl group alkylating agent at a concentration of 30 millimolar (mM) in 0.1 Normal (N) hydrochloric acid (HCl). This reagent facilitates accurate measurement of GSSG as it prevents the auto-oxidation of GSH (Asensi *et al.*, 1999).

5.2.3.1 Sample preparation for GSSG analysis

Whole blood was collected in ethylenediamine tetra-acetic acid (EDTA) tubes for the glutathione redox analysis. Of the EDTA treated blood, 100 μl was aliquoted into a 1.5 ml microcentrifuge tube containing 30 mM M2VP, for the GSSG test. The samples were stored in M2VP at -70°C, for no longer than 30 days. The samples were thawed and thoroughly mixed prior to analysis. The samples were subsequently mixed with 290 μl of 5% metaphosphoric acid (MPA), vortexed and centrifuged at 1,000 x g for 10 min. The acidic supernatant (25 μl) was carefully aspirated and diluted with 350 μl buffer A (500 mM sodium phosphate ($NaPO_4$) at pH of 7.5, 1 mM EDTA) for the GSSG analysis.

[1] Microsoft® is a registered trademark of Microsoft Corporation, Redmond, WA, U.S.A.

5.2.3.2 Sample preparation for total GSH (tGSH) analysis

For the GSH analysis, 50 µl of the EDTA blood was aliquoted into a separate sterile 1.5 ml microcentrifuge tube. The samples were stored at -70°C, until analysis, but were thawed and incubated at room temperature prior to analysis. To precipitate the proteins, 350 µl of 5% MPA was added to each of the samples. The precipitate was subsequently removed via centrifugation at 1,000 x g for 10 min. Subsequently, 5 µl of the MPA extract was diluted with 300 µl of buffer A, as discussed in Section 5.4.1.1.

5.2.3.3 GSH or GSSG analysis

The assay was performed in a microtitre plate via Fluorometry. A 3 µM GSH solution was prepared and used as a standard. The plate was set up as indicated in Table 5.6. The components specified in Table 5.6 are those of the standards and the blank, with a total reaction volume of 50 µl.

Table 5.6: Schematic representation of the set up of a microtitre plate for total GSH or GSSG analysis

	1	2	3	4	5	6	7
Standard (3 µM) in µl	0.0	8.3	16.7	25.0	33.3	41.7	50
Buffer A (µl)	50.0	41.7	33.3	25.0	16.7	8.3	0.0
Final concentration (µM)	0.0	0.5	1.0	1.5	2.0	2.5	3.0

Duplicates of each sample (50 µl of the samples diluted in buffer A) were aliquoted into separate wells. To each well 50 µl of 5, 5' dithiobis-(2-nitrobenzoic acid) solution (DTNB) at 0.3 mM in buffer A (500 mM $NaPO_4$ (pH 7.5), 1 mM EDTA) and glutathione reductase (GR, 0.02 $U.\mu l^{-1}$) were added. The solutions were mixed and incubated at 25°C for 5 min in a preheated microplate reader. To initialise the reaction, 50 µl of NADPH (1 mM) was aliquoted into each well. DTNB reacts with GSH resulting in coloured product, thiobis-(2-nitrobenzoic acid). The coloured product was measured kinetically at 412 nm for 3 min on a FL600 Bio-Tek microplate reader. The concentration of either GSSG or GSH, which is proportional to the concentration of the coloured product, was calculated utilising the linear slope of standards. The results of the GSH and GSSG assay were compared to obtain a ratio of the two, as depicted in Equation 5.4

Equation 5.4: Calculation of the GSH:GSSG ratio

GSH_t = μM x dilution factor (488)

GSSG = μM x dilution factor (60)

GSH:GSSG = (GSH_t – 2GSSG)/GSSG

GSH_t = GSH + GSSG. Asensi *et al.* (1999).

5.2.4 NADH:NAD^+ ratio analysis

As discussed in Section 3.1.5, the favoured reduction of pyruvate to lactate under defective OXPHOS conditions results in the production of a high concentration of NAD^+. The analysis of the NADH and NAD^+ is based on the reaction catalysed by the enzyme, alcohol dehydrogenase (ADH) that initiates the reduction of NAD^+ to NADH. NAD^+ is oxidised, upon the addition of N-ethyldibenzopyrazine ethyl sulphate (PES) which is in turn re-oxidised in the presence of 3-[4,5-dimethylthiazol-2-yl]-2,5-diphenyltetrazolium bromide (MTT), producing a colour change measured at 570 nm.

This test was performed in blood collected in fluoride tubes. The fluoride treated blood was mixed with a buffer solution composed of 10 mM nicotinamide, 20 mM sodium carbonate ($NaHCO_3$) and 100 mM di-sodium carbonate (Na_2CO_3). The mixture was snap frozen in liquid nitrogen and stored at –70 °C until the analysis was performed. The samples were thawed on ice before analysis, subsequent to which each of the samples were split into two. In the one sample aliquot, the NAD^+ was destroyed by the incubation of this mixture at 60°C for 30 min. The mixture was subsequently cooled on ice. At this point, the sample could be stored at -70°C if not analysed promptly.

To quantify the NADH present within each sample, 80 μl of each sample was aliquoted into each well of the microtitre plate. The standards were prepared from 0 nM to 1000 nM NADH to derive a standard curve, which was utilised to quantify the amount of NADH, present in each sample. To these standards and the samples the following reagents were added: 25 μl 1.0 M Tris-HCl (2-amino-2-hydroxymethyl)-1,3-propanediol hydrochloride (pH 8.0), 5 μl PES (100 mM), 12.5 μl MTT (10 mM), 7 μl ADH (29.4 milligrams (mg).ml^{-1}) and 96.5 μl double distilled water (ddH_2O). The mixture was incubated at room temperature for 5 min. To initialise the reaction catalysed by ADH i.e. the conversion of ethanol to acetaldehyde resulting in the reduction of NAD^+, 24 μl of 33% volume per total volume (v/v) ethanol was added. The absorbance at 560 nm was measured on the FL600

Bio-Tek microplate fluorescence for four minutes (min). The absorbance values were used to the NADH:NAD^+ ratio as illustrated in Equation 5.5.

Equation 5.5: Determination of the NADH:NAD^+ ratio

$$NADH:NAD^+ = (A_{NADH}/t)/ ([A_{NADHt}/t]-[A_{NADH}/t])$$

A_{NADH} = absorbance of sample in which NAD^+ was destroyed via heating; A_{NADHt} = absorbance of sample not heated; t = time min.

5.2.5 Lactate:pyruvate ratio analysis

The increase in the cellular concentration of L-lactate is characteristic of a defective OXPHOS or any of the pathways integral to the cellular energy metabolism. The lactate:pyruvate (L/P) ratio was determined in all groups of individuals. The pyruvate concentration was determined by the reversible reaction catalysed by lactate dehydrogenase (LDH), where pyruvate is favourably converted to lactate, with the concomitant reduction of NAD^+ to NADH. The increase in NADH which is measured at 340 nm is proportional to the amount of pyruvate converted to lactate. The addition of glutamate and glutamate-pyruvate transaminase (GPT) when determining the concentration of lactate which catalyses the transamination of pyruvate to alanine allowed for the precise determination of the concentration of lactate.

Blood utilised for this assay was collected in EDTA tubes. The blood sample was immediately deproteinised by the addition of 1 ml of 1 M PCA to 500 µl and centrifuged at 3,000 x g for 15 min. The supernatant was transferred to a 1.5 ml eppendorf tube and kept on ice for 15 min. To neutralise the solution, 3 M tripotassium buffer was added until a neutral pH was obtained, followed by incubation of the sample on ice. The potassium perchlorate precipitate was subsequently removed after centrifugation at 1,000 x g for 10 min.

The remaining clear supernatant was used for the lactate and pyruvate analyses. The reaction components were added into cuvettes as illustrated in Table 5.7 and 5.8. For the lactate analysis, the increase in the concentration of NADH was measured in an alkaline buffer whereas for the pyruvate analysis the decrease in NADH is measured in a neutral buffer.

Table 5.7: Reagents utilised in the lactate determination assay

Reagent	Blank	Standard	Sample	Rerun assay internal standard
Glycylglycine buffer (0.6 M, pH 10), glutamate (0.1 M) in µl	100	100	100	100
NAD (18 $mg.ml^{-1}$) in µl	20	20	20	20
GPT (0.1 $mg.ml^{-1}$) in µl	2	2	2	2
Sample in µl	--	--	20	10
Standard (0.15 $mg.ml^{-1}$) in µl	--	10/8/6/4/2	--	10
ddH_2O in µl	100	90/92/94/96/98	80	80

NAD = oxidised nicotinamide adenine dinucleotide; GPT = glutamate-pyruvate transaminase; ddH_2O = double distilled water; -- = no reagent added.

The reagents were gently mixed and incubated at room temperature for 5 min. The samples were aliquoted into cuvettes and placed in the Bio-Tek UVIKON UV-Vis double beam spectrophotometer. The absorbance was measured at 340 nm. Subsequent to the first reading, 5 µl of the enzyme, LDH (0.1 $mg.ml^{-1}$) was added and the samples were once again thoroughly mixed, incubated at room temperature for 30 min and the formation of NADH determined at 340 nm. The reading taken before the addition of LDH was referred to as A_1 and that taken after the addition is A_2. The concentration of lactate was determined by the use of Equation 5.6.

Equation 5.6: Determination of the lactate concentration

$$\text{Lactate } (mg.l^{-1}) = ([A_2-A_1]/t) \text{ X } (V \text{ x } MW) / (\varepsilon \text{ x } d \text{ x } v)$$

t = time (min); A_1 = absorbance value before the addition of LDH; A_2 = absorbance value after the addition of LDH; V = total reaction volume (ml) in cuvette; v = sample volume (ml); d = path of cuvette [10 millimetre (mm)]; ε = NADH extinction coefficient (0.63 l. $mmol^{-1}$. mm^{-1}); MW = molecular weight of lactate [90.1 grams per mole ($g.mol^{-1}$)].

The same procedure was followed for the determination of the pyruvate content. However, the reagents listed in Table 5.8 were utilised.

Table 5.8: Reagents utilised in the pyruvate determination assay

Reagent	Blank	Standard	Sample	Rerun assay internal standard
Triethanolamine (0.5 M), EDTA (5 mM) pH 7.6 in µl	100	100	100	100
NADH (5 $mg.ml^{-1}$) in µl	20	20	20	20
Sample solution in µl	-	-	10	20
Standard (0.15 $mg.ml^{-1}$) in µl	-	10/8/6/4/2	-	-
ddH_2O in µl	100	90/92/94/96/98	90	80

NADH = reduced nicotinamide adenine dinucleotide; EDTA = ethlenediamine tetra acetic acid (disodium salt); ddH_2O = double distilled water; - = no reagent added.

Following the addition of 5 µl of LDH (0.1 mg.ml^{-1}), the samples were thoroughly mixed, incubated at room temperature for 30 min, and the depletion of NADH determined at 340 nm. The reading that was taken before the addition of LDH was referred to as A_1 and that taken after the addition was A_2. These values were utilised in the equation below to determine the concentration of pyruvate.

Equation 5.7: Determination of the pyruvate concentration

$$\text{Pyruvate (mg.l}^{-1}) = ([A_2-A_1]/t) \text{ X } (V \text{ x } MW) / (\varepsilon \text{ x } d \text{ x } v)$$

t = time (min); A_1 = absorbance value before the addition of LDH; A_2 = absorbance value after the addition of LDH; V = total reaction volume (ml) in cuvette; v = sample volume (ml); ε = NADH extinction coefficient (0.63 l.mmol^{-1}.mm^{-1}); d = path of cuvette (10 mm); MW = molecular weight of pyruvate (88.1 g.mol^{-1}).

5.2.6 ATP:ADP ratio assay

The energy status of cells in whole blood was determined via the ATP:ADP assay. A 0.5 ml volume of fresh whole blood was thoroughly mixed with 1.5 ml ice cold 2 M PCA. The sample was placed on ice for 15 min. To precipitate the proteins, the mixture of blood and PCA was centrifuged at 1,000 x g for 15 min. The supernatant was transferred into a sterile tube, neutralised by the addition of 3 M tri-potassium buffer (pH 7.5) and centrifuged at 5,000 x g to remove the precipitated potassium perchlorate.

In order to measure the total cellular ATP (ATP + ADP converted to ATP), 150 µl of each of the neutralised samples was mixed with 140 µl of buffer A (3 mM phosphoenol pyruvate (PEP), 50 mM imidazole-HCl at pH 7.0, 2 mM magnesium chloride ($MgCl_2$), 75 mM potassium chloride (KCl) and 5 µl of pyruvate kinase (100 µg. ml^{-1} buffer A). The mixture was incubated at room temperature for 60 min. This reaction facilitated the conversion of cellular ADP to ATP, resulting in the formation of pyruvate. To inactivate the enzyme, the mixture was heated at 60°C for 10 min. Subsequent to the heat inactivation, 300 µl of buffer B (50 mM Tris-HCl at (pH 8.1), 10 mM glucose, 100 µg.ml^{-1} glucose 6-phosphate dehydrogenase, 100 µg.ml^{-1} hexokinase) was added before the first measurement was taken.

The first absorbance reading (A_1) was recorded at 340 nm in the Bio-Tek UVIKON UV-Vis double beam spectrophotometer. This reading gave an indication of the amount of ADP that was converted to ATP. To this mixture, 5 µl of $NADP^+$ (1 mM) was added to start the reaction that converts glucose 6-phosphate (formed via the reaction catalysed by

hexokinase) to 6-phophogluconate. The NADPH formed was measured at 340 nm, corresponding to the amount of total ATP present (ADP and ATP).

The ADP present in the sample was measured via the same procedure, however, pyruvate kinase was not added but substituted with buffer A (Lust *et al.*, 1981). A series of standards to quantify the concentration of ATP as well as ADP were prepared to range between 0 and 1,000 μM. From the data of both of the standards, as summarised in Table 5.9, a standard curve was plotted. The equation obtained from the standard curve was utilised to estimate the ATP and ADP concentration in each of the samples and from that data the ATP:ADP ratio was determined.

Table 5.9: Summary of concentrations for the ATP and ADP standards

Concentration of ATP (μM)	0 μM	200 μM	400 μM	600 μM	800 μM	1000 μM
Volume of ATP standard (μl)	0	30	60	90	120	150
Volume of buffer (μl)	150	120	90	60	30	0

5.3 CELL CULTURE FOR ROS ANALYSIS

Cells which were originally obtained from the cervical cancer cell line of Henrietta Lacks (HeLa) were obtained from the National Repository for Biological Materials (NRBM). These cells were cultured in Dulbecco's Modified Eagle's Medium supplied by Highveld Biological (Pty) Ltd (DMEM, with 4.5 grams per litre ($g.l^{-1}$) glucose, 0.110 $g.l^{-1}$ sodium pyruvate with L-glutamate) supplemented with 10% foetal calf serum (FCS, GIBCO®[1]), 100 units per millilitre ($U.ml^{-1}$) penicillin supplied by GIBCO® and 100 microgram per millilitre ($\mu g.ml^{-1}$) streptomycin. A 100 μl volume of previously cultured cells was aliquoted into a 1.5 ml Eppendorf tube under sterile conditions. A 250 μl aliquot of 0.4% Trypan blue together with 150 μl of 1 X phosphate buffered saline (PBS) were both supplied by Bio-Whittaker™[2], were added to the 100 μl aliquot of cells and mixed gently. The cells were counted via the use of a haemocytometer.

Subsequent to quantifying the cells, a desired number of cells were re-seeded into either sterile 25 cubic centimetre (cm^3) flasks or 96 well plates (Nunclon™[3]) depending on the analysis to be performed and incubated at 37 °C, 5% CO_2 in a humidified HERA cell Heraeus incubator. The process of cell seeding was performed every two to three days to

[1] GIBCO® is registered trademark of Invitrogen Corporation, Auckland, New Zealand.
[2] Bio-Whittaker™ is a trademark of Cambrex Bio Science, Walkersville Inc., Walkersville, MD, U.S.A.
[3] Nunclon™ is a trademark of Nalge Nunc International, Rochester, NY, U.S.A.

maintain the cells in a viable state. Once the cells were confluent, they were treated accordingly.

5.3.1 Treatment of control cells with *t*-BHP

A subset of control HeLa cell lines were treated with *t*-BHP (Sigma Aldrich), a compound that leads to increased presence of ROS, via the formation of peroxyl and alkoxyl radicals. Different concentrations of *t*-BHP (0.5 mM, 0.8 mM, 1 mM) were administered for 3 hrs, and the levels of ROS produced were determined for each dosage via the biochemical parameters described in Sections 5.4.7 and 5.4.8.

5.3.2 ROS determination in *t*-BHP-treated HeLa cells

To determine the production of ROS in *t*-BHP-treated HeLa cells, 3 x 10^4 cells per well were seeded on 96 well plates (Nunclon™ plates) in a total volume of 100 µl per well and incubated overnight. The method described by Wang and Joseph, (1999) was followed. Subsequent to the overnight incubation the media was discarded and the cells supplemented with media containing 1 mM, 0.8 mM and 0.5 mM *t*-BHP (made up in media) respectively. A subset of cells were utilised as a negative control, whereby no *t*-BHP was added. The exposure was allowed to occur for 3 hrs at 37°C. The detection of ROS production was enabled by the addition 10 µl of a 10 mM 2',7'-dichlorodihydrofluorescein diacetate (H_2DCFDA) solution as described by Shimizu *et al.* (2004). H_2DCFDA is widely utilised as a ROS probe (Wang and Joseph, 1999; Pérez and Cederbaum, 2003). The reactions were incubated for a further 30 min, at 37°C. The cells were subsequently washed with 200 µl PBS and 100 µl PBS added thereafter. The fluorescence (485 nm excitation and 530 nm emission) was measured via the FL600 Bio-Tek microplate reader. The sample measurements were normalised according to the protein content of the cells.

5.3.2.1 Protein assay

The standard Bicinchoninic Acid (BCA) method for protein determination was performed, using 1 $\mu g.\mu l^{-1}$ BSA as a standard. The BCA method is similar to the Lowry assay. It depends on the conversion of copper II (Cu^{2+}) to copper (Cu^{+}) ions under alkaline conditions. The formation of Cu^{+} leads to the formation of a purple colour reaction, which is measured at 560 nm. The production of Cu^{+} is proportional to the protein content. The

protein content of the samples is inferred from the known concentration of the BSA standard (Smith *et al.*, 1985). The standards were set up as illustrated in Table 5.10.

Table 5.10: Layout of the standard range on microtitre plate for the protein determination assay

Concentration (μg. μl^{-1})	0	2	4	6	8	10
BSA standard (μl)	0	2	4	6	8	10
dd$H_2$0 (μl)	10	8	6	4	2	0

ddH_2O = double distilled water; BSA = bovine serum albumin.

To each of the standards as well as the samples, 200 μl of a mixture of BCA and copper II sulphate (Cu_2SO_4) in a ratio of 50:1 was added. The plate was incubated at 37°C for 20 min, subsequent to which the absorbance of the reaction was measured at 560 nm in a FL600 Bio-Tek microplate reader.

5.3.3 Cell viability assay in *t*-BHP-treated HeLa cells

Similar to the ROS determination method described in Section 5.3.2, HeLa cells were seeded in 96 well plates at a density of 3 x 10^4 cell per well. The cells were treated with 0.5 mM, 0.8 mM and 1 mM *t*-BHP respectively, by incubating the plates for 3 hrs at 37°C with medium containing the respective concentrations of *t*-BHP. The method described by Denizot and Lang (1986) was followed. A positive control composed of 0.1% Triton X-100®[1] (supplied by Boehringer Mannheim) in PBS was added to cells not treated with *t*-BHP, 30 min prior to the completion of the 3 hrs incubation period.

Subsequent to the incubation period, the plate was centrifuged at 1,000 x g for 5 min, and the media discarded by pipetting. The cells were washed three times with 200 μl PBS and centrifuged for a further 5 min at 1,000 x g after each washing step. The residual PBS was subsequently removed. To each of the wells, 0.5 mg.ml^{-1} MTT was added and the cells incubated in the CO_2 incubator at 37°C for five hrs. During the incubation period, the reaction that occurred resulted in the formation of formazan crystals. The reaction was stopped by adding 10 μl dimethyl sulfoxide (DMSO), and shaken until the crystals were completely dissolved. The absorbance was measured in the FL600 Bio-Tek microplate reader at 560 nm and at 645 nm as the background wavelength. The measurements obtained for the samples were normalised according to the values obtained for protein content, and the results expressed in terms of the % cell viability.

[1] Triton X-100® is a registered trademark of Rohm & Haas Company, Philadelphia, PA, U.S.A.

5.4 RNA ISOLATION FROM CULTURED CELLS AND BLOOD

To quantify the amount of MT mRNA present in the cell lines as well as in whole blood, total ribonucleic acid (RNA) was firstly isolated by the use of the TRIzol®[1] Reagent. This is a mono-phasic solution composed of phenol and guanidine isothiocyanate. The phenol separates the lysate or blood sample into phases and guanidine isothiocyanate lyses the cells and is an effective protein denaturant.

RNA isolation from cultured cells was performed once the cells had reached an optimal level of confluency. They were centrifuged to obtain a pellet of cells, which was lysed by adding TRIzol® Reagent. The amount of TRIzol® Reagent added was 1 ml of the reagent per 5-10 $x10^6$ cells. Adequate mixing was accomplished by passing the lysate several times through the pipette, followed by the transfer of the cells to a 15 ml polypropylene tube. The homogenised sample was incubated at 30°C to permit the complete dissociation of nucleoprotein complexes. The addition of 0.2 ml of chloroform per 1 ml of TRIzol® Reagent followed by centrifugation at 12,000 x g for no more than 15 min lead to the separation of the solution into an aqueous phase and an organic phase. Subsequent to centrifugation, the mixture separated into a lower red coloured phenol-chloroform phase, a white interphase and a colourless upper aqueous phase. The RNA remained exclusively in the colourless upper aqueous phase.

The aqueous RNA-containing phase was transferred into a sterile 15 ml centrifuge tube. The remaining organic phase can be utilised for DNA or protein isolation. The RNA was subsequently precipitated by mixing the solution with 0.5 ml isopropanol per 1 ml of TRIzol® Reagent utilised for the initial homogenisation step, followed by centrifugation at 12,000 x g for 10 min at 2-8°C. The remaining supernatant was discarded and the gel-like pellet of RNA subsequently washed with 75% ethanol (1 ml of 75% ethanol per 1 ml of TRIzol® Reagent used for the initial homogenisation step). The sample was mixed thoroughly by vortexing and centrifuged at no more than 7,500 x g for 5 min at 2-8°C.

After this procedure, the pellet was air dried and rehydrated by the addition of RNase free water (supplied by Promega®[2]) and incubated at 60°C for 10 min. The quantity of RNA was determined via the use of the Eppendorf®[3] Biophotometer. The method described here was also followed for the isolation of RNA from blood, with the exception of the use of TRIzol® LS Reagent, which is more suitable for RNA isolation from liquid samples. The

[1] TRIZOL® is a registered trademark of Molecular Research Centre Inc., OH, U.S.A.
[2] Promega® is a registered trademark of Promega Corporation, Madison, WI, U.S.A.
[3] Eppendorf® is a registered trademark of Eppendorf, Hamburg, Germany.

concentration as well as the purity of the RNA was determined via spectrophotometry in TE buffer (10 mM Tris-HCl (pH 8.0), 1 mM Na_2EDTA). Agarose gel analysis of the RNA as discussed in Section 5.7.1 was also utilised to determine the purity and analyse the integrity of the isolated RNA.

5.4.1 Agarose gel electrophoresis

Mini submarine agarose gels of 2% weight per volume (w/v) were utilised to analyse the RNA isolated from blood. LE agarose was added into 1 X TBE [89.15 mM Tris® (pH 8.0), 88.95 mM boric acid, 2.498 mM disodium ethylenediamine tetra-acetic acid (Na_2EDTA) followed by the addition of 0.5 $\mu g.ml^{-1}$ ethidium bromide (EtBr) supplied by Sigma Aldrich, once a solution of TBE and agarose was obtained. Before loading the RNA product on the gel, it was mixed with gel loading dye (0.04% Orange G and 50% glycerol) to increase its density. A 100 bp molecular weight marker was loaded on every gel to enable sizing of the 12S rRNA as well as the 18S rRNA product. The gels were subsequently electrophoresed in 1 X TBE buffer at 10 volts per centimetre ($V.cm^{-1}$) unless stated otherwise. The RNA was visualised via UV fluorescence and the results photographed via a gel documentation system.

5.5 REAL-TIME POLYMERASE CHAIN REACTION FOR QUANTIFICATION OF METALLOTHIONEIN RNA

To determine the quantity of MT expressed in each of the patient samples as well as *t*-BHP treated HeLa cells, Real-Time polymerase chain reaction (PCR) was employed to obtain this objective. Two methods were utilised for this purpose. The first was the iScript™[1] one-step RT-PCR kit with SYBR® Green supplied by Bio-Rad laboratories that was utilised for the real-time quantification of the RNA templates. At the point of this investigation, this method had just been introduced into the market, and its efficiency was compared to the conventional reverse transcription polymerase chain reaction (RT-PCR) synthesis of complementary DNA (cDNA) method followed by Real-Time PCR of the cDNA product. For RT-PCR 100 nanograms (ng) of RNA isolated from blood of both groups of individuals as well as from *t*-BHP treated cell lines were utilised. This method facilitates the cDNA synthesis and PCR amplification in the same tube. The reaction conditions were suitable for the activity of both the Moloney Murine Leukemia Virus Reverse Transcriptase (M-MLV-RT) and the iTaq™ antibody-mediated hot-start DNA polymerase.

[1] iScript™ is a trademark of Bio-Rad, Hercules, CA, U.S.A.

All the reagents were supplied with the kit. The kit included the 2X SYBR Green®[1] RT-PCR reaction mix which was composed of the 2X reaction buffer (0.4 mM of each 2'-deoxynucleotide-5'-triphosphate (dNTP), [2'-deoxyguanosine-5'-triphosphate (dGTP), 2'-deoxycytidine-5'-triphosphate (dCTP), 2'-deoxyadenosine-5'-triphosphate (dATP), 2'-deoxythymidine-5'-triphosphate (dTTP)], 6 mM $MgCl_2$, 0.5 U of iTaq DNA polymerase and 20 nM fluorescein, SYBR Green® I dye), Nuclease free H_2O and an optimised 50X formulation of iScript M-MLV-RT. Oligonucleotide primers for the amplification of the MT genes were newly designed, via the use of the Primer3 output program (2004), and those for the housekeeping genes listed in Table 5.11 were obtained from the indicated references. Complementarity between the primer sequences as well as self annealing properties were analysed for each primer sequence before their use on the Oligonucleotide Properties Calculator. The respective primers whose sequences are listed in Table 5.11 were obtained from Inqaba Biotechnical Industries (Pty) Ltd.

Table 5.11: Nucleotide sequences of primer utilised for the Real-Time detection of Metallothionein isoforms

Primer name	Primer sequence	Optimised T_a	Reference	Product size (bp)
MT1B Fwd	5'-gaactccaggcttgtcttgg-3'	60	Newly synthesised	133
MT1B Rev	5'-gatgagcctttgcagacaca-3'			
MT1A Rev	5'-ttccaagtttgtgcaggtca-3'	60	Newly synthesised	185
MT2 Fwd	5'-tcctgcaaatgcaaagagtg-3'	60	Newly synthesised	187
MT2 Rev	5'-caggtttgtggaagtcgcgt-3'			
GAPDH Fwd	5'-gaaggtgaaggtcggagtc-3'	60	Radonic *et al.*, 2004	226
GAPDH Rev	5'-gaagatggtgatgggatttc-3'			
β-actin Fwd	5'-agcctcgcctttgccga-3'	60	Radonic *et al.*, 2004	174
β-actin Rev	5'-ctggtgcctggggcg-3'			
β-microglobulin Fwd	5'-agcgtactccaaagattcaggtt-3'	60	Radonic *et al.*, 2004	306
β- microglobulin Rev	5'-atgatgctgcttacatgtctcgat-3'			
RNA polymerase II Fwd	5'-gcaccacgtccaatgacat-3'	60	Radonic *et al.*, 2004	187
RNA polymerase II Rev	5'-gtgcggctgcttccataa-3'			

Fwd = forward primer; Rev = reverse primer; GAPDH = glyceraldehydes-3-phosphate dehydrogenase; T_a = annealing temperature; bp = base pair. The optimised T_a is further discussed in Section 6.4.

For the analysis of gene expression, 10 μM of each of the gene specific primers listed in Table 5.11 were utilised, and the total reaction volume was made up to 20 μl. The reaction was carried out in the Bio-Rad iCycler™[2] iQ optical system as depicted in Table 5.12. Data were collected throughout the melting curve analysis.

[1] SYBR Green® is a registered trademark of Molecular Probes, Eugene, OR, U.S.A.
[2] iCycler iQ ™ is a trademark of Bio-Rad, Hercules, CA, U.S.A.

Table 5.12: Real-Time PCR conditions utilising the iScript™ one-step RT-PCR kit

Reaction	Conditions
cDNA synthesis	50°C for 10 min
iScript Reverse Transcription activation	95°C for 3 min
PCR cycling and detection (for 30 cycles)	95°C for 20 sec
	63°C for 10 sec
	72°C for 20 sec
Melt curve analysis	95°C for 1 min
	55°C for 1 min
	55°C for 10 sec (80 cycles, increased by 0.5°C after each cycle)

PCR = polymerase chain reaction; cDNA = complementary deoxyribonucleic acid.

The second method of analysis included cDNA synthesis of the isolated RNA, followed by Real-Time PCR detection of the respective genes. For cDNA synthesis, 3 μg of total RNA was denatured together with 0.5 μg of random primer at 70°C for 5 min. Subsequent to the denaturation, 5 μl of 5 X M-MLV buffer and 0.3 mM dNTPs, 5 U of M-MLV-RT (Promega®) were added per reaction and ddH_2O to a total volume of 40 μl. The cDNA synthesis programme included synthesis at 37 °C for 60 min, denaturation at 80°C for 10 min. The reaction mixture was subsequently placed on ice until RT-PCR was performed.

Following cDNA synthesis, 1 μl (75 ng) of cDNA was utilised for Real-Time PCR with the iQ SYBR Green®[1] supermix supplied by Bio-Rad laboratories. The Bio-Rad iCycler™ iQ optical system was utilised for Real-Time PCR according to the following programme:

Table 5.13: Real-Time PCR conditions utilising the iQ SYBR Green® RT-PCR kit

Reaction	Conditions
iScript Reverse Transcription activation	95°C for 3 min
PCR cycling and detection (for 30 cycles)	95°C for 20 sec
	63°C for 10 sec
	72°C for 20 sec
Melt curve analysis	95°C for 1 min
	55°C for 1 min
	55°C for 10 sec (80 cycles, increased by 0.5°C after each cycle)

PCR = polymerase chain reaction.

[1] iQ SYBR Green® is a registered trademark of Molecular Probes, Eugene, OR, U.S.A.

In both methods, the expression on MT genes as well as the housekeeping genes listed in Table 5.11, was measured by in an increase in the fluorescence of SYBR Green. Every Real-Time PCR reaction included a negative control and the reactions for each sample were performed in duplicate. The mean values were utilised for calculations. The melt-curve analysis following the PCR contributed to distinguishing the specificity of the PCR products. In a case where non-specific amplification was detected, conventional PCR was utilised to optimise the conditions.

The fluorescence for each of the reactions was displayed graphically on the Bio-Rad iCycler™ iQ optical system software version 3.0. From this presentation of results the cycle threshold (Ct) value was determined by the software. The Ct value is defined as the number of cycles needed for the fluorescence signal to reach a specific threshold level of detection. A threshold level was determined and the value was maintained for all the analyses performed. This value was set to the log linear range of the amplification curve. To estimate the PCR efficiency of each of the primer sets listed in Table 5.11, the PCR efficiency was first analysed by measuring serial dilution from 75 $ng.\mu l^{-1}$ to 0.12 $ng.\mu l^{-1}$ via the use of Equation one indicated in Table 5.14. The GeNorm software version 1.4 was utilised to determine the normalisation values. The formulas indicated in Table 5.14 were utilised to evaluate the relative expression ratio for each for the MT genes.

Table 5.14: Equations utilised for the determination of the relative expression of MT-2A and housekeeping genes

Equation number	Equation
1	$E = 10^{(-1/s)} - 1$
2	$Q = E^{(\text{minCt} - \text{sampleCt})}$
3	$SDQ = E^{(\text{minCt} - \text{sampleCt})} \ln E.\ SD\ \text{sample}$
Normalisation factor	
4	$NF_n = \sqrt[n]{QHKG_1 \cdot QHKG_2}$
5	$SDNF_n = \sqrt{\left(\frac{SDQHKG_1}{n.QHKG_1}\right)^2 + \sqrt{\left(\frac{SDQHKG_n}{n.QHKG_n}\right)^2}}$
Normalised expression	
6	$NE = \frac{Q}{NF}$

E = PCR efficiency; s = slope of graph; Ct = cycle threshold; Q = Relative quantity of gene expression; *min* = minimum; SDQ = standard deviation of the relative quantity; NF = normalisation factor; n = total number of housekeeping genes; HKG = housekeeping gene; $SDNF_n$ standard deviation of the normalisation factor; NE = normalised expression; SD = standard deviation. Adapted from Muller *et al.* (2002) and Pfaffl *et al.* (2002).

5.6 ELISA FOR HUMAN METALLOTHIONEIN

The detection of metallothionein protein was achieved by the utilisation of the enzyme-linked immunosorbent assay (ELISA) that provided a non radioactive measurement of MT proteins. This method is based on the competitive ELISA setup reported by Butcher *et al.* (2003) with modification described in Section 6.5. 96-well microtitre plates were coated with 100 µl coating buffer (2 $\mu g.ml^{-1}$ standard metallothionein obtained from rabbit liver, (Sigma Aldrich) and 0.1 M $NaHCO_3$ at pH 9.6). The plates were coated overnight at 4°C to obtain maximum coating. A dilution series of MT standards were simultaneously prepared in Eppendorf tubes, ranging from 0.02 $\mu g.ml^{-1}$ to 200 $\mu g.ml^{-1}$. Primary antibody (mouse monoclonal antibody to metallothionein in PBS, supplied by Stressgen) at a concentration of 1:1,000 in 1% Tween 20®[1] in PBS, was added to the standards, and to the samples, to a total volume of 320 µl (160 µl sample or standard and 160 µl primary antibody) . The mixtures incubated at 4°C overnight.

The coating buffer was decanted and followed by the addition of the blocking buffer (0.3% BSA in 0.05% Tween 20®). The buffer was incubated in the plates for 1 hr at room temperature and all unbound areas blocked to prevent non-specific binding of the primary antibody. The blocking buffer was decanted subsequent to the 1 hr incubation period and the plate washed three times with the wash buffer (1 X PBS, 0.05% Tween 20®). To each of the wells, 100 µl of the standards-primary antibody and sample–primary antibody mixtures were added in triplicate subsequent to the wash step. The plate was incubated at room temperature for 60 min with shaking. The reaction that occurred during the incubation period entailed the binding of the unbound primary antibody to the antigen coated onto the surface of the plate. Thus after incubation the sample-primary antibody and standard-primary antibody conjugates were washed off. The remaining primary antibody was bound onto the MT-coated plate.

To each well, 100 µl (1:5,000) of the detection antibody (Goat anti-mouse immunoglobulin G (IgG): horse radish peroxidase (HRP) conjugate, Zymed™[2]), was added and incubated for 60 min at room temperature with shaking, followed by a wash step 5 times. A 100 µl of the detection antibody substrate 3,5,3',5'-tetramethylbenzidine (TMB), which yields a coloured product upon reacting with HRP. The reaction was stopped by the addition of 100 µl of 1 M HCl. The absorbance was measured at 460 nm on a FL600 Bio-Tek

[1] Tween 20® is a registered trademark of Atlas Chemical Industries Inc., Wilmington, DE, U.S.A.
[2] Zymed™ is a trademark of Zymed laboratories, San Francisco, CA, U.S.A.

microplate reader. Protein determination assay was performed as described in Section 5.4.7.1 for each of the standards and the samples. The concentration of MTs was expressed as μg MT per μg protein.

5.7 STATISTICAL ANALYSIS OF DATA

All of the statistical parameters such as the mean, median and standard deviation of the data obtained were measured via the use of Statistica©[1] version 6.1 software package unless stated otherwise. In cases where the data distribution was normal, the means were indicated by a small box. The larger box indicated the standard error of the mean and the whiskers of the box plots indicated the standard deviation. Whenever the data was not normally distributed, the median was indicated by a small box within the whisker plot. The spread of the values was represented by the larger 25-75% box, and the minimum and the maximum values of the variable were indicated by the whiskers on either end of the larger box.

The statistical significance of the results obtained from the tests performed was expressed in terms of a p-value. This value represented the probability that an error is involved in accepting the observed difference. A p-value equal to or less than 0.05 was selected in this investigation as the level of significance required. The value was selected on the basis of its conventional use, although, other levels of significance such as 0.01 may be utilised (Samuels, 1989).

In order to measure the level of statistical difference, the distribution of the data had to be determined. The Shapiro Wilk's test was performed to test for normality, where a p-value above 0.05 indicated a normal distribution of the data, i.e. Gaussian distribution. However, any p-value below the above-mentioned value was indicative of data that was not normally distributed (Watt, 1993).

In cases where the data was normally distributed, the one-way analysis of variance (ANOVA) was performed to analyse the variation between the mean values of each of the groups for each of the parameters analysed and determine the significance of the observed difference in terms of a p-value (Pavlidis, 2003). To correct for the multiple comparisons that were performed subsequent to analysing the difference in the means or medians, the Bonferroni correction was performed. This correction compensates for the

[1] Statistica© is a copyright of Statsoft Inc., Tulsa, OK, U.S.A.

probability that multiple comparisons may result in false rejection of the null hypothesis (Rice, 1995). The Student t-test was not used initially because multiple comparisons were being performed. It has been reported that the use of the Student t-test for multiple comparisons is not ideal as the chance of making a type I error, i.e. the probability of rejecting a true hypothesis, are higher, thus there is a need to correct for multiple testing bias. In addition, the estimation of the standard deviation when more than two groups are being analysed is more precise with the one-way ANOVA (Samuels, 1989). Therefore, due to the abovementioned limitations of using the Student t-test for multiple comparisons, in cases where a significant difference between the means of the data was obtained via the ANOVA, the Bonferroni corrected Student t-test was performed. This test enabled the determination of significantly different inter group comparisons.

In instances where the data was not normally distributed, the Kruskal-Wallis test was utilised to analyse the observed difference in the median values (Watt, 1993). A p-value equal to, or less than (≤) 0.05 was indicative of a 95% probability that the observed difference was due to the factors analysed and not due to chance. To further analyse the observed difference in the median values, multiple comparisons were performed via the Bonferroni corrected Mann-Whitney test. Unlike the t-test, the Mann-Whitney test is a distribution-free type of test, and was therefore utilised for data that was not normally distributed (Samuels, 1989).

One of the aims of this investigation was to determine if there was a relation between increased levels of ROS and MT genes expression. To determine if there was a correlation between the data obtained from the biochemical parameters, the Spearman ranked correlation analysis for non-parametric data was performed on Statistica©. This analysis provided the correlation coefficient (r), which is a measure that indicates the degree to which two variables have a linear relationship as well as the p-values for this association. The correlation coefficient can range from -1.00 to +1.00, with -1.00 representing a perfect negative correlation, +1.00 indicating a perfect positive correlation and 0.00 representing no correlation. Correlation coefficients less than 0.33 indicate weak relationships, those between 0.34 and 0.66 indicate a medium relationship, whereas those greater than 0.67 indicate a strong relationship (Cann, 2003). P-values greater than or equal to 0.05 were selected, and this value indicated whether the distribution of the data sets compared were distributed close to the linear regression line. The correlation analysis was performed for the Real-Time PCR data as well as the ELISA data.

The materials and methods presented in this chapter were utilised to generate the data presented in Chapter Six. A discussion of the clinical as well as anthropometric data of all 73 individuals included in the investigation is presented in Section 6.1. The results of the biochemical parameters are presented in Section 6.2, whereas those of the Real-Time PCR and ELISA are discussed in Sections 6.4 and 6.5 respectively. The data obtained for analyses performed with HeLa cells is discussed in Section 6.3.

CHAPTER SIX

RESULTS AND DISCUSSION

Reactive oxygen species have been implicated in the pathogenesis of various disorders such as T2D, which is the focus of the current research project. The mitochondrion is the primary source of ROS production via the leakage of electrons mainly from complex I and complex III as illustrated in Figure 3.2. Choski *et al.* (2004) as well as others, have postulated that the resultant protein modifications due to elevated levels of ROS within the mitochondria may lead to alterations in the functioning of the respiratory complexes, resulting in their dysfunction. This could contribute to the pathogenesis of metabolic diseases with a mitochondrial involvement. Diabetes mellitus, which may be classified as a secondary mitochondrial disorder and various mitochondrial cytopathies due to a defect in the mitochondrial proteins, such as those forming part of the OXPHOS have been reported to have a ROS aetiology (Segrouchni *et al.*, 2002). It may be concluded that although genetic alterations play a vital role in the pathogenesis of an array of metabolic disorders they are not the only factors leading to aberrant protein functioning, but other factors such as elevated ROS production may contribute to disease pathogenesis as discussed in Section 3.3. These observations emphasise the need for early detection of ROS or their metabolites.

Oxidative stress is particularly detrimental in the pathogenesis of a disorder, as it does not present with any symptoms in the initial stages and is therefore difficult to recognise. The aim of the investigation was to determine the effect of oxidative stress on the expression of MT genes under pathological oxidative stress conditions in T2D individuals. Based on recent reports, various forms of stress including the presence of these reactive species result in the induction of MT synthesis (Fornance *et al.*, 1988; Kling and Olsson, 2000). The mechanism of induction as well as the tissue specific expression still need to be elucidated.

Various techniques were employed to determine the redox status, and the ROS levels within whole blood of each member of the three groups of individuals. Real-Time PCR was utilised to analyse the expression levels of the MT genes and the MT proteins were analysed using the ELISA. The results obtained with these analyses are presented in the

subsequent Sections. Any deviations from the protocols described in Chapter Five are indicated and it is also explained why the respective alterations were performed.

6.1 PATIENT POPULATION

In this molecular investigation, three groups of individuals were recruited into the study, subsequent to the acquisition of informed consent. During the recruitment of these individuals, various questions were asked to obtain information on their life style patterns, history of diabetes in the family, medical treatment as well as anthropometric data. A summary of the responses obtained to these questions is presented in Appendix A.

Group-1, i.e. the diabetic individuals, was composed of 19 individuals who were clinically diagnosed with T2D. This group was composed of 12 males and seven females. These individuals were between the ages 48 and 79 yrs, with an average age of 66. Group-2 was a group of 12 elderly individuals who were not diagnosed with T2D, but were afflicted with other age related disorders such as hypertension and rheumatoid arthritis. The minimum and maximum ages in this group of individuals were 40 and 78 yrs respectively, with the average age being 61. This Group of individuals was not sex matched with Group-1 as it was composed of four males and eight females. When Group-1 and Group-2 were combined, 19.4% of this cohort was below the age of 50, whereas the remaining 80.6% were older than 50 yrs of age.

Group-3 included 42 individuals who were at risk for developing diabetes. The individuals comprising Group-3 formed part of the POWIRS2 study. In contrast to Group-1 and Group-2 combined, these individuals ranged between the ages 21 and 48 yrs, with 97.6% being younger than 48 yrs. Although both Group-2 and Group-3 were composed of non-diabetic individuals, Group-3 had a mean age of 29, whereas Group-2 had a mean age of 61. Therefore, based on age as well as the effect of ROS on aging, as discussed in Section 3.3.3, it was expected that a distinct difference between the levels of ROS of Group-2 and Group-3 would be obtained. The age comparisons throughout the study were based on the combined ages of Group-1 and Group-2 in comparison to those of Group-3. As discussed in Section 5.1 the criteria for classification of these individuals as being at risk of developing diabetes was based on a high BMI as well as family history of diabetes mellitus, particularly, T2D.

Due of the effect that cigarette smoking and alcohol intake have on the production of ROS, the individuals recruited into this investigation were required to indicate whether they smoked or not. Of the individuals comprising Group-1, 16% indicated that they were smoking during the time of the study and none of those in Group-2 smoked. In addition 16% of Group-1 and 17% of Group-2 were ex-smokers. When the results from the responses in Group-3 were analysed, 11.9% of this group indicated that they were smokers at the time of sampling, whereas 7.1% were ex-smokers. Approximately 42% and 33% of the individuals comprising Group-1 and Group-2 respectively consumed alcohol, although, in moderate volumes. In Group-3, 9.5% indicated that they did not take any alcohol, while the remaining 90.5% consumed alcohol, although not on a regular basis.

As presented in Table 3.11, one of the symptoms of the effect of oxidative stress particularly in the eye is corneal opacities and cataract. The aforementioned eye complications are observed at a higher incidence in diabetic individuals as opposed to non-diabetic individuals and in older individuals (Bhattacharya *et al.*, 2003). For this reason, the individuals that were recruited into this investigation were asked if they had cataract removal. When Group-1 and Group-2 were combined, 35.5% of the combined group had undergone an operation to have their cataracts removed. None of the POWIRS2 group of individuals had cataracts removed. Another eye complication that has been reported in diabetic individuals is retinopathy, which occurs mainly due to high blood glucose levels over time (Porta and Allione, 2004). Laser therapy is currently utilised to treat retinopathy, and because of this, the individuals were asked if they had ever had laser therapy. Individuals who had not undergone surgery for cataract removal also did not undergo laser therapy. However, early onset retinopathy could not be excluded, since it was not investigated by an ophthalmologist in this study. These individuals reported that they were not clinically evaluated for this condition by an ophthalmologist prior to their recruitment into this study.

At the time of recruitment, the diabetic individuals were already on medical treatment. The majority of these patients also presented with hypertension and were on medical treatment for hypertension as well. The effect of medication is further discussed in Section 6.2.1.1 on page 86. The presence of hypertension was not exclusive to diabetic individuals. Of the 12 individuals in Group-2, six were undergoing treatment for hypertension, whereas one was being treated for high cholesterol and the remaining five were not on any medication.

Other parameters that were analysed were the BMI as well as the waist hip ratio (WHR), due to these factors being characteristic in most diabetic individuals or those prone to developing diabetes, as discussed in Section 3.3.2.1. Obesity is characterised by inflammation as well as increased ROS production (Hotamisligil and Spiegelman, 1994; Dhindsa *et al.*, 2004) which eventually leads to the activation of NF-κB. Individuals with BMI values less than 25 were classified as being normal, those with BMI values between 26 and 29 were overweight and those above 30 were characterised as being obese (Hotamisligil and Spiegelman, 1995). Due to the presence of GREs within the promoter sequence of MT genes, as discussed in Section 4.1.7.3, it was expected that individuals who were obese, would present with high levels of ROS and thus higher expression of MT genes. Of the individuals comprising Group-1, 16% had a normal BMI, 37% were overweight and the remaining 47% were obese. Group-2 had 42% of individuals with normal BMI values, 17% overweight and the remaining 41% were obese. On the other hand, the majority of individuals in Group-3 (45.2%) had BMI ratios within the normal range, and 31% of this group were obese. Unlike Group-1 and Group-2 combined, a smaller percentage (16.1%) of Group-3 was overweight.

Based on the clinical as well as the lifestyle patterns presented in this Section and a detailed description in Appendix A, it was evident that although Group-2 was age matched with Group-1, it could not serve as a control group for Group-1. The presence of age related pathological conditions within Group-2 also make it unsuitable to use as a control group. Thus, the POWIRS2 group (Group-3) of individuals were designated to be the control group in this investigation, even though they were not age matched. It was envisaged that this factor would minimise the reported increase in the levels of ROS with age (Lenaz,1998).

6.2 OXIDATIVE STRESS IN DIABETIC AND NON-DIABETIC INDIVIDUALS

It has been reported that various forms of stress lead to an increase in MT expression, particularly in the liver (Karin *et al.*, 1980; Sato and Bremner, 1993; Fraga and Oteiza, 2002). Even though oxidative stress has been suggested to also lead to an over expression of MT, the mechanism of how this occurs and which tissues it occurs in still requires clarification. Therefore, the aim was to investigate the role of ROS production in T2D individuals in the expression of MT genes during this molecular study.

6.2.1 Biochemical analyses

Due to the fact that various metabolic and biochemical pathways are affected by the presence of high levels of ROS, a few of these processes were analysed in the respective samples. The profiles obtained from these biochemical analyses including the RNA and protein data are discussed in detail in the subsequent paragraphs.

6.2.1.1 d-ROMs test

The reactive oxygen metabolites that were measured via this assay are characterised by having an odd number of electrons in the most external orbit of the oxygen. Because of their reactivity, they form derivatives that maintain good chemical reactivity and good oxidising power. Upon the addition of the chromogenic solution provided with the d-ROMs test kit, a coloured complex, which was measured at 510 and 550 nm, was produced. According to Table 5.4 healthy individuals have values ranging between 250-300 CARR U. This value has been noted to differ depending on the season of the year the samples were collected and analysed. In summer, the majority of healthy individuals range within 260-270, whereas in winter their values ranged from 280-290 CARR U. All individuals included in this investigation were recruited during winter. A factor that may lead to elevated ROS in winter may be the increased activity of the immune system via the increased respiratory action of activated phagocytic cells which produce ROS (Iorio, 2002). The increased activity of the OXPHOS system during the winter period to produce heat via the coupling of oxidation and phosphorylation may also in turn lead to high production of ROS, as discussed in Section 3.1.5.

Upon analysis of the d-ROMs data with the Shapiro Wilk's test on Statistica©, a p-value of 0.045 was obtained, indicating that the data did not have a normal distribution, i.e. a non-Gaussian distribution, as illustrated in Graph 6.1. As discussed in Section 5.7, according to the Shapiro Wilk's test, a p-value of greater than 0.05 indicated a normal distribution of the data. The raw data from which Graph 6.1 was derived from is presented in Appendix B.

Graph 6.1: Representation of the d-ROMs test data distribution for all groups

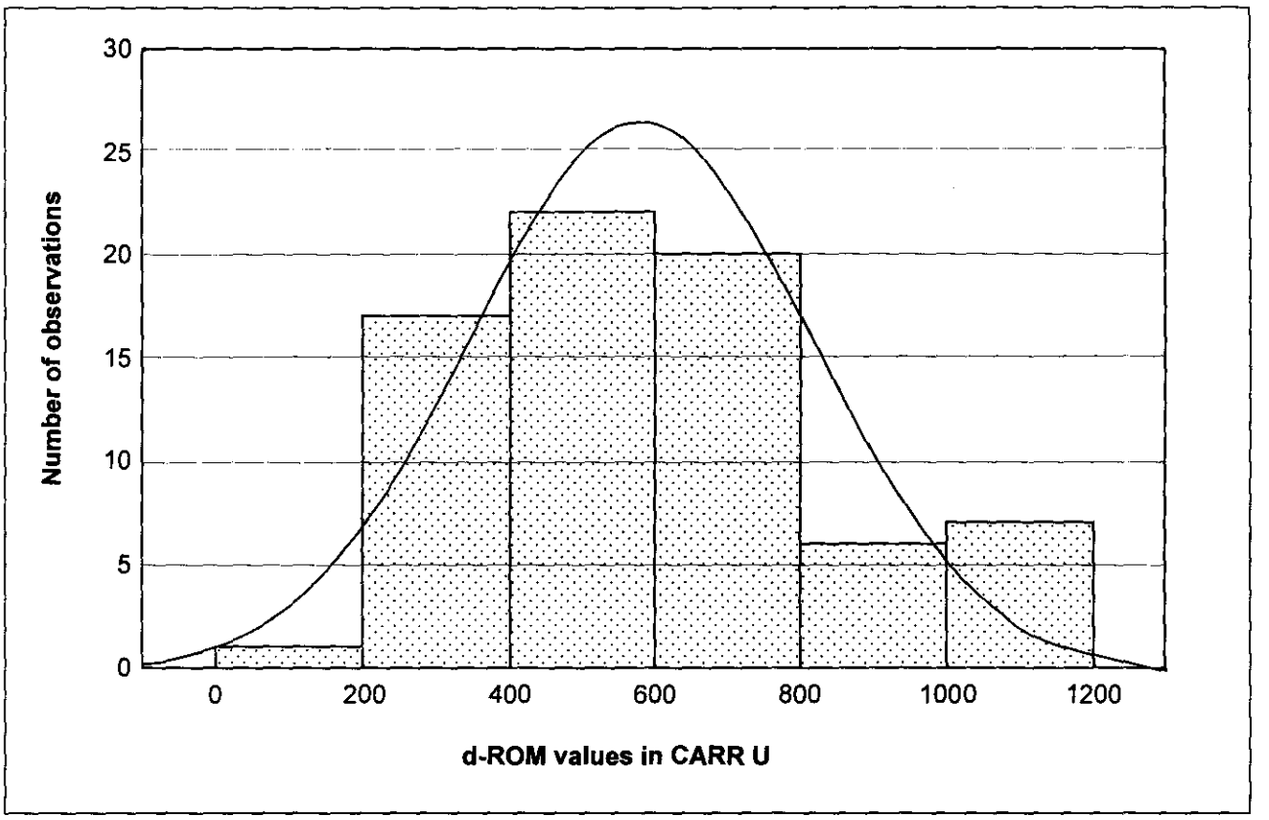

The curve indicates the expected distribution curve if the data is normally distributed; the bar graph indicates the distribution of d-ROM data in CARR U analysed in this investigation.

The mean values, median, and standard deviation for each group of individuals are presented in Table 6.1. The mean value observed for Group-2 was much greater than that of Group-1 and Group-3. This could be attributed to the observation that 75% of this group presented with values greater than 500 CARR U. The largest variation was observed in Group-1 as indicated by a standard deviation value greater than that of the Group-2 and Group-3, as well as the overall standard deviation.

Table 6.1: Summary of the results of the d-ROMs test

Group	Mean	Median	Minimum	Maximum	Standard deviation
Group-1	584.1	550.0	200.0	1015.0	243.5
Group-2	761.2	766.5	394.0	1162.0	229.5
Group-3	540.5	514.5	214.0	1118.0	220.9
Group-1 and Group-2	652.6	629.0	200.0	1162.0	250.2
All groups	588.1	546.0	200.0	1162.0	238.7

All non-diabetic individuals (Group-2) were within the moderate oxidative stress to heavy oxidative stress range as indicated by the minimum and maximum values in Table 6.1. The T2D patients (Group-1), on the other hand, varied from normal ranges to heavy

oxidative stress. The at-risk group of individuals (Group-3) displayed a broader range of values. However, the median value for Group-3 was lower than that of the other two groups. This difference was also observed when the elderly individuals, i.e. Group-1 and Group-2, were grouped together and compared to Group-3.

A graphical illustration of the results obtained from T2D patients (Group-1), elderly non-diabetic individuals (Group-2) as well as individuals forming part of the POWIRS2 group (Group-3) is presented in Graph 6.2. Elderly non-diabetic individuals (Group-2) who were expected to have d-ROMs values lower than the patient group (Group-1) exhibited the opposite result, as depicted in Graph 6.2. This observation can be explained by the fact that the diabetic individuals (Group-1) were already on medication such as Glucophage®[1]. This antihyperglycaemic agent improves glucose tolerance and lowers basal and postprandial plasma glucose. The treatment of T2D with such medication may have reduced ROS production in this group of individuals. The d-ROMs values of Group-2 were found to be higher than those of Group-3. This observation was expected due to the reported effect of ROS on ageing and the increase of ROS production with age (Lenaz, 1998). However, the difference between the d-ROMs values of Group-2 and Group-3 were not significantly different, as indicated in Table 6.2.

As discussed in Section 3.3.2.1 high levels of glucose increase intracellular ROS production from the mitochondria in the β-cells, which in turn results in reduced glucose induced insulin secretion. Hyperglycaemia also destroys the overall effect of the cellular antioxidant mechanisms. Although the levels of oxidative stress are high in the circulatory system of individuals in Group-1, it is still relatively lower than in individuals who are not on any medication for the treatment of diabetes, i.e. Group-2. This indicates that, to a certain extent, the medication does influence the oxidative status in blood of these individuals.

[1] Glucophage® is a registered trademark of Merck Santé S.A.S., associate of Merck KGaA, Darmstadt, Germany.

Graph 6.2: Representation of the d-ROMs test results

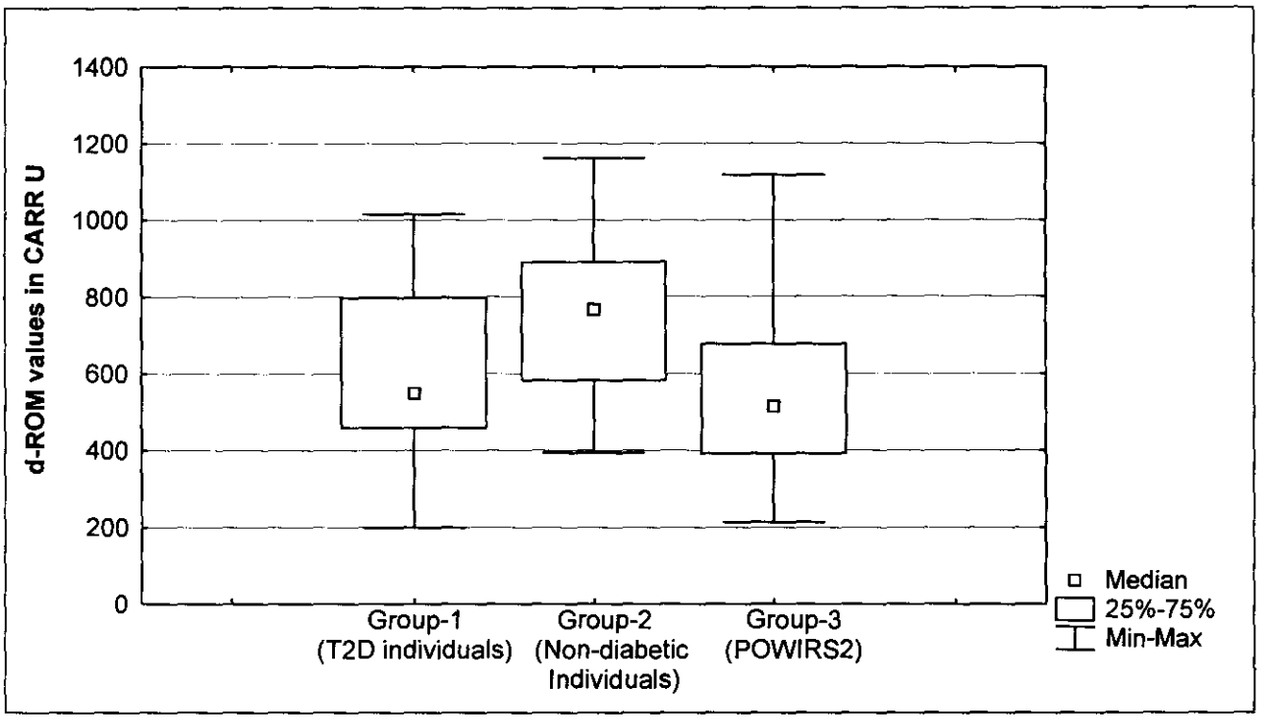

Due to the non-Gaussian distribution of the d-ROMs data, the Kruskal-Wallis test was employed for the analysis of variation between the medians of the three groups. An overall difference (p-value = 0.020) was detected by the Kruskal-Wallis test between the three groups. It was imperative to perform multiple comparisons via the Mann-Whitney U test to establish whether the difference obtained was due to the intracellular levels of ROS or if it was by chance, as well as to determine the significance of the difference observed. However, given the probability of multiple testing bias, Bonferroni corrected Mann-Whitney U tests were performed. The values indicated in Table 6.2 are the p-values obtained from this test.

Table 6.2: p-values obtained for intra group comparisons via the Bonferroni corrected Mann-Whitney U tests for the d-ROMs analyses

Group number	Group-1	Group-2	Group-3
Group-1			
Group-2	0.167		
Group-3	1.000	**0.016**	

The values indicated are rounded off to the third decimal; p-values < 0.05, indicating statistical significance, are presented in bold. Grey shaded cells contain no data.

It can be suggested from Table 6.2, that there is no significant difference between the d-ROMs values of Group-1 and Group-3, as indicated by a p-value of 1.000, which is greater than the statistically significant p-value of 0.05. However, Group-2 and Group-3 presented a significant difference with a p-value of 0.016, as indicated by the bold text in

Table 6.2. Even though there is a difference between Group-1 and Group-2, it is below the 95% level of statistical significance, as indicated by a p-value of 0.167. This observation supported the conclusion stated in Section 6.1 that Group-2 should not serve as a control in this investigation. It is also suggested that a larger sample size should be analysed in order to provide results that are more representative of these groups. When Group-1 and Group-2 were combined and the Bonferroni corrected Mann-Whitney U tests were performed, as discussed in Section 5.7, to determine if there is a significant difference between this combined group and Group-3, a p-value of 0.409 was obtained. This value indicated that there is no statistically significant difference between Group-3 and the combined Group-1 and Group-2.

The d-ROMs test has been demonstrated to be a valuable tool in the evaluation of metabolism in obese and diabetic patients (Dandona and Aljada, 2002). Because of the significantly high levels of lipid peroxides in individuals with high BMI as compared to those with normal BMI (Hotamisligil and Spiegelman, 1994), the d-ROMs values obtained in this study were expected to be higher in obese individuals. This would be in agreement with the reported presence and the role of ROS and obesity in the pathogenesis of diabetes. In the cohort of T2D individuals (Group-1) and non-diabetic individuals (Group-2), 77.4% had BMI values greater than the normal value of 25. The rest of the group had lower BMI values, although their d-ROMs values were indicative of heavy oxidative stress. The lack of significant difference obtained for the d-ROMs data may be attributed to the lack of a strong correlation ($r = -0.007$ with a corresponding p-value of 0.950) between the BMI values and the d-ROMs data in these three groups. Another factor may have been the presence of a small difference in the percentage of obese individuals between the three groups as discussed in Section 6.1 page 83. From these d-ROMs test results, as well as the effect that the lifestyle factors discussed in Section 6.1 have on oxidative stress, it is evident that various factors affect the oxidative status within serum. The effect of incorrect life styles, e.g. smoking and alcohol intake on ROS production observed in this study is consistent with that reported by Dhindsa *et al.* (2004). These life style factors will collectively affect the outcome of the d-ROMs test. Although this data was present at the beginning of the study, due to a large proportion of the general population being exposed to pollutants that increase the production of ROS (Prithivirajsingh *et al.*, 2004), selection against these parameters would not have provided an accurate representation of the population at large.

Due to the complex nature of diabetes, this test can not serve as a reliable indicator of increased reactive metabolites on its own. Based on the factors discussed in Section 6.1,

the d-ROMs test results and the reports by Dhindsa *et al.* (2004) and Prithivirajsingh *et al.* (2004), a conclusion regarding the oxidative status within a biological sample cannot be made from measuring a single parameter, lending credence to the analysis of the antioxidant activity within serum obtained from these individuals.

6.2.1.2 ORAC assay

The primary antioxidant activity of serum is derived from micro molecules such as ascorbic acid, Vitamin E, β-carotene and macromolecules such as transferin. Even though antioxidant enzymes such as SOD and GSHPx have lower antioxidant capacity in serum, they also aid in eradicating free radicals. The different antioxidant components active in the serum make it difficult to measure the antioxidant capacity of each of them. This limitation lends credence to the use of an assay that measures the total antioxidant capacity, such as the ORAC assay (Cao *et al.*, 1996). When measuring the antioxidant capacity in each of the serum samples via the ORAC assay two major factors were considered, that is, the time that the inhibition lasted as well as the percentage of inhibition at different time intervals, in terms of fluorescence. The ability to define these two parameters is an advantage of the use of the ORAC assay (Cao and Prior, 1998). An additional advantage of the ORAC assay is that it does not distinguish between the hydrophilic and lipophilic antioxidants (Prior *et al.*, 2003).

The antioxidant capacity of the various antioxidants differs, thus not resulting in the general lag phase, as depicted in Graph 6.3. This difference in the decay of the fluorescence of fluorescein is illustrated for various concentrations of Trolox (vitamin E). The decrease in emission of florescence due to the damage to fluorescein does not follow zero-order kinetics (i.e. linear with time), thus suggesting that the interpretation of the antioxidant capacity based of the standard curve should not assume zero-order kinetics. To overcome these difficulties, the area under the curve was utilised to quantify the antioxidant capacity of each sample, in Trolox Units. Another factor that could have masked the antioxidant response was the presence of proteins within the serum sample. This was eliminated by precipitating the proteins with the addition of 0.5 M PCA in a 1:1 ratio.

Graph 6.3: Representation of results generated with Trolox standards via the ORAC assay

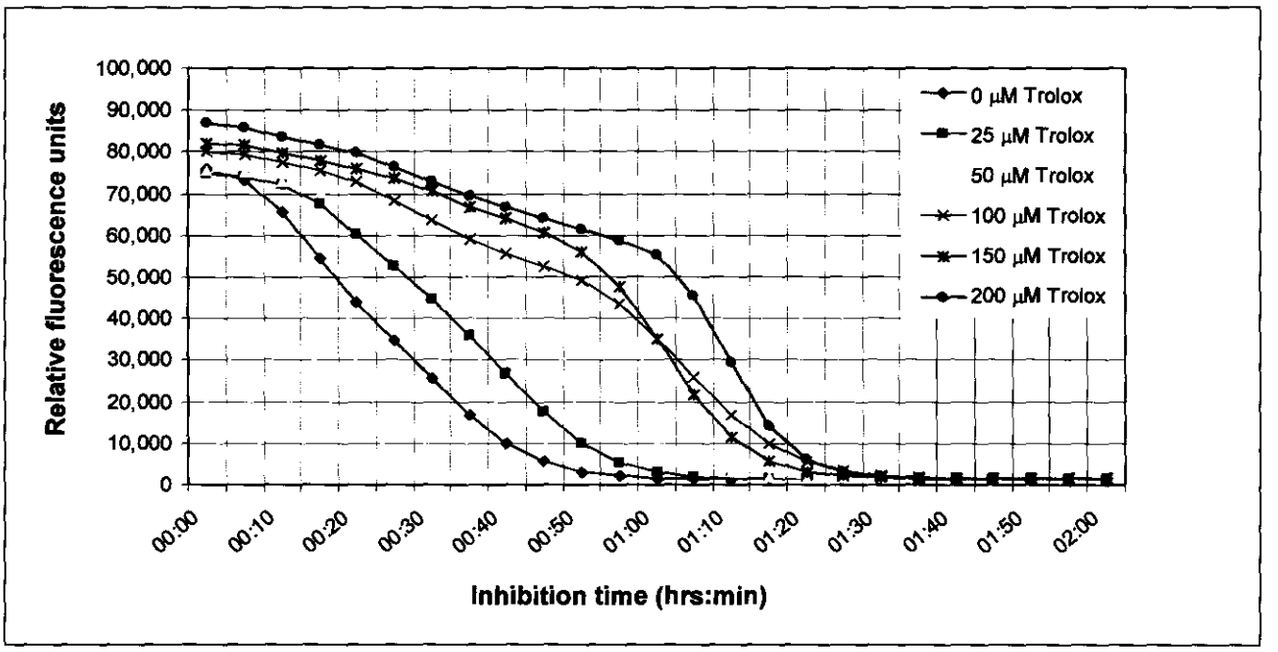

hrs = hours; min = minutes.

To determine the total antioxidant capacity of each sample, the ORAC value in Trolox Units was estimated using the standard curve depicted in Graph 6.4 representing the area under the curve of each of the Trolox standards presented in Graph 6.3. The standard curve was drawn from the results obtained from the standards with varying concentration of Trolox (as indicated in Table 5.5) as well as Equations 5.2 and 5.3. From this data, the total antioxidant capacity within the serum samples was determined. The ORAC values of the samples were within the same range as those of the standards. The readings were performed over a period of 2 hrs and no significant differences were observed after 1.5 hrs.

It was reported in a study by Sacheck *et al.* (2003), that in older individuals, between the ages of 65 and 80 yrs , the baseline ORAC value in Trolox Units is ca. 675 µM, whereas in younger individuals between 18 and 35 years this value is ca. 720 µM. This data was, however, based on the antioxidant capacity of lipophilic antioxidants. Prior *et al.* (2003) reported that the total antioxidant capacity taking into account both the hydrophilic and the lipophilic antioxidant components in serum, as measured with the ORAC assay is ca. 1,807 µM for individuals between 60 and 71 years of age and 1,909 µM for individuals between ages 22 and 40 yrs. The low ORAC values that were detected in all three groups as indicated in Appendix B, may be attributed to various factors such as the type of nutrients consumed before blood collection and whether these individuals were taking antioxidant supplements. These aspects, which are further discussed in the subsequent

paragraphs of this section, may affect the outcome of both the d-ROMs test data and the ORAC data.

Graph 6.4: Standard curve of Trolox standards at varying concentrations

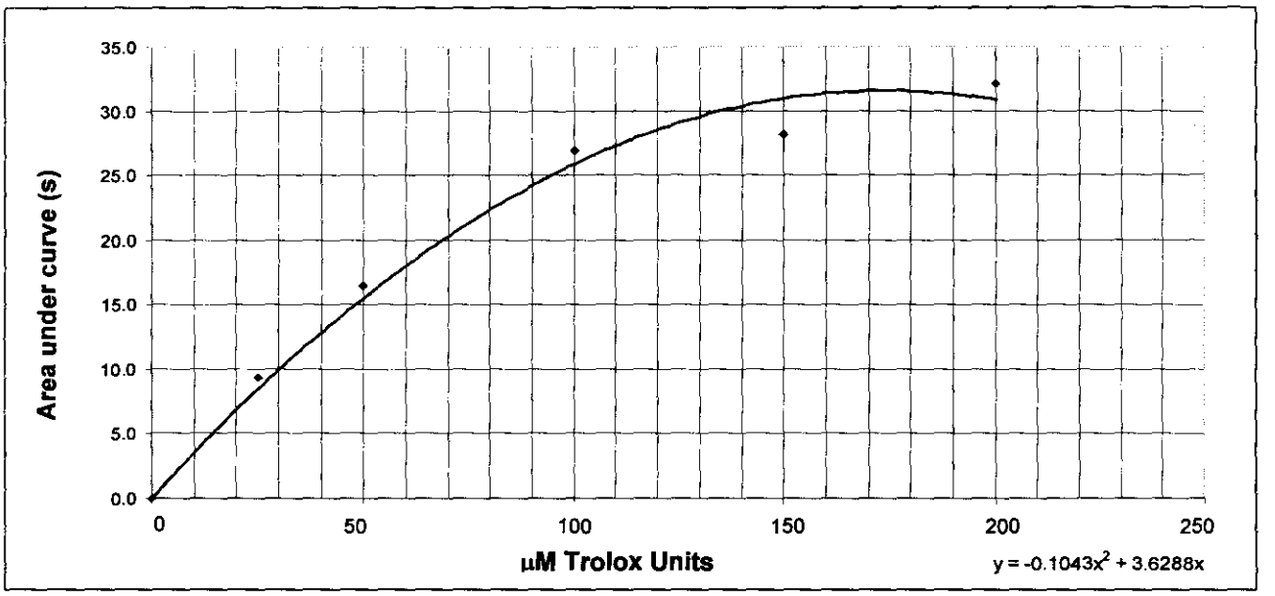

S = area under the fluorescence curve for each of the Trolox standards.

Subsequent to analysis of the data via the Shapiro Wilk's test, it was evident that the ORAC data obtained for the three groups of individuals was not normally distributed (p-value = 0.013) as depicted in Graph 6.5. The one-way ANOVA was thus not performed.

Graph 6.5: Representation of the analysis of the distribution of the ORAC data

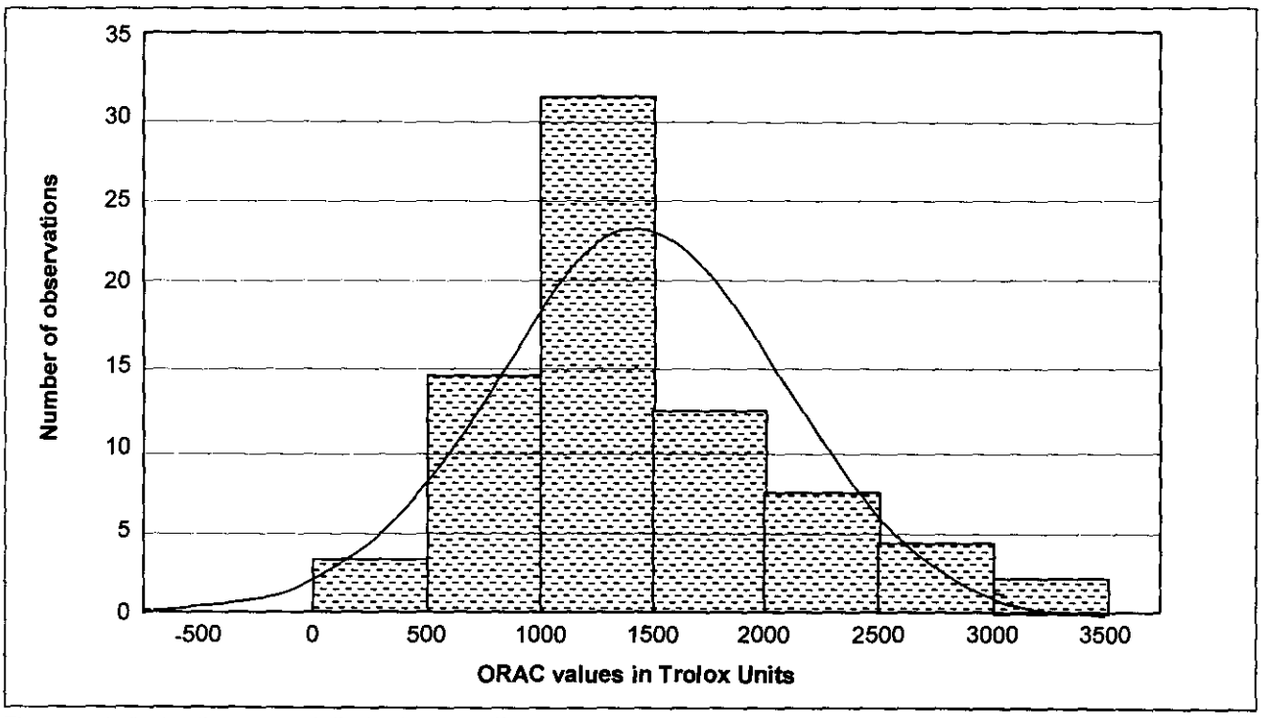

The curve indicates the expected distribution curve if the data is normally distributed; the bar graph represents the distribution of the ORAC data in Trolox units, analysed in this investigation.

A summary of the results for the ORAC values in Trolox Units for each group is presented in Table 6.3. As indicated by the mean values in Table 6.3, Group-3 had a mean value closest to the normal range. However, the standard deviation within this group was the highest of the three groups. This can be attributed to the high variation in the ORAC data of this group of individuals. The values obtained for each individual are presented in Appendix B.

Table 6.3: Summary of the results of the ORAC test

Group	Mean	Median	Minimum	Maximum	Standard deviation
Group-1	1366.5	1212.0	615.0	2633.0	539.3
Group-2	1392.8	1382.0	554.0	2566.0	564.6
Group-3	1510.1	1379.5	198.0	3253.0	719.5
Group-1 and Group-2	1376.6	1313.0	554.0	2633.0	540.0
All groups	1453.5	1359.0	198.0	3253.0	648.6

The observed high standard deviation in Group-3 may be due to the high variation in the BMI values of individuals comprising this group, as illustrated in Appendix A. A family history of diabetes mellitus was present in 38% of Group-3. However, a cohort of the individuals with a family history of diabetes did not present with low ORAC values. Within this cohort, no distinct group of characteristics could be identified. From this observation it can be suggested that various factors, such as those discussed in Section 6.1, as well as genetic predisposition may affect the antioxidant capacity, however their contribution varies in each individual.

A graphical representation of the distribution of the ORAC values in Trolox Units for the three groups of individuals is illustrated in Graph 6.6, where the minimum and the maximum values of Group-3 represent the largest range of the three groups. The results presented in this Section highlight the importance of the early detection of hyperglycaemia which eventually has an effect of the production of ROS by the respective cells.

Graph 6.6: Illustration of the ORAC data between the three groups

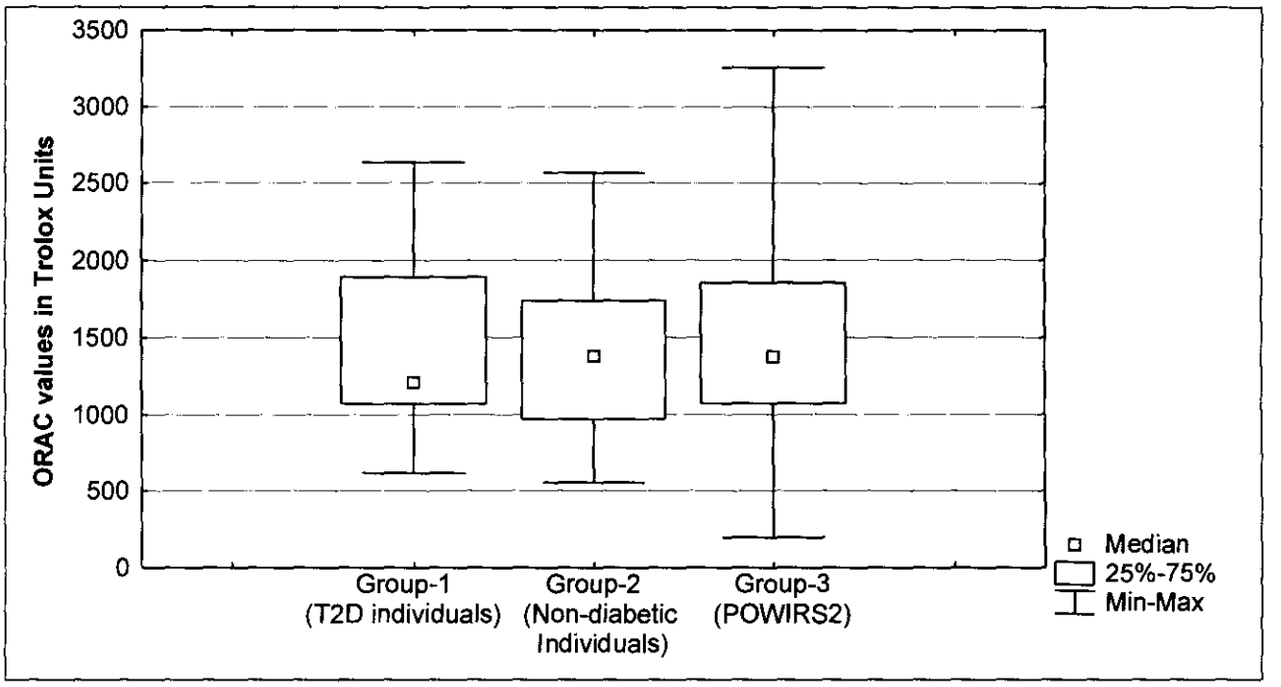

The Kruskal-Wallis test was carried out to test for a significant difference between the median values of the three groups. From this analysis, no significant difference for the ORAC analyses (p-value = 0.711) was observed within this data set.

In this investigation, 3 of the 31 individuals in Group-1 and Group-2 combined, exhibited high levels of antioxidant capacity i.e. 9.67%, as indicated by the values above the reported 1909 μM in Appendix B. Of this group, 38.7% presented with antioxidant capacity much lower than the normal range, i.e. values between 554 and 984 μM. The remaining 51.63% were within the normal range and the threshold of 1,200 μM. In Group-3 (POWIRS2), 23.8% displayed high levels of antioxidant capacity, 28.6% demonstrated low values, whereas the rest of the group presented with values within the normal range and the threshold value.

It can be suggested from the low ORAC values of the 38.7% of Group-1 combined with Group-2 and the 23.8% of Group-3, that there is depletion in the endogenous antioxidants at a period, which, according to the d-ROMs test data, corresponds to high levels of oxidative stress. Another important factor to consider with regard to Group-1 and Group-2 is that most individuals were elderly and were also affected by other ROS related disorders such as hypertension, which could affect their antioxidant status. As discussed in Section 6.2.1.1, the individuals comprising Group-1 were already on medication. It was expected that if the medication did reduce the levels of ROS, by reducing hyperglycaemia, as

illustrated from the results obtained for the d-ROMs test, the values for the ORAC assay would be lower than those of Group-2 and Group-3. This observation, as depicted in Table 6.3, may be due to the lower antioxidant capacity required in blood of the diabetic individuals (Group-1).

To obtain an indication of the effects of the aforementioned factors on the antioxidant capacity within whole blood of these individuals, it would be essential to perform an oral glucose tolerance test in a future study, in order to determine the glycaemic state of these individuals. It is suggested that various factors such as BMI, age, as well as predisposition to hyperglycaemia may have affected the antioxidant status in whole blood of these individuals.

There are reports indicating that the intake of fruits and vegetables (2-3 servings) provides ca. 1,640 Trolox Units (Silliman *et al.*, 2003). The dietary antioxidants that are found in foods such as fruits, vegetables, wine, beer and other foods were not taken into consideration during the recruitment of Group-1 individuals. This is mainly due to the fact that these were patients who came to the diabetes clinic to collect medication, therefore making it difficult to put them on a specific diet prior to blood collection. This factor may have thus influenced the results obtained from this analysis. Although diet was envisaged to affect the outcome of the ORAC data, this test was performed to analyse the feasibility of using it in the absence of a controlled diet. However, prior to fasting the individuals comprising Group-3 (POWIRS2) were put on a controlled diet, composed of complex carbohydrates, low fat and protein. Thus for this group of individuals, the effects of these foods were negligible.

The ORAC assay is widely accepted as a standard tool to measure the antioxidant activity in the pharmaceutical and food industries (Prior and Cao, 1999; Huang *et al.*, 2002). The ORAC assay detects the radical absorbance capacity and not directly oxidative stress. The inability to distinguish between the T2D patients and the elderly non-diabetic individuals based on the ORAC data highlights the importance of a molecular biomarker for the detection of the antioxidant capacity as well as oxidative stress in ROS related disorders. The proportion of individuals who displayed high antioxidant capacity, presented with high oxidative stress levels as indicated by the d-ROMs test. This observation, which was not expected, supports the utilisation of a combination of techniques to characterise the oxidative stress levels within a specific tissue. Detailed results of the ORAC assay for each sample are presented in Appendix B.

6.2.1.3 Glutathione redox analysis

GSH, a low molecular weight γ-glutamylcysteinylglycine tripeptide with a free thiol group is an important biomarker for oxidative stress. It plays a vital role in the resistance to oxidative stress by providing reducing equivalents of enzymes, such as GSHPx and glutathione reductase and other protein thiols involved in eradicating ROS. The measurement of the glutathione status in blood is a valuable tool as it reflects of both GSH and GSSG in other less accessible tissues, thus making this test a reliable indicator of oxidative stress. As discussed in Section 3.3.2, the hyperglycaemia in diabetic patients indirectly leads to the depletion of GSH by means of the consumption of NADPH via the pentose phosphate pathway (Lee and Chung, 1999). It was therefore hypothesised that in insulin resistant diabetic individuals (T2D), the levels of GSH will be greatly reduced as compared to the control samples. This result would provide evidence for the consumption of the antioxidant molecule to combat oxidative stress. The decrease in GSH and the increase in GSSG levels, with the result being the reduction of the GSH:GSSG ratio are therefore important contributing factors to consider in the pathogenesis of T2D, ageing and other associated complications. In a case where the cell is exposed to increased oxidative stress, the ratio will also be decreased as a result of the increased GSSG content.

During sampling, GSH oxidation, which is driven by unidentified reactions in which oxyhaemoglobin is involved, results in the artificial oxidation of GSH. This auto-oxidation leads to an overestimation of GSSG (Asensi *et al.*, 1999). Due to this fact, the accuracy of this test was highly dependent on the prevention of auto-oxidation of GSH during sample preparation by the addition of M2VP, thus giving a true representation of the concentration of GSSG within the sample at the time of sampling. Various other thiol trapping agents such as *N*-ethylmaleimide (NEM) or iodoacetic acid (IAA) can be utilised to prevent the auto-oxidation process (Giustarini *et al.*, 2003), however, M2VP was chosen due to its fast binding characteristics to GSH compared to other trapping agents listed above (Asensi *et al.*, 1999).

A variety of techniques are currently utilised to determine the GSH and GSSG ratio. These include high performance liquid chromatography (HPLC), nuclear magnetic resonance (NMR), capillary electrophoresis and spectrophotometry. In this investigation, spectrophotometry was readily available and was the method of choice. From an investigation by Giustarini *et al.* (2003) where a variation of the conventional HPLC method for glutathione status determination was utilised, it was reported that in healthy individuals,

the GSH:GSSG ratio is 349.30 (GSH = 1,359 μM and GSSG = 4 μM). The ratio reported by Giustarini *et al.* (2003) was utilised in the current investigation as a reference to characterise the observed GSH:GSSG ratio. According to the Shapiro Wilk's Test, the data for the GSH:GSSG ratio was not normally distributed (p-value = 0.000), as indicated in Graph 6.7. The data was skewed to the left.

Graph 6.7: Representation of the analysis of the distribution of the GSH:GSSG ratio data

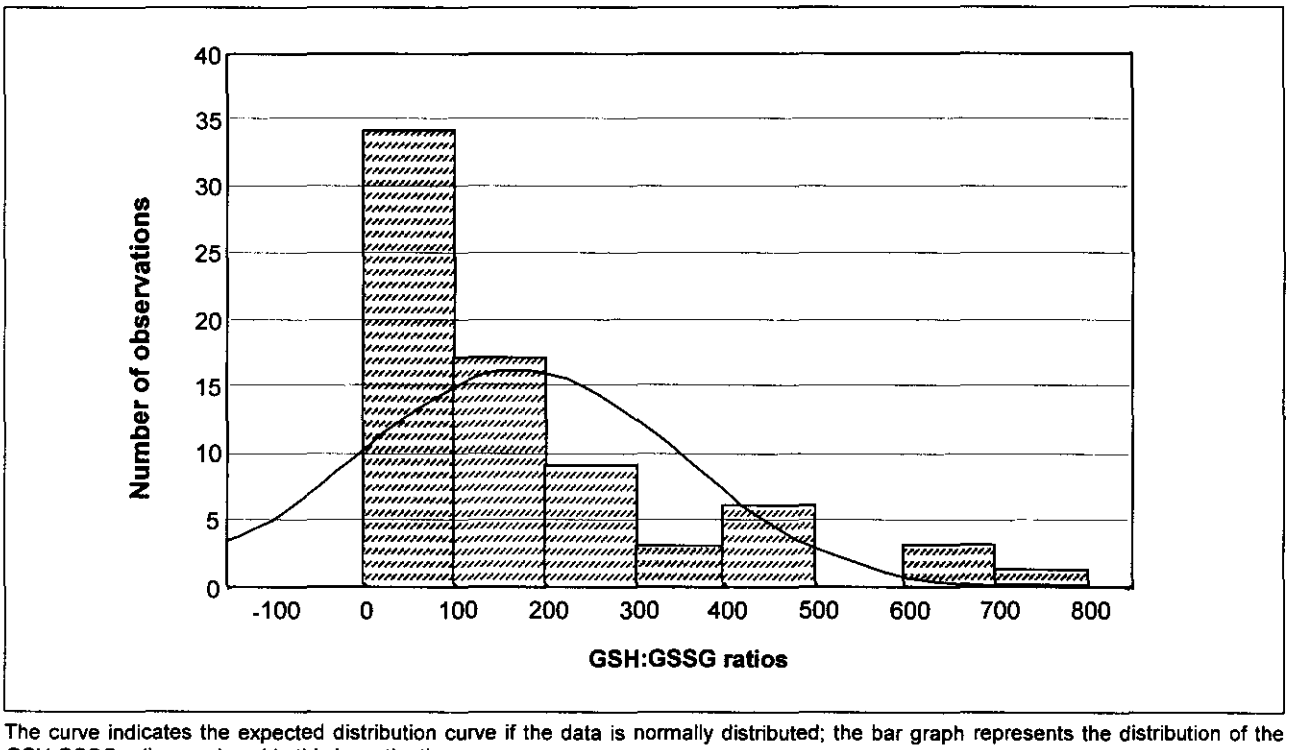

The curve indicates the expected distribution curve if the data is normally distributed; the bar graph represents the distribution of the GSH:GSSG ratios analysed in this investigation.

A mean value of 79.36 was obtained for Group-1 as indicated in Table 6.4. Upon analysis of the GSH:GSSG ratio in Group-2, it was evident that these individuals had a low mean ratio (166.67) when compared to the reported value in normal individuals. However, this value was higher than that of the diabetic individuals, i.e. Group-1. This result was expected due to the results obtained from the d-ROMs test. The high standard deviations obtained for Group-2 and Group-3 compared to Group-1, as presented in Table 6.4, may be attributed to the high variation observed in the GSH:GSSG ratios in these two groups of individuals. The observed variation may be due to the varied effects of other antioxidant mechanisms utilised by the cells such as SOD and catalase, which were not individually analysed in this investigation.

Group-3 had a mean ratio closer to that observed in normal individuals. Two individuals in Group-3 (1521 and 1523) displayed very high values, 1776.82 and 1515.87 respectively,

for this analysis as indicated in Appendix B. These two samples were repeated and similar results were obtained. These outliers were omitted for the purpose of statistical analysis since they resulted in a high standard deviation as well as high maximum values for this group of individuals. Individual 1521 who presented with a GSH:GSSG ratio of 1776.82, had a BMI value of 40.2 and a maternal history of T2D, whereas individual 1523 had a value of 23.4, and consumed alcohol. This difference in the BMI values of these individuals with high ratios indicates that various factors affect oxidative stress. It is therefore suggested that in the future study a comprehensive clinical and lifestyle profile of each individual be included.

Table 6.4: Summary of the results of the GSH:GSSG ratio analysis

Group	Mean	Median	Minimum	Maximum	Standard deviation
Group-1	79.4	33.2	5.0	393.0	100.6
Group-2	166.7	32.4	7.0	697.8	262.7
Group-3	218.0	159.3	5.6	713.2	170.1
Group-1 and Group-2	113.2	33.2	5.0	697.8	182.3
All groups	173.5	123.96	5.0	713.2	181.8

A distinct variation in the mean values for the GSH:GSSG ratio was observed between the individuals who formed part of Group-3 and those of Group-1 and Group-2 combined. It is therefore suggested that the GSH concentration in individuals comprising Group-3 was much higher than Group-1 and Group-2 and that the GSSG levels were much lower. Even though the mean GSH:GSSG ratio, i.e. 217.99 in the POWIRS2 group of individuals was below that reported by Giustarini *et al.* (2003), it was however, not as greatly reduced as the values of Group-1 and Group-2. From this data it can be suggested that the high oxidative stress conditions illustrated in the d-ROMs test and the ORAC results may have resulted in a low GSH:GSSG ratio, and are thus indicative of a lowered concentration of GSH available to scavenge the ROS. A graphical representation of these results is presented in Graph 6.8, indicating the median as well as minimum and maximum values of this data set.

Graph 6.8: Representation of GSH:GSSG ratio between the three groups

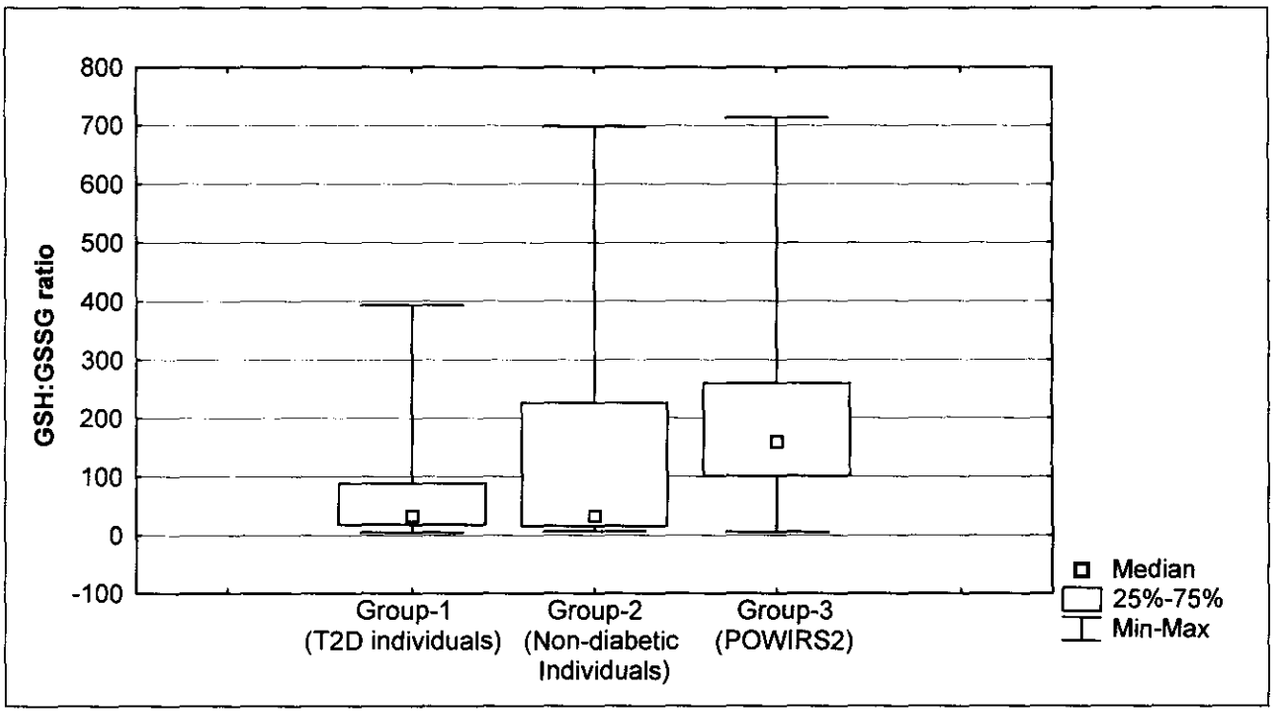

To analyse the differences between the median values of the three groups, the Kruskal-Wallis test was performed and a p-value of 0.0002 was generated. This indicated that a significant difference existed between the medians of the three groups. Bonferroni corrected Mann-Whitney U tests were performed to analyse the inter group median differences. The p-values obtained from these analyses are indicated in Table 6.5.

Table 6.5: p-values obtained for inter group comparisons via Bonferroni corrected Mann-Whitney U tests for the GSH:GSSG ratios

Group	Group-1	Group-2	Group-3
Group-1			
Group-2	1.000		
Group-3	**0.001**	**0.021**	

The values indicated are rounded off to the third decimal; p-values < 0.05, indicating statistical significance, are presented in bold. Grey shaded cells contain no data.

A significant difference was observed (p-value of 0.001) between Group-1 and Group-3, as well as a significant difference between Group-2 and Group-3 with a p-value of 0.021, as indicated by the bold text in Table 6.5. However, no significant difference was observed between Group-1 and Group-2 (p-value = 1.000). The low median values observed for Group-1 and Group-2 when compared to that of Group-3, as illustrated in Table 6.4 indicate that due to the probable high levels of oxidative stress associated with ageing (Lenaz, 1998), this low molecular weight thiol was highly oxidised, resulting in a lowered ratio in the elderly groups (Group-1 and Group-2) compared to the younger group of individuals (Group-3).

When the combined Group-1 and Group-2 was compared to Group-3 a p-value of 0.0003 was obtained indicating a significant difference between these groups. Although there was no significant difference between these groups based on the d-ROMs data (p-value = 0.409), the data of the GSH:GSSG ratio indicated that the redox status in the individuals comprising Group-1 and Group-2 was compromised when compared to that of Group-3.

6.2.1.4 NADH:NAD$^+$ redox analysis

NAD$^+$ is involved in various biological processes, such as regulation of energy metabolism, DNA repair, transcription and is also a coenzyme for various enzymatic pathways. NAD$^+$ is synthesised from tryptophan, or via the recycling of degraded NAD$^+$ products such as nicotinamide. It is converted to NADH mainly in catabolic reactions including glycolysis and the citric acid cycle, as depicted in Figure 3.3. To maintain a proper redox state, NADH is re-oxidised, by means of several mechanisms including complex I of the respiration chain. Due to the impermeability of NAD$^+$ from the mitochondrial matrix to the cytosol, the ethanol acetylaldehyde shuttle system is involved in the transfer of NAD$^+$. Therefore an increase in the mitochondrial NAD$^+$, will lead to the production of acetylaldehyde by the mitochondrial ADH. Acetylaldehyde diffuses freely to the cytosol and is reduced to ethanol via the cytosolic ADH, resulting in an increase in cytosolic NAD$^+$. This process forms the basis of the experimental method utilised in this investigation to analyse the NADH:NAD$^+$ ratio.

This ratio plays an important role in the regulation of the intracellular redox state and is often considered as an indication of the metabolic state. Various reports have indicated that the NADH:NAD$^+$ ratio fluctuates in response to changes in metabolism. Many metabolic enzymes are regulated by this ratio, such as those involved in the glycolytic pathway, for example glyceraldehyde-3-phosphate dehydrogenase and pyruvate dehydrogenase complex. Swierczynski *et al.*, 2001 reported that the NADH:NAD$^+$ ratio in mammalian blood is 3.3 (10:3).

A variety of age related diseases as well as metabolic disorders have been indirectly associated with an aberration in the NADH:NAD$^+$ ratio (Lin and Guarente, 2003). An example of this postulated association is the role of this ratio in diabetic vascular dysfunction (Dandona and Aljada, 2002). Hyperglycaemia, which induces vascular complications, has been reported to cause a decrease in the NADH:NAD$^+$ ratio, due to an influx of glucose into the pentose phosphate pathway as discussed in Section 3.3.2. In another investigation, an association between lower complex I activity and T2D was found

(Suzuki *et al.*, 1999). It can be concluded from these reports that in a diabetic state the ratio is more difficult to regulate and will consequently affect the activity of complex I. The wide range of ratios as depicted in the data distribution graph in Graph 6.9, obtained in the current study for all three groups, strongly supports the above statement. To determine the distribution of the data, the Shapiro Wilk's Test was performed and a p-value of 0.000 was obtained, indicating that the data distribution was not normal.

Graph 6.9: Representation of the NADH:NAD$^+$ ratio data distribution

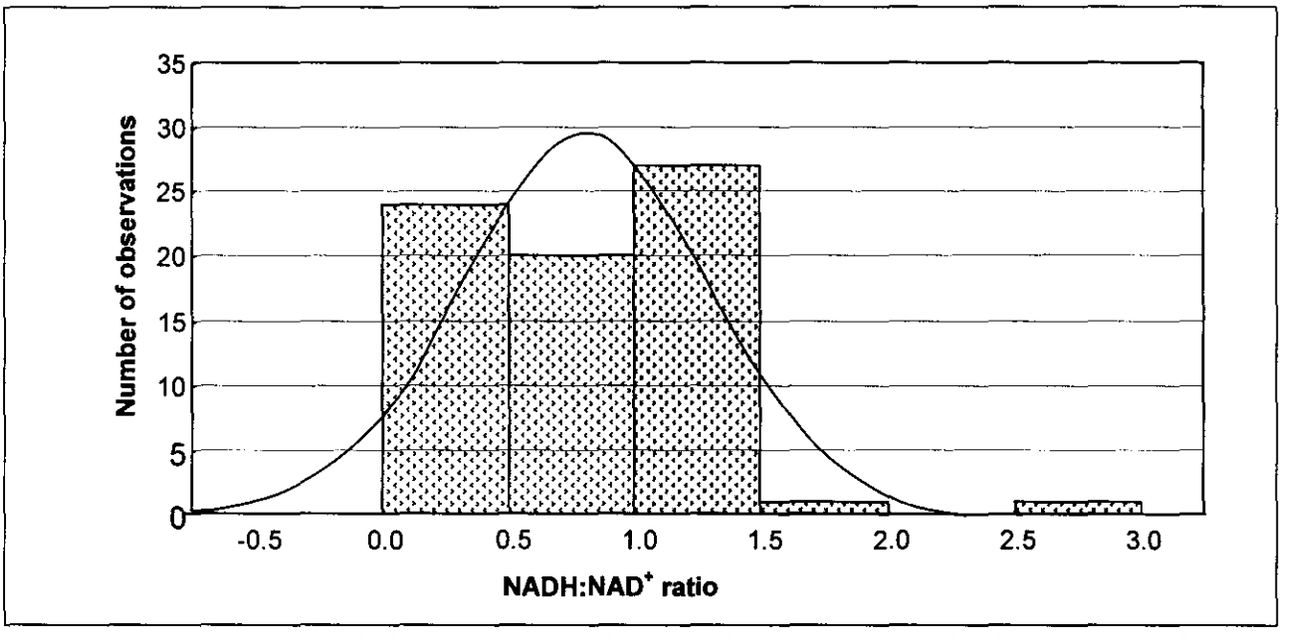

The curve indicates the expected distribution curve if the data is normally distributed; bar graph indicates the distribution of the NADH:NAD$^+$ ratios analysed in this investigation.

Of the individuals included in this investigation only one individual from Group-3 had an NADH:NAD$^+$ ratio within the range of that reported by Swierczynski *et al.* (2001). This analysis was performed in duplicate for each sample. The deviation of these results from the values reported by Swierczynski *et al.* (2001) could be attributed to the fact that in their analysis, Swierczynski *et al.* (2001) analysed this ratio in rat liver. Due to the unavailability of reports stating the normal ratio in human blood at the time of this investigation, the value reported by Swierczynski *et al.* (2001) was used as a reference. From this observation, it can be suggested that each laboratory has to define a normal value for this analysis for the respective tissues.

A summary of the statistical parameters analysed from the NADH:NAD$^+$ ratio data are presented in Table 6.6. The NADH:NAD$^+$ ratio for Group-3 has a higher standard deviation as depicted in Table 6.6, due to the maximum value of 2.8 obtained for one of the individuals in this group.

Table 6.6: Summary of NADH:NAD$^+$ ratios between Group-1, Group-2 and Group-3

Group	Mean	Median	Minimum	Maximum	Standard deviation
Group-1	1.0	1.0	0.7	1.8	0.2
Group-2	1.1	1.1	0.8	1.4	0.2
Group-3	0.6	0.3	0.1	2.8	0.6
Group-1 and Group-2	1.1	1.0	0.7	1.8	0.2
All groups	0.8	0.9	0.1	2.8	0.5

A graphical representation of the distribution of the data for the three groups of individuals is presented in Graph 6.10. The median, minimum and maximum values are indicated.

Graph 6.10: Representation of the NADH:NAD$^+$ ratio in the three groups of individuals

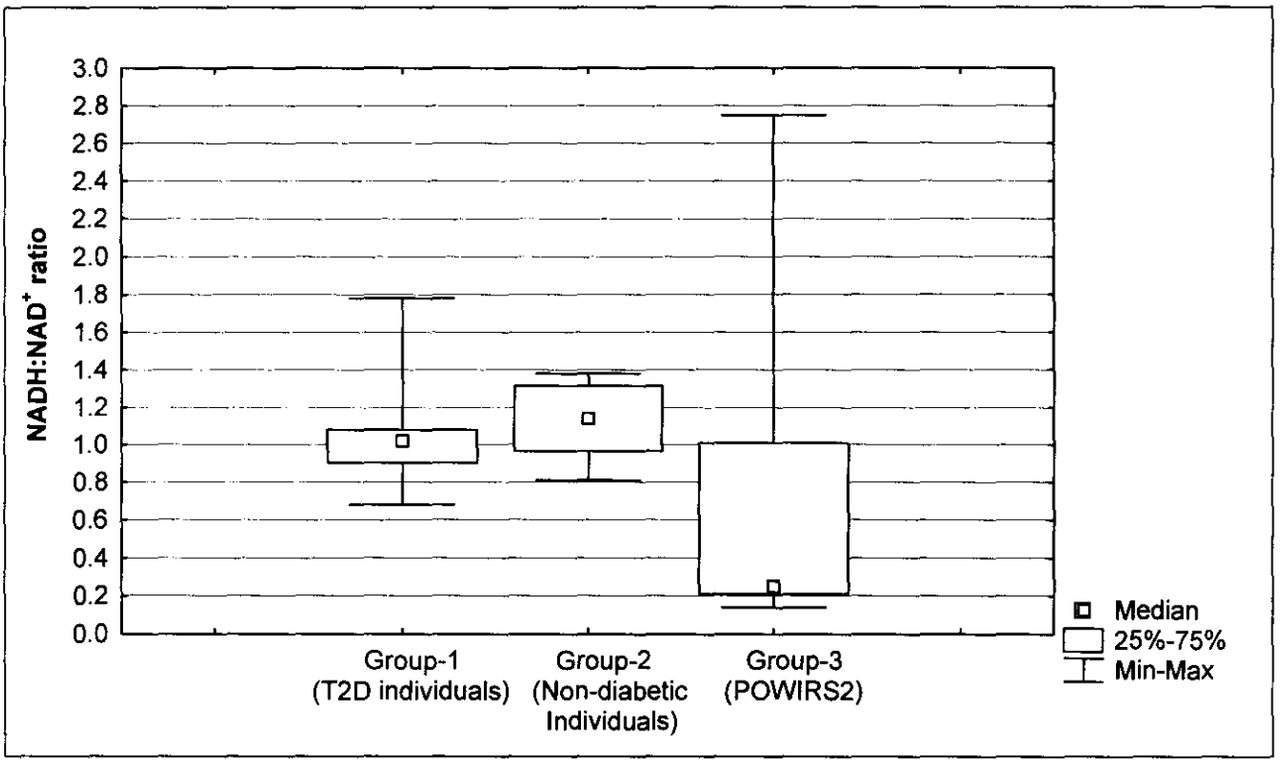

Despite the lack of a reference value for normal individuals, the differences in the median values of the NADH:NAD$^+$ ratios between the three groups of individuals was still analysed utilising the Kruskal-Wallis test. A p-value of 0.0003 was obtained indicating that there is significant difference in the median values of the three groups. To determine the inter group differences, Bonferroni corrected Mann-Whitney U tests were performed.

As depicted in Table 6.7, the difference observed between Group-1 and Group-3 (p-value = 0.019) as well as the difference between Group-3 and Group-2 (p-value = 0.001) were above the 95% level of statistical significance. However, no

significant difference, (p-value = 0.836) was observed between Group-1 and Group-2. The lack of a significant difference between Group-1 and Group-2 corresponds with the results obtained for the GSH:GSSG ratio and the d-ROM tests.

Table 6.7 p-values obtained for inter group comparisons via Bonferroni corrected Mann-Whitney U tests for the NADH:NAD$^+$ ratios

Group	Group-1	Group-2	Group-3
Group-1			
Group-2	0.836		
Group-3	**0.019**	**0.001**	

The values indicated are rounded off to the third decimal; p-values < 0.05, indicating statistical significance, are presented in bold. Grey shaded cells contain no data.

The results presented for the ATP:ADP ratios in Section 6.2.1.6 and the lactate:pyruvate ratios in Section 6.2.1.5 also indicate that there is no significant difference (below the 95% level of statistical significance) in the biochemical parameters analysed in this investigation between Group-1 and Group-2. This observation supports the postulated role of ROS in aging as well as in the pathogenesis of various metabolic disorders, such as T2D and mitochondrial cytopathies. The suggested lack of sensitivity of these biochemical analyses, particularly in a heterogeneous tissue such as blood, highlights the importance of a biomarker for the detection of increased levels of ROS.

It has been postulated that if the NADH:NAD$^+$ ratio is very high, the regulation thereof will be more sensitive to a change in the concentration of NADH than NAD$^+$. Since NAD$^+$ is a cofactor in the reaction catalysed by glyceraldehyde phosphate dehydrogenase as depicted in Figure 3.4, the variation in this ratio will affect this step within the glycolytic pathway, resulting in altered energy metabolism. As discussed previously any impairment within Complex I of the OXPHOS pathway affecting the oxidation of NADH will also affect this ratio. It can also be suggested that the process of energy metabolism will be compromised if the NADH:NAD$^+$ ratio is impaired. This suggestion was further explored in this investigation by measuring the ATP:ADP ratio for these individuals and the results thereof are presented in Section 6.2.1.6.

6.2.1.5 Lactate:Pyruvate ratio analysis in blood

Under physiological conditions, the lactate and pyruvate levels in blood are regulated by their production from glycolysis and the utilisation thereof during gluconeogenesis as well as in mitochondrial oxidation. In blood, the lactate:pyruvate (L/P) ratio reflects the redox state. In a case where there is a defect in the glucose metabolism, or mitochondrial

impairment, the oxidation of pyruvate to acetyl-CoA by pyruvate dehydrogenase complex does not occur. Due to the only other possible reaction being the conversion thereof to lactate, a shift in the pyruvate to lactate ratio will occur, which eventually leads to metabolic acidosis.

Various methods can be utilised in the determination of the L/P ratio (Vassault *et al.*, 1991), however due to the sensitivity of the spectrophotometry, this was the method of choice. T2D is one of the many diseases that present with ketoacidosis, as discussed in Section 3.3.2. Ketoacidosis in a hyperglycaemic state leads to high lactate levels within the blood, which is characteristic of T2D. Under normal metabolic conditions, the L/P ratio is maintained within the range of 15-25 (Wanders *et al.*, 1992; Minniti *et al.*, 2001; ter Hofstede *et al.*, 2004). Ratios exceeding 25 are indicative of a disturbance in the cellular oxidation-reduction state. Minniti *et al.* (2001) reported that lactate values differ in various body fluids such as arterial blood, which exhibits the lowest values, venous blood and cerebrospinal fluid, which has the highest values. Thus, results obtained in this investigation are based on the reported normal range for venous blood. According to the Shapiro Wilk's Test, the L/P ratio data for the groups of individuals did not have a normal distribution (p-value = 0.000) as indicated in Graph 6.11.

Graph 6.11: Representation of the analysis of the distribution of the lactate:pyruvate ratios

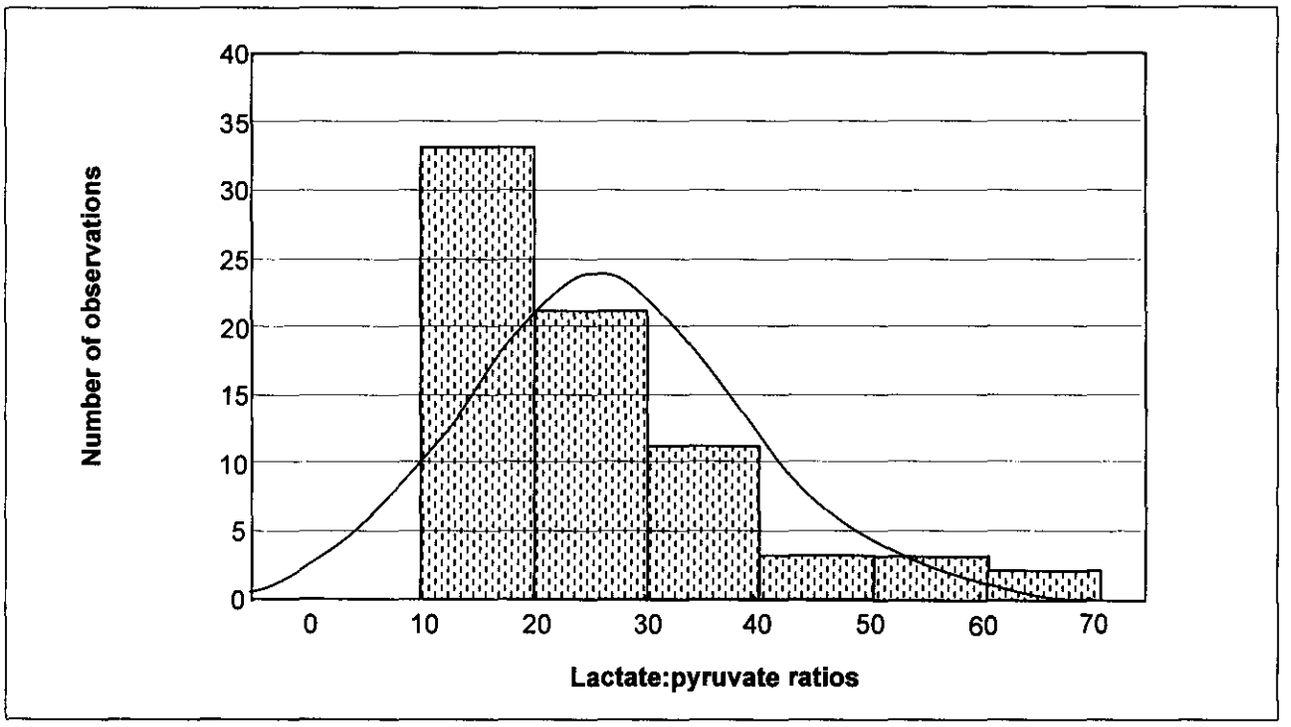

The curve indicates the expected distribution curve if the data is normally distributed; the bar graph indicates the distribution of the lactate:pyruvate ratios analysed in this investigation.

In T2D individuals (Group-1), high levels of lactate were observed in this investigation as indicated by the median L/P ratio of 33.3 observed for this group, as listed in Table 6.8. The elderly non-diabetic individuals (Group-2) also presented with a high median value of 28.9 when compared to the 17.4 obtained for the POWIRS2 group (Group-3) of individuals. This difference indicates an alteration in the redox states within the various groups of individuals. The relatively high L/P ratios obtained for all three groups, as opposed to the reported ratio between 15 and 20, may be attributed to the fact that during blood drawing a tourniquet was utilised, thus inhibiting the free flow of oxygenated blood. Hypoxaemia has been reported to result in high concentrations of lactic acid in blood due to the preferential conversion of pyruvate to lactic acid under anaerobic conditions (Joulia *et al.*, 2003). Therefore, the procedure followed to obtain blood may have led to high L/P ratios. However, because this procedure was performed for all three groups, a relative estimation of the L/P ratios could be made.

Table 6.8: Summary of the lactate:pyruvate ratios between the three groups of individuals

Group	Mean	Median	Minimum	Maximum	Standard deviation
Group-1	35.6	33.3	18.8	68.3	15.1
Group-2	30.0	28.9	16.3	55.1	11.4
Group-3	19.3	17.4	10.2	49.9	8.0
Group-1 and Group-2	33.4	31.0	16.3	68.3	13.8
All groups	25.27	20.94	10.2	68.3	12.9

A representation of the statistical parameters listed in Table 6.8 is presented in Graph 6.12. The large variation in the L/P ratios between and within the groups is indicated by the large distribution of the minimum and maximum values observed for each of the groups. The constant metabolism of pyruvate to either enter the citric acid cycle as depicted in Figure 3.3, or to form lactic acid could be a factor that led to this variation. The inability to monitor the diet of Group-1 and Group-2, thereby not regulating the uptake of carbohydrates, protein or fats, may also have led to the observed variation.

Graph 6.12: Representation of the lactate:pyruvate ratios in the three groups of individuals

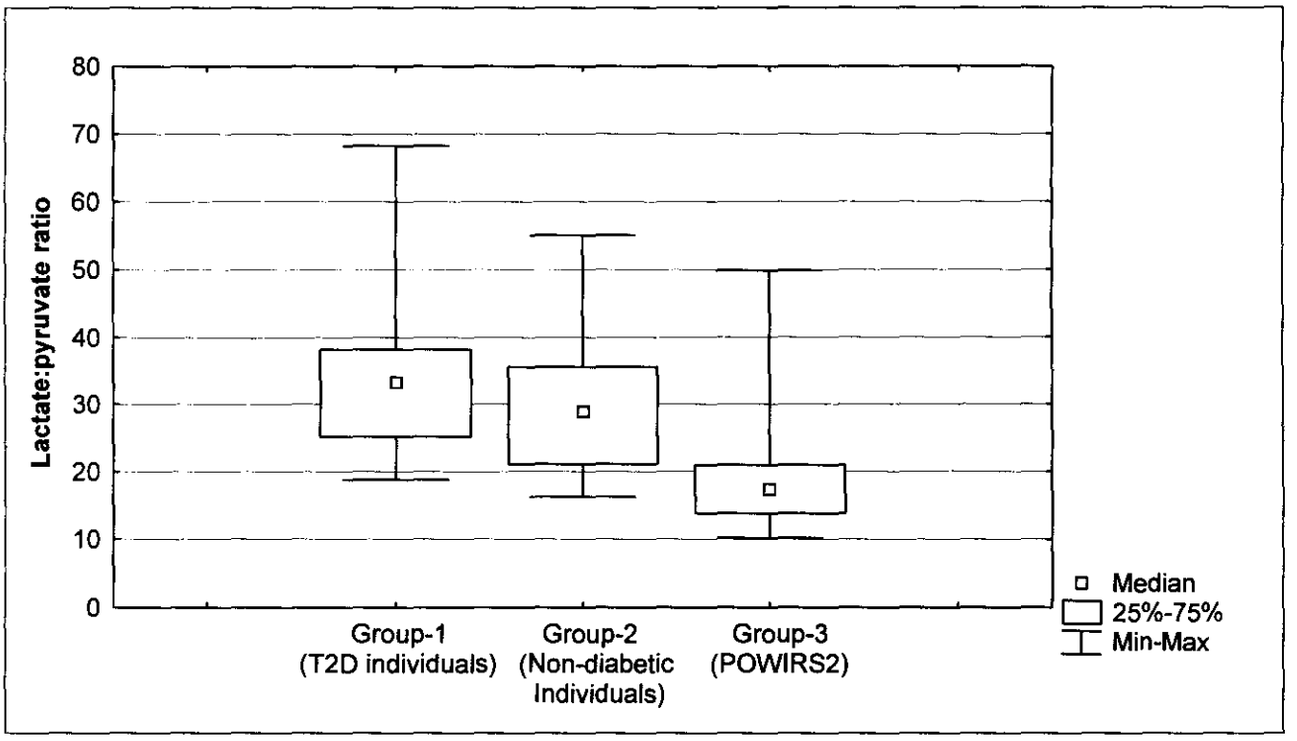

Due to the data of the L/P ratios of these three groups having a non-parametric distribution as indicated in Graph 6.11, the Kruskal-Wallis test was performed to analyse the difference between the median values. A p-value of 0.000 was obtained, indicating a significant difference between these three groups. To determine the inter group differences, Bonferroni corrected Mann-Whitney U tests were performed. The results of these analyses are listed in Table 6.9.

Table 6.9: p-values obtained for inter group comparisons via the Bonferroni corrected Mann-Whitney U tests for the lactate:pyruvate ratios

Group number	Group-1	Group-2	Group-3
Group-1			
Group-2	1.000		
Group-3	**0.000**	**0.005**	

The values indicated are rounded off to the third decimal; p-values < 0.05, indicating statistical significance, are presented in bold. Grey shaded cells contain no data.

A significant difference (p-value = 0.000) was observed between Group-1 and Group-3, as indicated by the bold text in Table 6.9. It is also evident from the p-value of 0.005 obtained when comparing Group-2 and Group-3 that a statistically significant difference exists between these two groups. However, no difference was observed between Group-1 and Group-2. This data supports the conclusion made subsequent to the analysis of the anthropometric data, the lifestyle patterns as discussed in Section 6.1, as well as the

d-ROMs test data presented in Section 6.2.1.1, namely that Group-2 should not serve as a control for Group-1.

6.2.1.6 ATP:ADP ratio analysis in whole blood

In a metabolic disorder, energy production is decreased. Since the mitochondria produce the most amount of energy, any impairment within these organelles will be identified by decreased levels of energy in the form of ATP. It is thus hypothesised in this investigation that due to the high levels of ROS (present in individuals within the various groups) resulting in mitochondrial dysfunction, a low energy status will be detected.

In order to measure the energy status within blood, the method describe by Lust *et al.* (1981) was employed. In this procedure, the total cellular ATP (ATP and ADP converted to ATP) was measured spectrophotometrically by detecting the formation of NADPH in the reaction catalysed by hexokinase and glucose-6-phosphate dehydrogenase.

The Shapiro Wilk's Test was performed to determine the distribution of the ATP:ADP ratios obtained for all three groups. From this analysis, a p-value of 0.001 was observed, indicative of data not normally distributed, as depicted in Graph 6.13.

Graph 6.13: Representation of the analysis of the distribution of the ATP:ADP ratios

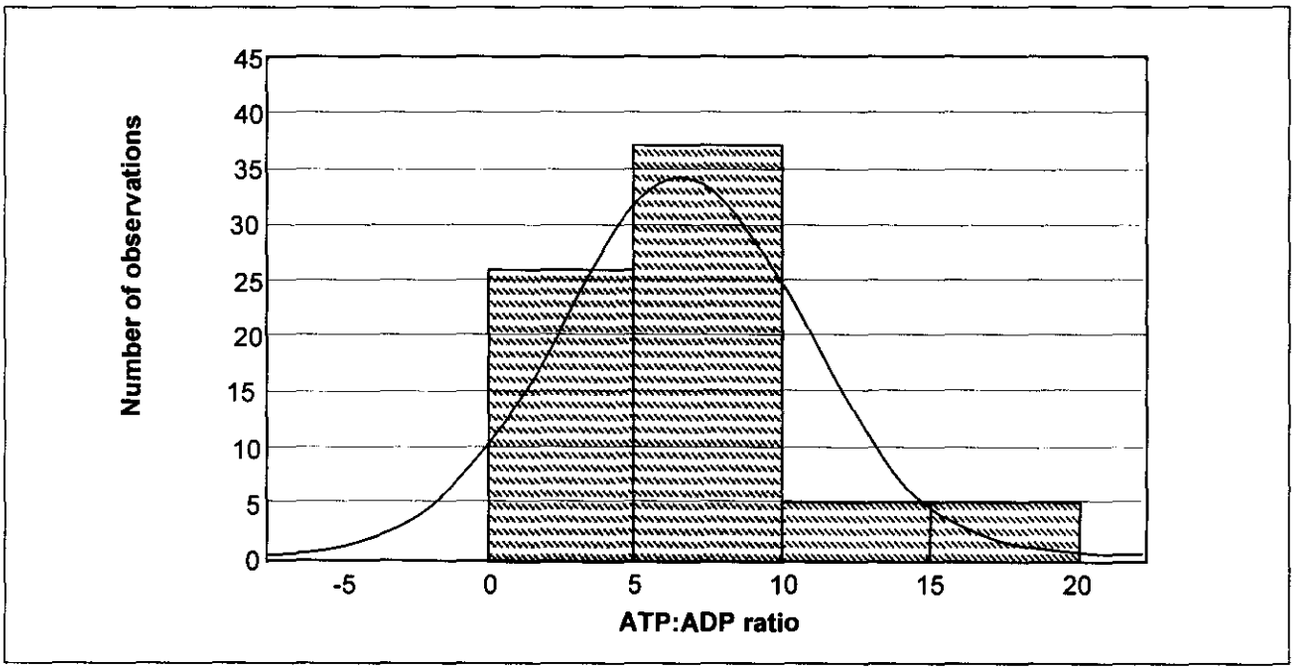

The curve indicates the expected distribution curve if the data is normally distributed; the bar graph indicates the distribution of the ATP:ADP ratios analysed in this investigation.

Nadlinger *et al.* (2002) reported in their investigation that the blood ATP:ADP ratio in a normal individual who is not under any physical stress is between 10 and 12. This value was used as a reference in this investigation. A summary of the results of the ATP:ADP analysis is presented in Table 6.10.

Table 6.10: Summary of the ATP:ADP ratios between the three groups of individuals

Group number	Mean	Median	Minimum	Maximum	Standard deviation
Group-1	4.5	2.6	1.3	10.0	3.3
Group-2	4.6	5.0	1.3	9.0	2.5
Group-3	8.4	8.3	1.2	19.3	4.4
Group-1 and Group-2	4.5	4.2	1.3	10.0	3.0
All groups	6.7	6.3	1.2	19.3	4.3

From the results presented in Table 6.10 it was apparent that individuals comprising Group-1 and Group-2 had reduced energy levels as indicated by the mean values, which are greatly decreased when compared to the normal range. Even though Group-3 presented with a lowered mean value, it was higher than that of Group-1 and Group-2. A graphical illustration of these results is presented in Graph 6.14, where the median values for each group are indicated. Group-3 had a higher standard deviation due the great variation in the ATP:ADP ratios between the individuals comprising this group, as indicated in Appendix B by the large range of values obtained.

Graph 6.14: Representation of the ATP:ADP ratios in the three groups of individuals

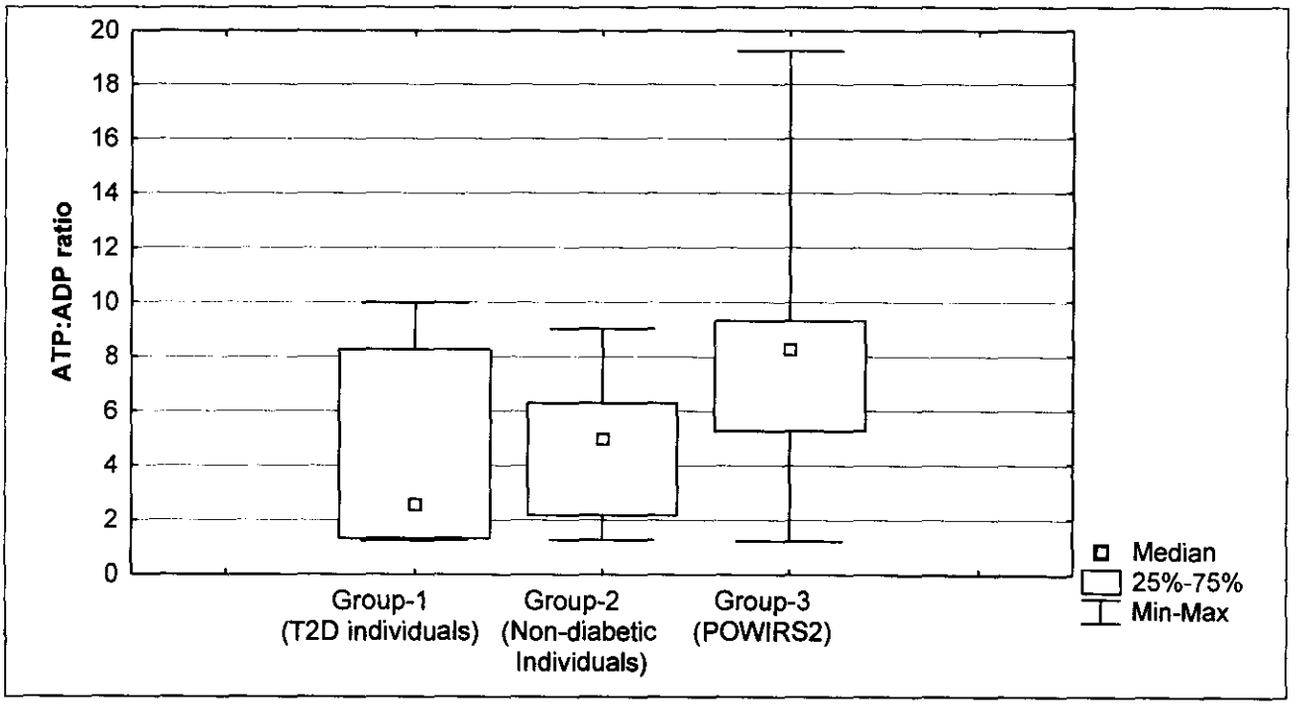

Due to the data having a non-Gaussian distribution pattern according to the Shapiro Wilk's Test, the Kruskal-Wallis test was performed and a p-value of 0.0017 was generated. This indicated that a significant difference existed between the medians of the three groups. Bonferroni corrected Mann-Whitney U tests were performed to analyse the inter group median differences and the results thereof are presented in Table 6.11 in terms of p-values.

Table 6.11: p-values obtained for inter group comparisons via the via Bonferroni corrected Mann-Whitney U tests for the ATP:ADP ratios

Group number	Group-1	Group-2	Group-3
Group-1			
Group-2	1.000		
Group-3	**0.007**	**0.027**	

The values indicated are rounded off to the third decimal; p-values < 0.05, indicating statistical significance, are presented in bold. Grey shaded cells contain no data.

No significant difference was observed between the diabetic elderly (Group-1) and non-diabetic elderly (Group-2) individuals (p-value of 1.000). However, a significant difference was observed between Group-3 and Group-2, with a p-value of 0.027, as well as Group-3 and Group-1 (p-value of 0.007). When the data for Group-1 and Group-2 was combined and compared to the results obtained for Group-3 via the Bonferroni corrected Mann-Whitney U test, a significant difference was obtained with a p-value of 0.001.

The results obtained for the ATP:ADP ratio for these groups correlates with those obtained for the NADH:NAD ratio. These results are also consistent with those presented by Nadlinger *et al.* (2002), where it was observed that post physical exercise, lower NADH concentrations were obtained as well as lower ATP levels. None of the individuals comprising the three groups took part in physical exercise during recruitment, or indicated that they had undergone any physical training prior to sampling. However, the results follow a similar trend as those of Nadlinger *et al.* (2002), which indicate that where there is a decrease in NADH for utilisation in the OXPHOS, it will result in a decrease in the ATP levels.

It is apparent from the analysis of the aforementioned biochemical parameters that Group-1 and Group-2 cannot be clearly distinguished based on these parameters. This is mainly due to various factors such as that individuals comprising Group-2 were affected with other ROS related disorders, were elderly, and had BMI ratios above the normal range. This may indicate that the ROS related complications observed in Group-1 and Group-2 may in both cases be related to their age and not necessarily to T2D. Therefore,

because of the age difference between Group-3 and the combined Group-1 and Group-2, Bonferroni corrected Mann-Whitney U tests (non-parametric data) were performed for all six biochemical parameters assayed to analyse the significance of differences observed between these groups.

A significant difference was obtained for four of the six biochemical parameters analysed as indicated in Table 6.12. The text indicated in bold, denotes the parameters where a level of statistical significance was attained.

Table 6.12: p-values obtained from the Bonferroni corrected Mann-Whitney U tests when the combined Group-1 and Group-2 was compared to Group-3

Parameter	p-value
d-ROMs test	0.409
ORAC analysis	0.825
GSH:GSSG ratio analysis	**0.000**
NADH:NAD ratio analysis	**0.000**
Lactate:pyruvate ratio analysis	**0.000**
ATP:ADP ratio analysis	**0.001**

The values indicated are rounded off to the third decimal; p-values < 0.05, indicating statistical significance, are presented in bold.

Based on the results presented in Table 6.12, the combined Group-1 and Group-2 had significantly different redox capacity as well as energy states when compared to Group-3. However, the difference that was observed for oxidative stress as indicated by the p-values of the d-ROMs and ORAC assays was not significantly different. Therefore, based on the redox and energy states between Group-3 and the combined Group-1 and Group-2, these two groups can be distinguished from each other. However, the inability to distinguish between these groups based on the ROS data indicates the need to use alternative methods for the detection of ROS.

The data of all six biochemical parameters analysed for the three groups of individuals was further analysed via Statistica© to determine and measure the correlation between the various analyses. Each of the values for all of the parameters for each group were utilised for this analysis. As discussed in Section 5.7, the Spearman ranked correlations test was performed. The results of the analysis of correlation are indicated in Table 6.13.

Table 6.13: Correlation coefficients of all six biochemical parameters generated with the Spearman ranked test for the three groups of individuals

Biochemical parameter		d-ROM	ORAC	Lactate: pyruvate ratio	GSH:GSSG ratio	NADH:NAD$^+$ ratio	ATP: ADP ratio
d-ROM							
ORAC	All three groups	r = 0.014 p = 0.905					
	Group-1	**r = 0.039 p = 0.875**					
	Group-2	r = 0.273 p = 0.391					
	Group-3	r = -0.028 p = 0.861					
Lactate:pyruvate ratio	All three groups	r = 0.067 p = 0.574	r = -0.034 p = 0.778				
	Group-1	**r = -0.299 p = 0.213**	**r = -0.001 p = 0.997**				
	Group-2	r = -0.098 p = 0.762	r = 0.322 p = 0.308				
	Group-3	r = 0.000 p = 0.998	r = -0.062 p = 0.696				
GSH:GSSG ratio	All three groups	r = -0.110 p = 0.355	r = -0.113 p = 0.341	**r = -0.281 p = 0.016**			
	Group-1	**r = 0.037 p = 0.881**	**r = -0.174 p = 0.477**	r = -0.363 p = 0.126			
	Group-2	r = -0.301 p = 0.342	r = -0.413 p = 0.183	r = 0.224 p = 0.484			
	Group-3	r = 0.062 p = 0.694	r = -0.068 p = 0.671	r = 0.026 p = 0.872			
NADH:NAD$^+$ ratio	All three groups	r = -0.040 p = 0.732	r = 0.026 p = 0.830	**r = 0.344 p = 0.003**	r = -0.163 p = 0.167		
	Group-1	**r = -0.091 p = 0.710**	**r = -0.016 p = 0.949**	**r = 0.221 p = 0.364**	**r = 0.171 p = 0.485**		
	Group-2	r = -0.063 p = 0.846	r = -0.217 p = 0.499	r = 0.455 p = 0.138	r = 0.713 **p = 0.009**		
	Group-3	r = -0.289 p = 0.063	r = 0.190 p = 0.229	r = 0.002 p = 0.989	r = -0.170 p = 0.283		
ATP:ADP ratio	All three groups	r = 0.022 p = 0.795	r = -0.088 p = 0.461	**r = -0.301 p = 0.010**	r = 0.205 p = 0.082	**r = -0.304 p = 0.008**	
	Group-1	**r = 0.305 p = 0.205**	**r = 0.050 p = 0.839**	**r = 0.216 p = 0.375**	**r = -0.167 p = 0.495**	**r = 0.155 p = 0.527**	
	Group-2	r = -0.063 p = 0.846	r = 0.070 p = 0.829	r = -0.007 p = 0.983	r = -0.035 p = 0.914	r = 0.042 p = 0.897	
	Group-3	r = 0.050 p = 0.751	r = -0.193 p = 0.221	r = -0.116 p = 0.465	r = -0.022 p = 0.889	**r = -0.317 p = 0.041**	

Grey shaded cells contain no data; the yellow shaded cell indicates a strong positive correlation in Group-2 between the NADH:NAD$^+$ ratios and the GSH:GSSG ratio, with a significant p-value; the green shaded cells indicate a weak relationship in the groups with significant p-values; the blue shaded cell indicates a medium relationship between the NADH:NAD+ ratios and the lactate:pyruvate ratios for all three groups.

The values listed in Table 6.13 indicate the correlation coefficients (r) as well as the p-values of the regression analysis for all three groups and the individual groups. A positive correlation between the d-ROMs test and ORAC data was expected. According to the Spearman ranked test, a weak relationship was detected as indicated by a correlation coefficient of 0.014, with a corresponding p-value of 0.905 for all three groups. Weak relationships were also observed for the d-ROMs test and ORAC data in each of the three groups.

In cases of high energy production i.e. high ATP:ADP ratio, a negative correlation between the ATP:ADP ratio and the lactate:pyruvate ratio is expected, with the ATP:ADP ratio having a positive correlation to the NADH:NAD^+ ratio. A weak negative correlation between the ATP:ADP ratio and the NADH:NAD^+ ratio was observed (r-value = -0.304) for all three groups. However, a p-value of 0.009 was generated, indicating that there is a 0.9% probability of obtaining this result due to chance. A weak negative correlation between the ATP:ADP ratio and the lactate:pyruvate ratio (r-value = -0.301) was observed with a p-value of 0.010. A medium strength positive correlation between the NADH:NAD^+ ratio and the lactate:pyruvate ratio (r-value = 0.344, p-value = 0.003) was obtained. As indicated in Table 6.13, a strong positive relationship between the NADH:NAD^+ ratio and the GSH:GSSG ratio (r = 0.713) exists in Group-2, with a p-value of 0.009, indicating a 99.1% probability of observing this relationship in this sample group. According to the values indicated in Table 6.13, the lactate:pyruvate ratio, ATP:ADP ratio, GSH:GSSG ratio and the NADH:NAD^+ ratio had significant p-values for the regression analysis. It may be suggested from the results of the correlation analyses that relationships between the aforementioned biochemical parameters do exist, even though the correlation coefficients obtained did not indicate strong relationships.

From the results obtained during correlation analyses via the Spearman ranked test, it may be suggested that the cohort size was not large enough to be representative of the diabetic population and the non-diabetic population group. Due to the number of individuals that were selected in the study to test the effect of ROS in T2D individuals as according to Samuels (1989), a larger sample size would aid in providing a more accurate estimation of this effect of ROS, particularly in a complex disorder such as T2D. Thus it is suggested that a true profile of the biochemical parameters in T2D individuals can be obtained via the analysis of a larger population group. The use of a heterogeneous tissue such as blood, which has not been reported for such analyses, may have also lead to the low sensitivity observed for these biochemical assays. The effect of the endogenous levels

of ROS on MT gene expression in these three groups of individuals was analysed via Real-Time PCR and ELISA. The results thereof are discussed in Sections 6.4.2 and 6.5.2, respectively.

6.3 OXIDATIVE STRESS IN CONTROL CELL LINES TREATED WITH *t*-BHP

For the purpose of this investigation, a positive control for ROS-induced expression of MT genes was required. MT expression was therefore analysed in ROS producing HeLa cells as discussed in Section 6.3.1. As stated in Sections 5.3.2 and 5.3.3, the ROS determination, and the cell viability assay were performed to quantify the oxidative stress. The results obtained for these two parameters were normalised to the protein content of the cells. The BCA method discussed in Section 5.3.2.1 was utilised for the protein determination. Real-Time PCR was used to analyse the differential expression of MT genes and the ELISA was used for the detection of the MT proteins. The results of these analyses are presented in Sections 6.4.1 and 6.5.1 respectively.

6.3.1 Analysis of ROS production in *t*-BHP treated HeLa cells

t-BHP has been proved to induce free radical damage in lymphocytes and many other cell types (Wölfler *et al.* 1999), via the formation of peroxyl- and alkoxyl radicals in the presence of transition metal ions. These intermediates initiate lipid peroxidiation, DNA damage, and affect cell integrity. HeLa cell lines were treated with 0.5 mM, 0.8 mM, 1 mM *t*-BHP. A three hour incubation period was optimal, since longer periods of incubation led to too much cell damage, resulting in a loss of cells, therefore producing erroneous results.

Each of the *t*-BHP concentrations as well as the control were performed in replicates of seven, to analyse the reproducibility of the results and the homogeneity between the different wells. As discussed in Section 6.3.2, it was observed that HeLa cell viability was affected by the presence of *t*-BHP. Cell viability decreased when the concentration of *t*-BHP was increased.

The production of ROS within the *t*-BHP treated cells was measured, as discussed in Section 5.3.2 by a fluorometric analysis via the use a H_2DCFDA. The oxidation of the non-fluorescent H_2DCFDA to the highly fluorescent 2',7'-dichlorofluorescein (DCF) is commonly used to detect the generation of reactive oxygen intermediates within cells. Oxidation of H_2DCFDA has been reported to not be directly sensitive to free radicals, but rather that free radicals can indirectly contribute to the formation of DCF through their reaction with cellular substrates that yield peroxy products and peroxyl radicals (Wang and Joseph, 1999).

The mean absorbance values which were measured at an excitation of 485 nm and emission of 530 nm for all seven replicates of each of the *t*-BHP concentrations are listed in Table 6.14. The data were plotted using each of the medians of the absorbance values divided by the protein concentration in order to express the results in relative fluorescence units (RFU) per μg protein. To obtain a relative quantification of the production of ROS, RFU per μg protein values of each of the different concentrations of *t*-BHP were subtracted from the mean value obtained for the negative control.

Table 6.14: Summary of the statistical analysis of the *t*-BHP treated HeLa cells

Parameter	0 mM *t*-BHP	0.5 mM *t*-BHP	0.8 mM *t*-BHP	1 mM *t*-BHP
Protein concentration ($\mu g.ul^{-1}$)	17.17	14.18	13.40	13.40
Mean (RFU. μg^{-1} protein)	1478.92	4637.45	5963.47	4530.41
Median(RFU. μg^{-1} protein)	1396.61	4784.23	6026.56	6270.09
Median-Blank (0 mM *t*-BHP)	0.00	3387.62	4629.95	4873.48
Standard deviation	294.77	542.30	971.70	3152.20

μg = micro grams; mM = millimolar; *t*-BHP = *tert*-butyl hydroperoxide; RFU = relative fluorescence units.

As depicted in Graph 6.15 there was a linear increase in the production of ROS with an increase in the concentration of *t*-BHP. These results support the report by Wang *et al.* (2000) that cells exposed to *t*-BHP have an increased production of ROS.

Graph 6.15: Representation of the extent of ROS production in *t*-BHP treated cell lines

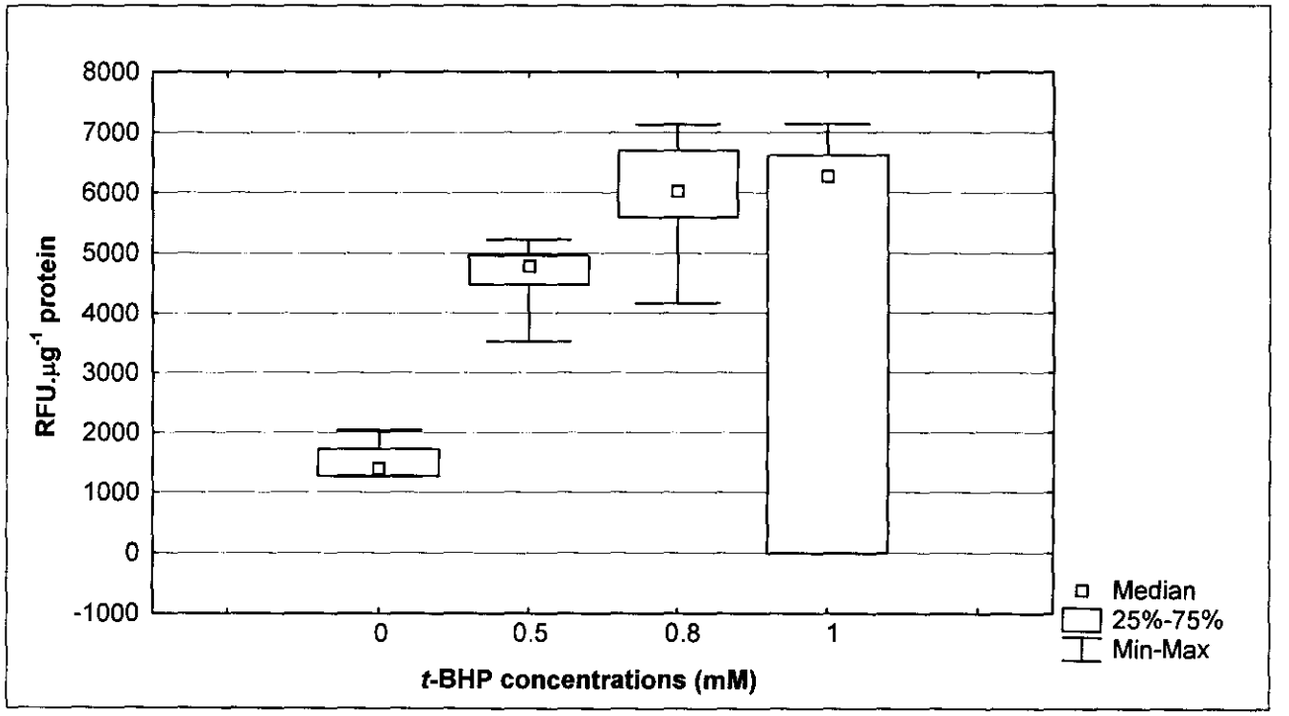

RFU = relative fluorescence units; μg = micrograms; mM = millimolar.

In this investigation, as presented in Table 6.14 and Graph 6.15, an increase in the standard deviation was observed with an increase in *t*-BHP concentrations. This observation could be explained by a possible differential production of ROS by the cells within the 96 well plates. It is also suggested that at the 0.8 mM and 1 mM *t*-BHP concentrations, a subset of the cells may have activated the endogenous cellular antioxidant mechanisms discussed in Section 3.3, thus resulting in increased variation. At the 1 mM *t*-BHP concentration, values close to those detected at 0 mM *t*-BHP were also observed, further supporting the hypothesis that the activation of endogenous cellular antioxidant mechanisms result in decreased ROS production.

The significance of the differences between the median values of the different *t*-BHP concentrations and the negative control was analysed via the Kruskal-Wallis test. A 95% level of statistical significance was utilised with a corresponding p-value equal to 0.05 or less. A p-value of 0.006 was obtained, indicating that the difference observed between the median values is significant. To analyse the inter group median differences, Bonferroni corrected Mann-Whitney U tests were performed. The results of this test are in presented in Table 6.15.

Table 6.15: p-values obtained for inter group comparisons via the Bonferroni corrected Mann-Whitney U tests for the *t*-BHP treated HeLa cells

Treatment	0.5 mM *t*-BHP	0.8 mM *t*-BHP	1 mM *t*-BHP
0 mM t-BHP	0.413	**0.003**	0.074

The values indicated are rounded off to the third decimal; p-values < 0.05, indicating statistical significance, are presented in bold.

A significant difference was observed between the 0 mM *t*-BHP and 0.8 mM *t*-BHP concentrations (p-value = 0.003). Even though a difference was present between the 0 mM *t*-BHP and 0.5 mM *t*-BHP as well as 0 mM *t*-BHP and 1 mM *t*-BHP, it was not statistically significant. It may be concluded from this observation that at 0.8 mM *t*-BHP concentration, ROS production was greatly increased when compared to the 0 mM *t*-BHP concentration. It is suggested that at 1 mM *t*-BHP, the cellular endogenous antioxidant mechanisms were activated in a subset of cells, leading to a distribution that is not significantly different from those of the 0 mM *t*-BHP, thus creating the overlap in the results of the ROS production.

6.3.2 Analysis of cell viability in *t*-BHP treated HeLa cells

The MTT assay is commonly used to analyse cell viability. Within a living cell, MTT is reduced by mitochondrial dehydrogenases to a blue-magenta coloured formazan precipitate. The absorption of the dissolved formazan in the visible region correlates with the number of metabolically active cells, since tetrazolium are only reduced by metabolically active cells. Cytotoxic compounds such as Triton-X 100®, high concentration of *t*-BHP, and Glacial acetic acid (supplied by Merck) were used in this analysis as positive controls. These compounds have been reported to damage and destroy cells, and thus decreasing the reduction of MTT to formazan (Mueller *et al.*, 2004). HeLa cells were seeded in 96 well plates at a density of 3 x 10^4 cell per well. Each of these cytotoxic agents were added 30 min prior to the MTT analyses of the 0.5 mM, 0.8 mM, 1 mM *t*-BHP concentrations. A graphical illustration of the effects of the aforementioned positive controls is presented in Graph 6.16.

Graph 6.16: Representation of the effects of the different cytotoxic agents on HeLa cell viability

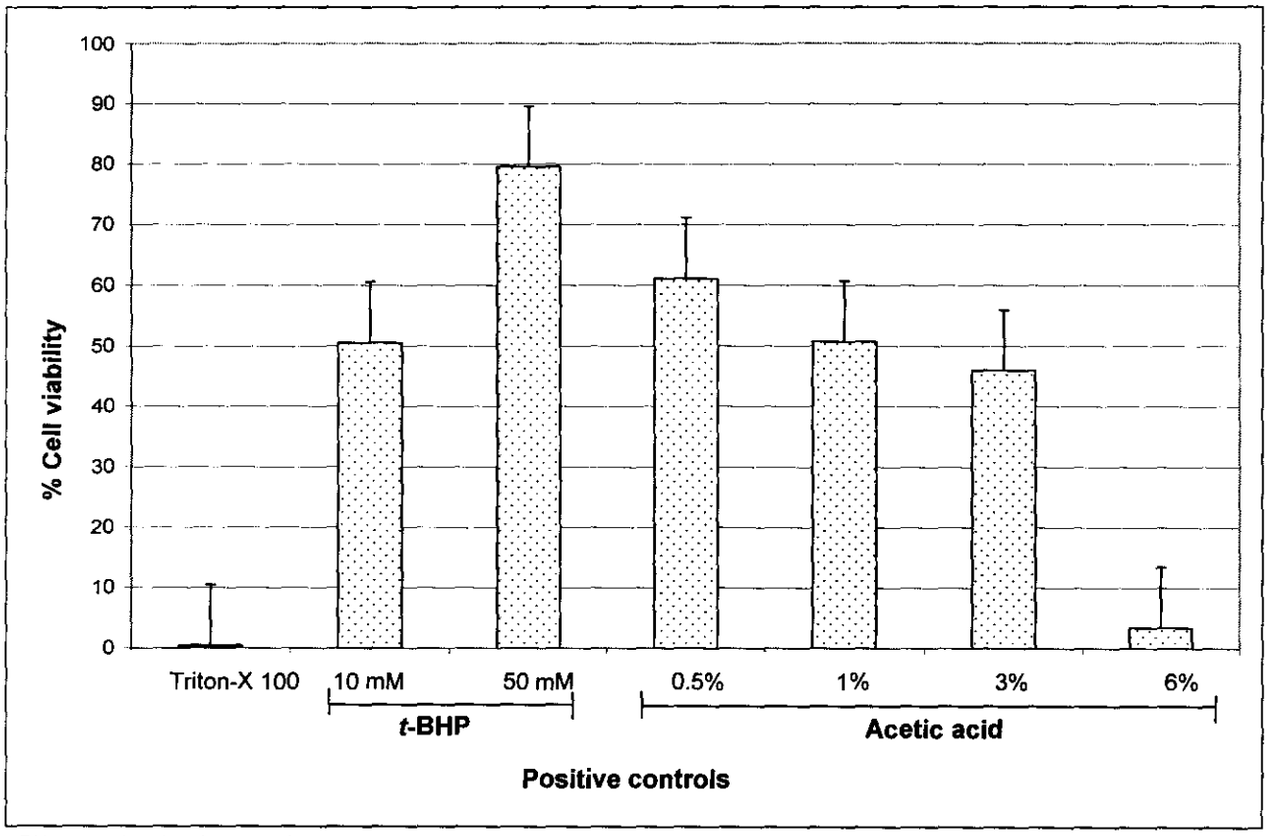

t-BHP = *tert*-butyl hydroperoxide.

As depicted in Graph 6.16, Triton-X 100 resulted in the least cell viability, however it was not the compound of choice because it resulted in the detachment of metabolically active cells from the plate. It was not clear whether the low cell viability was due to the reduction

of live cells, or due to the toxic effects thereof. The positive control of choice was therefore 6% acetic acid for the MTT analysis, as it was evident that very little cell detachment occurred subsequent to the analyses of the cells under the microscope. From the results presented in Graph 6.16, it is evident that although *t*-BHP is toxic to the cells, it does not lead to excessive cell death during the 30 min incubation period as compared to Triton-X 100.

The effects of the three hour incubations with 0.5 mM, 0.8 mM, 1 mM *t*-BHP concentrations were subsequently analysed with 6% Glacial acetic acid as a positive control. The results of these analyses are present in Graph 6.17.

Graph 6.17: Representation of the effects of the *t*-BHP and Acetic acid on cell viability

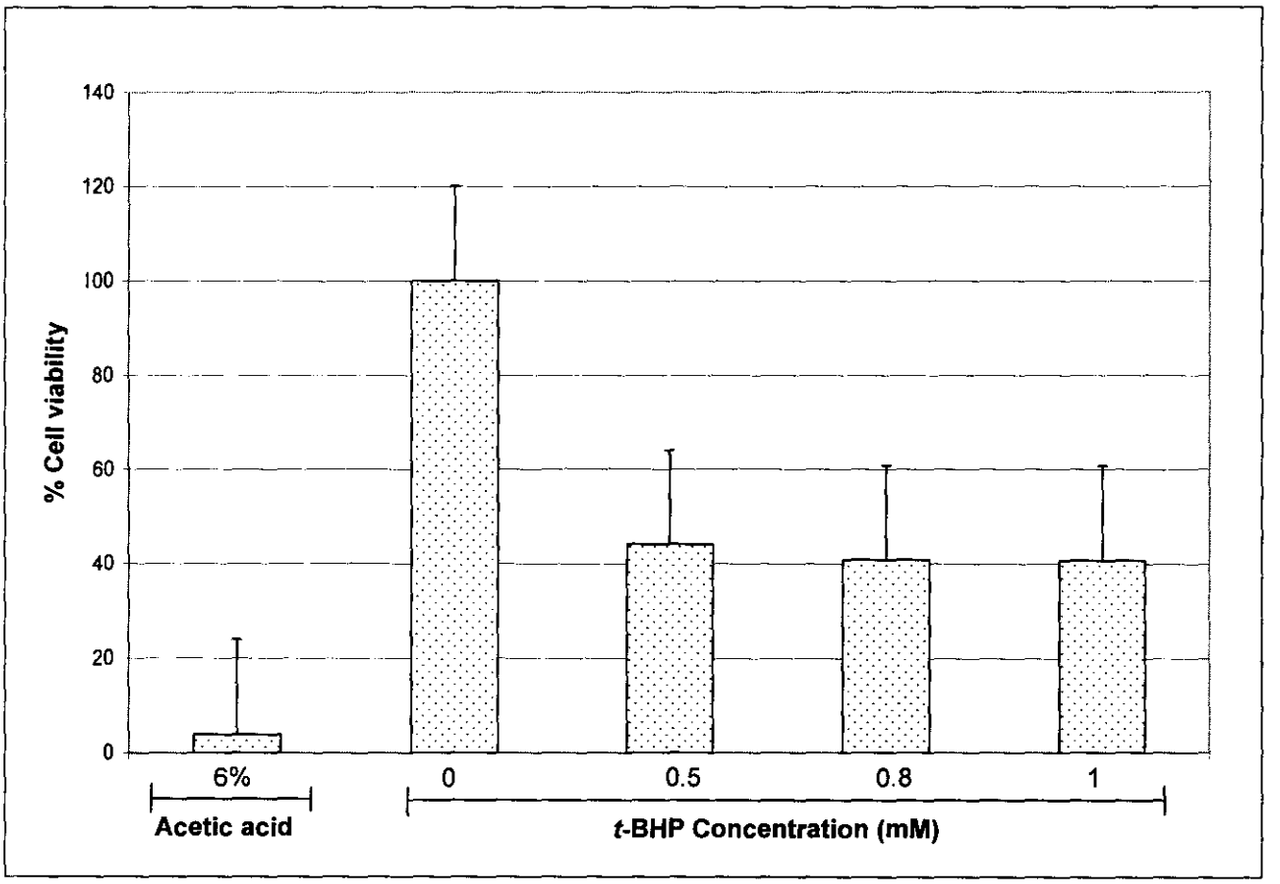

mM = millimolar; *t*-BHP = *tert*-butyl hydroperoxide.

It can be concluded from the data presentation in Graph 6.17, that the concentration of *t*-BHP utilised to induce ROS production did affect the cell viability. The protein concentrations for each of the treatments were measured and cell viability expressed in RFU per μg protein, as indicated in Table 6.16. Measuring the protein content enabled the normalisation of the data based on their protein content (Wang and Joseph, 1999).

Table 6.16: Summary of the cell viability analysis in *t*-BHP treated cells

Parameter	6% Glacial acetic acid	0 mM *t*-BHP	0.5 mM *t*-BHP	0.8 mM *t*-BHP	1 mM *t*-BHP
Protein concentration ($\mu g.\mu l^{-1}$)	10.90	10.62	10.32	8.86	9.50
Median (absorbance at 560nm)	0.01	0.30	0.13	0.10	0.11
Absorbance per μg protein	0.00	0.03	0.012	0.01	0.01

μg = micro grams; *t*-BHP = *tert*-butyl hydroperoxide.

According to the Kruskal-Wallis test, the difference in the median values of the cell viability assay for the various *t*-BHP treatments was not significantly different (p-value = 0.39), and the ROS measurements were therefore based on a similar quantity of cells for all treatments. It can therefore be concluded from the ROS assay as well as the MTT assay that the HeLa cells eventually produced ROS leading to both apoptosis and necrosis. The effect of the ROS production on MT gene expression was further analysed and the results thereof are presented in Section 6.4.1.

6.4 REAL-TIME PCR ANALYSIS OF METALLOTHIONEIN RNA

The Guanidinium thiocyanate and phenol-chloroform extraction method utilising the TRizol LS reagent was employed for RNA isolation from blood as well as from HeLa cells treated with varying concentrations of *t*-BHP for three hours. Subsequent to the RNA isolation, the purity, concentration and integrity of the isolated RNA, was analysed via spectrophotometry and agarose gel electrophoresis, respectively. Upon analysis of the RNA isolated from blood, it was observed that there was DNA contamination of the isolated RNA. To overcome this obstacle, RNase free DNase was utilised to destroy the DNA as described in Section 5.7.2, yet keeping the RNA intact. The RNA was further analysed on a 2% (w/v) agarose gel. The results thereof are presented in Figure 6.1.

Figure 6.1: Photographic representation of untreated RNA and DNase treated RNA

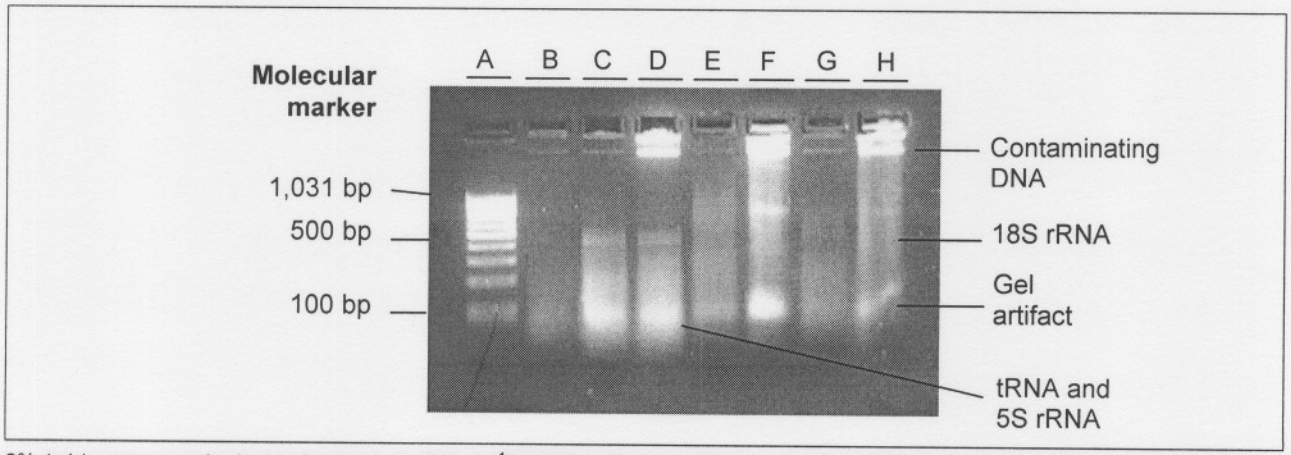

2% (w/v) agarose gel, electrophoresed at 10 $V.cm^{-1}$ in TBE buffer. A = 100 bp molecular weight maker; B = DNase treated RNA for sample 1414; C = DNase treated RNA for sample 1424; D = untreated RNA for sample 1424; E = DNase treated RNA for sample 1531; F = untreated RNA for sample 1531; G = DNase treated RNA for sample 1521; H = untreated RNA for sample 1521; tRNA = transfer RNA; rRNA = ribosomal RNA, S = Svedberg units.

The DNA contamination of RNA was also observed subsequent to the Real-Time PCR analysis of the RNA where amplification of the MT-2A pseudogene was observed upon analysis of the Real-Time PCR products on a 2% agarose. The MT-2A primer set listed in Table 5.11 was analysed for complementarity to other MT genes via the Basic Local Alignment Search Tool (BLAST). The forward primer sequence had 96% complementarity to the MT-2A pseudogene, whereas the reverse primer had 95% complementarity. A fragment of ca. 400 base pairs, as indicated in Figure 6.2 was observed which corresponded to a fragment size that would the obtained if the MT-2A pseudogene was amplified. From these two observations it was thus concluded that the RNA had DNA contamination.

Figure 6.2: Photographic representation the MT-2A pseudogene product amplified via Real-Time PCR

2% (w/v) agarose gel electrophoresed at 10 $V.cm^{-1}$ in TBE buffer. A = 100 bp molecular weight maker; B = Real-Time PCR product from RNA isolated from HeLa cells, which was utilised as a positive control of MT-2A; C = control sample 1; D = control sample 2; E = sample 1524; F = sample 1414; G = sample 1415; H = negative control.

cDNA synthesis was performed with 3 μg of total RNA using the MMLV-RT enzyme, and was subsequently utilised for Real-Time PCR. Real-Time PCR was the method of choice due to its accuracy, sensitivity, and minimal amount of RNA required. As discussed in Section 5.6, two methods were initially employed for Real-Time PCR, however, the iScript™ one step Real-Time PCR was omitted as the method of choice, because the PCR efficiency was lower than that of the iQ SYBR Green® Real-Time PCR kit. The optimised temperatures listed in Table 5.11 were utilised for the Real-Time PCR amplification of the receptive genes.

6.4.1 Real-Time PCR detection of the expression of MT genes in HeLa cells

To analyse the effect of ROS production via treatment with *t*-BHP on the expression of MT genes, Real-Time PCR was employed. Due to the requirement of internal controls, as indicated by Radonić *et al.* (2004), four housekeeping genes listed in Table 5.11 were analysed. The annealing temperature for all the primer sets listed in Table 5.11 was optimised at 60°C. In this investigation glyceraldehyde-3-phosphate dehydrogenase (GAPDH) and β-microglobulin were found to be the most stably expressed genes, and were used for the normalisation of the MT expression profile. These genes were listed by Radonić *et al.* (2004) as suitable genes to use as housekeeping genes for the normalisation of Real-Time PCR experiments. It was observed that the increased ROS production led to an increase of MT-2A gene expression and not increased expression of MT-1 isoforms, even though ROS-dependent induction was reported by Dalton *et al.* (1994). To compare the different RNA transcription levels, the Ct values for MT-2A for the *t*-BHP treated cell lines were compared via the GeNorm software version 1.4. The Ct is defined as the number of cycles needed for the fluorescence signal to reach a specific threshold level of detection. At this point, a significant increase in the quantity of the PCR product was detected.

To ensure comparability between the two housekeeping genes as well as the MT-2A, the PCR efficiency was first determined for each gene by measuring serial dilution from 15 $ng.\mu l^{-1}$ to 0.12 $ng.\mu l^{-1}$. Ct values less than 40 were used for calculation of the PCR efficiency, via the Relative expression software tool (REST) as discussed by Pfaffl *et al.* (2002). The PCR efficiency for GAPDH, β-microglobulin and MT-2A were 1.94, 1.99, and 1.99 respectively. In this analysis, a PCR efficiency value of 2 indicated a 100% amplification efficiency. For the analysis of gene expression in each of the *t*-BHP HeLa cell lines, the Real-Time PCR for each sample was performed in triplicate. The GeNorm software version 1.4 program was utilised to determine the normalisation and the formulas indicated in Table 5.14 utilised in the Microsoft Excel® software programme to measure the relative expression of MT-2A. A summary of this data obtained is presented on Table 6.17.

Table 6.17: Summary of MT-2A gene expression in *t*-BHP treated cells

Conditions	Mean Ct	Standard deviation of Ct	Normalised quantity	Expression ratio	Standard deviation of Expression ratio
0 mM *t*-BHP	19.4	0.173	0.259	1.000	0.187
0.5 mM *t*-BHP	18.5	0.173	0.523	2.018	0.285
0.8 mM *t*-BHP	17.4	0.402	0.672	4.613	0.549
1 mM *t*-BHP	20.3	0.208	1.330	5.127	1.148

As graphically presented in Graph 6.18, there was a proportional increase in putative ROS induced expression of MT genes. The 0.5 mM *t*-BHP concentration treatment resulted in a two fold expression of the MT-2A gene. A four and a half-fold and five-fold increase in expression of MT-2A as compared to the control cell lines was observed for the 0.8 mM and 1 mM *t*-BHP concentrations respectively. A high standard deviation was however, obtained for both the 0.8 mM (0.549) and 1 mM *t*-BHP (1.148) concentrations, indicating varied responses of cells to the *t*-BHP treatment, resulting in a high variation of the expression of MT genes. This increase in the standard deviation with an increase in the *t*-BHP concentration was also observed when the ROS production was measured as discussed in Section 6.3.1. This observation supports the suggestions made in Section 6.3.1, that a subset of cells may have activated endogenous antioxidant mechanisms to overcome the effect of ROS. This postulation was however not tested due to the large quantity of cells required for the ORAC assay as discussed in Section 5.2. It was also noted, as indicated in Graph 6.18, that the difference in MT expression between the 0.5 mM *t*-BHP and 0.8 mM *t*-BHP concentrations was greater than the difference between 0.8 mM *t*-BHP and 1 mM *t*-BHP treatments. This observation may illustrate that at the former concentrations, the endogenous cellular antioxidant mechanisms were not sufficient to scavenge the ROS, thus resulting in a robust ROS-dependant MT expression. However, at the latter concentrations, the antioxidant mechanisms were more efficient at diminishing ROS, although there was still high enough levels of ROS to result in the expression of MT genes.

Graph 6.18: Representation of the effects of the *t*-BHP treatment on the expression of MT-2A *in vitro*

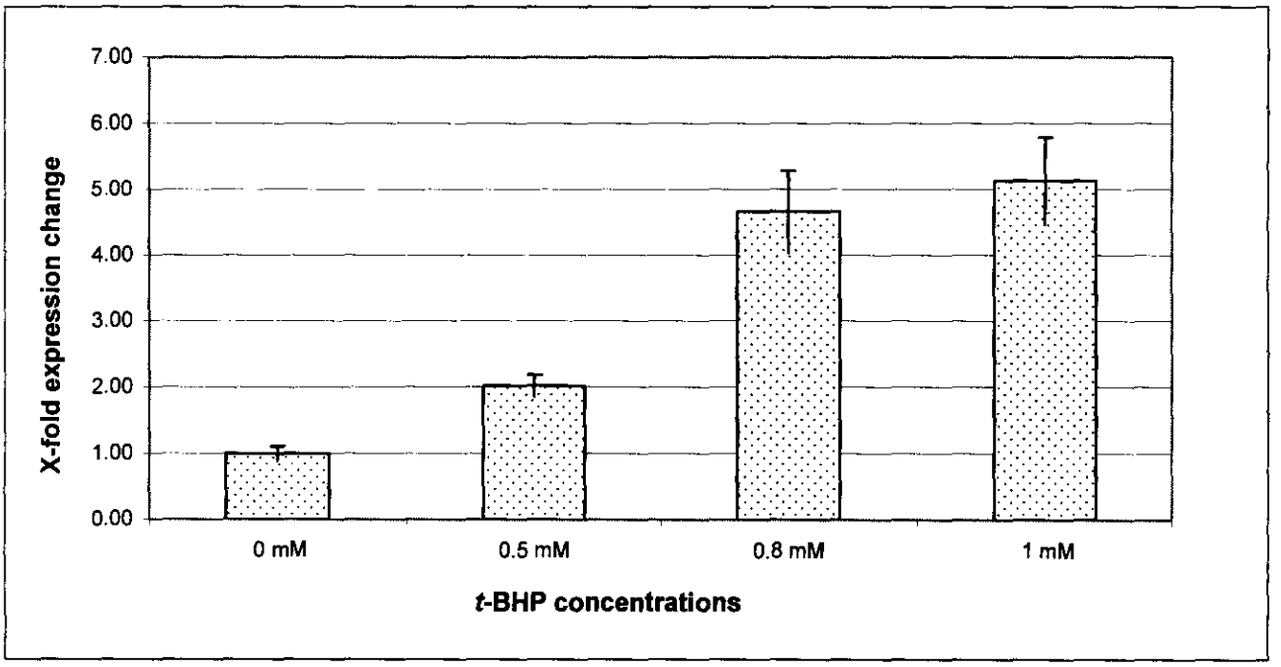

t-BHP = *tert*-butyl hydroperoxide.

It can therefore be concluded from the results presented in this Section that the increase in ROS production, induced by the treatment of cells with *t*-BHP, does result in an increase in the expression of MT genes. However, in this cell line MT-2A was the only MT isoform that was expressed at a level above the threshold value. Even though these results are derived from *in vitro* work, they serve as a positive control for the ROS-induced expression of MT genes, since at the time of this investigation no *in vivo* analysis, particularly in humans, of ROS-induced MT expression had been reported.

6.4.2 Real-Time PCR detection of the Metallothionein gene expression in whole blood

It has previously been reported that quantitative changes in MT mRNA content in lymphocytes exposed to high Cd concentrations can be detected (Yamada and Koizumi, 2001). The report by Yamada and Koizumi (2001) supports the postulated metal-induced expression of MT genes. However, the limiting factor of such investigations is that the cells were isolated and grown in culture prior to RNA isolation. Therefore, this observation still requires to be elucidated *in vivo*. It was the aim of this investigation to quantify the expression levels of MT mRNA from RNA isolated from whole blood of T2D individuals as well as individuals not affected with T2D and to explore the possibility of utilising the differential expression of MT genes as a biomarker for oxidative stress in T2D individuals.
RNA was isolated from whole blood as described in Section 5.6.1. In order to estimate the differences in the mRNA content of whole blood, all five housekeeping genes listed in Table 5.8 were initially analysed to evaluate their use as internal controls in reactions containing control RNA isolated from whole blood. All reactions were performed in duplicate. From the experimental results obtained from control samples the expression of GAPDH was the most stable, with Ct values ranging between 30 and 42.7. The expression of β-actin, β-microglobulin and RNA polymerase II exhibited great variation, where in some samples expression of these genes above the threshold position was not detected. It was thus concluded that GAPDH was the most stably expressed housekeeping gene and thus ideal to be utilised for normalisation of the expression of MT genes. It has been suggested by Ullmannová and Haškovec (2003) as well as by Radonić *et al.* (2004) that it is best to utilise two housekeeping genes for normalisation. In this regard, it was concluded that utilising a single stably expressed gene would provide more accurate results as opposed to the use of a second gene whose expression was not stable. Therefore, GAPDH was the only housekeeping gene utilised for normalisation in this investigation.

In contrast to the 35 cycles utilised for Real-Time PCR performed on RNA isolated from *t*-BHP treated cell lines, 45 cycles for RNA isolated from whole blood were performed. This is mainly due to the low PCR efficiency that was obtained for RNA isolated from blood utilising the method discussed in Section 6.4.1. When determining the PCR efficiency a linear increase in the Ct values with an increase in the concentration of cDNA utilised is required. This was observed for HeLa cells. However, for RNA obtained from whole blood of individuals in the three groups, the Ct values were within the same range even with an increase in cDNA concentration. The procedure for determining the expression profile for MT in HeLa cells, i.e. determining the normalised expression via Equation 1.0 listed in Table 5.14, was not followed in this regard.

As indicated in Appendix C the expression profile was classified as below the experimentally defined threshold position or above. Out of the three MT gene isoforms analysed, i.e. MT-1A, MT-1B and MT-2A, only MT1B was detected above the threshold level in all the individuals analysed. In contrast, MT-2A was detected in only 13.7% of the 73 individuals at levels above the threshold. Statistical parameters of the cycle threshold values obtained were measured and are listed in Table 6.18.

Table 6.18: Summary of the cycle threshold values obtained for the expression of MT and GAPDH genes

MT-1B					
Group	**Mean**	**Median**	**Minimum**	**Maximum**	**Standard deviation**
Group-1	36.09	36.00	32.20	39.20	2.02
Group-2	35.96	36.65	32.20	39.20	2.09
Group-3	35.83	35.60	31.00	42.80	2.64
MT-2A					
Group	**Mean**	**Median**	**Minimum**	**Maximum**	**Standard deviation**
Group-1	37.8	38.50	35.20	39.80	2.37
Group-2	38.70	38.70	37.90	39.50	1.13
Group-3	34.38	34.25	32.00	37.00	2.10
GAPDH					
Group	**Mean**	**Median**	**Minimum**	**Maximum**	**Standard deviation**
Group-1	36.71	36.90	31.80	41.30	2.67
Group-2	37.67	38.20	32.50	42.70	2.82
Group-3	37.42	37.70	30.30	43.70	2.71

From the analysis of the median values via the Kruskal-Wallis test for all three genes presented in Table 6.18, it was observed that no significant difference (p-value = 1.000)

was present between the individuals in the three groups who presented with Ct values above the threshold level. The Ct values of MT-2A and MT-1B expression for the samples that were above the threshold position are indicated in Appendix C and graphically presented in Graph 6.19. Due to the Bio-Rad iCycler™ iQ optical system software version 3.0 providing the Ct values for those above the threshold levels only, the samples with gene expression below the threshold level are indicated as NA in Appendix C and are therefore not indicated in Graph 6.19a. The Ct values of GAPDH are also indicated in Appendix C, and the distribution of these values is depicted in Graph 6.19.

Graph 6.19: Scatter plots of the cycle threshold values for the expression of MT and GAPDH genes in vivo

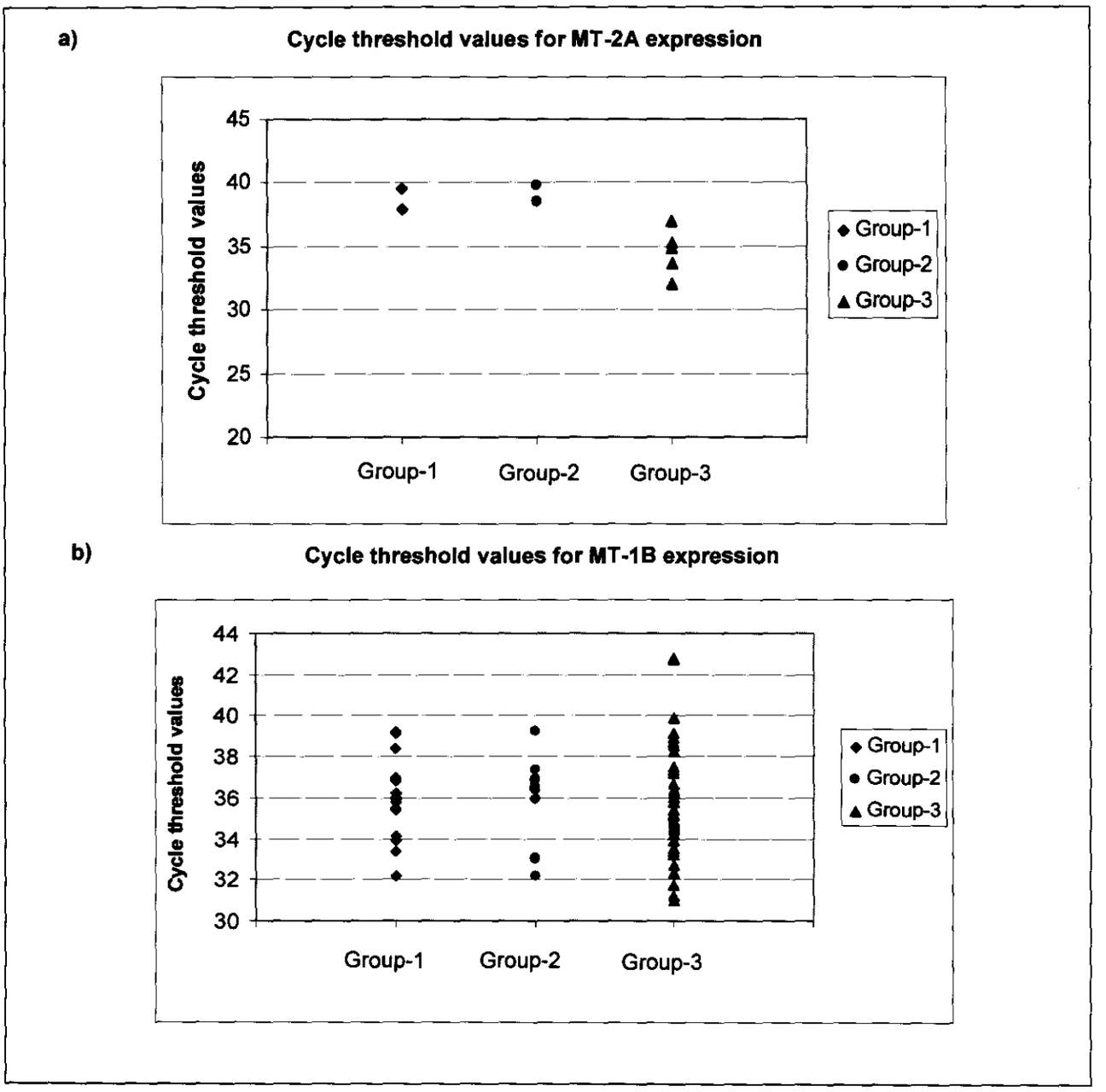

Graph 6.19: continued ...

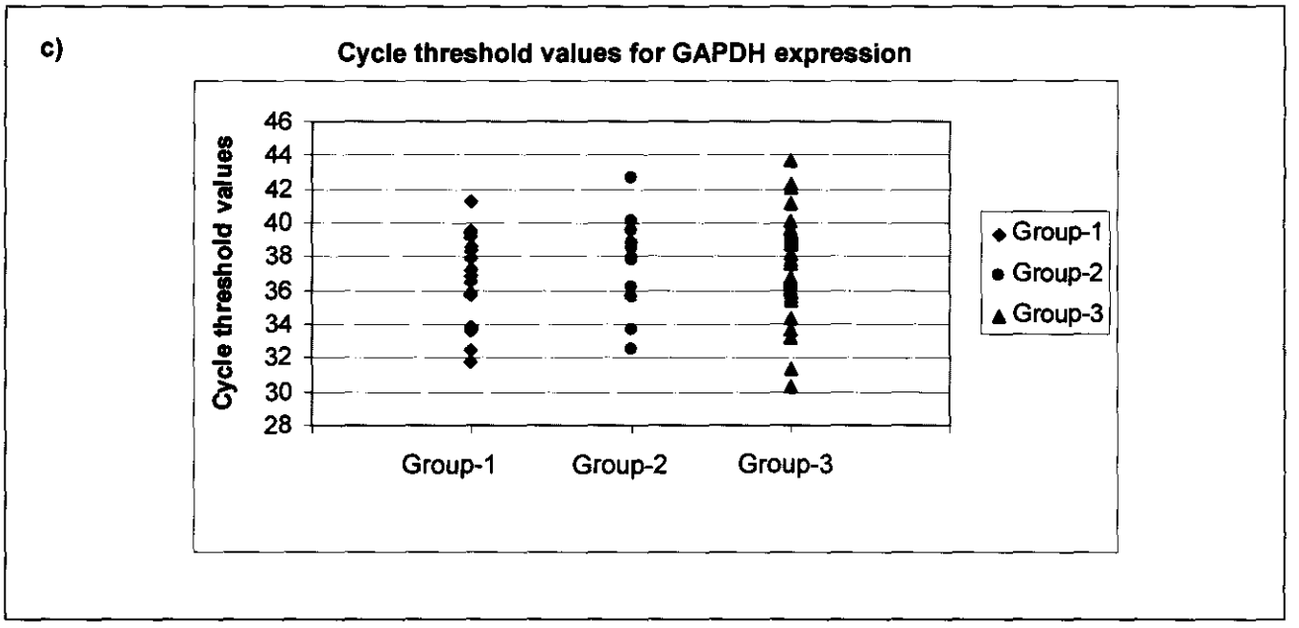

As discussed below Table 6.17, according to the Kruskal-Wallis test, no significant difference between the Ct values of GAPDH and those of MT-1B was observed (p-value = 1.000). From this result it was concluded that there is no significant difference between the expression profile of GAPDH and that of MT-1B, indicating that the MT-1B mRNA that was detected was the baseline expression of this gene.

Of the individuals comprising Group-1, 21% had Ct values for MT-2A above the threshold level, whereas in the remaining 79% no Ct values above the threshold level were detected. The above-mentioned 21% of individuals comprising Group-1 presented with high values for the d-ROMs test, low values for the ORAC assay and lowered GSH:GSSG ratios. However, there are individuals within this group who had similar biochemical profiles but did not present with Ct values above the threshold level.

In Group-2, 16.7% presented with Ct values for MT-2A above the threshold level. In 83.3% of this cohort, no expression of MT-2A was observed above the threshold level. The GSH:GSSG ratio of the 16.7% was greatly reduced as indicated in Appendix B. The reactive oxygen metabolites were also increased as depicted by the high value obtained for the d-ROMs test for one of these individuals, whereas the other individual presented with a relatively low value for the d-ROMs test.

In Group-3, 9.5% of individuals presented with Ct values for MT-2A above the threshold level and for the remaining 90.5% no expression above the threshold level was observed.

The values of the d-ROMs test for the 9.5% also ranged between border line threshold and high oxidative stress similar to those of the individuals in Group-1 and Group-2. The values for the GSH:GSSG ratio were however significantly higher that those of the individuals in Group-1 and Group-2 presenting with Ct-values for MT-2A above the threshold level. From these observations, it is suggested that no relationship between the results of the biochemical parameters analysed is present in this cohort of 73 individuals. To obtain a true reflection of the effects of increased levels of ROS on the expression of MT genes in humans, it is suggested that alternative methods be explored for the detection of MT expression.

Another suggestion that may be put forward from this data is that blood is not an ideal tissue to utilise for analysis of differential expression of MT genes due to its heterogeneous nature, leading to the non-specificity of the results obtained. Even though the expression of MT-1B was above the threshold level in the three groups, no significant difference in the median values according to the Kruskal-Wallis test was obtained (p-value = 1.000).

6.5 DETECTION OF METALLOTHIONEIN PROTEINS VIA ELISA

In order to further evaluate the expression of MT genes in *t*-BHP treated HeLa cells, as well as serum from individuals in Group-1, Group-2 and Group-3, the competitive ELISA as discussed in Section 5.7 was performed. Each sample was performed in triplicate. The factors listed in Table 6.19 were modified to fit the experimental conditions of this investigation.

Table 6.19: Summary of the factors that were optimised for the competitive ELISA

Parameter	Optimised conditions
Plate coating	4 μg. ml^{-1} MT in freshly prepared 0.1 M $NaHCO_3$ at pH 9.6
Sample volume	The amount of sample utilised was based on protein content instead of volume. 250 μg sample protein per 160 μl volume was utilised
Primary antibody	Polyclonal antibody was utilised instead of the monoclonal antibody
Blocking	Blocking was carried out for 2 hrs to obtain optimal blocking, thus preventing non-specific binding of the antibody.
Detection antibody	1:10,000 detection antibody (Goat anti-rabbit immunoglobulin G (IgG): horse radish peroxidase (HRP) conjugate) concentration was prepared in block buffer

μg. ml^{-1} = microgram per millilitre; μl = microlitre; $NaHCO_3$ = sodium bicarbonate; hrs = hours; M = molar; IgG = immunoglobulin G; HRP = horse radish peroxidase.

It has been suggested by Dabrio *et al.* (2002) that pre-treatment of the sample with β-mercaptoethanol aids in overcoming oxidation of the protein, which results in

overestimation of the protein concentration. However, in this investigation adding β-mercaptoethanol resulted in the standard series reacting at a slower rate than that of the samples. For this reason, this procedure was not followed. The sensitivity of the competitive ELISA as well as the small amount of starting material required for this assay were the main reasons why this method of analysis was included in this study. The low immunogenicity of MT as well as the risk of polymerisation, could lead to lowered detection efficiency. However, these limitations were overcome by comparing the data obtained via the ELISA assay with results of the Real-Time PCR.

6.5.1 ELISA detection of the Metallothionein protein *t*-BHP treated HeLa cells

As previously discussed, HeLa cells treated with varying concentration of *t*-BHP to induce ROS production were utilised as a positive control for the ROS-induced expression of MT genes. Subsequent to the Real-Time PCR analysis of gene expression, the competitive ELISA was performed to analyse the presence of MT proteins. The protein content of the cells was determined according to the method described in Section 5.3.2.1. A mean value for the absorbance values at 460 nm was obtained for the triplicates and the presence of MT proteins expressed as μg MT per μg protein. The reproducibility of this assay was low. It is therefore suggested that further optimisation of this method is required for the use of the competitive ELISA in the detection of MT proteins. Although there was low reproducibility the data was still further analysed to determine the expression of MT protein in HeLa cells treated with *t*-BHP. The results of this assay are presented in Table 6.20.

Table 6.20: Summary of the ELISA data obtained from *t*-BHP treated HeLa cells

Parameter	0 mM *t*-BHP	0.5 mM *t*-BHP	0.8 mM *t*-BHP	1 mM *t*-BHP
Protein concentration ($\mu g.\mu l^{-1}$)	0.71	0.61	1.32	0.23
Mean (absorbance at 460 nm)	0.04	0.02	0.13	0.07
μg MT per μg protein	0.00	0.54	3.40	1.68

μg = micro grams; *t*-BHP = *tert*-butyl hydroperoxide; nm = nanometre; mM = millimolar; MT = metallothionein.

For the analysis of the data, the 0 mM *t*-BHP concentration was utilised as a reference, with no induced expression of MT gene, thus no MT protein. The presence of MT protein in terms of μg MT per μg protein is indicated in Graph 6.20. The high standard deviation observed, as indicated in Graph 6.20, may be due to the low reproducibility of the ELISA, thus resulting in high variation. However, it can also be suggested that, as discussed in Section 6.4.1, other cellular antioxidant mechanisms may have been activated thus scavenging the ROS and therefore resulting in the variable translation of MT mRNA to MT

protein. This factor could also explain the low levels of MT protein in the HeLa cells treated with 1 mM t-BHP.

Graph 6.20: Representation of the ELISA data of *t*-BHP treated HeLa cells

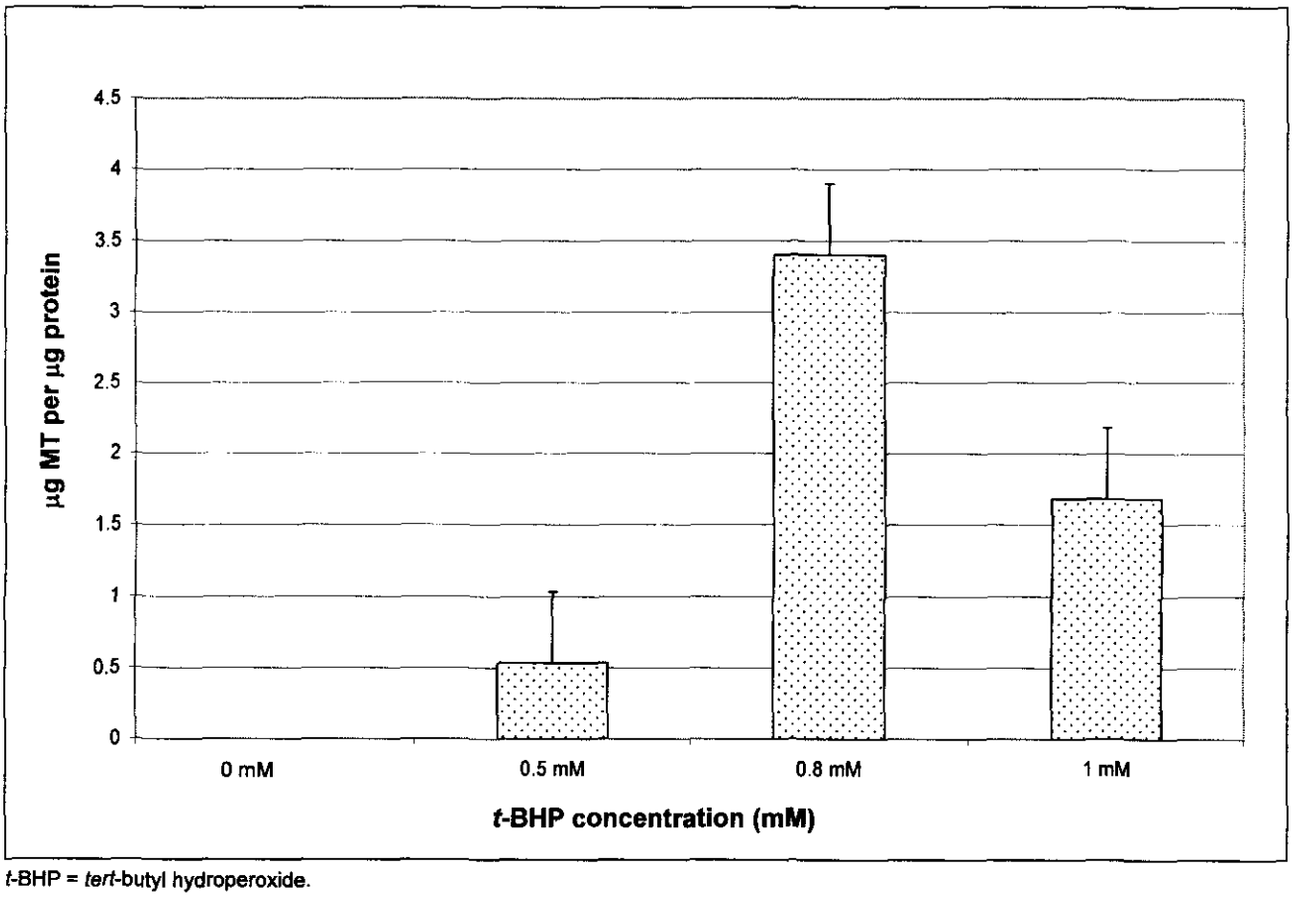

t-BHP = *tert*-butyl hydroperoxide.

6.5.2 ELISA detection of the Metallothionein protein in serum

Due to the unavailability of a reported reference group or sample for physiological levels of MT in serum, results reported by Sullivan *et al.* (1998) of MT concentration in isolated erythrocytes were utilised in this investigation as a reference. Sullivan *et al.* (1998) reported that in erythrocytes of control individuals, i.e. not undergoing Zn supplementation, an MT concentration of 0.027 µg MT. μg^{-1} protein was detected. This value was greatly increased in individuals supplemented with Zn. In the current investigation, low levels of MT were detected for all three groups as presented in Appendix D, however 24.6% of the individuals as indicated by asterisks in Appendix D, did present with a high level of MT protein. As depicted in Graph 6.21, most values cluster within the range of 0 to 0.02 particularly in Group-1 and Group-3. This result was not expected for Group-1 based on the significantly higher oxidative stress detected within this group when compared to Group-3. The factors that may have led to this result are discussed in the subsequent paragraphs.

Graph 6.21: Scatter plots of the ELISA data for all three groups

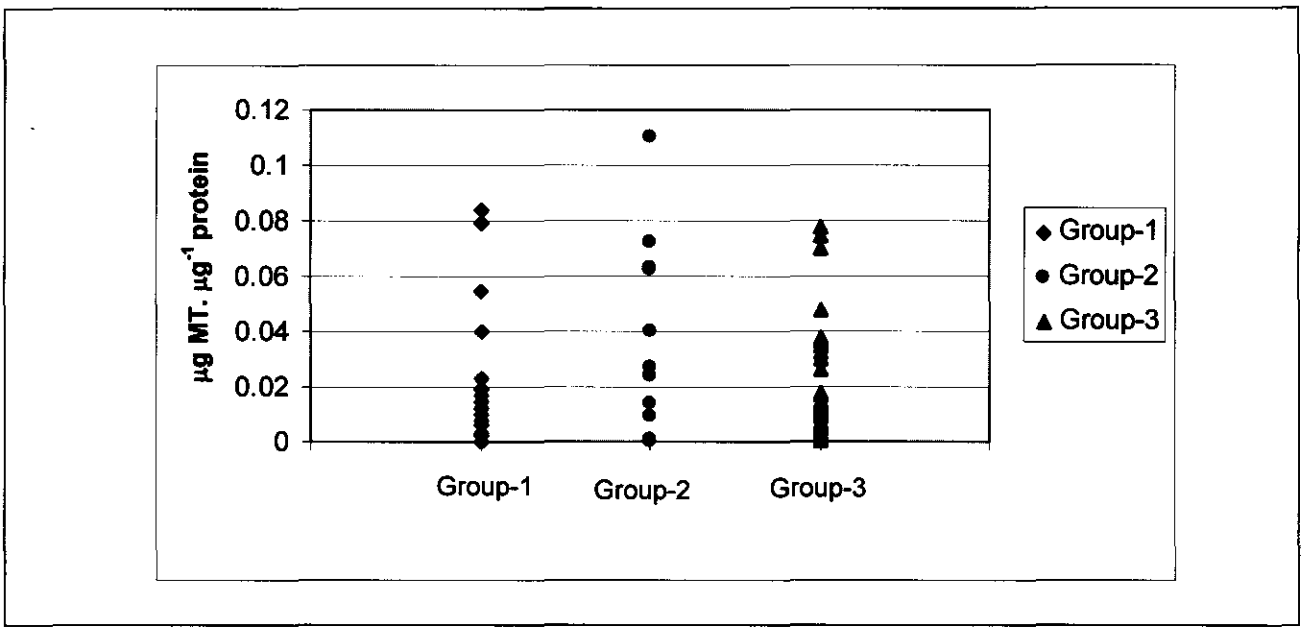

It has been reported by Butcher *et al.* (2003) that the reproducibility of the competitive ELISA is very low at low concentrations of MT. This was also observed in the current investigation, where samples were analysed in triplicate and a low reproducibility was detected. Although two of the three replicates were in most cases within the same range, the third replicate was always out of range. A high standard deviation was thus observed between the three values obtained for each sample.

Even though there was great variation between the replicates, the data obtained was still analysed via Statistica© based on the values listed in Appendix D to determine the significance of the differences obtained for the presence of MT proteins between the three groups. The mean value for Group-3 and Group-1 were low, as indicated in Table 6.21. This observation was however expected due to the lower d-ROMs values, as well as the higher GSH:GSSG ratio, that was obtained for Group-3, however it was not expected for Group-1. The low mean value could also be attributed to the result presented in Graph 6.21, where it is illustrated that in the majority of individuals within these two groups values lower than 0.02 µg MT.µg^{-1} protein were detected. Therefore it may be suggested from this observation that there was a lower concentration of MT protein within Group-1 and Group-3 when compared to Group-2.

Table 6.21: Summary of the statistical parameters analysed for the ELISA data

Group	Mean	Median	Minimum	Maximum	Standard deviation
Group-1	0.02	0.01	0.00	0.08	0.03
Group-2	0.04	0.03	0.00	0.11	0.03
Group-3	0.02	0.01	0.01	0.08	0.02

According to the Shapiro Wilk's W test performed via the Statistica© software program the ELISA data was not normally distributed, with a p-value less than 0.01. A great proportion of the values were clustered within the range from 0.00 to 0.02. The Kruskal-Wallis test was performed via the Statistica© software program to determine the level of significance in the differences obtained between the median values of three groups. A p-value of 0.414 was obtained indicating that no statistically significant difference between the median values existed.

No statistically significant difference in the presence of the MT protein between these three groups was observed. From this investigation, as well as those of Olivier, 2004 and Reinecke, 2004, it is evident that the competitive ELISA is not the ideal method to utilise for analysis of MT proteins, or that further optimisation, may be required. Other methods such as western blot, capillary zone electrophoresis, immunohistochemistry and the Cd binding assay which have previously been utilised for the detection of MT could be employed for this purpose (Harley *et al.*, 1989; Kubo *et al.*, 1999; Hasumi *et al.*, 2003). However, due to the time efficiency and sensitivity of Real-Time PCR, it was the method of choice. Harley *et al.* (1989) reported that an induction in MT expression as well as increased levels of the protein were observed utilising northern blot and the Cd binding assay, respectively.

6.6 SUMMARY OF THE RESULTS

One of the objectives of this study was to determine the levels of ROS in the three groups. From the results obtained, it seems as though elevated levels of ROS were present in elderly diabetic individuals (Group-1), supporting the reported presence of high levels of ROS in T2D (Dandona *et al.*, 1996; Sakai *et al.*, 2003). Elevated levels of ROS were also detected in elderly non-diabetic individuals (Group-2), in contrast to the POWIRS2 group (Group-3) of individuals, where lower levels of ROS were detected. These results illustrate that ROS does not only play a role in the pathogenesis of T2D but is also involved in the presentation of other age related complications observed in Group-2. The high standard deviation, obtained with the various biochemical analyses reported in this thesis, may

suggest the instability of these parameters, thus making them unsuitable for the determination of ROS and the redox status in pathological conditions. However, other factors such as obesity, smoking as well as the possible genetic predisposition (as suggested by a family history of diabetes) of a subset of the individuals included in this study may have led to the high variation observed in the biochemical parameters analysed.

From the results presented in this chapter in Sections 6.3, 6.4.1 and 6.5.1, on the analyses performed *in vitro,* it is evident that MT expression is induced by elevated levels of ROS. Therefore the objective of elucidating the expression pattern of MT genes in HeLa cells and using this cell line as a positive control as discussed in Section 4.2.1 was attained.

However, these results were not observed in *in vivo* conditions. Despite the observed high oxidative stress in Group-1, it could not be concluded with certainty that the elevated ROS in T2D does not result in increased MT expression. This observation could suggest that other cellular endogenous antioxidant mechanisms are involved in the eradication of ROS, thus the levels of ROS may not be sufficient in pathological conditions such as T2D to induce ROS-dependant expression of MT genes. In support of this observation, Aksenov and Markesbery (2001) suggested in their report subsequent to the analysis of the expression pattern of key glutathione redox system genes (GSHPx and glutathione reductase) in the hippocampus of patients with Alzheimer's disease, that there was insufficient induction of these genes therefore contributing to the elevated levels of ROS within the tissue analysed.

Although a distinct expression pattern of MT genes was not observed in the three groups of individuals to enable differentiation between these groups based on the MT gene expression profile, the second objective of this study as outlined in Section 4.2.1 was accomplished. The aim was to investigate the expression profile of MT genes in T2D individuals. Therefore, from the results presented here the hypothesised ROS-induced MT expression in T2D individuals due to the increased levels of ROS as discussed in Section 4.2.1 can not be rejected with certainty.

Oxygen free radicals formed in tissues can be spontaneously degraded by endogenous cellular mechanisms, such as GSH or SOD. Thus, the lack of detection of induced MT gene expression may be due to the action of these cellular mechanisms. The particularly short half-life of the free radicals could be another factor that may have led to the high

variation observed in the biochemical parameters analysed as well as the lack of detection of MT expression *in vivo*. It has also been reported that MT and other scavengers can only be effective if they are within close proximity of the site of radical production in order to interact with the radicals before they react with other cellular compartments (Fahn and Cohen, 1992). The aforementioned postulation thus supports the suggested analysis of the affected tissue in T2D individuals. Furthermore, the high level of variation in the concentration of metallothionein proteins in different species and tissues that was detected by Miura *et al.* (1997) and Esposito *et al.* (2000) reflected the effects of age and cell function on the expression of these genes. However, it was observed in this investigation that blood is not an ideal tissue to utilise for the analysis of MT gene expression.

From the p-values presented in Section 6.5.2, which were obtained via the Kruskal-Wallis test, it may be suggested that no significant difference in the presence of the MT protein exists between the three groups. It is further illustrated in Graph 6.19, by the clustering pattern of the Ct values of MT-1B and those of GAPDH that the distribution of the Ct values for MT-1B is similar to those of GAPDH. The expression of MT-2A above the threshold level was only detected in a subset of individuals, as indicated in Graph 6.19 and in Appendix C. However, no distinct group of characteristics among this cohort could be identified. However, to obtain a better representation of MT expression in the T2D population group, a larger cohort may need to be analysed. Therefore, it is suggested that the remaining functional MT isoforms discussed in Table 4.1 should be analysed to obtain a comprehensive expression profile of MT genes in T2D individuals and those not affected.

It may also be concluded from the results presented in this chapter that further analyses are, however, required in order to optimise the ELISA. Alternatively, as mentioned earlier, other methods could be utilised for the detection of MTs. If this could be accomplished in the future, analysis of MT expression in specific tissues involved in the pathogenesis of T2D would prove to be significant in the evaluation of the effects of pathophysiological levels of ROS on the expression of MT.

CHAPTER SEVEN

CONCLUSIONS

Various reports have demonstrated that oxygen free radicals, which are mainly produced via the reduction of O_2 to H_2O, are at the centre of the pathogenesis of various disorders (Fahn and Cohen, 1992; Dandona *et al.*, 1996; Segrouchni *et al.*, 2002). A cell utilises 10^{13} molecules of O_2 per day. It is estimated that 1% of the respired molecular O_2 will be converted to superoxide. Thus, this means that 10^{11} free radical species are produced by each cell per day. Therefore, the higher the energy demands of a cell, the more O_2 used with a resultant increase in the production of ROS. This occurs particularly in high energy demanding tissues. If there is an imbalance between the oxidants and the antioxidant mechanisms these tissues will be affected and this is commonly referred to as "oxidative stress". This phenomenon is observed to a great extent in disorders such as Alzheimer's disease, diabetes mellitus and mitochondrial cytopathies, where the brain, muscles and heart present with symptoms earlier than the rest of the body (Suzuki *et al.*, 1999; Zhu *et al.*, 2004).

High levels of ROS result in various effects such as DNA damage, oxidative modification of proteins, lipid peroxidation, modification of sugars (increased glycation and glycoxidation) and eventually leads to apoptosis (Dandona *et al.*, 1996; Suzuki *et al.*, 1999). When a cell is exposed to oxidative stress, endogenous mechanisms such as enzymatic and chemical antioxidants, as discussed in Section 3.3, are employed to destroy ROS and reduce their harmful effects. Under normal conditions, these mechanisms are sufficient to counteract the free radical damage. Based on these effects of ROS it was decided to investigate the role of ROS in the pathogenesis of diabetes mellitus, particularly T2D.

7.1 OXIDATIVE STRESS IN T2D, NON-DIABETIC AND INDIVIDUALS AT RISK FOR DEVELOPING DIABETES

Diabetes mellitus is a metabolic disorder that is recognised as one of the leading causes of mortality and morbidity in the world, affecting ca. 5-6% of the world population (King *et al.*, 1998). The effects of increased levels of ROS in the pathogenesis of T2D have not been fully understood. However, as illustrated in Section 6.2, in T2D individuals the antioxidant

mechanism previously mentioned are overwhelmed due to the increased oxidative stress. T2D is characterised by among other features glucose auto-oxidation, protein glycation, and activity of the pentose phosphate pathway as discussed in Section 3.3. These features reflect increased ROS production and metabolic stress resulting from changes in the energy metabolism (Lee and Chung, 1998; Orie *et al.*, 1999; Suzuki *et al.*, 1999).

The use of the d-ROMs test in this investigation enabled the analysis of a broader range of reactive oxygen metabolites as presented in Section 6.2.1.1, thus providing a holistic view of the level of reactive oxygen metabolites in blood samples of these individuals. Oxidative stress was found to be significantly increased in elderly individuals (Group-2) when compared to the younger, non-diabetic individuals (Group-3), with a p-value of 0.016. The minimum and the maximum ages in Group-2 were 40 and 78 respectively, with 8.3% of the individuals being equal to or younger than 40 years of age, and the remaining 91.7% older than 40 years. In contrast, 7.1% of the individuals in Group-3 were above or at the age of 40, whereas 92.9% were younger than 48 years. The results obtained in this study, where increased oxidative stress was detected in Group-2 when compared to Group-3, support the postulated increase in the production of ROS with an increase in age (Lenaz, 1998). It was reported in studies performed by Dandona *et al.* (1996) and Segrouchni *et al.* (2002), where oxidative stress was measured, that diabetic individuals had an increased ROS production in comparison to their control groups. Even though different techniques were utilised, the difference between these reports and the current investigation may be due to the fact that individuals comprising Group-1 were already on medical treatment for T2D, which may have resulted in the reduction of ROS production, and thus no significant difference between Group-1 and Group-3. These results are the first to use the d-ROMs test in diabetic individuals to analyse the levels of the reactive oxygen species.

As previously mentioned, the endogenous antioxidant capacity is compromised in high oxidative stress conditions. This observation was detected upon the use of the ORAC assay for the three groups of individuals. The total antioxidant capacity in serum obtained from diabetic and elderly non-diabetic individuals was reduced, but not to the level of statistical significance (see page 93), when compared to the group of individuals at risk for developing diabetes. This result is a reflection of the results obtained via the d-ROMs test.

Another parameter indicative of oxidative stress that was analysed was the GSH:GSSG ratio. The results presented in Section 6.2.1.3, support the hypothesis made in Section 3.3.2.2, that hyperglycaemia leads to a depletion of GSH. However, a depletion of GSH

was not exclusive to Group-1 but was also noted in Group-2. The aforementioned observations indicate that ROS production via various mechanisms presented throughout the literature leads to the consumption of GSH, resulting in a decreased GSH:GSSG ratio in these two groups of individuals. This result is in accordance with that presented by Aksenov and Markesbery (2001) where sulfhydryl containing proteins were found to be reduced in patients with Alzheimer's disease, due to the increased oxidative stress in the hippocampus of these patients. The increased oxidative stress detected in individuals comprising Group-1 and Group-2 may be due to the unavailability of GSH to scavenge the ROS thus leading to the many complications observed in these individuals, as presented in Appendix A.

Due to the NADH:NAD^+ ratio being an important marker of the cellular redox status as well as the metabolic state, it was investigated in this molecular study. This ratio was found to be affected by the presence of high levels of ROS. The observation was furthermore supported by the analysis of the energy status in whole blood of all groups of individuals. It can be suggested from the results presented in Section 6.2.1.6 that the energy levels in terms of the ATP:ADP ratio in Group-1 and Group-2 was significantly reduced (p-value = 0.001) when compared to Group-3. An overall increase in the lactate:pyruvte ratios was also noted in Group-1 and Group-2 suggesting that less pyruvate is formed for metabolism via the TCA cycle, more lactate is formed, thus resulting in the lowered energy levels as detected via the ATP:ADP ratio. The afore-mentioned observations eventually lead to lactic acidosis, which is one of the characteristic symptoms of T2D. According to the results of the correlation analyses no relationship existed between the d-ROM and the ORAC data. However from the results of all three groups, relationships between the ATP:ADP ratio, NADH:NAD^+ ratio, GSH:GSSG ratio and the Lactate:pyruvate ratio do exist, even though the correlation coefficients obtained did not indicate strong relationships.

The detection of increased levels of oxidative stress in these biological samples is a step closer to elucidating the relation between free radical production and disease pathogenesis. The chronic ROS exposure observed in disorders such as T2D leads to decreased functioning of the 'power house' of the cell, the mitochondrion. The early detection of the reactive oxygen species is likely to improve disease treatment as well as set a platform for therapeutic intervention with antioxidant agents to prevent cellular damage. The results presented here support the hypothesis that increased oxidative stress contributes to the pathogenesis of T2D. However, these results also indicate the

complexity of diabetes mellitus as well as an array of factors that may lead to diabetes such as the type of diet, obesity, genetic predisposition and lack of physical exercise. The production of ROS is influenced by various factors such as those discussed in Section 6.1 and the effects thereof are variable. Based on the results presented in this study, it is suggested that it would be important to monitor and obtain information pertaining to such factors when classifying and characterising individuals since these factors will influence the results. For a study focusing on a disorder such as diabetes and an intricate process such as ROS production the aforementioned suggestion will add value to the outcome of the study.

7.2 ROS-DEPENDENT INDUCTION OF METALLOTHIONEIN GENE EXPRESSION

There are several reports that indicate that MT expression is associated with certain neurological diseases such as facioscapulohumeral muscular dystrophy (FSHD), Amyotrophic lateral sclerosis, Alzheimer's and Parkinson's disease (Blaauwgeers *et al.*, 1996; Winokur *et al.*, 2003). Due to the hypothesised role of ROS in these disorders, it has been suggested that the expression of MT genes is induced by the presence of ROS. The investigation outlined in this thesis, was aimed at elucidating whether in T2D individuals, where high levels of ROS were detected, the afore-mentioned genes were expressed.

An *in vitro* phase of the study was also performed to serve as a positive control. To induce MT gene expression in HeLa cells, *t*-BHP was utilised. The increased ROS production was found to lead to a proportional increase in the expression of MT genes. In this cell line, a five-fold increase in the expression of MT-2A was observed at the 0.8 mM *t*-BHP concentration. No over expression of MT-1 isoforms was detected. However, from the results obtained from the ELISA as presented in Section 6.5.1, it can not be stated with certainty that an increase in the MT proteins was detected. A parallel study to that discussed in this thesis was also performed by Olivier (2004), where it was found that ROS production via induced complex I deficiency resulted in the selective induction of expression of the MT-2 genes. Therefore, from the results of the *in vitro* analyses as well as other reports, it can be concluded that MT expression is indeed induced by elevated levels of ROS.

The expression profile of MT genes was also investigated in T2D elderly individuals (Group-1), non-diabetic elderly individuals (Group-2) as well as individuals at risk of developing T2D (Group-3) via Real-Time PCR. There was expression of the MT-2A gene

in 13.7% of 73 individuals. Although expression was detected, these results could not be matched to the ROS profile of these individuals. MT-1A and MT-1B gene expression were also analysed. No expression of MT-1A was detected in any of these individuals. No MT-1B over-expression was detected in all individuals. However, MT-1B expression was detected at the level of the GAPDH housekeeping gene. It can be suggested from these results that only basal expression of MT-1B was detected. These observations indicate that although there is a ROS dependent increase in the expression of MT genes as observed with the *t*-BHP treatment of HeLa cells (*in vitro* conditions), in pathological conditions it cannot be stated with certainty that the present ROS leads to the induction of expression of these genes. This is due to the fact that no significant difference in ROS induced expression of MT genes was attained in the individuals presenting with high levels of ROS.

Another factor that may have led to the ambiguity of the gene expression data is that whole blood, which is a heterogeneous medium, was utilised and it has been reported that there is tissue specific expression of MT genes (Fornance *et al.*, 1988). However, if a specific tissue such as the pancreas was analysed, a more definite and precise profile may have been obtained. Although the protective role of MTs has been investigated in transgenic mouse models with targeted over expression of MT in the heart and in cultured pancreatic β-cells (Chen *et al.*, 2001; Liang *et al.*, 2002), as well as cell cultures of dopaminergic and hippocampal neurons (Køhler *et al.*, 2003), the pathological ROS-dependant induction of MT expression has not been analysed. Thus, the next phase of such an investigation would be to analyse the ROS status in specific tissues, and thereafter analyse the expression profile of MT genes in the respective tissues.

In the investigation performed by Reinecke (2004), it was illustrated that over expression of MT genes confers resistance of HeLa cells to the effects of elevated ROS produced by the treatment of cells with *t*-BHP as well as rotenone. From the results of the *in vitro* work it can be concluded that metallothioneins play a vital role in the protection of these cells from ROS. This provides evidence to the hypothesised antioxidant function of metallothionein. These results support the observation made by Suzuki *et al.* (2000) that the levels of H_2O_2 in cultured astrocytes over-expressing MT-1 were the lowest, while those of MT-1 and MT-2 null mice were the highest.

Due to the instability and short half-life of reactive oxygen species, the currently utilised techniques are not optimal. This factor thus highlights the need to establish sensitive and

reliable methods. The results generated in this investigation are one step closer to attaining this objective. Identification of molecular markers such as metallothioneins will in the future prove to be pivotal in the field of molecular diagnostics. Such techniques will make the early detection of diseases more feasible and will thus aid the treatment of various ROS-related disorders.

7.3 FUTURE DIRECTIONS FOR THE ANALYSIS OF METALLOTHIONEIN GENE EXPRESSION.

Despite the large number of methods that can be employed to detect MT mRNA as well as MT protein, the unavailability of a reference material for *in vivo* analysis of these proteins makes it difficult to quantify expression levels. Thus a reference group or reliable standards for the various tissues will aid in the characterisation of the expression of MT within biological samples.

Although MT have been proposed by the European Commission and other international scientific organisations to be included in environmental monitoring programmes as biomarkers to assess metal pollution in aquatic animals (Ren *et al.*, 1998), it is evident from the current research that this proposition can not be applied to humans yet, particularly if MTs are to be used as biomarkers for oxidative stress. Thus, further *in vivo* studies need to be performed to elucidate the differential expression of metallothioneins in ROS-related disorders. The investigation presented here is the first to perform *in vivo* analysis of the expression of MT genes in a ROS-related disorder.

Yamada and Koizumi (2001) indicated in their investigation that blood cadmium levels between 0.1 μM and 0.5 μM resulted in the increase in MT mRNA in cultured human peripheral blood lymphocytes. Blood cadmium levels of exposed humans have been reported to be ca. 0.5 μM, thus suggesting that Cd-induced expression of MT genes should be detected in these individuals. Further investigations to test this suggestion have yet to be performed. It would be vital to obtain the outcome of such studies to investigate the *in vivo* pattern of MT gene expression, in response to various inducers such as those discussed in Section 4.1.7. However, due to the toxic nature of some of these inducers, such a study would not be ethical to perform.

Rasilainen *et al.* (2002) suggested in their investigation that the administration of cysteine in cultured pancreatic β-cells increased the antioxidant capacity by providing reducing

equivalents and enhancing GSH synthesis. It may be suggested from this report and the results presented in this thesis that increased concentrations of MT in pancreatic β-cells may improve ROS scavenging together with GSH due to its high cysteine content. This approach will aid in the therapeutic intervention in diabetes mellitus and many other ROS-related disorders.

Although various cellular antioxidant mechanisms such as the SOD, and glutathione redox systems have previously been investigated (Rahman and MacNee, 2000; Zelko *et al.*, 2002), the precise role of these mechanisms in disease pathogenesis as well as the regulation of their expression remains to be elucidated. It is important to note that these antioxidant genes, including MTs have common inducers, such as pro-inflammatory agents as well as oxidants. Based on the aforementioned characteristic of these genes, an investigation of the cumulative effect of various antioxidant genes on disease pathogenesis will therefore be important in the future. The analysis of the expression pattern of these genes in specific tissues affected in the respective ROS-related disorders will provide a holistic view on the regulation of expression of this class of proteins.

7.4 MODEL FOR THE DETECTION OF METALLOTHIONEIN GENE EXPRESSION

It has become evident over the past decade that elevated levels of ROS have an important role in the pathogenesis of diabetes mellitus as well as various complications associated with this metabolic disease (Suzuki *et al.*, 1999; Dandona *et al.*, 1996). The prevalence of disorders such as diabetes mellitus, mitochondrial cytopathies, Alzheimer's and Parkinson's disease is slowly increasing. Even though a proportion of the population has a genetic predisposition for these disorders, the life style patterns may play a vital role in the development of many of these disorders. A common element of these metabolic disorders is the elevated levels of ROS. As previously described in Section 3.3, the effects of ROS on the cell are detrimental, eventually leading to disease presentation. It is postulated in Figure 7.1, that the early detection of ROS may aid in the pre-symptomatic diagnosis of various metabolic disorders.

The effects of ROS on the induction of expression of metallothioneins has been explored and proven to occur in *in vitro* conditions. Thus, as indicated in Figure 7.1, the establishment of standard methods for the analysis of gene expression patterns of metallothioneins in individuals at risk for developing any of the afore-mentioned disorders

will add value to the current diagnostic procedures. Another advantage of this approach is that early therapeutic intervention in this class of disorders will be feasible.

Figure 7.1: Schematic representation of the proposed model for the detection of metallothionein gene expression for diagnostic purposes

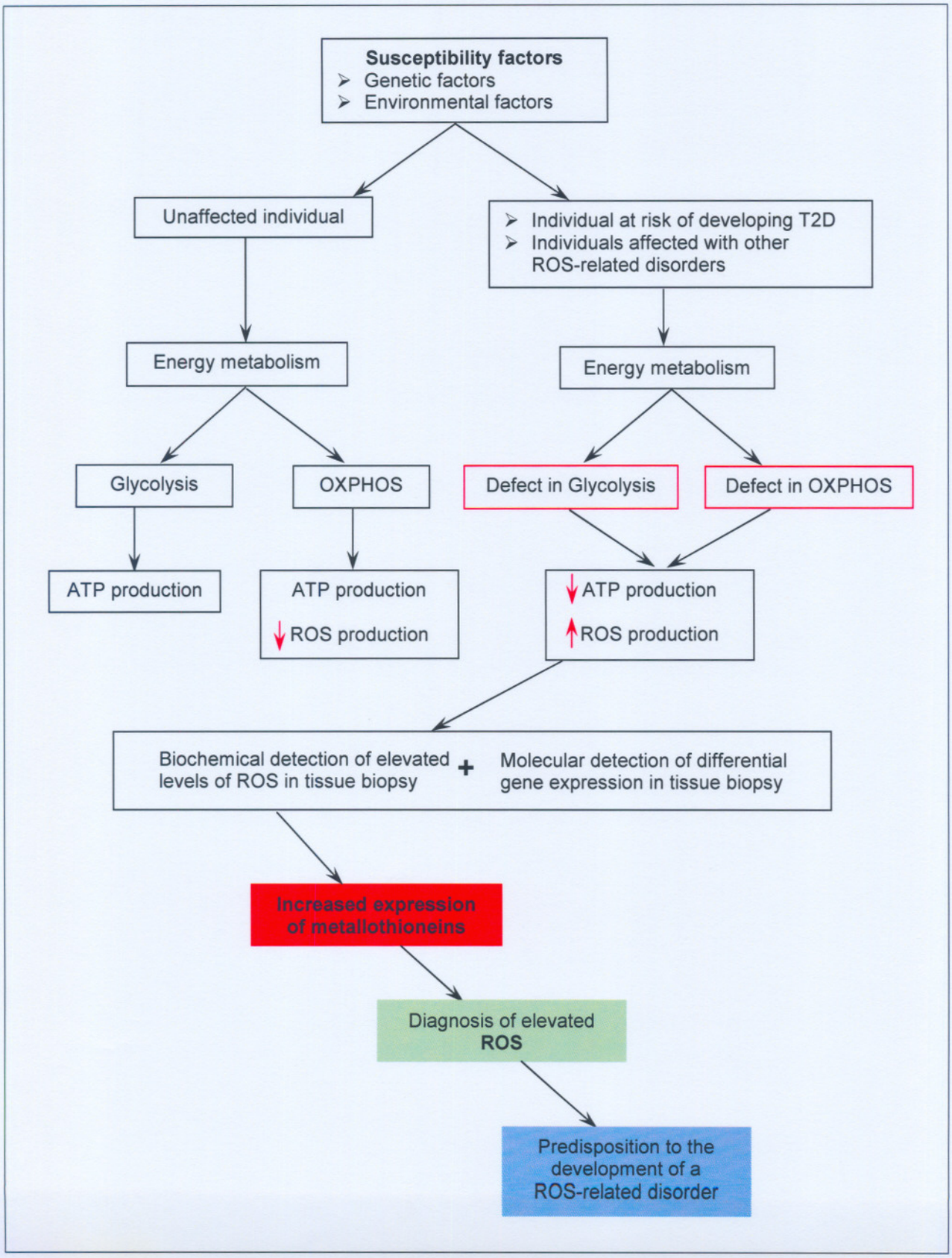

Although differential expression of MT genes was not detected *in vivo*, the results presented indicate the presence of high levels of ROS in T2D individuals as well as elderly individuals. Due to the heterogeneous nature of whole blood, it is suggested that for the analysis of MT expression, specific tissues affected in the respective disorders be analysed. It is hypothesised that if that approach is undertaken the expression profile of these proteins, postulated to have an antioxidant role, will be elucidated.

The study presented here supports the reported role of ROS in disease pathogenesis and ageing as indicated by the differences in the d-ROMs test data and the ORAC data of Group-1 and Group-2 combined when compared to Group-3. Although there was a difference in the levels of ROS between the three groups, no correlation was observed between the high levels of ROS in the elderly diabetic and non-diabetic individuals and MT gene expression, even though the expression of these proteins has been reported to be induced by oxidative stress. The postulated ROS-dependent induction of MT expression, reported by Sato *et al.* (1995) and Van der Westhuizen *et al.* (2003) was, however, made from *in vitro* studies. This postulation is however still supported in this investigation where increased ROS production in HeLa cells was observed to result in a proportional increase in MT-2A gene expression, as discussed in Section 6.4.1. This phenomenon, however, requires further elucidation via *in vivo* studies. The results generated in this study represent the first investigation of MT gene expression in a human pathological condition. This investigation highlights the fact that blood is not an optimal medium in which MT gene expression can be analysed. It can therefore be suggested that MTs can not yet be utilised as biomarkers for the detection of elevated levels of ROS in whole blood, particularly in pathological conditions with ROS aetiology.

The analysis of differential gene expression is currently one of the major focus areas in genetics and molecular medicine. This application will be valuable in different areas of science, including plant genetics, drug discovery as well as personalised medication. This investigation facilitates understanding of the intricate nature of complex disorders such as diabetes mellitus, shedding light on one of the nodes in the network of biological events that culminate in the expression of disease phenotype.

CHAPTER EIGHT

REFERENCES

8.1 GENERAL REFERENCES

Adams P.L. and Turnbull D.M. Disorders of the electron transport chain. *J. Inherit. Dis.*, **19**, 463-469, 1996.

Agarwal S. and Sohal R.S. Differential oxidative damage to mitochondrial proteins during aging. *Mech. Ageing. Dev.*, **85**, 55-63, 1995.

Alberts B., Bray D., Johnson A., Lewis J., Raff M., Roberts K. and Walter P. Essential cell biology, an introduction to the use of molecular biology of the cell. Garland Publishing, Inc., NY, 584-587, 1998.

Anderson S., Bankier A.T., Barrell B.G., de Bruijn M.H.L., Coulson A.R., Drouin J., Aperon I.C., Nierlich D.P., Roe B.A., Sanger F., Schreir P.H., Smith A.J.H., Staden R. and Young I.G. Sequence and organisation of the human mitochondrial genome. *Nature*, **290**, 457-465, 1981.

Anderson R.S., Patel K.M. and Roesijadi G. Oyster metallothionein as an oxyradical scavenger: implications for hemocyte defence responses. *Dev. Comp. Immunol.*, **23**, 443-449, 1999.

Andrews G.K., Huet-hudson Y.M., Paria B.C., McMaster M.T., De S.K. and Dey S.K, Metallothionein gene expression and metal regulation during preimplatation mouse embryo development (MT mRNA during early development). *Dev. Biol.*, **145**, 13-27, 1991.

Andrews R.M., Kubacka I., Chinnery P.F., Lightowlers R.N., Turnbull D.M. and Howell N. Reanalysis and revision of the Cambridge reference sequence for the human mitochondrial DNA. *Nat. Genet.*, **23**,147,1999.

Aksenov M.Y. and Markesbery W.R. Changes in thiol content and expression of the glutathione redox system genes in the hippocampus and cerebellum of Alzheimer's disease. *Neurosci. Lett.*, **302**, 141-145, 2001.

Asensi M., Sastre J., Pallardo V., Lloret A., Lehner M., Asuncion J.G. and Vina J. Ratio of reduced to oxidised glutathione as indicator of oxidative stress status and DNA damage. In Methods of enzymology, **299**,267-277, 1999.

Banci L. Molecular dynamic simulations of metalloproteins. *Curr. Opin. Chem. Biol.*, **7**, 143-249, 2003.

Barrell B.G., Bankier A.T. and Drouin J. A different genetic code in human mitochondria. *Nature*, **282**, 189-194, 1979.

Barnett A.H., Eff C., Leslie R.D.G. and Pyke D.A. Diabetes in identical twins. A study of 200 pairs. *Diabetologia*, **20**, 87-93, 1981.

Baumann J.W., Liu J., Liu Y.P. and Klaassen C.D. Increase in Metallothionein produced by chemicals that induce oxidative stress. *Toxicol. Appl. Pharmacol.*, **110**, 347-354, 1991.

Benda C. The spermatogenesis of vertebrates and higher invertebrates. The histology of sperm (German). *Arch. Anal. Physiol., (Physiol. Abt)*, 393-398, 1898.

Bhattacharya K., Rahman S. and James L. Diagnosis and managements of mitochondrial respiratory chain disorders. *Curr. Paediat.*, **13**, 536-542, 2003.

Blaauwgeers H.G.T., Chand A.M., Van der Berg F.M., de Jong V.J.M.B. and Troost D. Expression of different metallothionein messenger ribonucleic acids in the motor cortex, spinal cord and liver from patients with amyotrophic lateral sclerosis. *J. Neurol. Sci.*,**142**, 39-44, 1996.

Bogenhagen D. and Clayton D.A. The number of mitochondrial deoxyribonucleic acid genomes in mouse and human HeLa cells. *J. Biol. Chem.*, **249**, 7991-7995, 1974.

Bogenhagen D., Applegate E.F. and Yoza B.K. Identification of a promoter for transcription of the heavy strand of human mtDNA: *in vitro* transcription and deletion mutagenesis. *Cell*, **36,** 1105-1113, 1984.

Borst P. Structure and function of mitochondrial DNA. *TIBS*, February, 31-34, 1977.

Braun H-P. and Schmitz U.K. The mitochondrial processing peptidase. *Int. J. Biochem. Cell. Biol.*, **29**, 1043-1045, 1997.

Bremner I. and Davies N.T. The induction of metallothionein in rat liver by zinc injection and restriction of food intake. *Biochem J.*, **149**, 733-738,1975.

Brown M.D., Starikovskaya E., Derbeneva O., Hosseini S., Allen J.C., Mikhailovskaya I.E., Sukernik R.I. and Wallace D.C. The role of mtDNA background in disease expression: a new primary LHON mutation associated with Western Eurasian haplogroup. *J, Hum Genet.*, **110**, 130-138, 2002.

Bühler R.H.O. and Kägi H.R.J. Human hepatic metallothioneins. *FEBS lett.*, **39**, 229-234, 1974.

Butcher H., Kennette W., Collins O., Demoor J. and Koropatnick J. A sensitive time-resolved fluorescent immunoassay for metallothionein protein. *J. Immunol., Methods*, **272**, 247-256, 2003.

Cadenas E., Boveris A., Ragan C.I. and Stoppani A.O.M. Production of superoxide radicals and hydrogen peroxide by NADH-ubiquinone reductase and ubiquinol-cytochrome c reductase from beef-heart mitochondria. *Arch. Biochem. Biophys.*, **180**, 248-257, 1977.

Cagen X.Z. and Klaasen C.D. Protection of carbon tetrachloride (CCl_4) - induced hepatotoxicity by zinc: Role of metallothionien. *Toxicol. Appl. Pharmacol.*, **51**, 107-116, 1979.

Campbell S.R.J. Biochemistry. Second Edition, Saunders College Publishing, 391-404; 525, 1995.

Cann R.L., Stoneking M. and Wilson A.C. Mitochondrial DNA and human evolution. *Nature,* **325**, 31-36, 1987.

Cann A.J. Maths from scratch for biologist. John Wiley & Son Ltd, Sussex, England, 136-140, 2003.

Cao G., Giovanoni M. and Prior R.L. Antioxidant capacity decreases during growth but not aging in rat serum and brain. *Arch. Geront. Geriat.*, **22**, 27-37, 1996.

Cao G. and Prior R.L. Measurement of oxygen radical absorbance capacity in biological samples. In Methods in Enzymology, Oxidants and antioxidants. Packer, L. ed (New York: Academic Press) **299**, 50-62, 1998.

Chang D.D. and Clayton D.A. Priming of human mitochondrial DNA replication occurs at the light strand promoter. *Proc. Natl. Acad. Sci. USA.*, **82**, 351-355, 1985.

Chimienti F., Jourdan E., Favier A. and Seve M. Zinc resistance impairs sensitivity to oxidative stress in HeLa cells: protection through metallothionein expression. *Free Radic. Biol. Med.*, **31**, 1179-1190, 2001.

Chen H., Carlson E.C., Pellet L., Moritz J.T. and Epstein P.N. Overexpression of Metallothionein in pancreatic β-cells reduces Streptozotocin-induced DNA damage and diabetes. *Diabetes*, **50**, 2040-2046, 2001.

Chen Q., Vazquez E.J., Moghaddaas S., Hoppel C.L. and Lesnefsky E.J. Production of reactive oxygen species by mitochondria: central role of complex III. *J. Biol Chem.*, **278**, 36027-36031, 2003.

Choi C-H. Cloning and functional study of a novel human metallothionein-I isoforms induced by paraquat. *Biochem. Biophys. Res.Commun.*, **304**, 236-240, 2003.

Choski K.B., Boylston W.H., Rabek J.P., Widger W.R. and Papaconstantinou J. Oxidatively damaged proteins of heart mitochondrial electron transport complexes. *Biochim. Biophys. Acta.*, **1688**, 95-101, 2004.

Chvapil M., Ryman J N. and Zukoshi C.F. Effect of zinc on lipid peroxidation in liver microsomes and mitochondria. *Proc. Soc. Exp. Biol. Med.*, **141**, 150-153, 1972.

Clayton D.A. Replication of animal mitochondrial DNA. *Cell*, **28**, 693-705, 1982.

Clayton D.A. Transcription of the mammalian mitochondrial genome. *Ann. Rev. Biochem.*, **53** ,573-594, 1984.

Clayton D.A. Replication and transcription of vertebrate mitochondrial DNA. *Ann. Rev. Cell Biol.*, **7**, 453-478, 1991.

Clausen J.O., Hansen T., Bjørbaek C., Echwald S.M., Urhammer S.A., Rasmussen S., Anderson C.B., Hansen L., Almid K., Winther K. Haraldsdottir., Borch-Jonhnsen K. and Pedersen O. Insulin resistance: interactions between obesity and a common variant of insulin receptor substrate-1. *Lancet,* **346**, 397-402, 1995.

Conrad C.C., Grabowski D.T., Walter C.A., Sabia M. and Richardson A. Using $MT^{-/-}$ mice to study metallothionein and oxidative stress. *Free Radic. Biol. Med.*, **28**, 447-462, 2000.

Cross A.R. and Jones O.T.G. Enzymatic mechanisms of superoxide production. *Biochim. Biophys. Acta.*, **1057**, 281-298, 1991.

Dabrio M., Rodríguez A.R., Bordin G., Bebianno M.J., De Ley M., Šestáková, Vašák M. and Nordberg M. Recent developments in quantification methods for metallothionein. *J. Inorg. Biochem.*, **88**, 123-124, 2002.

Dalton T.P., Palmiter R.D. and Andrews G.K. Transcriptional induction of the mouse metallothionein-1 gene in hydrogen peroxide treated Hepa cell involves a composite major late transcription factor/antioxidant response element and metal response promoter elements. *Nucleic. Acids. Res.*, **22**, 5016-5023, 1994.

Dalton T., Paria B.C., Fernanado L.P., Huet-Hudson Y.M., Dey S.K. and Andrews G.K. Activation of the chicken metallothionein promoter by metals and oxidative stress in cultured cells and transgenic mice. *Comp. Biochem. Physiol.*, **116B**, 75-86, 1997.

Dandona P., Thusu K., Cook S., Snyder B., Makowski J., Armstrong D. and Nicotera T. Oxidative damage to DNA in diabetes mellitus. *The Lancet*, **347**, 444-445, 1996.

Dandona P. and Aljada A. A rational approach to pathogenesis and treatment of type 2 diabetes mellitus, insulin resistance, inflammation and atherosclerosis. *Am. J. Cardiol.*, **90**, 27G-33G, 2002.

Dandona P., Aljada A. and Bandyopadhyay. Inflammation: the link between insulin resistance, obesity and diabetes. *Trends Immunol.*, **25**, 4-7, 2004.

Denizot F. and Lang R. Rapid colorimetric assay for cell growth and survival. *J. Imm. Methods*, **89**, 271-277, 1986.

Dhindsa S., Tripathy D., Mohanty P., Ghanim H., Syed T., Aljada A. and Dondona P. Differential effects of glucose and alcohol on reactive oxygen specie generation intranuclear nuclear factor -κB in mononuclear cells. *Metabolism*, **53**, 330-334, 2004.

DiMauro S. and Wallace D.C. Mitochondrial DNA in human pathology. Raven Press, New York, 8-10, 1993.

DiMauro S. and Schon E.A. Mitochondrial DNA mutations in human disease. *Am. J. Med. Genet.*, **106**, 18-26, 2001.

Dincer Y., Akcay T., Alademir Z. and Iikova H. Effects of oxidative stress on glutathione pathway in red blood cells from patients with insulin dependant diabetes mellitus. *Metabolism*, **51**, 1360-1362, 2002.

Eckert A., Keil U., Marques C.A., Bonert A., FreyC., Schüssel K. and Müller W.E. Mitochodnrial dysfunction, apoptotic cell death and Alzheimer's disease. *Biochem. Pharmacol.*, **66**, 1627-1634, 2003.

Esposito L.E., Kokoszka J.E., Waymire K.G., Cottrell B., MacGregor G.R. and Wallace D.C. Mitochondrial oxidative stress in mice lacking the glutathione peroxidase-1 gene. *Free Radic. Biol. Med.*, **28**, 754-766, 2000.

Fahn S. and Cohen G. The oxidant stress hypothesis in Parkinson's disease: evidence supporting it. *Ann. Neurol.*, **32**, 804-812, 1992.

Filipović V. and Rapor B. Metallothionein and metal in cytosol of liver, kidney and brain in relation to growth parmaters of *Mullus surmuletus* and *Liza aurata* from the Eastern Adriatic sea. *Water Res*, **37**, 3252-3262, 2003.

Fornace A.J., Schalch H. and Alamo I JR. Coordinate induction of metallothioneins I and II in rodent cells by UV irradiation. *Mol. Cell. Biol.*, **8**, 4716-4720, 1988.

Fraga C.G. and Oteiza P.I. Iron toxicity and antioxidant nutrients. *Toxicology*, **180**, 23-32, 2002.

Friedman J., Peleg E., Kagan T., Shnizer S. and Rosenthal T. Oxidative stress in hypertensive, diabetic and diabetic hypertensive rats. *Am. J. Hyper.*, **16**, 1049-1052, 2003.

Furuta M., Yano Y., Ito K., Gabazza E.C., Katsuki A., Tanaka T., Ohtake K., Hirata N., Hori Y., Araki-Sasaki R., Sumida Y. and Adachi Y. Relationship of the tumor necrosis factor-α-308 A/G promoter polymorphism with insulin sensitivity and abdominal fat distribution in Japanese patients with type 2 diabetes mellitus. *Diabetes, Res., Clin., Pract.*, **56**, 141-145, 2002.

Galdes A., Vasak M., O.Hill H.A. and Kägi H.R. HNMR spectra of Metallothioneins. *FEBS Lett.*, **92**, 17-21, 1978.

Giacconi R., Cipriano C., Muzzioli M., Gasparini G., Orlando F. and Mocchegiani E. Interrelationships among brain, endocrine and immune response in ageing and successful ageing: role of metallothionein III isoform. *Mech. Ageing Dev.*, **124**, 371-378, 2003.

Giles R.E., Blanc H., Cann H., and Wallace D.C. Maternal inheritance of human mitochondrial DNA. *Proc. Natl. Acad. Sci. USA.*, **77** (11), 6715-6719, 1980.

Gille L. and Nohl H. The ubiuinol/bc_1 redox couple regulates mitochondrial oxygen radical formation. *Arch. Biochem. Biophys.*, **388**, 34-38, 2001.

Giustarini D., Dalle-Donne I., Colombo R., Milzani A. and Rossi R. An improved HPLC measurement for GSH and GSSG in human blood. *Free Radic. Biol. Med.*, **35**, 1365-1372, 2003.

Godowski P., Rusconi S., Meisfeld R. and Yamamoto K.R. Glucocorticoid receptor mutants that are constitutive activators of transcriptional enhancement. *Nature*, **325**, 365-368, 1987.

Green A. Prevention of NIDDM: the epidemiologic perspective. *Diabetes Res. Clin. Pract.*, **34**, 101-106, 1996.

Greenfield J.R. and Campbell L.V. Insulin resistance and obesity. *Clin Dermatol.*, **22**, 289-295, 2004.

Griendling K.K. and Harrison D.G. Out, damned dot: studies of the NADPH oxidase in atherosclerosis. *J. Clin. Invest.*, **108**, 1423-1424, 2001.

Grigorieff N. Structure of the respiratory NADH:ubiquinone oxidoreductase (complex I). *Curr. Opin. Struc. Biol.*, **9**, 476-483, 1999.

Hamer D.H. Metallothioneins. *Annu. Rev. Biochem.*, **55**, 913-951, 1986.

Harman D. Free radical theory of ageing: applications. *Asian Pac. J. Heart*, **7**, 169-177, 1998.

Harley C.B., Menon C.R., Rachubinski R.A. and Neiboer E. Metallothionein mRNA and protein induction by cadmium in peripheral-blood leucocytes. *Biochem J.*, **262**, 873-879, 1989.

Harris D.A. Bioenergetics at a glance, Blackwell Science Ltd, 18-19, 24-29, 84-46,1995.

Hasumi M., Suzuki K., Matsui H., Koike H., Ito K. and Yamanaka H. Regulation of metallothionein and zinc transporter expression in human prostate cancer cells and tissues. *Cancer Lett.*, **200**, 187-195, 2003.

Haq F., Mahoney M. and Koropatnick J. Signalling events for metallothionein induction. *Mut. Res.*, **533**, 211-226, 2003.

Hecht N.B., Liem H., Kleene K.C., Distel R.J. and Ho S-M. Maternal inheritance of the mouse mitochondrial genome is not mediated by a loss or gross alteration of the paternal mitochondrial DNA or by methylation of the oocyte mitochondrial DNA. *Dev. Biol.*, **102**, 452-61, 1984.

Hernández J., Carrasco J., Belloso E., Giralt M. Bluethmann H., Lee D.K., Andrews G.K. and Hildago J. Metallothionein induction by restraint stress: role of glucorcorticoids and IL-6. *Cytokine*, **12**, 791-796, 2000.

Hess J.F., Paris M.A., Bennett J.L. and Clayton D.A. Impairment of mitochondrial transcription termination by a point mutation associated with the MELAS subgroup of mitochondrial encephalomyopathies. *Nature*, **351**, 236-239, 1991.

Heuchel R., Radtke F., Georgiev O., Stark G., Aguet M. and Schaffner W. The transcription factor MTF-1 is essential for basal and heavy metal induced metallothionein gene expression. *EMBO J*, **13**, 2870-2875, 1994.

Hildago J., Aschner M., Zatta P. and Vašàk M. Roles of the metallothionein family of proteins in the central nervous system. *Brain, Res, Bulletin.*, **55**, 133-145, 2001.

Himsworth H.P. Diabetes mellitus: its differentiation into insulin-sensitive and insulin insensitive types. *Lancet*, **1**, 127-130, 1936.

Hirano T., Nakajima K. and Hibi M. Signalling mechanisms through gp130: A model for the cytokine system. *Cytokine Growth Factor Rev.*, **8**, 241-252, 1997.

Hixson J.E., Wong T.W. and Clayton D.A. Both the conserved stem-loop and divergent 5'-flanking sequences are required for initiation at the human mitochondrial origin of light-strand DNA replication. *J. Biol. Chem.*, **261,** 2384-2390, 1986.

Hotamisligil G.S., Shargill N.S. and Spiegelman B.M. Adipose expression of tumor necrosis factor-α: direct role in obesity-linked insulin resistance. *Science,* **259**, 87-91, 1993.

Hotamisligil G.S. and Spiegelman B.M. Tumor necrosis factor-α: a key component of the Obesity-diabetes link. *Diabetes*, **43**, 1271-1278, 1994.

Hotamisligil G.S., Arner P., Caro J.F., Atkinson R.L. and Spiegelman B.M. Increased adipose tissue expression of tumor necrosis factor-α in human obesity and insulin resistance. *J. Clin. Invest.*, **95**, 2409-2415, 1995.

Hovi T. Molecular epidemiology of enteroviruses with special reference to their potential role in the etiology of insulin-dependent diabetes mellitus (IDDM). *Clin. Diag. Vir.*, **9**, 89-98.1998.

Huang M-C., Pan P.K. Zheng Z.F., Chen N.C., Peng J.Y. and Huang P.C. Multiple isoforms of metallothionein are expressed in the porcine liver. *Gene*, **211**, 49-55, 1998.

Huang D., Ou B., Hampsch-Woodill M., Flanagan J.A. and Prior R.L. High throughput assay of oxygen radical absorbance capacity (ORAC) using a multichannel liquid handling system coupled with a microplate fluorescence reader in 96-well format. *J. Agric. Food Chem.*, **50**, 4437-4444, 2002.

Iorio E.L. d-ROMs test and oxidative stress assessment. Diacron International, Grosseto, Italy, 2002.

Joulia F., Steinberg J.G., Faucher M., Jamin T., Ulmer C., Kipson N. and Jammes Yves. Breath-holding training of humans reduces oxidative stress and blood acidosis after static and dynamic apnea. *Respir. Physiolo. Neurobiol.*, **137**, 19-27, 2003.

Jun H-S., Bae H.K., Lee B.R., Koh K.S., Kim Y.S., Lee K.W., Kim H. and Yoon J-W. Pathogenesis of non-insulin –dependent (type II) diabetes mellitus (NIDDM)-genetic predisposition and metabolic abnormalities. *Adv. Drug Del.*, **35**, 157-177, 1999.

Kadonaga J.T., Carner K.R., Masiarz F.R. and Tjian R. Isolation of cDNA encoding transcription factors Sp1 and functional analysis of the DNA biding domain. *Cell*, **51**, 1079-1090, 1987.

Kägi J.H.R. and Vallee B.L. Metallothionein: a Cadmium and zinc-containing protein from Equine Renal cortex. *J. Biol. Chem.*, **235**, 2435-2442, 1960.

Kägi J.H.R. and Vallee B.L. Metallothionein: a Cadmium and zinc-containing protein from Equine Renal cortex: physicochemical properties. *J. Biol. Chem.*, **236**, 3537-3542, 1961.

Kägi J.H.R., Himmelhoch S.R., Whanger P.D., Bethune J.L. and Vallee B.L. Equine hepatic and renal metallothioneins: Purification, molecular weight and amino acid composition and metal content. *J. Biol. Chem.*, **249**, 2435-2442, 1974.

Kaneda H., Hayashi J-L., Takahama S., Taya C., Lindahl K.F. and Yonekawa H. Elimination of paternal mitochondrial DNA in intraspecific crosses during early mouse embryogenesis. *Proc. Natl. Acad. Sci. USA.*, **92**, 4542-4546, 1995.

Karin M., Andersen R.D., Slater E., Smith K. and Herschman H.R. Metallothionein mRNA induction in HeLa cells in response to zinc or dexamethasone is a primary induction response. *Nature*, **286**, 295-297, 1980.

Karin M. and Richards R.I. Human metallothionein genes: Molecular cloning and sequence analysis of the mRNA. *Nucleic Acids Res.*, **10**, 3165-3173, 1982a.

Karin M. and Richards R.I. Human metallothionein genes-primary structure of the metallothionein-II gene and related processed gene. *Nature,* **299**, 797-802, 1982b.

Karin M., Eddy R.L., Henry W.M., Haley L.L., Byers M.G. and Shows T.B. Human metallothionein genes are clustered on chromosome 16. *Proc. Natl. Acad. Sci. USA.*, **81**, 5494-5498, 1984.

Kasutani K., Itoh N., Kanekiyo M., Muto N. and Tanaka K. Requirement for a responsive element in the synergistic activation of mouse metallothionein-1 gene by interleukin-6 and glucocorticoid. *Toxicol. Appl. Pharmacol.*, **151**, 143-151, 1998.

Kimura T., Itoh N., Takehara M., Oguro I., Ishzaki J-I., Nakanishi T. and Tanaka K. MRE-binding transcription factor-1 is activated during endotoxemia: a central role for metallothionein. *Toxicol. Lett.*, **129**, 77-84, 2002.

King H., Aubert R.E. and Herman W.H. Global burden of Diabetes, 1995-2025. *Diabetes Care*, **21**, 1414-1431, 1998.

Kissling M.M. and Kägi H.R. Primary structure of human hepatic metallothionein. *FEBS lett.*, **82**, 247-250, 1977.

Kling P.G. and Olsson P-E. Involvement of differential metallothionein expression in free radical sensitivity of RTG-2 and CHSE-214 cells. *Free Radic.Biol. Med.*, **28**, 1628-1637, 2000.

Kondoh M., Inoue Y., Atagi S., Futakawa N., Higashimoto M. and Sato M. Specific induction of metallothionein synthesis by mitochondrial oxidative stress. *Life Sci.*, **69**, 2137-2146, 2001.

Kondoh M., Tsukahara R., Kuronga M., Higashimoto M., Takiguchi M. and Sata M. Enhancement of MT synthesis by leptin in fasted mice. *Life Sci.*, **71**, 2425-2433, 2002.

Kondoh M., Kamada K., Kuronaga M., Higashimoto M., Takiguchi M., Watanabe Y. and Sata M. Antioxidant property of metallothionein in fasted mice. *Toxicol. Lett.*, **143**, 301-306, 2003.

Koolman J. and Röhm K. Color Atlas of biochemistry, Theime Medical publishers, New York, 1996.

Køhler L.B., Berezin V., Bock E., and Penkowa M. The role of metallothionein II in neuronal differentiation and survival. *Brain Res.*, **992**, 128-136, 2003.

Kristal B.S., Matsuda M. and Yu B.P. Abnormalities in the mitochondrial transition in diabetic rats. *Biochem. Biophys. Res. Commun.*, **222**, 519-523, 1996.

Kubo K., Sakita Y., Okazaki Y., Otaki N., Kimura M., Minami T. Identification of metallothionein on capillary zone electrophoresis by adding anti-metallothionein antibody. *J. Chromat.*, **736**, 185-190, 1999,

Lass A., Sohal B.H., Weindruch R., Forster M.J. and R.S. Caloric restriction prevents age associated accrual of oxidative damage to mouse skeletal muscle mitochondria. *Free, Rad. Biol. Med,* **25**, 1089-1097, 1998.

Larsson N-G. and Clayton D.A. Molecular genetic aspects of human mitochondrial disorders. *Ann. Rev. Genet.*, **29**, 151-178, 1995.

Lazo J.S., Kondo Y., Dellapiazza D, Michalska A.E., Choo K.H. and Pitt B.R. Enhanced sensitivity to oxidative stress in cultured cells from transgenic mice deficient in metallothionein I and II genes. *J. Biol. Chem.*, **270**, 5506-5510, 1995.

Lee A.Y.W. and Chung S.S.M. Contributions of the polyol pathway to oxidative stress in diabetic cataract. *FASEB*, **13**, 24-30, 1999.

Lee W., Haslinger A., Karin M. and Tjian R. Activation of transcription by two factors that bind promoter and enhancer sequences of the human metallothionein gene and SV40. *Nature*, **325**, 362-372, 1987.

Lenaz G. Role of mitochondria in oxidative stress and ageing. *Biochem. Biophys. Acta,* **1366**, 53-67, 1998.

Liang Q., Carlson E.C., Donthi R.V., Kralik P.M., Shen .X. and Epstein P.N. Overexpression of metallothioneins reduces diabetic cardiomyopathy. *Diabetes,* **51**, 174-181, 2002.

Lin S-J. and Guarente L. Nicotinamide adenine dinucleotide, a metabolic regulator of transcription, longevity and disease. *Curr. Opin. Cell. Biol.,* **15**, 241-246, 2003.

Liu J., Kimler B.F., Liu Y. and Klaassen C.D. Metallothionein–I transgenic mice are not protected from gamma-radiation. *Toxicol. Lett.*, **104**, 183-187, 1999.

Lubrano V., Vassalle C., L'Abbate A. and Zucchelli G.C. A new method to evaluate oxidative stress in humans. *Immuno Analy. Biol. Spec.*, **17**, 172-175, 2002.

Lust W.D. Feussner G.K., Barbehenn E.K. and Passonneau J.V. The enzymatic measurement of adenine nucleotides and P-creatine in picomole amounts. *Anal. Biochem.*, **110**, 258-266, 1981.

Lundberg K.C. and Sweda L.I. Initiation of mitochondrial-mediated apoptosis during cardiac reperfusion. *Arch. Biochem. Biophys.*, **432**, 50-57, 2004.

Margoshes M. and Vallee B.L. A cadmium protein from equine kidney cortex. *J. Am. Chem. Soc.*, **79**, 4813-4814, 1957.

Min K-S., Mukai S., Ohta M., Onosaka S. and Tanaka K. Glucocorticoid inhibition of inflammation-induced metallothionein synthesis in mouse liver. *Toxicol. Appl, Pharmacol.*, **113**, 293-298, 1992.

Minniti G., Cerone R. and De Toni E. Determination of lactic acid, pyruvic acid and ketone bodies in serum and cerebrospinal fluid by HPLC. *Am. Clic. Lab.*, 21-23, 2001.

Miura T., Muraoka S. and Ogiso T. Antioxidant activity of metallothionein compared with reduced glutathione. *Life Sci.*, **60**, 301-309, 1997.

Moller D.E., Benecke H. and Flier J. Biological activities of naturally occurring human insulin receptor mutations. *J. Biol. Chem.,* **266**, 10995-11001, 1991.

Montoya J., Christianson T., Levens D., Rabinowitz M. and Attardi G. Identification of initiation sites for heavy-strand and light strand transcription in human mitochondrial DNA. *Proc. Natl. Acad. Sci. USA.,* **79**, 7195-7199, 1982.

Montoya J., Gaines G.L. and Attardi G. The pattern of transcription of the human mitochondrial rRNA genes reveals two overlapping transcription units. *Cell*, **34**, 151-159, 1983.

Mueller R.F. and Young I.D. Emery's elements of medical genetics, Ninth edition, Churchill Livingstone, 127-141, 1995.

Mueller H., Kassack M.U. and Wiese M. Comparison of the usefulness of the MTT, ATP, and Calcein assay to predict the potency of cytotoxic agents in various human cancer cell lines. *J. Biomol. Screening*, **9**, 506-515, 2004.

Muller P.Y., Janovjak H., Miserez A.R. and Dobbie Z. Processing of gene expression data generated by quantitative Real-Time RT-PCR. *Biotechniques*, **32**, 2-7, 2002.

Murray R.K., Granner D.K., Mayes P.A. and Rodwell V.W. Harper's biochemistry, 23rd edition, Appleton and Lange, 119-120, 1993.

Nadlinger K., Westerthaler W., Storga-Tomic D. and Birkmayer J.G.D. Extracellular metabolism of NADH by blood cells correlates with intracellular ATP levels. *Biochem. Biophys. Acta,* **1573**, 177-182, 2002.

Nass M.M.K. and Nass S. Intramitochondrial fibres with DNA characteristics I. Fixation and electron staining reactions. *J. Cell Biol.*, **19**, 593-611, 1963a.

Nass S. and Nass M.M.K. Intramitochondrial fibres with DNA characteristics I. Enzymatic and other hydrolytic treatments. *J. Cell Biol.*, **19**, 613-629, 1963b.

Okazawa K., Yoshimasa Y., Miyamoto Y., Takahashi-Yasuno A., Miyawaki T., Masuzaki H., Hayashi T., Hosoda K., Inuoe G., and Nakao K. The haplotypes of IRS-2 gene affect insulin sensitivity in Japanese patients with type 2 diabetes. *Diabetes Research and Clinical Practice*, 2004. Accepted for publication.

Olivier Y. Identifying isoform specific metallothionein expression in rotenone induced NADH:ubiquinone oxidoreductase-deficient HeLa cells. MSc Thesis, North-West University (Potchefstroom campus) South Africa, 2004.

Orie N.N., Zidek W. and Tepel M. Reactive oxygen species in essential hypertension and non-insulin dependent diabetes mellitus. *Am. J. Hypertens.*, **12**, 1169-1174, 1999.

Owen K. and Hattersley A.T. Maturity-onset diabetes of the young: from clinical description to molecular genetic characterisation. *Res Clinc Endo Metab.*, **15**, 309-323, 2001.

Palmiter R.D., Findley S.D., Whitmore T.E. and Durnam D.M. MT-III, a brain specific member of the metallothionein gene family. *Proc. Natl. Acad. Sci. USA.*, **89**, 6333-6337, 1992.

Pavlidis P. Using ANOVA for gene selection from microarray studies of the nervous system. *Methods,* **31**, 282-289, 2003.

Pérez M.J. and Cederbaum A.I. metallothionein 2A induction by zinc protects HEPG2 cells against CYP2E1-dependent toxicity. *Free Rad. Biol. Med.*, **34**, 443-455, 2003.

Pfaffl M.W., Horgan G.W. and Dempfle L. Relative expression software tool (REST) for group wise comparison and statistical analysis of relative expression results in real-time PCR. *Nucleic. Acids. Res.*, **30**, 1-10, 2002.

Piccolo G., Banfi P. and Azan G. Biological markers of oxidative stress in mitochondrial myopathies with chronic progressive external ophthalmoplegia. *J. Neurol. Sci.*, **105**, 57-60, 1991.

Porta M. and Allione A. Current approaches and perspectives in the medical treatment of diabetic retinopathy. *Pharmacol. Ther.*, **103**, 197-177, 2004.

Prior R.L. and Cao G. *In vivo* total antioxidant capacity: comparison of different analytical methods. *Free Rad. Biol. Med.*, **27**, 1173-1181, 1999.

Prior R.L., Hoang H., Gu L., Wu X., Bacchiocca M., Howard L., Hampsch-Woodill M., Huang D., Ou B. and Jacob R. Assay for hydrophilic and lipophilic antioxidant capacity [oxygen radical absorbance ($ORAC_{FL}$)] of plasma and other biological and food samples. *J. Agric. Food Chem.*, **51**, 3273-3279, 2003.

Prithivirajsingh S., Story M,D., Bergh S.A., Geara F.B., Ang K.K., Ismail S.M., Stevens C.W., Buchholz T.A. and Brock W.A. Accumulation of the common mitochondrial DNA deletions induced by ionizing radiation. *FEBS lett.*, **571**, 227-232, 2004.

Quaife C.J., Findley S.D., Erickson J.C., Froelick G.J., Kelly E.J., Zambrowicz B.P. and Palmiter R.D Induction of a new metallothionein isoform (MT-IV) occurs during differentiation of stratified squamous epithelia. *Biochemistry*, **33**, 7250-7259, 1994.

Radonić A., Thulke S., Mackay I.M., Landt O., Siegert W. and Nitsche A. Guidelines to reference gene selection for quantitative real-time PCR. *Biochem. Biophys. Res. Commun.* **313**, 856-862, 2004.

Rahman I. and MacNee W. Regulation of the redox glutathione levels and gene transcription in lung inflammation: therapeutic approach. *Free Radic. Biol. Med.*, **28**, 1405-1420, 2000.

Rasilainen S., Nieminen J.M., Levonen A-L., Otonkoski T. and Lapatto R. Dose-dependent cysteine-mediated protection of insulin-producing cells from damage by hydrogen peroxide. *Biochem. Pharmacol.*, **63**, 1297-1304, 2002.

Ren L., Shi D., Dai J., Ru B. Expression of the mouse metallothionein-I gene conferring cadmium resistance in transgenic cynobacterium. *FEMS Microbiol. Lett.*, **158,** 127-132, 1998.

Reinecke F. Functional properties of metallothionein over expression in rotenone induced NADH:ubiquinone oxidoreductase-deficeint HeLa cells. MSc Thesis, North-West University (Potchefstroom campus) South Africa, 2004.

Rice J.A. Mathematical statistics and data analysis, Wadsworth Publishing company, Belmont, CA, 423-424, 453, 1995.

Riggio M., Filosa S., Parisi E. and Scudeiro R. Changes in zinc, copper and metallothionein contents during oocyte growth and early development of the teleost *Danio rerio* (zebra fish). *Comp. Biochem. Physiol C.*, **135**, 191-196, 2003.

Romero-Isart N. and Vašák M. Advances in the structure and chemistry of metallothioneins. *J. Inorg. Biochem.*, **88**, 388-396, 2002.

Rossman T.G., Goncharova E.I, Nada A. and Dolzhanskaya N. Chinese hamster cells expressing antisense to metallothionein become spontaneous mutators. *Mutat. Res.*, **373**, 75-85, 1997.

Rossmanith W., Tullo A., Potuschak T., Karwan. and Sbis E. Human mitochondrial tRNA processing. *J. Biol. Chem.*, **270**, 12885-12891, 1995.

Rusanen H., Majamaa k. and Hassinen I.E. Increased activities of antioxidant enzymes and decreases ATP concentration in cultured myoblast with the 3243A-G mutation in mitochondrial DNA. *Biochim. Biophys. Acta*, **1500**, 10-16, 2000.

Sacheck J.M., Milbury P.E., Cannon J.G., Roubenhof R. and Blumberg J.B. Effect of vitamin E and eccentric exercise on selected biomarkers of oxidative stress in young and elderly men. *Free Radic. Biol. Med.*, **34**, 1575-1588, 2003.

Sadhu C. and Godamu L. Regulation of human metallothionein (MT) genes. Differential expression of MT1-F, MT1-G, and MTII-A genes in the hepatoblastoma celll line (HepG2). *J. Biol. Chem.*, **263**, 2679-2684, 1988.

Sakai K., Matsumoto K., Nishikawa T., Suefuji M., Nakamaru K., Hirashima Y., Kawashima J., Shirotani T., Ichinose K., Brownlee M. and Araki E. Mitochondrial reactive oxygen species reduce insulin secretion by pancreatic B-cells. *Biochem. Biophys. Res. Commun.*, 300, 216-222, 2003.

Samuels M.L. Statistics for the life sciences. Dellen publishing company, a division of Macmillian, Inc., CA, 179-180, 218-222, 393-404, 1989.

Samuni A.Y., Degraff W., Cook J.A., Krishna M.C., Russo A. and Mitchell J.B. The effects of antioxidants on radiation induced apoptosis pathways I TK6 cells. *Free Radic.Biol. Med.*, **37**, 1648-1655, 2004.

Sato M. and Brenmer I. Oxygen free radicals and metallothionein. *Free Radic.Biol. Med.*, **14**, 325-337, 1993.

Sato M. Dose-dependent increase in metallothionein synthesis in the lung and liver of paraquat-treated rats. *Toxicol. Appl, Pharmacol.* **107**, 98-105, 1991.

Sato M., Sasaki M. and Hojo H. Antioxidant roles of metallothionein and manganese superoxide dismutase induced by tumor necrosis factor-α and interleukin-6. *Arch. Biochem. Biophys.*, **316**, 738-744, 1995.

Satoh M., Naganuma A. and Imura N. Metallothionein induction prevents toxic side effects of cisplatin and adriamycin used in combination. *Cancer Chemother. Pharmacol.*, **21**, 176-178, 1988.

Şardaş S., Yilmaz M., Öztok U., Çakir N. and Karakaya A.E. Assessment of DNA strand breakage by comet assay in diabetic patients and the role of antioxidant supplementation. *Mut. Res.*, **490**, 123-129, 2001.

Schmidt C. J., Hamer D. H. and McBride O. Chromosomal location of human metallothionein genes: implications for Menkes' disease. *Science*, **224**, 1104-1106, 1984.

Schmidt C.J., Jubier M.F.and Hamer D.H. Structure and expression of two human metallothionein-I isoform genes and a related pseudogene. *J. Biol. Chem.*, **260**, 7731-7737, 1985.

Schmidt M.I., Duncan B.B., Sharrett A.R., Lindberg G., Savage P.J., Offenbacher S., Azambuja M.I., Tracy R.P. and Heiss G. Markers of inflammation and prediction of diabetes mellitus in adults (Atherosclerosis risk in communities study): a cohort study. *The Lancet*, **353**, 1649-1652, 1999.

Scholte H.R. The biochemical basis of mitochondrial diseases, *J. Bioenerg. Biomembr.*, **20**, 161-191, 1987.

Seghrouchni I., Drai J., Bannier E., Rivière J., Calmard P., Garcia I., Orgiazzi J. and Revol A. Oxidative stress parameters type I, Type II and insulin-treated type II diabetes mellitus, insulin treatment efficiency. *Clin. Chim. Acta*, **321**, 89-96, 2002.

Shimuzu T., Numata T. and Okada Y. A role of reactive oxygen species in apoptotic activation of volume-sensitive Cl^- channel. *Proc. Natl. Acad. Sci.*, **101**, 6770-6773, 2004.

Smeitink J. and van den Heuvel, L. Human mitochondrial complex I in health and disease. *Am. J. Hum. Genet.*, **64**, 1505-1510, 1999.

Smeitink J., van den Heuvel, L. and DiMauro S. The genetics and pathology of oxidative phosphorylation. *Nat. Rev. Genet.*, **2**, 342-352, 2001.

Silliman K., Parrys J., Kirk L.L and Prior R.L. Pycnogenol does not impact the antioxidant or vitamin C status of healthy young adults. *J. Am. Diet. Assoc.*, **103**, 67-72, 2003.

Simpkins C.O., H-liao Z., Gebrehiwot R., Tyndall J.A., Torrence C.A., Fonong T., Balderman S., Mensah E. and Sokolove P.M. Opposite effects of metallothionein I and spermine on mitochondrial function. *Life Sci.*, **58**, 2091-2099, 1996.

Smirnova I.V., Bittel D.C., Ravindra H., Jiang G.K. and Andrews G.K. Zinc and cadmium can promote the rapid nuclear translocation of MTF-1. *J. Biol, Chem.*, **275**, 9377-9384, 2000.

Smith P.K., Krohn R.I., Hermanson G.T., Mallia A.K., Gartner F.H., Provenzano M.D., Fujimoto E.K., Goeke N.M., Olson B.J. and Klenk D.C. Measurement of protein using Bicinchoninic Acid. *Anal. Biochem.*, **150**, 76-85,1985.

Sonksen P. and Sonksen J. Insulin: understanding its action in health and disease. *Br. J. Anaesth.*, **85**, 96-79, 2000.

Staneik K. and Nohl H. Are mitochondria a permanent source of reactive oxygen species? *Biochim. Biophys. Acta.* **1460**, 268-275, 2000.

Stennard F.A., Holloway A.F., Hamilton J. and West A.K. Characterisation of six additional human metallothioneins genes. *Biochim. Biophys. Acta.*, **1218**, 357-365, 1994.

Stephens J.W., and Hurel S.J., Cooper J.A., Acharya J., Miller G.J. and Humphires S.E. A common functional variant in the interleukin-6 gene is associated with increased body mass index in subjects with type 2 diabetes mellitus. *Mol. Gent. Metabol.*, **82**, 180-186, 2004.

Sullivan V.K., Burnatt F.R. and Cousins R. Metallothionein expression is increases in monocytes and erythrocytes of young men during zinc supplementation. *J. Nutr., 128*, 707-713, 1998.

Sugihara T., Wadhwa R., Kaul S.C. and Mitsui Y. A novel testis-specific metallothionein-like protein, tesmin, is an early maker of male germ cell differentiation. *Genomics*, **57**, 130-136, 1999.

Suzuki S., Hinokio Y., Komatu K., Ohtomo M., Onada M., Hirai M., Hirai S., Hirai A., Chiba M., Kasuga S., Akai H. and Toyota T. Oxidative damage to mitochondrial DNA and its relationship to diabetic complications. *Diabetes, Res. Clin. Pract.*, **45**, 161-168, 1999.

Suzuki Y., Apostolova M.D. and Cherian M.G. Astrocyte cultures form transgenic mice to study the role of metallothionein in cytotoxicity of tert-butyl hydroperoxide. *Toxicology,* **145**, 51-62, 2000.

Suzuki S., Oka Y., Kadowaki T., Kantsuka A., Kuzuya T., Kobayashi M., Sanke T., Seino Y. and Nanjo K. Clinical features of diabetes mellitus with mitochondrial DNA 3243 (A-G) mutation in the Japanese: Maternal inheritance and mitochondrial-related complication. *Diabet. Res. Clin. Prac.,* **59**, 207-217, 2003.

Sydow K. and Münzel T. Diabetes mellitus, Oxidative stress and endothelial dysfunction. International Congress Series, 1253, 125-138, 2003.

Swierczynski J., Slominska E., Smolenski R.T and Mayer D. Increase in NAD but not ATP and GTP concentrations in rat liver by dehydroepiandrosterone feeding. *Pol. J. Pharmacol*, **53**, 125-130, 2001.

Taanman J-W. The mitochondrial genome: structure, transcription, translation and replication. *Biochim. Biophys. Acta.,* **1410**, 103-123, 1999.

Talbot D.A., Lambert A.J. and Brand M.D. Production of endogenous matrix superoxide from mitochondrial complex I leads to activation of uncoupling protein 3. *FEBS lett.*, **556**, 111-115, 2004.

ter Hofstede H., Willems H.L. and Koopmans P.P. Serum L-lactate and pyruvate in HIV-infected patients with and without presumed NRTI-related adverse events compared to healthy volunteers. *J. Clin. Vir.*, **29**, 44-50, 2004.

Thomas J.P., Bachowski G.J. and Girotti A.W. Inhibition of cell membrane lipid peroxidation by cadmium and zinc-metallothioneins. *Biochim. Biophys. Acta.,* **884**, 448-461, 1986.

Thornalley P.J. and Vasak M. Possible role for metallothionein in protection against radiation-induced oxidative stress. Kinetics and mechanism of its reaction with superoxide and hydroxyl radicals, *Biochim. Biophys. Acta.* **872**, 36-44, 1985.

Turrens J.F., Alexandre A. and Lehninger A.L. Ubisemiquinone is the electron donor for superoxide formation by complex III of heart mitochondria. *Arch. Biochem. Biophys.*, **237**, 408-414, 1985.

Ullmannová V. and Haškovec C. The use of housekeeping genes (HKG) as an internal control for the detection of gene expression by quantitative Real-Time PCR. *Folia Biol.*, **49**, 211-216, 2003.

Unger R.H., Zhou Y-T. and Orci L. Regulation of fatty acid homeostasis in cells: Novel role of leptin. *Proc. Natl. Acad. Sci. USA.*, **96**, 2327-2332, 1999.

Van der Westhuizen F.H., van der Heuvel, L.P., Smeets R., Veltman J.A., Pfundt R., Geurts van Kessel A., Ursing B. and Smeitink J. Human mitochondrial complex I deficiency: investigating transcriptional responses by microarray. *Neuropeadiatrics*, **34**, 14-22, 2003.

Vašák M., Berger C. and Kagi J.H.R. Dynamic structure of metallothionein. *FEBS*, **168**,174-178, 1984.

Vašák M., and Hasler D. Metallothionein: new functional and structural insights. *Curr. Opin. Chem. Biol.*, **4**, 177-183, 2000.

Vassault A., Bonnefont J.P., Specola N. and Saudary J.M. Lactate, Pyruvate and Ketone bodies. Techniques in diagnostic human biochemical genetics: A laboratory manual, 285-308, 1991.

Vendrell J., Fernandez-Real J-M., Gutierrez C., Zamora Alberto., Simon I., Bardaji A., Ricart W. and Richart C. A polymorphism in the promoter of the tumour necrosis factor-α gene (-308) is associated with coronary heart diseases in type 2 diabetic patients. *Atherosclerosis*, **167**, 257-264, 2003.

von Kleist-retzow J-C., Cormeir-Daire V., de Lonlay P., Parfait B., Chretein D., Rustin P., Feingold P., Rötig A. and Munnich A. A high rate of (20%-30%) parental consanguinity in cytochrome – oxidase defieciency. *Am. J. Hum. Genet.*, **63**, 428-435, 1998.

Waalkes M.P and Peratoni A. Isolation of a novel metal binding protein from rat testes. Characterisation and distinction form metallothioneins. *J. Biol. Chem.*, **261**, 13097-13103, 1986.

Walker J.E. Determination of the structures of the respiratory enzyme complexes from mammalian mitochondria. *Biochim. Biophys. Acta.*,1271, 221-227, 1995.

Wallace D.C., Singh G., Lott M.T., Hodge J.A., Schurr T.G., Lezza A.M.S., Elsas L.J. and Nikoskelainen E.K. Mitochondrial DNA mutation associated with Leber's Heriditary Optic Neuropathy. *Science*, **242**, 1427-1430, 1988

Wallace D.C. Disease of the mitochondrial DNA. *Ann. Rev. Biochem.*, **61**, 1175-1212, 1992a.

Wallace D.C. Mitochondrial genetics: A paradigm fro aging and degenerative disease? Science, 256, 628-629, 1992b.

Wanders R.J.A., Wijburg F.A., Ruiter J., Trijbels J.M.F., Ruitenbeek W., Sengers R.C.A., Bakkeren J.A.J.M. and Feller N. Prenatal Diagnosis of systemic disorders of the respiratory chain in cultured amniocytes and chroninc villus fibroblasts by studying the formation of lactate and Pyruvate from glucose. *J., Inher. Metab. Dis.*, **15**, 84-91, 1992.

Wang H. and Joseph J.A. Quantifying cellular oxidative stress by dichlorofluorescein assay using a microplate reader. *Free Radic. Biol. Med.*, **27**, 912-616, 1999.

Wang C-J., Wang J-M., Lin W-L., Chu C-Y., Chou F-P. and Tseng T-H. Protective effect of *Hibiscus* anthocyanins against *tert*-butyl hydroperoxide-induced hepatic toxicity in rats. *Food Chem. Toxicol.*, **38**, 411-416, 2000.

Watt T.A. Introductory statistics for biology students, Chapman Hall, NY, 3-6, 15-21, 123-133, 1993.

West A.K., Stallings R., Hildebrand C.E., Chiu R., Karin M. and Richards R.I. Human metallothionein genes: structure of the functional locus at 16q13. *Genomics*, **8**, 513-518, 1990.

Williams I.A., and Mayer R.F. Subacute proximal diabetic neuropathy. *Neurology*, **26**, 108-116, 1976.

Winge D.R. and Miklossy K-A. Domain nature of metallothionein. *J. Biol. Chem.*, **257**, 3471-3476, 1982.

Winokur S.T., Chen Y.W. Masny P.S., Martin J.H., Ehmsen J.T., Tapscott S.J. van der Maarel S.M., Hayashi Y. and Flanigan K.M. Expression profiling of FSHD muscle supports the defect in specific stages of myogenic differentiation. *Hum. Mol. Gent.*, **12**, 2895-2907, 2003.

Wolf N.I. and Smeitink J.A.M. Mitochondrial disorders: A proposal for consensus diagnostic criteria in infants and children. *Neurology*, **59**, 1402-1405, 2002.

Wölfer A., Abuja P.M., Schauenstein K. Liebmann P.M. *N*-acetylserotonin is a better extra-and intracellular antioxidants than melatonin. *FEBS lett.*, **449**, 206-210, 1999.

Yamada H. and Koizumi S. Lymphocyte Metallothionein-mRNA as a sensitive biomaker of Cadmium exposure. *Ind. Health.*, **39**, 29-32, 2001.

You J.H., Lee K.J. and Jeong H.G. Over expression of human metallothionein-III prevents hydrogen peroxide-induced oxidative stress in human fibroblasts. *FEBS Lett.*, **521**, 175-179, 2002.

Zelko I.N., Mariani T.J. and Folz R.J. Superoxide dismutase multigene family: a comparison of the CuZn-SOD (SOD1), Mn-SOD (SOD2), and EC-SOD (SOD3) gene structures, evolution and expression. *Free Radic. Biol. Med.*, **33**, 337-349, 2002.

Zeng J., Heuchel R., Schaffner W. and Kagi J.H.R. Thionein (apometallothionein) can modulate DNA binding and transcription activation by zinc finger containing factor SP1. *FEBS*, **279**, 310-312, 1991.

Zheng H., Liu J., Liu Y. and Klaassen C.D. Hepatocytes from metallothionein I and II knock out mice are sensitive to cadmium -- and Tert-butylhydroperoxide induced cytotoxicity. *Toxicol. Lett.*, **87**, 139-145, 1996.

Zhou J. and Goldsbrough P.B. Structure, organisation and expression of the metallothionein gene family in *Arabidopsis. Mol. Gen. Genet.*, **248,** 318-328, 1995.

Zhu X., Raina A.K., Lee H., Casadesus G., Smith M.A. and Perry G. Oxidative stress signalling in Alzheimer's disease. *Brain Res.*, **1000**, 32-39, 2004.

8.2 ELECTRONIC REFERENCES

MITOMAP, A human mitochondrial genome database: http://www.mitomap.org, 2003.

Naviaux R.K. Mitochondrial and metabolic disorders. The spectrum of mitochondrial diseases. A primary care physicians's guide, http://biochemgen.ucsd.edu/mmdc/ep-toc.htm, 1997.

Oligonucleotide Properties Calculator: http://www.basic.nwu.edu/bitools/oligocalc, 2004.

OMIM: Online Mendelian Inheritance in Man, http//www.ncbi.nlm.gov/entrez, 2004

Primer3 output program: http://www-genome.wi.mit.edu/genome_software/other/primer3.html, 2004.

APPENDIX A

SUMMARY OF CLINICAL DATA OF INDIVIDUALS INCLUDED IN THE INVESTIGATION

A summary of the clinical data obtained from the individuals forming part of this investigation. The clinical and anthropometric data, life style patterns as well as the family history of diabetes mellitus are all included in Table A.1. A discussion of this data is presented in Section 6.1.

Table A.1: Summary of clinical parameters of diabetic patients, non-diabetic individuals as well as individuals recruited into this investigation

Individual number	Age	BMI	WHR	Gender	Alcohol intake	Cigarette smoking	Cataract removal	Family history of Diabetes Mellitus	Medication
1415-PT	73	30.4	1.00	Male	Yes	Ex-smoker	No	No known family history	Treatment for T2D and hypertension
1416-PT	66	27.3	1.00	Male	Yes	Ex-smoker	No	No known family history	Treatment for T2D and hypertension
1418-PT	76	24.8	0.96	Male	No	Yes	Yes	Maternal parent history	Treatment for T2D
1419-PT	78	26.9	0.95	Male	No	No	No	One Biological sibling	Treatment for T2D and hypertension
1421-PT	76	33.9	0.90	Male	No	No	Yes	Paternal parent, maternal family history, biological sibling as well as own child	Treatment for T2D and hypertension
1423-PT	62	27.7	0.96	Male	No	No	No	No known family history	Treatment for T2D and hypertension
1424-PT	62	32.9	0.84	Female	No	Yes	No	Maternal family history	Treatment for T2D
1425-PT	64	28.1	0.80	Female	Yes	No	Yes	Maternal parent	Treatment for T2D and hypertension
1427-PT	64	37.1	0.76	Female	Yes	No	Yes	None	Treatment for T2D and arthritis
1429-PT	79	20.9	0.98	Male	Yes	No	Yes	Maternal family history	Treatment for T2D
1431-PT	48	33.6	0.85	Female	No	No	No	No known family history	Treatment for T2D
1432-PT	63	29.9	0.98	Female	No	No	No	Maternal history	Treatment for T2D and hypertension

Table A.1: continued ...

Individual number	Age	BMI	WHR	Gender	Alcohol intake	Cigarette smoking	Cataract removal	Family history of Diabetes Mellitus	Medication
1433-PT	68	36.9	1.05	Male	No	Ex-smoker	No	Maternal parent affected	Treatment for T2D
1435-PT	48	30.9	1.06	Male	Yes	Yes	No	No known family history	Treatment for T2D and hypertension
1437-PT	68	23.8	0.99	Male	Yes	No	No	No known family history	Treatment for T2D and hypertension
1438-PT	67	26.1	1.00	Male	No	No	Yes	Paternal grandmother	Treatment for T2D
1439-PT	50	46.3	0.80	Female	No	No	No	Maternal and Paternal history	Treatment for T2D and hypertension
1440-PT	73	26.9	0.94	Male	Yes	No	Yes	Paternal parent and biological siblings	Treatment for T2D and hypertension
1444-PT	63	28.9	0.82	Female	No	No	No	Maternal parent	Treatment for T2D and hypertension
1414-CT	78	28.8	0.75	Female	No	None	Yes	No known family history	Treatment for hypertension
1417-CT	64	30.8	0.84	Female	Yes	No	No	Parental history and maternal family history	High cholesterol treatment
1420-CT	72	20.2	0.86	Female	No	No	Yes	None	None
1422-CT	67	27.6	0.90	Female	Yes	No	No	Maternal parent	None
1426-CT	66	25.1	1.00	Male	No	No	No	None	Treatment for hypertension
1428-CT	62	24.8	0.98	Male	No	Ex-smoker	No	Maternal parent and biological sibling	Treatment for hypertension
1430-CT	49	35.3	0.82	Female	No	No	No	Paternal history of diabetes mellitus	Treatment for hypertension
1434-CT	68	23.8	0.72	Female	Yes	No	Yes	No known family history	Treatment for hypertension
1436-CT	47	33.2	0.91	Female	No	No	No	No known family history	No medication
1441-CT	70	29	0.98	Female	No	No	Yes	No known family history	Treatment for hypertension
1442-CT	47	48.3	1.17	Male	Yes	Ex-smoker	No	Paternal grandmother	No medication
1445-CT	40	19	0.89	Male	No	No	No	No known family history	None
1501-PW	35	42.7	0.93	Female	Yes	No	No	None	No diabetes or hypertension related medication
1502-PW	23	28.1	0.84	Female	Yes	No	No	Maternal family history	No diabetes or hypertension related medication

Table A.1: continued ...

Individual number	Age	BMI	WHR	Gender	Alcohol intake	Cigarette smoking	Cataract removal	Family history of Diabetes Mellitus	Medication
1503-PW	23	29.5	0.72	Female	Yes	No	No	None	No diabetes or hypertension related medication
1504-PW	22	30.6	0.78	Female	Yes	Yes	No	Paternal family history	No diabetes or hypertension related medication
1505-PW	22	29.2	0.94	Female	Yes	No	No	None	No diabetes or hypertension related medication
1506-PW	35	29.4	0.91	Female	Yes	No	No	Maternal parent	No diabetes or hypertension related medication
1507-PW	37	19.7	0.69	Female	No	No	No	No known family history	No diabetes or hypertension related medication
1508-PW	35	21.5	0.75	Female	Yes	No	No	None	No diabetes or hypertension related medication
1509-PW	42	27.5	0.91	Female	Yes	No	No	None	No diabetes or hypertension related medication
1510-PW	27	20.3	0.77	Female	No	No	No	Paternal parent and paternal grandmother	No diabetes or hypertension related medication
1511-PW	38	29.2	0.88	Female	Yes	No	No	Paternal grandmother	No diabetes or hypertension related medication
1512-PW	31	19.3	0.70	Female	Yes	No	No	None	No diabetes or hypertension related medication
1513-PW	35	21.0	0.73	Female	Yes	Yes	No	None	No diabetes or hypertension related medication
1514-PW	26	20.2	0.69	Female	Yes	No	No	None	No diabetes or hypertension related medication
1515-PW	25	22.6	0.69	Female	Yes	No	Unknown	Maternal family history	No diabetes or hypertension related medication
1516-PW	25	40.4	0.75	Female	Yes	Ex-smoker	No	Maternal grandmother	No diabetes or hypertension related medication

Table A.1: continued ...

Individual number	Age	BMI	WHR	Gender	Alcohol intake	Cigarette smoking	Cataract removal	Family history of Diabetes Mellitus	Medication
1517-PW	28	30.7	0.80	Female	Yes	No	No	No known family history	No diabetes or hypertension related medication
1518-PW	22	25.1	0.76	Female	Yes	Ex-smoker	No	Maternal history	No diabetes or hypertension related medication
1519-PW	22	32.2	0.78	Female	Yes	Yes	No	No known family history	No diabetes or hypertension related medication
1520-PW	23	21.7	0.77	Female	Yes	No	No	None	No diabetes or hypertension related medication
1521-PW	23	40.2	0.80	Female	Yes	No	No	Maternal grandmother	No diabetes or hypertension related medication
1522-PW	29	36.1	0.70	Female	Yes	No	No	Maternal history	No diabetes or hypertension related medication
1523-PW	23	23.4	0.72	Female	Yes	No	No	None	No diabetes or hypertension related medication
1524-PW	23	25.8	0.76	Female	Yes	Ex-smoker	No	Maternal family history	No diabetes or hypertension related medication
1525-PW	24	24.5	0.76	Female	Yes	Yes	No	None	No diabetes or hypertension related medication
1526-PW	42	38.0	0.77	Female	No	No	No	None	No diabetes or hypertension related medication
1527-PW	48	23.6	0.76	Female	Yes	No	No	Maternal family history	No diabetes or hypertension related medication
1528-PW	35	18.6	0.70	Female	Yes	No	No	None	No diabetes or hypertension related medication
1529-PW	35	24.4	0.72	Female	Yes	No	No	No known family history	No diabetes or hypertension related medication

Table A.1: continued ...

Individual number	Age	BMI	WHR	Gender	Alcohol intake	Cigarette smoking	Cataract removal	Family history of Diabetes Mellitus	Medication
1530-PW	30	23.8	0.66	Female	Yes	No	No	None	No diabetes or hypertension related medication
1531-PW	21	32.8	0.77	Female	Yes	No	No	None	No diabetes or hypertension related medication
1532-PW	30	21.2	0.70	Female	Yes	No	No	None	No diabetes or hypertension related medication
1533-PW	30	30.5	0.83	Female	Yes	No	No	None	No diabetes or hypertension related medication
1534-PW	35	20.8	0.73	Female	Yes	No	No	None	No diabetes or hypertension related medication
1535-PW	23	21.7	0.73	Female	Yes	No	No	Maternal grandmother	No diabetes or hypertension related medication
1536-PW	23	32.4	0.87	Female	Yes	No	No	None	No diabetes or hypertension related medication
1537-PW	22	27.2	0.85	Female	Yes	No	No	None	No diabetes or hypertension related medication
1538-PW	22	28.6	0.80	Female	No	No	No	Maternal family history	No diabetes or hypertension related medication
1539-PW	35	22.0	0.70	Female	Yes	No	No	None	No diabetes or hypertension related medication
1540-PW	37	34.3	0.77	Female	Yes	Yes	No	Paternal grandmother	No diabetes or hypertension related medication
1541-PW	35	20.0	0.68	Female	Yes	No	No	Paternal parent	No diabetes or hypertension related medication
1542-PW	42	30.1	0.72	Female	Yes	No	No	No known family history	No diabetes or hypertension related medication

BMI = body mass index; WHR = waist hip ratio; PT = T2D patients (Group-1); CT = control individual (Group-2); PW = POWIRS2 group of individuals (Group-3).

APPENDIX B

SUMMARY OF BIOCHEMICAL DATA OF INDIVIDUALS INCLUDED IN THE INVESTIGATION

The data for all six biochemical parameters analysed in this investigation for all three groups of individuals is presented in Table B.1. The classification of individuals is according to groups. Group-1 represents the T2D diabetic individuals, Group-2 represent the non-diabetic elderly individuals and Group-3 is comprised of individuals who are classified as being at risk of developing diabetes.

Table B.1: Summary of biochemical parameters of diabetic patients, non-diabetic individuals as well as individuals recruited into this investigation

Individual Number	Group	d-ROM (CARR U)	ORAC (Trolox U)	Lactate: Pyruvate ratio	GSH:GSSG ratio	NADH: NAD^+ ratio	ATP: ADP ratio
1415	Group-1	797	1093	25.16	28.13	0.82	9.25
1416	Group-1	1012	1158	19.25	42.47	0.76	1.25
1418	Group-1	200	1361	19.25	134.21	1.04	1.26
1419	Group-1	630	1410	33.25	16.13	0.68	6.28
1421	Group-1	479	1241	29.35	18.05	0.98	2.39
1423	Group-1	880	2633	22.25	35.39	1.26	9.36
1424	Group-1	229	1984	59.26	15.62	0.91	2.36
1425	Group-1	1015	2208	28.26	73.01	0.93	4.27
1427	Group-1	868	1388	34.26	255.48	1.09	1.33
1429	Group-1	330	1195	36.25	88.73	0.90	2.37
1431	Group-1	459	961	38.20	27.42	1.24	1.26
1432	Group-1	284	1891	33.42	81.81	1.00	4.24
1433	Group-1	550	1945	68.25	5.01	1.02	2.57
1435	Group-1	486	1072	18.84	393.01	1.04	1.33
1437	Group-1	501	1212	35.27	8.32	1.08	5.24
1438	Group-1	583	1204	33.10	33.21	1.07	8.27
1439	Group-1	629	714	51.18	32.58	1.78	9.24
1440	Group-1	519	678	65.42	188.47	1.04	9.99
1444	Group-1	646	615	25.61	30.74	0.68	2.37
1414	Group-2	1162	1405	28.59	12.95	1.00	4.68
1417	Group-2	846	2566	31.25	27.72	1.31	6.28
1420	Group-2	935	1659	19.25	47.46	1.13	5.27
1422	Group-2	623	1533	43.25	14.85	1.15	9.03
1426	Group-2	736	1313	25.26	47.56	1.38	2.36
1428	Group-2	394	1906	29.26	16.23	0.81	1.29
1430	Group-2	543	984	16.29	31.03	1.06	6.29
1434	Group-2	1075	1359	22.90	6.98	0.81	1.27
1436	Group-2	729	663	17.58	33.80	0.93	7.27
1441	Group-2	809	1813	55.07	405.50	1.18	6.26
1442	Group-2	485	554	39.93	697.84	1.37	2.01
1445	Group-2	797	958	31.00	658.10	1.32	3.26
1501	Group-3	392	1314	49.89	149.94	2.75	1.26
1502	Group-3	330	1440	14.29	123.96	0.95	3.36

Table B.1: continued ...

Individual Number	Group	d-ROM (CARR U)	ORAC (Tolox U)	Lactate: Pyruvate ratio	GSH:GSSG ratio	NADH: NAD^+ ratio	ATP: ADP ratio
1503	Group-3	385	1486	13.99	180.01	1.03	1.25
1504	Group-3	341	2293	15.50	260.10	1.30	10.25
1505	Group-3	214	3253	13.80	252.87	0.91	2.35
1506	Group-3	247	2186	22.39	177.18	1.50	4.03
1507	Group-3	234	1144	25.39	208.94	1.29	11.27
1508	Group-3	469	1376	11.70	132.02	1.37	10.26
1509	Group-3	448	2772	10.30	150.53	0.30	6.24
1510	Group-3	602	2478	15.30	139.92	0.24	9.27
1511	Group-3	629	3141	20.94	194.26	0.22	8.27
1512	Group-3	643	1434	28.10	138.53	0.25	18.25
1513	Group-3	817	1442	19.10	5.58	0.22	1.24
1514	Group-3	734	1150	16.33	101.04	0.21	9.00
1515	Group-3	295	2510	19.82	146.16	0.22	7.27
1516	Group-3	287	1550	12.77	75.25	0.22	13.25
1517	Group-3	686	1854	12.37	256.03	0.21	17.27
1518	Group-3	537	1480	17.31	49.86	0.22	9.27
1519	Group-3	526	455	18.60	378.78	0.17	9.33
1520	Group-3	395	677	17.25	359.77	0.23	9.27
1521	Group-3	751	2346	27.13	1776.82	0.28	9.24
1522	Group-3	1093	966	20.54	496.30	0.21	15.24
1523	Group-3	586	1283	16.59	1515.87	0.20	8.26
1524	Group-3	604	1073	12.23	648.48	0.14	5.27
1525	Group-3	518	531	17.32	412.66	0.18	5.27
1526	Group-3	324	945	42.15	713.24	0.14	9.24
1527	Group-3	466	1269	10.51	84.20	0.25	11.27
1528	Group-3	676	1237	17.29	139.30	0.15	8.27
1529	Group-3	466	1658	12.62	165.17	0.17	19.25
1530	Group-3	664	1591	20.37	71.42	0.14	16.25
1531	Group-3	546	464	24.09	209.90	0.17	8.66
1532	Group-3	427	1026	17.49	47.86	0.18	9.27
1533	Group-3	511	2343	26.50	25.24	0.98	2.36
1534	Group-3	230	739	24.67	33.83	1.01	8.27
1535	Group-3	426	1755	18.32	488.49	1.00	6.24
1536	Group-3	742	1383	12.23	153.40	1.06	6.26
1537	Group-3	392	198	13.25	110.99	1.22	9.24
1538	Group-3	470	800	20.07	93.97	1.08	8.27
1539	Group-3	708	2477	31.52	222.53	0.92	2.36
1540	Group-3	766	1283	18.15	299.18	0.93	5.26
1541	Group-3	1004	1340	20.97	65.45	0.78	8.24
1542	Group-3	1118	1284	10.17	204.38	1.06	8.27

APPENDIX C

RESULTS OF THE EXPRESSION PROFILES FOR METALLOTHIONEIN GENE ISOFORMS AND GAPDH

The cycle threshold values (Ct) obtained for the expression of MT-1B and MT-2A are presented in Table C.1 including those obtained for GAPDH. The Bio-Rad iCycler™ iQ optical system software version 3.0 provided the Ct values for the expression of genes that were above the threshold level. Therefore, those samples in which Ct values were not provided by the software are indicated as NA. A summary of the data presented in Table C.1 is presented in Graph 6.19.

Table C.1: Expression ratios of MT genes based on Real-Time PCR detection of MT mRNA

Patient number	Group	Real-time PCR (expression profile of MT-2A)[1]	Ct value of MT-2A	Ct value of MT-1B	Ct value of GAPDH
1415	Group-1	Above	38.5	36.0	38.4
1416	Group-1	Below	NA	36.8	41.3
1418	Group-1	Below	NA	35.9	39.2
1419	Group-1	Below	NA	39.1	35.9
1421	Group-1	Above	39.8	39.2	35.8
1423	Group-1	Below	NA	38.4	35.7
1424	Group-1	Below	NA	36.8	36.9
1425	Group-1	Below	NA	39.2	37.9
1427	Group-1	Below	NA	36.2	33.6
1429	Group-1	Below	NA	33.9	39.5
1431	Group-1	Below	NA	36.9	38.6
1432	Group-1	Above	38.7	34.1	36.5
1433	Group-1	Below	NA	37.0	39.5
1435	Group-1	Below	NA	35.4	37.2
1437	Group-1	Below	NA	35.8	39.4
1438	Group-1	Below	NA	32.2	33.8
1439	Group-1	Below	NA	33.9	31.8
1440	Group-1	Above	35.2	35.5	32.5
1444	Group-1	Below	NA	33.4	33.9
1414	Group-2	Above	37.9	36.9	42.7
1417	Group-2	Below	NA	36.8	38.9
1420	Group-2	Below	NA	35.9	35.6
1422	Group-2	Below	NA	37.3	38.7
1426	Group-2	Below	NA	39.2	37.8
1428	Group-2	Above	39.5	36.9	40.1
1430	Group-2	Below	NA	33.0	36.2
1434	Group-2	Below	NA	36.5	38.5

Table C.1: continued ...

Patient number	Group	Real-time PCR (expression profile of MT-2A)[1]	Ct value of MT-2A	Ct value of MT-1B	Ct value of GAPDH
1436	Group-2	Below	NA	36.4	32.5
1441	Group-2	Below	NA	33.1	33.6
1442	Group-2	Below	NA	37.3	39.5
1445	Group-2	Below	NA	32.2	37.9
1501	Group-3	Above	37.0	31.7	36.1
1502	Group-3	Below	NA	37.3	38.2
1503	Group-3	Below	NA	34.8	36.5
1504	Group-3	Below	NA	34.9	36.7
1505	Group-3	Below	NA	31.0	35.9
1506	Group-3	Below	NA	33.9	35.4
1507	Group-3	Below	NA	33.5	34.4
1508	Group-3	Below	NA	35.1	36.1
1509	Group-3	Above	32.0	34.8	42.3
1510	Group-3	Above	33.7	38.9	36.0
1511	Group-3	Below	NA	32.7	41.2
1512	Group-3	Below	NA	36.0	39.3
1513	Group-3	Below	NA	36.7	38.7
1514	Group-3	Below	NA	34.4	37.8
1515	Group-3	Below	NA	34.2	39.2
1516	Group-3	Below	NA	39.9	34.3
1517	Group-3	Below	NA	42.7	38.9
1518	Group-3	Below	NA	36.4	37.6
1519	Group-3	Below	NA	35.4	43.7
1520	Group-3	Below	NA	35.8	38.7
1521	Group-3	Below	NA	42.8	39.0
1522	Group-3	Below	NA	37.5	33.6
1523	Group-3	Below	NA	33.2	36.1
1524	Group-3	Below	NA	34.7	39.2
1525	Group-3	Below	NA	38.2	36.4
1526	Group-3	Below	NA	39.1	38.1
1527	Group-3	Below	NA	38.7	35.6
1528	Group-3	Below	NA	33.4	36.7
1529	Group-3	Below	NA	35.2	39.4
1530	Group-3	Below	NA	34.7	40.1
1531	Group-3	Above	34.8	36.3	30.3
1532	Group-3	Below	NA	36.3	36.8
1533	Group-3	Below	NA	36.2	36.4
1534	Group-3	Below	NA	34.8	38.2
1535	Group-3	Below	NA	38.5	39.1
1536	Group-3	Below	NA	31.2	42.1
1537	Group-3	Below	NA	32.3	38.1
1538	Group-3	Below	NA	34.6	38.7
1539	Group-3	Below	NA	35.8	39.7
1540	Group-3	Below	NA	37.2	33.2
1541	Group-3	Below	NA	36.7	36.4
1542	Group-3	Below	NA	37.3	31.3

1 = indicates expression of MT-2A gene, either above or below the threshold level; NA = Ct values below the threshold level which are indicated as being not available; Ct = cycle threshold value; MT-1A = metallothionein-1A; MT-2A = metallothionein-2A; GAPDH = glyceraldehydes-3-phosphate dehydrogenase; PCR = polymerase chain reaction.

APPENDIX D

RESULTS FROM THE ELISA ANALYSIS OF METALLOTHIONIEN PROTEINS

The results presented in Table D.1 indicate the presence of MT proteins as obtained via the ELISA from serum samples of individuals comprising Group-1, Group-2 and Group-3. A graphical representation of these results is presented in Graph 6.21.

Table D.1: Expression profile of MT based on the ELISA data

Patient number	Group	ELISA (μg MT per μg protein)	Patient number	Group	ELISA (μg MT per μg protein)
1415	Group-1	0.023	1507	Group-3	0.000
1416	Group-1	0.079*	1508	Group-3	0.000
1418	Group-1	0.084*	1509	Group-3	0.000
1419	Group-1	0.010	1510	Group-3	0.001
1421	Group-1	0.055*	1511	Group-3	0.015
1423	Group-1	0.008	1512	Group-3	0.000
1424	Group-1	0.015	1513	Group-3	0.001
1425	Group-1	0.008	1514	Group-3	0.070*
1427	Group-1	0.006	1515	Group-3	0.009
1429	Group-1	0.019	1516	Group-3	0.017
1431	Group-1	0.017	1517	Group-3	0.015
1432	Group-1	0.006	1518	Group-3	0.011
1433	Group-1	0.012	1519	Group-3	0.013
1435	Group-1	0.008	1520	Group-3	0.037*
1437	Group-1	0.002	1521	Group-3	0.010
1438	Group-1	0.002	1522	Group-3	0.015
1439	Group-1	0.003	1523	Group-3	0.038*
1440	Group-1	0.000	1524	Group-3	0.036*
1444	Group-1	0.040*	1525	Group-3	0.007
1414	Group-2	0.063*	1526	Group-3	0.017
1417	Group-2	0.110*	1527	Group-3	0.015
1420	Group-2	0.024	1528	Group-3	0.026
1422	Group-2	0.027	1529	Group-3	0.048*
1426	Group-2	0.040*	1530	Group-3	0.026
1428	Group-2	0.009	1531	Group-3	0.032*
1430	Group-2	0.062*	1532	Group-3	0.035*
1434	Group-2	0.009	1533	Group-3	0.078*
1436	Group-2	0.001	1534	Group-3	0.012
1441	Group-2	0.014	1535	Group-3	0.075*
1442	Group-2	0.000	1536	Group-3	0.011
1445	Group-2	0.072*	1537	Group-3	0.030*
1501	Group-3	0.000	1538	Group-3	0.013
1502	Group-3	0.003	1539	Group-3	0.006
1503	Group-3	0.000	1540	Group-3	0.018
1504	Group-3	0.000	1541	Group-3	0.006
1505	Group-3	0.000	1542	Group-3	0.006
1506	Group-3	0.005	--	--	--

* = individuals with levels of MT protein higher than the reported value of 0.027 μg MT. μg^{-1} protein.

APPENDIX E

CONFERENCES AND MEETING AT WHICH THE RESEARCH WAS PRESENTED DURING THE STUDY

The research in this thesis was presented at the following national meetings during the period of this study. The name of the presenting author is underlined for each presentation.

E.1 PRESENTIONS AT NATIONAL CONFERENCES

E.1.1 **South African Society of Biochemistry and Molecular biology,** Stellenbosch, January 2005.
Olivier Y., Reinecke F., Levanets O., Semete B., Louw R., Olckers A. and van der Westhuizen F.H. Identifying isoform- specific Metallothionein expression in Rotenone induced NADH:ubiquinone oxidoreductase deficiency in HeLa cells (Poster presentation).

E.1.2 **South African Society of Biochemistry and Molecular biology,** Stellenbosch, January 2005.
Van der Westhuizen F.H., Olivier Y., Reinecke F., Levanets O., Semete B., Louw R., and Olckers A. Metallothionein expression and its role in rotenone-induced Complex I-deficient HeLa cells (Oral presentation).

E.1.3 **South African Society of Biochemistry and Molecular biology,** Stellenbosch, January 2005.
Reinecke F., Levanets O., Louw R., Semete B., Olivier Y., Olckers A. and van der Westhuizen F.H. Functional properties of Metallothionein overexpression in rotenone induced NADH:ubiquinone oxidoreductase-deficient HeLa cells (Poster presentation).

E.2 PRESENTION AT A NATIONAL MEETING

E.2.1 **30th Annual General Meeting of the National Muscular Dystrophy Foundation,** Gauteng, September, 2004.

Semete B., van der Westhuizen F.H., Levanets O., and Olckers A. Analysis of Metallothionein gene expression in patients with oxidative stress related disorders.